Bulletin de la

Commission Géologique

de Finlande

N:o 229

Suomen Geologisen Seuran julkaisuja
Meddelanden från Geologiska Sällskapet
i Finland
Comtes Rendus de la Société Géologique
de Finlande

XXXIX

Geologinen tutkimuslaitos · Otaniemi 1967

Bulletin de la Commission Géologique de Finlande N:o 229

SUOMEN GEOLOGISEN SEURAN JULKAISUJA
MEDDELANDEN FRÅN GEOLOGISKA SÄLLSKAPET I FINLAND
COMPTES RENDUS DE LA SOCIÉTÉ GÉOLOGIQUE DE FINLANDE

XXXIX

Published yearly by The Geological Society of Finland
Helsinki 1967

SISÄLLYSLUETTELO — CONTENTS

Sivu—Page

KIRJOITUKSIA — PAPERS

(*Contents continued*) Sivu—Page

This bulletin is the journal of the Geological Society of Finland. It contains articles on geology and related scientific subjects.

Manuscripts for publication should be sent to the Editor before March 1st. The papers should be in English, German or French. References to other publications should be in accordance with the forms used in this issue. The headings should generally be restricted to three classes. The articles should be brief and should be preceded by a short Abstract (Zusammenfassung, Résumé). The illustrations, in black and white, should be kept separate from the text. The author's name and the figure number to be on each illustration.

The contributors may have 100 reprints without covers free of charge. Additional author's reprints can be supplied at printer's rates if ordered in advance of publication.

Comptes Rendus de la Société géologique de Finlande
N:o XXXIX (1967), pp. 3—9

A GEOBAROMETER FOR CERTAIN MIGMATITES

BY

R. V. DIETRICH

Department of Geological Sciences, Virginia Polytechnic Institute
Blacksburg, Virginia, U.S.A.

ABSTRACT

Where a K-feldspar-, quartz-rich rock occurs in juxtaposition with a plagioclase-, quartz-rich rock and it can be demonstrated that either or both of the rocks have undergone partial anatexis, it may be possible to determine whether the anatexis took place at a pressure below, near, or above approximately 1.7 kilobars. Laboratory data indicate that at pressures greater than approximately 1.7 kilobars, Na-rich plagioclase plus quartz starts to melt — and thus gains at least potential mobility — at lower temperatures than K-feldspar plus quartz, whereas at pressures of less than approximately 1.7 kilobars the reverse relationship obtains (*i.e.*, K-feldspar plus quartz starts to melt at lower temperatures than plagioclase plus quartz). Of course, the effects of differences in viscosities of the anatectic fluids, of volatile contents, *etc.*, must become better known before at all acceptable values can be assigned.

Occurrences of such rocks in juxtaposition are not uncommon in migmatite terrains. A banded migmatite of southern Finland is described and concluded to exhibit features probably attributable to anatexis above approximately 1.8 kilobars.

INTRODUCTION

A large percentage of migmatites are characterized in the literature as »granitic» in composition. Nonetheless, close examination has shown that many of them actually contain either plagioclase or K-feldspar, almost to the exclusion of the other, along with quartz and the other mineral constituents. Not uncommonly a rock unit containing the one feldspar and quartz occurs contiguous with another unit containing the other feldspar and quartz (see, *e.g.*, Dietrich, 1959 or 1960).

A banded migmatite from southern Finland that exhibits this relationship and which subsequent to the formation of its banding underwent fracturing and apparently partial anatexis serves as the basis for this brief note.

The exact geological occurrence of the described specimen is not known. The specimen was discovered by the writer in the collections of the U. S. National Museum about ten years ago when Dr. William F. Foshag and Dr. George Switzer were kindly helping him look for ptygmatic features. According to museum records, the specimen, along with type locality ptygmatic features, was sent to the museum by Dr. J. J. Sederholm. The only location given was »southern Finland.» This lack of information, of course, reduces the significance of this example. The specimen, however, constitutes too fine an example for calling attention to certain phenomena to be ignored.

The terms used in this paper to apply to certain features (*e.g.*, restite) and processes (*e.g.*, anatexis) are used as defined by Dietrich and Mehnert (1960).

DESCRIPTION

A tracing of the interesting part of the specimen is given as Figure 1. The dark bands consist chiefly of approximately millimeter grains of hornblende, biotite, and oligoclase (An_{24-26}) with abundant sphene and minor apatite. As is shown, the lighter colored bands are tripartite — their central portions consist almost wholly of 3—5 millimeter grains of microcline and quartz whereas the generally thinner zones to either side (*i.e.*, between the »central portions» and the dark bands) consist of 2—3 millimeter grains of oligoclase (An_{24-26}) and quartz. Each of these contains trace amounts of hornblende and biotite. The microcline, a small proportion of which is slightly microperthitic, exhibits »grid» twinning. Most microcline-microcline and microcline-oligoclase boundaries (the latter of which occur near the boundaries between the predominantly microcline plus quartz bands and the predominantly oligoclase plus quartz bands) exhibit plagioclase rims similar to those pictured and described by Tuttle (1952). Index of refraction measurements indicate these rims to be albitic in composition. As Tuttle *(op. cit.)* suggested, the albite may have been derived by unmixing from the microcline.

A very interesting veinlet transects the bands. This veinlet consistently cuts across the relatively well foliated hornblende-biotite richer bands at a more acute angle than it does across the predominately feldspar-quartz bands. The veinlet, like the rock proper, consists of three differently constituted sections — 1. wholly plagioclase (An_{24-26}), 2. microcline plus quartz, and 3. plagioclase (An_{24-26}) plus quartz. The boundaries between the differently constituted portions are abrupt, *i.e.*, there are no segments that exhibit compositional zoning parallel to their walls. The minerals of the veinlet are of markedly coarser grain size than the same minerals in the rock proper. The hornblende and biotite grains of the dark bands are slightly more concentrated and do not exhibit so well defined a preferred orientation directly adjacent to the veinlet as they do away from it; this may be a restite and the probable *re*orientation may represent »pushing aside» as a result of the vein-filling process. The microcline of the veinlet, like that of the bands, exhibits »grid» twinning but with less regular distribution than that of the microcline in the rock proper. A few, sporadic grains of the oligoclase in the veinlet are antiperthitic; contrariwise, none of the grains in the rock proper was seen to be either visibly or microscopically anti-

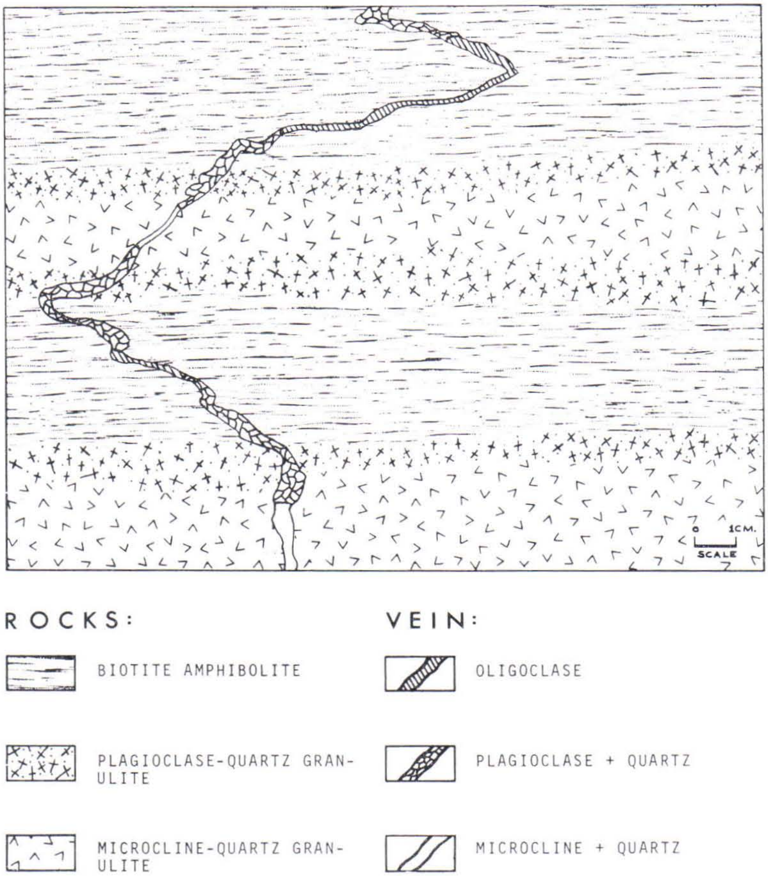

FIG. 1. Tracing of Banded Migmatite specimen from Southern Finland. (The symbol for the vein plagioclase should not be construed to imply that all of the vein plagioclase is of the same orientation; it is not.)

perthitic. Each of the portions of the veinlet contains the low melting constituents of one of the rocks constituting the banded host rock. *BUT*, the boundaries between the differently constituted parts of the veinlet do not coincide with the boundaries between the differently constituted bands of the host. The plagioclase-quartz segments of the veinlet extend farther into the chiefly hornblende-biotite-plagioclase bands than into the predominantly microcline-quartz bands.

DISCUSSION

So far as the subject of main concern in this paper, evaluation of diverse conjectures as to origin of the banding may be omitted. It is sufficient to state that the banding must have been established before formation of the veinlet. (The fact that the veinlet cuts across the dark, relatively well foliated bands at a nearly consistent and acute angle and across the light, only poorly foliated bands also at a nearly consistent but less acute angle appears to establish the fracturing, certainly pre-vein formation, as post-banding.)

The lack of correspondence of the compositional boundaries within the veinlet with those of the contiguous rock precludes the possibility that the vein minerals were deposited under overall substrate control. On the other hand, local derivation of the vein minerals is certainly indicated although not proved.

The distribution of the minerals within the veinlet indicates that: 1. the plagioclase-quartz composition fluid became mobile while the K-feldspar-quartz and the plagioclase composition, potential fluids were still immobile; 2. the fluid was rather viscous; and 3. later the K-feldspar-quartz composition fluid and still later the plagioclase composition fluid also gained mobility. This alternative of prior mobility, rather than greater but simultaneous mobility, of the plagioclase-quartz composition fluid as compared to the K-feldspar-quartz and the plagioclase composition fluids is considered applicable because the arrangement of constituents within the vein can be accounted for rather easily on the basis of sequential events, whereas if each of the three fluids had come into existence essentially simultaneously (even if with notable differences of fluidity) it would appear that the compositional boundaries of at least the border zones of the veinlet would correspond with the compositional boundaries within the contiguous host rock. A relatively high viscosity for at least the plagioclase-quartz composition fluid is indicated by the distribution of the plagioclase plus quartz portion of the vein — it would appear that had the fluid been of low viscosity essentially all, if not all, of the border zones of the entire vein would have been composed of plagioclase plus quartz. The later (albeit probably only slightly so) sequence of mobilization apparently involving first the mobilization of the K-feldspar-quartz composition fluid and subsequently the mobilization of the plagioclase composition fluid is indicated by the fact that the fluid from which the plagioclase and quartz portion of the vein was deposited encroached further into the plagioclase-rich bands than into the microcline-, quartz-rich bands. This indicated sequence would be that expected under the herein hypothesized — essentially isobaric, rising-temperature — conditions. The sequence, if correct, would strongly support the conclusion that the probably relatively highly viscous plagioclase-quartz fluid was formed as the result of melting and, thus, most probably was a local, anatectic magma. This, in turn, would support the further dependent conclusion that these relationships permit making of the geobarometric statement that this vein was formed at a pressure of greater than approximately 1.8 kilobars (see Figure 2).

This is true because, as has been shown by several laboratory experiments, the albite plus quartz liquidus crosses the orthoclase plus quartz liquidus at approximately 1.7 kilobars pressure and about 770°C. Of course, the oligoclase plus quartz liquidus would cross the orthoclase plus quartz liquidus at a higher pressure (but lower tem-

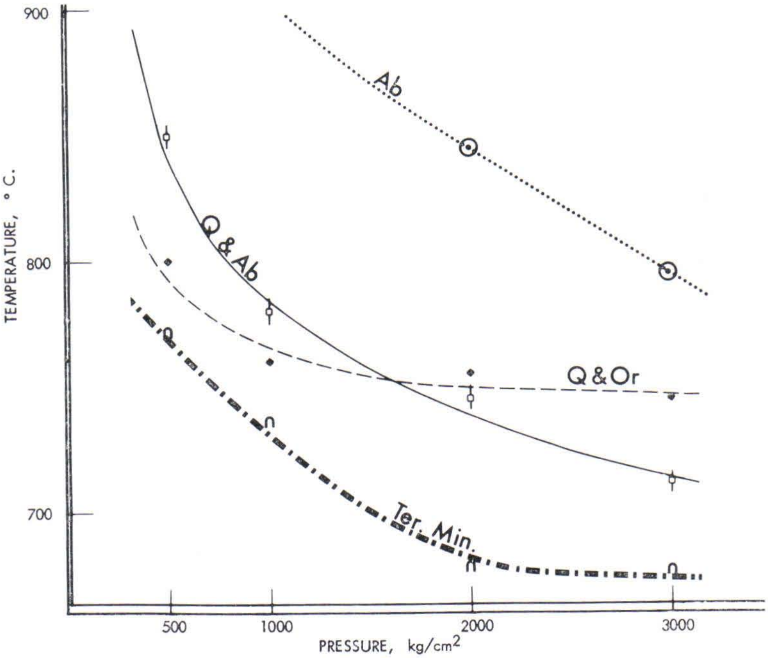

FIG. 2. Relationships of liquidus curves of quartz + albite (Q + Ab), quartz + K-feldspar (Q + Or), and the »ternary minimum» (Ter. Min.); after Tuttle and Bowen, 1958.

perature). The 1.8 kilobars figure is suggested for this specimen instead of the 1.7 kilobars figure to emphasize the fact that the oligoclase (An_{24-26}) plus quartz liquidus would cross the K-feldspar plus quartz liquidus at a higher pressure than the albite plus quartz liquidus does.

CONCLUSIONS

The features of the described specimen suggest that at the time its included veinlet was filled the rock was under pressure and temperature conditions that promoted earlier mobility of plagioclase plus quartz composition fluid than of either K-feldspar plus quartz composition fluid or plagioclase composition fluid. Rising temperature at some pressure of greater than approximately 1.8 kilobars would apparently fulfill the conditional requirements.

Careful search will certainly lead to the discovery of several rocks the low melting temperature phase of which would have either a K-feldspar or plagioclase plus quartz composition rather than the more common »ternary-minimum» composition. Those occurrences where K-feldspar-, quartz-rich rocks occur in juxtaposition with plagioclase-, quartz-rich rocks should be examined closely for features that may make possible a greater than, nearly equal to, or less than some single value pressure-of-formation statement.

It must always be kept in mind, however, that not only must there be juxtaposition of the two types of rock, but also the absence of a nearby rock containing both plagioclase and K-feldspar along with quartz. Such a rock would serve as a source for »ternary minimum» fluid which should fill both real and potential openings under lower temperature and pressure conditions thus precluding the events herein hypothesized. Also, mere movement of anatectic fluids of either plagioclase plus quartz (see, *e.g.*, Härme, 1962) or K-feldspar plus quartz composition (alone) within a rock can not be considered indicative of any condition other than a superliquidus one for the fluid which moved.

Perhaps the major loophole in applying these laboratory data to most occurrences is the necessary assumption that the mobile material was a melt. So far as the writer is aware, there are no definite data that show, for example, volatilization temperatures to have necessarily the same temperature order relationships as fusion temperatures.

Also problematic are questions such as what volatiles were present (?) and how would these have affected the temperature-pressure position of the pertinent intersection (?). The work of Wyllie and Tuttle (*e.g.*, 1961 and 1964) suggest that the effect could be noteworthy.

Furthermore, there is essentially no published data relating to viscosities of quasi-natural magmas and a dearth of data relating to viscosities of fluids of anything even approaching rock compositions (see, *e.g.*, Shaw, 1963). Such data are needed not only because they could add much to considerations of this type but also to petrogenetic considerations in general.

Therefore, present day observations of these kinds of features must be considered mainly as the recording of occurrences to be investigated more fully when more pertinent data become known. Then, they may become very important — particularly since there is a general lack of pressure-of-formation (or pressure-of-change, *inter alia)* information. For example, essentially all so-called geothermometers are pressure dependent. Such pressure information, if proved valid and well-defined, would permit much greater insight into considerations of several things like depth of formation. This is true not only because the pressure gradient of the crust of the earth is apparently better known than the geothermal gradient is, but also because for some rocks it may become possible to correlate the two gradients.

Manuscript received, September 1, 1966.

REFERENCES CITED

Dietrich, R. V., 1959, Development of ptygmatic features within a passive host during partial anatexis: Beitr. Min. u. Petr., v. 6, p. 357—366.

—»— 1960, Genesis of ptygmatic features: Int. Geol. Congr., XXI Sess., Norden, Pt. XIV, p. 138—148.

—»— 1966, Partial anatexis above and below approximately 1.7 kilobars (Abst.): Program Ann. Mtg. S.E.Sect. Geol. Soc. America, p. 23.

Dietrich, R. V. & Mehnert, 1960, Proposal for the nomenclature of migmatites and associated rocks: Int. Geol. Congr., XXI Sess., Norden, Pt. XXVI, Suppl. v., Sect. 1—21, p. 56—67.

Härme, Maunu, 1962, An example of anatexis: C. R. Soc. Géol. Finlande XXXVI, Bull. Comm. Géol. Finlande, No. 204, p. 113—125.

Shaw, H. R., 1963, Obsidian-H_2O viscosities at 1 000 and 2 000 bars in the temperature range 700° to 900° C: Jour. Geophysical Research, v. 68, p. 6337—6343.

Tuttle, O. F., 1952, Origin of the contrasting mineralogy of extrusive and plutonic salic rocks: Jour. Geol., v. 60, 00. 107—124.

Tuttle, O. F. & N. L. Bowen, 1958, Origin of granite in the light of experimental studies in the system $NaAlSi_3O_8$—$KAlSi_3O_8$—SiO_2—H_2O: Geol. Soc. America, Mem. 74, 153 p.

Wyllie, P. J. & Tuttle, O. F., 1961, Experimental investigation of silicate systems containing two volatile components. Part II. The effects of NH_3 and HF, in addition to H_2O on the melting temperatures of albite and granite: Am. Jour. Sci., v. 259, p. 128—143.

—»— 1964, Experimental investigation of silicate systems containing two volatile components. Part III. The effects of SO_3, P_2O_5, HCl, and Li_2O, in addition to H_2O on the melting temperature of albite and granite: Am. Jour. Sci., v. 262, pp. 930—939.

ADDENDUM

After the discovery of above described relationship, the ptygmatic vein pictured and figured in detail (Dietrich, 1959 and 1960, respectively) was reëxamined to see if it also could be cited as a possible example of this type of phenomenon. The specimen exhibits slight encroachment of the microcline plus quartz portions of the veins, that transect the compositional boundary of the host, into the vein segments within the rock that is composed chiefly of plagioclase plus quartz (and biotite). If the same hypothesis of origin fits this rock as appears to fit best the above described rock from southern Finland, this Northwestern Adirondack Province rock would appear to have been formed at pressures of less than approximately 1.7 kilobars. But, an additional point must be raised with regard to this rock — the microcline of the microcline plus quartz portion of these veins is markedly perthitic so the controlling conditions, as indicated by the liquidus curves, may have been those permitting formation of a »ternary minimum» composition fluid and then a quartz plus plagioclase composition fluid. If such were the case, the relationships within this rock could have been formed as the result of either rising temperature under essentially isobaric conditions or of rising pressure under essentially isothermal conditions *(etc.)* with *no* pressure value alternative within the temperature pressure range generally considered applicable to petrogenesis of »granitic» and similarly constituted migmatites.

R. V. D.

Comptes Rendus de la Société géologique de Finlande
N:o XXXIX (1967), pp. 11—16

REMARKS ON THE PAPER »A GEOBAROMETER FOR CERTAIN MIGMATITES» BY R. V. DIETRICH

BY

VLADI MARMO

Geological Survey of Finland, Otaniemi

In his paper, professor R. V. Dietrich makes an interesting approach to the petrology of migmatites. He starts from the laboratory data indicating that at pressures above approx. 1.7 kilobars, Na-rich plagioclase + quartz starts to melt at lower temperatures than K-feldspar + quartz, whereas at pressures of less than approx. 1.7 kilobars the reverse relationship occurs.

He presents a very careful and detailed investigation of a specimen from the collections of the U.S. National Museum, sent to the museum by J. J. Sederholm to illustrate the ptygmatic features. The only location given was »southern Finland».

On the basis of the examination of this single handspecimen, prof. R. V. Dietrich made, however, quite a generalization (p. 3): »A banded migmatite of southern Finland is described and concluded to exhibit features probably attributable to anatexis above approximately 1.8 kilobars.»

The migmatites of southern Finland are, in general, very inhomogeneous rocks especially as far as the paleosome is concerned. They may be composed of mica schists, mica gneiss, amphibolites of different origin, and also of equigranular quartz -and granodiorites, rarely also of rocks of granite composition, even if only a small area is concerned. Figs 1 to 3, for instance, represent an area (Otaniemi) 1 by 1 km in size. Figs 4 to 5, are taken from an outcrop at the airport of Helsinki (Seutula). The neosome, on the contrary, is mostly microcline-albite aplite also often forming homogeneous masses within the migmatites.

Furthermore, if the paleosome is amphibolite, the contacts with migmatite- forming aplite are always sharp (Fig. 4). Sometimes amphibolite occurs as fragments, and the migmatite is breccialike. If the paleosome is mica schist or mica gneiss, the contacts are often gradational or even diffuse (Fig. 3), the paleosome itself often being so rich in microcline that its composition is granitic.

FIG. 1. Migmatite with paleosome of amphibolite. Neosome to the right is aplite, at the hammer it is made up by coarse microcline with pockets, blebbs and veinlets of quartz. Otaniemi.

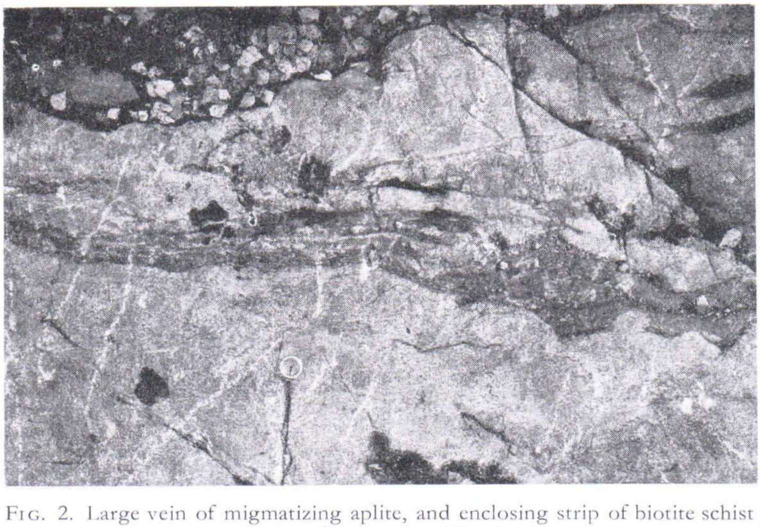

FIG. 2. Large vein of migmatizing aplite, and enclosing strip of biotite schist — restite of paleosome. Otaniemi.

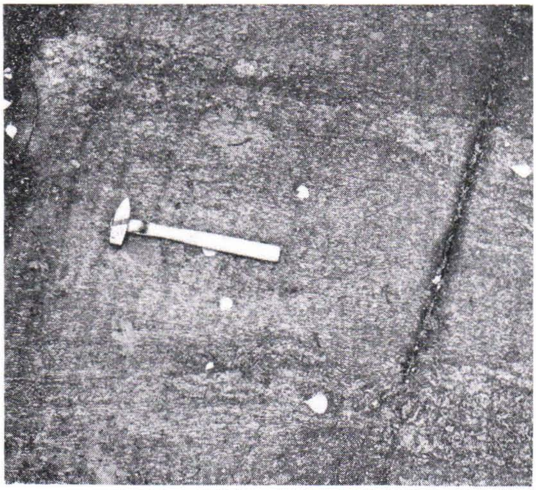

FIG. 3. Paleosome of mica gneiss containing microcline in abundance. Aplitic material forms neosome, but the margins are very diffuse. Otaniemi.

In his paper, prof. Dietrich is using the name granulite for the neosome of the specimen he describes. In Finland the name is not used at all in this sense, because the migmatizing material here, and also in Sweden, is predominantly aplite, rich in potassium. K-feldspar is invariably microcline of high triclinicity (0.9 to 1.0), and plagioclase is albite or acid oligoclase. Sometimes the neosome is coarse-grained, pegmatitic, or pegmatite. In Fig. 1, it consists only of coarse microcline with pockets and veinlets of quartz. True pegmatite, if occurring as neosome, may be made up solely of quartz.

The ptygmatic veins are not very characteristic of the migmatites of southern Finland. In the Otaniemi area they are occasionally present. At the airport (Fig. 5) they may be excellently developed.

Distribution of plagioclase + quartz and microcline + quartz, as illustrated by Dietrich may be found. Mostly, however, the migmatizing veins and patches are made up homogeneously of aplite (= microcline + albite + quartz).

Thus, generalization of observations based on one hand specimen for areas such as those occupied by the migmatites of southern Finland, is both dangerous and may be even misleading.

Some remarks must also be made concerning the actual discussion of prof. Dietrich, on the determination of the pressure conditions under which anatexis was produced.

According to Fig. 2 of the paper of Dietrich, his starting point is based on temperatures above roughly 650°C. Such temperatures are unexpected for the migmatites. Aplitic granites, if using feldspars as thermometers, give much lower temperatures —

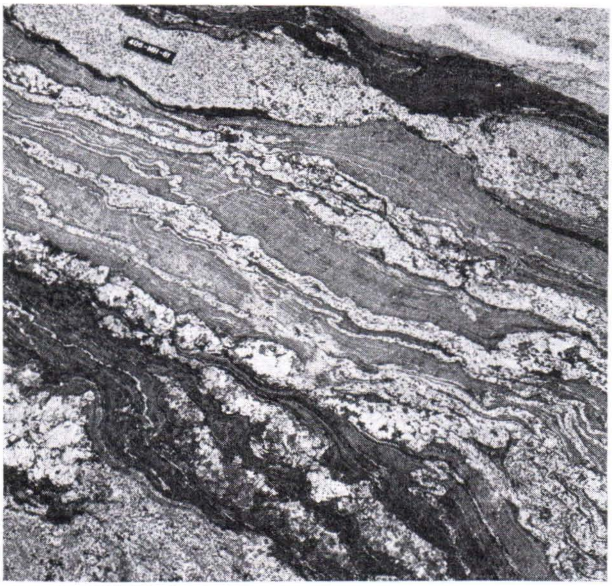

Fig. 4. Banded migmatite. Darkest strips of paleosome are biotite amphibolite; light gray is mica schist. The lightest gray is leptite. Neosome is pegmatitic (upper part), and aplitic. Seutula airport.

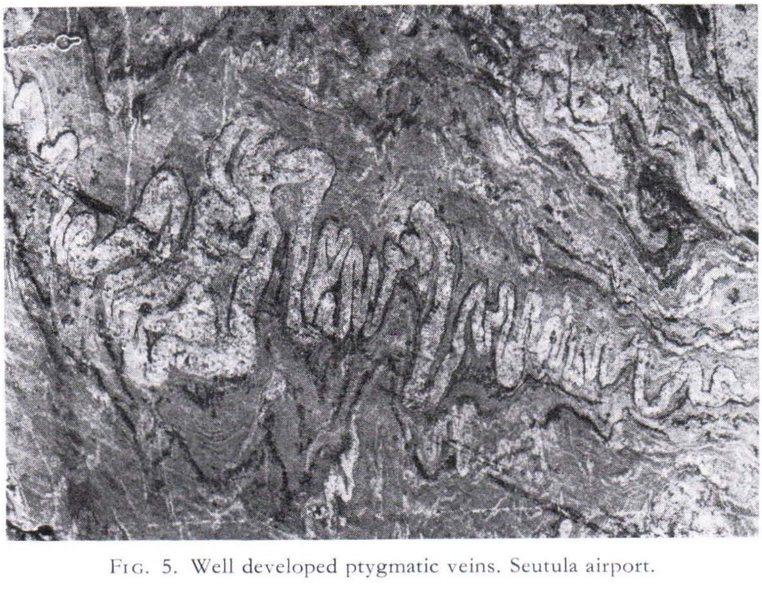

Fig. 5. Well developed ptygmatic veins. Seutula airport.

as low as 350°C. The high and constant triclinicity of microcline also indicates temperatures below 500°C. The modern opinions of granite petrologists are more inclined in favour of the hydrothermal emplacement of the migmatizing material, and also in favour of palingenesis, and still more of anatexis in the presence of water. On this model is also based the assumption of Walton (1960), who named it »Anatectic». For this model, Tuttle and Bowen (1958) have supplied much supporting material. According to Tuttle, in such rocks, which are rich in water, and correspond to granite in composition, the granite liquids must be important, because the stability field of granitic liquids extends into the PT-conditions prevailing at the depth of high-grade regional metamorphism. According to Walton (1960) a granite melt can already exist at roughly 650°C and at water-vapour pressure of about 2.000 kg cm^{-2}. At a still higher water-vapour pressure, the crystallization of two separate feldspars will be intensified, and at the same time the necessary temperature *decreases*. This result was supported by the experiments of Yoder, Stewart and Smith (1957) in the ternary feldspar-water system Ab—Or—An—H_2O. According to these, even low concentration in Ca-feldspar can cause the crystallization of separate K- and Na-feldspars at still lower water concentration.

It is also important to note here that the results mentioned above (Tuttle and Bowen) are based on the system $NaAlSi_3O_8$—$KAlSi_3O_8$—SiO_2—H_2O.

As a matter of fact, the »anatectic» model is close to the model set forth by Sederholm. The mechanism of them both works in principally the same way.

In his »hydrothermal model» the present author has paid still more attention to the importance of water, and thus could explain the formation of aplites at temperatures below 500°C.

Manuscript received, October 17, 1966.

REFERENCES

DIETRICH, R. V., 1967, A geobarometer for certain migmatites. C. R. Soc. géol. Finlande 39.

TUTTLE, C. F., BOWEN, N. L., 1958 Origin of granite in the light of experimental studies in the system $NaAlSi_3O_5$—$KAlSi_3O_8$—SiO_2—H_2O. Geol. Soc. Amer. Mem. N:o 74.

WALTON, MATT, 1960. Granite problems. Science, vol. 131, pp. 635—645.

YODER, H. S., STEWART, D. B., SMITH, J. R., System Ab—Or—An—H_2O. Carnegie Inst. Wash. Year Book N:o 56, p. 206.

REPLY

BY

R. V. DIETRICH

College of Arts and Sciences, Virginia Polytechnic Institute
Blacksburg, Virginia, U.S.A.

I believe that most of Dr. Marmo's points are covered sufficiently in the original note. Incidentally:

The described specimen was not, in my opinion, sent by Dr. Sederholm to illustrate ptygmatic features.

The term granulite was used in the paper strictly as a descriptive term to refer to the granular character of the unit.

No general significance of the reported relationships in this one hand specimen, so far as its possible bearing upon interpretations of geologic events in any large area, was stated or intended. Perhaps it would have been better to have said »A banded migmatite *specimen* from southern Finland is described and concluded to exhibit features *possibly* attributable to anatexis above approximately 1.8 kilobars.»

Comptes Rendus de la Société géologique de Finlande
N:o XXXIX (1967), pp. 17—28

IRON CONTENT OF MELILITE

BY

TH. G. SAHAMA

University of Helsinki, Finland

ABSTRACT

This paper presents a review of the analytical data available of rock forming melilite. The following statements may be made:

According to the mode of occurrence, melilite can be divided into three groups.

1. Contact metamorphic group. Composition covers virtually the entire åkermanite-gehlenite series, often with more or less predominating gehlenite component. The atomic ratio $Al/(Na + K)$ is a little or very much greater than 1 : 1. The contents of the alkali melilite and iron melilite components extend down to negligible.

2. Volcanic group. The atomic ratio of aluminum to the alkalies is usually almost 1 : 1 or, in a few analyzed specimens, aluminum shows a slight excess over this ratio. Accordingly, the alkali melilite component is quantitatively important and the gehlenite component proper plays just a minor or even a negligible role. The main variation in composition is found in the ratio of the åkermanite component to the iron åkermanite (iron gehlenite) component. The composition is conveniently illustrated in an Al-Fe-Mg diagram indicating the relative contents of alkali melilite (plus the small amount of gehlenite), iron åkermanite (plus iron gehlenite) and åkermanite.

3. Plutonic-subvolcanic group. This group seems to be intermediate between the two previous groups. Data available so far are, however, too scanty for any review.

Microprobe study of a number of zoned volcanic melilite specimens indicates that the zoning is not caused by a variation in åkermanite/alkali melilite (gehlenite) ratio but mainly by a variation in the Fe/Mg ratio. In this respect melilite is analogous to rock forming olivine, orthopyroxene etc.

There is no need to include an Al-free alkali melilite component in the list of natural melilite end members.

More data for the composition of rock forming melilite are highly desirable.

INTRODUCTION

It is, of course, just a formal matter to put up specific end members for complicated solid solutions like for many of the rock forming silicates. This principle is certainly valid also for the melilite group. It seems, however, that for natural melilite the range of variation of the chemical composition will be illustrated best on the basis of the end members.

The history of the study of the melilite group, with a discussion of the end members proposed in literature, has been thouroughly reviewed by Christie (1961 a and b; 1962 a and b) and will not be repeated here. Leaving aside the zinc- and beryllium-bearing silicates with melilite-type structure, the following end members of natural melilite can be established:

Åkermanite	$Ca_2MgSi_2O_7$
Iron åkermanite	$Ca_2FeSi_2O_7$
Gehlenite	$Ca_2Al_2SiO_7$
Iron gehlenite	$Ca_2Fe_2SiO_7$
Soda melilite	$CaNaAlSi_2O_7$

Of these compounds åkermanite is the only one to have been found pure or nearly so in Nature (Zambonini, 1910). Åkermanite and gehlenite have been synthesized long ago. Iron åkermanite was prepared by devitrifying glass at 700°C by Bowen, Schairer and Posnjak (1933). Synthetic iron gehlenite has been described by Nurse and Midgley (1953). Recently, Yoder (1964) has shown that soda melilite represents a stable compound at pressures above 4 kb. Its optical properties have been determined by Schairer, Yoder and Tilley (1965).

Most studies of the melilite group published in literature deal with the åkermanite-gehlenite series and pay little or no attention to the alkali and iron contents of the mineral. As has been remarked already by Winchell (1924), Berman (1929) and recently by Yoder (1964), Mittempergher (1965) and Edgar (1965), the soda melilite is known to be a constant component in the melilite of alkaline magmas and, accordingly, is of considerable petrological importance. The significant content of iron in many melilites is also well known and has been stressed by Sahama (1961).

The aim of this paper is to review the alkali and, especially, the iron content of melilite. It will be done partly on the basis of the chemical melilite analyses available and partly on the basis of electron microprobe study of the melilite zoning. The presentation of the melilite compositions in triangular diagrams is given in atomic percent.

MATERIALS

Table I summarizes the analyzed melilite specimens used in this paper. Most of the chemical analyses have been published in literature and will not be reproduced here. Only the analysis of melilite No. 17 is previously unpublished and is given in the table. No. 29 presents an unpublished microprobe analysis. Nos. 30—35 represent partial microprobe analyses of aluminum, iron and magnesium in zoned melilite phenocrysts. The results of these partial analyses are indicated in the diagrams of Figs. 3, 7 and 8. The microprobe work was done by the author using the »Geoscan» electron microprobe (Cambridge Instrument Co.) of the Geological Survey of Finland. A fairly large homogeneous phenocryst of melilite No. 13 served as a standard.

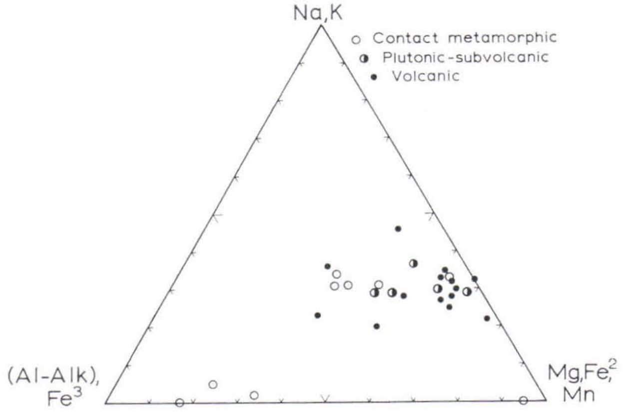

FIG. 1. Melilite specimens Nos. 1—28 of Table I plotted in a Na,K-(Al-alk),Fe^{III}-Mg,Fe^{II},Mn diagram. Illusrating the contents of alkali melilite, gehlenite (iron gehlenite) and åkermanite (iron åkermanite).

The mode of occurrence of rock forming melilite is essentially threefold. 1) The mineral is a characteristic constituent of high temperature contact metamorphic limestone or dolomite where it evidently represents a product of reaction between carbonates and silicates. Such a mode of occurrence, denoted in this paper as contact metamorphic, also includes the occurrence in calcareous blocks ejected by volcanoes. Of the melilite specimens listed in Table I, Nos. 1—9 belong to the group of contact metamorphic origin. 2) Melilite is a wide spread constituent in highly alkaline, silica deficient volcanic rocks where it must be considered as a crystallization product of the melt. In this paper, the latter mode of occurrence is denoted volcanic. Nos. 10—23 and 29—35 of Table I are representatives of the volcanic group. 3) Melilite specimens Nos. 24—28 of Table I are not contact metamorphic nor volcanic but represent the third group denoted plutonic-subvolcanic in this paper.

THE GEHLENITE COMPONENT

The conventional way of presenting melilite compositions diagrammatically is to plot the analyses in a soda melilite-gehlenite-åkermanite triangle adding the iron gehlenite component to gehlenite and the iron (manganese) åkermanite component to åkermanite. Fig. 1 presents such a plot. However, instead of the compounds $Ca(Na,K)AlSi_2O_7$, $Ca_2(Al,Fe)_2SiO_7$ and $Ca_2(Mg,Fe,Mn)Si_2O_7$, the cation sums $Na + K$, $(Al - alk) + Fe^{III}$ and $Mg + Fe^{II} + Mn$ were taken as coordinates. The use of the cations as coordinates was preferred because these coordinates can be calculated direct from the analytical data without having to account for a possible excess or deficiency of silica etc. over the ideal chemical formulas and, further, without having to consider any possible ordering or disordering in the occupation of the tetrahedral sites of the melilite structure by Al, Mg, Si etc.

Fig. 1 illustrates the remark made by Yoder (1964, p. 86) that 'a significant number of melilites plot near the middle portion of the soda melilite-åkermanite join, even though emphasis in the past has been directed toward the gehlenite-åkermanite join'. This statement holds true especially for the group of volcanic melilite whereas the contact metamorphic group extends down to the gehlenite-åkermanite join.

The iron (manganese) end members proper contain neither aluminum nor alkalies. Therefore, for a moment, we can forget about the iron (manganese) content of the melilite specimens used and plot the analyses referred to in Table I in the (Na, K)-Al-Mg triangle of Fig. 2. In this figure, only two of the analyzed melilite specimens, *viz.*, No. 12 (volcanic) and No. 27 (plutonic-subvolcanic), plot slightly above the dashed line which indicates a one-to-one ratio of aluminum to the alkalies. The analyses of these two melilites show an excess of the alkalies over aluminum. For melilite No. 12 it is not possible to decide whether this excess is real or just a result of analytical inaccuracy. The analysis of melilite No. 27 shows a low total and a very high P_2O_5 content indicating that the material was probably contaminated. Leaving these two exceptions aside, the figure illustrates the fact that volcanic melilite plots on or slightly below the dashed line. In the contact metamorphic melilite group, on the other hand, the excess of aluminum over the alkalies is more pronounced. The plutonic-subvolcanic melilite group seems to be intermediate between the volcanic and the contact metamorphic groups. Accordingly, in volcanic melilite, most of the aluminum content of the mineral is used up by the alkali melilite component and the gehlenite component proper plays actually a very minor role.

The fact that aluminum (with two exceptions) is in excess over the alkalies in natural melilite justifies the presentation of the melilite composition diagrammatically in an Al-Fe(Mn)-Mg triangle of Fig. 3. This figure illustrates the fact that the contact metamorphic melilite covers virtually the whole range of the Al-Mg join with mostly small contents of iron whereas the main variation in the composition of the volcanic melilite is found in the Fe/Mg ratio.

MELILITE ZONING

Volcanic melilite is commonly zoned. The melilite phenocrysts of volcanic rocks mostly show a narrow margin with a birefringence slightly higher than that of the crystal core. By using a rotating (elliptical) mica compensator (Sahama, 1959) the zoning can often be seen under the microscope even in crystals where no zoning can be detected without the compensator. The circularly polarized light produced by the compensator is extremely sensitive to minute changes in retardation and makes small variations in birefringence visible. In many cases the zoning is oscillatory with alter-

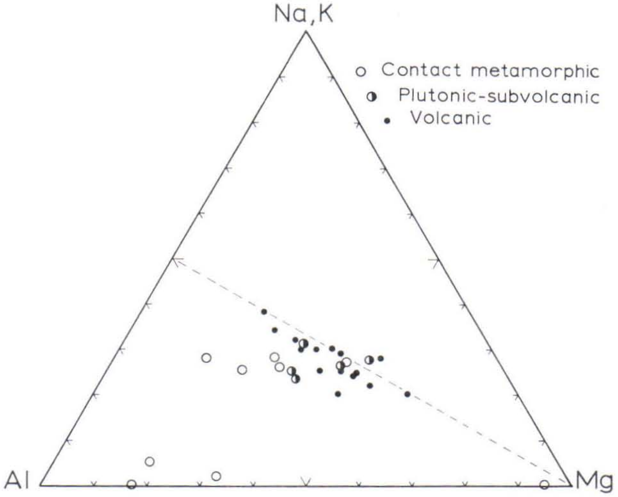

FIG. 2. Melilite specimens Nos. 1—29 of Table I plotted in a Na,K-Al-Mg diagram. Illustrating the excess of aluminum over the alkalies.

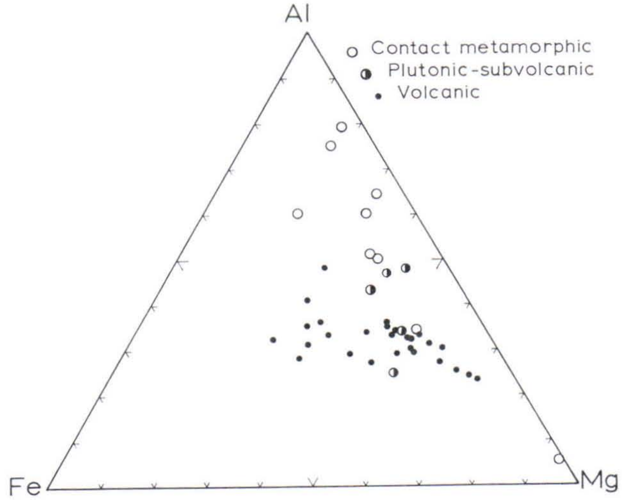

FIG. 3. Melilite specimens Nos. 1—35 of Table I (of specimens Nos. 30—35 core and margin separately) plotted in an Al-Fe(Mn)-Mg diagram.

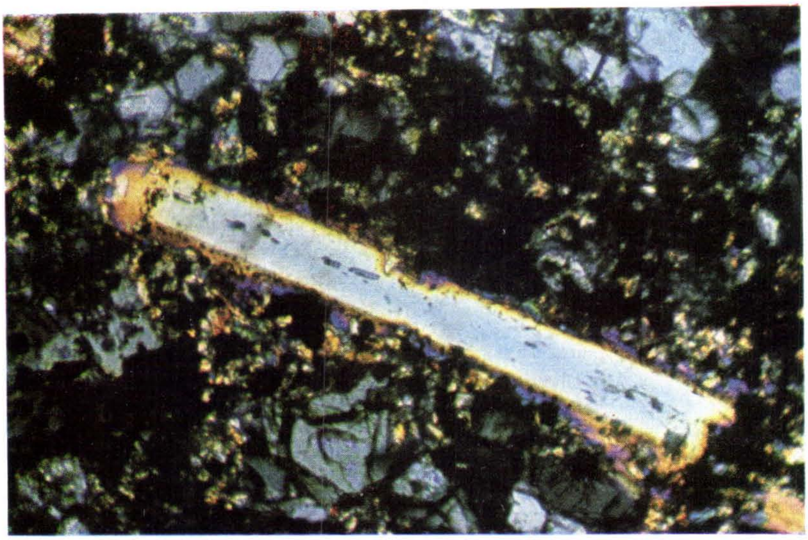

FIG. 4. Strongly zoned melilite phenocryst in melilite nephelinite lava. Mt. Nyiragongo (specimen VM 611), Congo. Magnification 200 x.

nating higher and weaker birefringent zones. Such an oscillatory zoning apparently reflects rhythmic changes in conditions of crystallization. The zoning is difficult to reproduce in a black-and-white print. Therefore, Fig. 4 illustrates in color a heavily zoned phenocryst. The change of optical retardation across the same phenocryst, measured with the Berek compensator, is illustrated in Fig. 5.

As has been shown by Sahama (1961), the exceptionally strong increase in birefringence towards the margins of the melilite phenocrysts in certain rocks of the Nyiragongo volcano is caused by an increase in iron content. To study the phenomen-

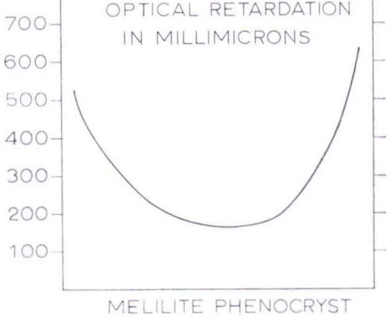

FIG. 5. Change of optical retardation across the melilite phenocryst of Fig. 4.

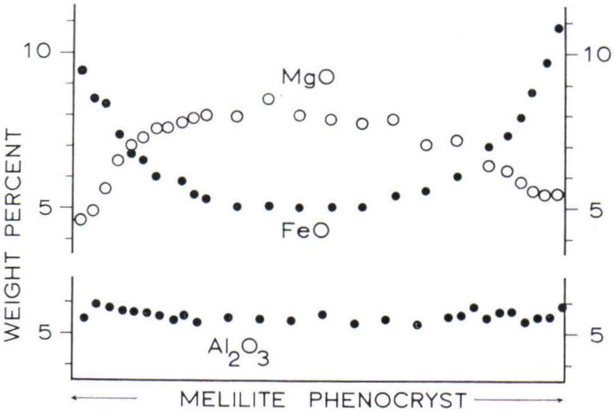

FIG. 6. Variation of the content of aluminum, iron and magnesium across the melilite phenocryst of Fig. 4.

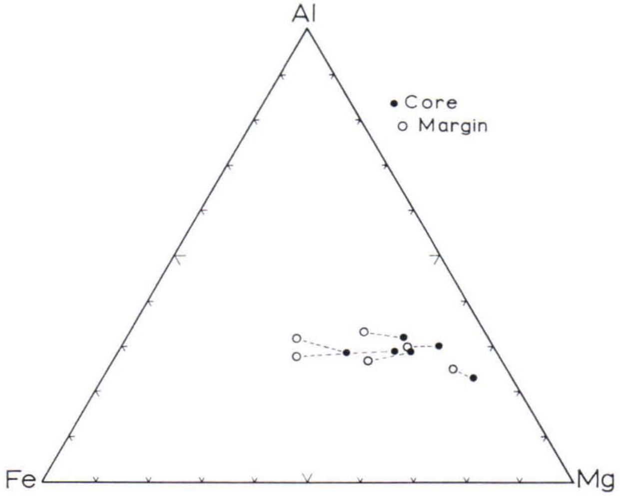

FIG. 7. Al : Fe : Mg ratio in the core and in the margin of a selected melilite phenocryst in specimens Nos. 30—35.

on further, a number of melilite phenocrysts of several volcanic rocks were analyzed with the electron microprobe. Fig. 6 reproduces the variation of FeO (total iron), MgO and Al_2O_3 across the zoned phenocryst of Fig. 4. Fig. 6 illustrates the fact that the FeO content increases and the MgO content decreases towards the margin of the crystal whereas the Al_2O_3 content remains virtually constant. To test the trend revealed by Fig. 6, partial analyses of Al, Fe and Mg were made with the mi-

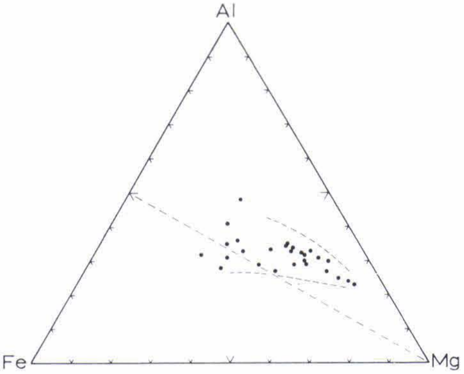

FIG. 8. Range of variation of the composition of volcanic melilite in an Al-Fe-Mg diagram.

croprobe of melilite specimens Nos. 30—35. The determinations of the core and of the margin of a selected phenocryst in each rock were carried out separately. The results of these determinations are summarized in Fig. 7. In this figure, the points indicating the composition of core and margin of the same crystal are connected with each other by a dashed line. The figure shows that the main difference in composition between core and margin is in the ratio of iron to magnesium and that the aluminum content remains nearly unchanged. Accordingly, the common zoning in volcanic melilite is not caused by a variation of the åkermanite-alkali melilite (gehlenite) ratio but mainly by the variation of the åkermanite-iron åkermanite (iron gehlenite) ratio. In this respect melilite is comparable with, *e.g.*, rock forming olivine, orthopyroxene etc. where the zoning is caused by the variation of the Fe/Mg ratio.

Further to illustrate the range of variation of the composition of volcanic melilite, all the points of Fig. 3 representing volcanic melilite are collected in Fig. 8. As is shown by this summary, the field covered by the volcanic melilite composition extends over a considerable range of the Fe/Mg ratio whereas the range of the Al/Fe ratio is more narrow.

Acknowledgments — The author is indebted to Mr. J. Siivola, M. A., of the Geological Survey of Finland, for helping with the microprobe work and to Mr. M. Lehtinen, M. A., of the University of Helsinki, for various assistance during the work.

Manuscript received, November 8, 1966

TABLE I. List of the analyzed melilite specimens which have been used in this paper.

No. 1. Melilite (åkermanite), Monte Somma, Italy. From calcareous block. Published by Zambonini (1910).

» 2. Melilite, Iron Hill, Colorado. From uncompahgrite. Published by Smith (1953), Neuvonen (1955) and Edgar (1965).

» 3. Melilite, Iron Hill, Colorado. From uncompahgrite. Published by Larsen (1942).

» 4. Melilite (gehlenite), Fassathal, Tyrol. Contact metamorphic. Published by Smith (1953), Neuvonen (1955) and Edgar (1965).

» 5. Melilite (gehlenite), Luna County, New Mexico. Contact metamorphic. Published by Neuvonen (1952, 1955), Smith (1953) and Edgar (1965).

» 6. Melilite, Albano, Latium, Italy. Contact metamorphic. Published by Tilley and Henry (1953).

» 7. Melilite, Scawt Hill, Co. Antrim, Ireland. Contact metamorphic. Published by Tilley (1929).

» 8. Melilite, Monte Somma, Italy. Average from three analyses. Contact metamorphic. Published by Bodländer (1893).

» 9. Melilite, Tulare County, California. Contact metamorphic. Published by Shannon (1922).

» 10. Melilite, Katunga Flow, Uganda. From katungite lava. Published by Neuvonen (1955, 1956) and Edgar (1965).

» 11. Melilite, Sugar Loaf Series, Honolulu, Hawaii. From melilitite lava. Published by Neuvonen (1952, 1955), Smith (1953) and Edgar (1965).

» 12. Melilite, Mt. Elgon, Uganda. From melilitite lava. Published by Smith (1953), Neuvonen (1955) and Edgar (1965).

» 13. Melilite, Kabfumu Flow (specimen FEAE 83), Mt. Nyiragongo, Congo. From melilitite lava. Published by Sahama and Meyer (1958).

» 14. Melilite, Mt. Nyiragongo (specimen VM 569), Congo. From melilitite lava. Published by Sahama (1961).

» 15. Melilite, Mt. Nyiragongo (specimen FEAE 93), Congo. From melilite nephelinite lava. Published by Sahama and Meyer (1958).

» 16. Melilite, Baruta crater (specimen S 96 = VM 355), Mt. Nyiragongo, Congo. From melilitite lava. Published by Sahama and Meyer (1958).

» 17. Melilite, Baruta crater (specimen VM 372), Mt. Nyiragongo, Congo. Unpublished chemical analysis by Mr. Pentti Ojanperä: SiO_2 42.73, TiO_2 0.15, Al_2O_3 6.97, Fe_2O_3 1.39, FeO 3.54, MnO 0.30, MgO 7.28, CaO 31.13, Na_2O 3.70, K_2O 0.63, CO_2 0.00, H_2O+ 2.08, H_2O- 0.10, total 100.00 (corrected for 2.20 % clinopyroxene admixture).

» 18. Melilite, Shaheru crater (specimen VM 391), Mt. Nyiragongo, Congo. From melilitite lava. Published by Sahama (1961).

» 19. Melilite, Mt. Nyiragongo (specimen RG 22778), Congo. From vesicles in melilitite lava. Published by Sahama (1961).

» 20. Melilite, Mt. Nyiragongo (specimen VS 217), Congo. From melilite nephelinite lava. Published by Sahama (1961).

» 21. Melilite, Capo di Bove, Italy. From leucite melilite lava. Average of the analyses I, III, IV and V compiled by Smith (1953).

» 22. Melilite, Hochbohl near Oven, Württemberg, Germany. From melilitite lava. Published by Stelzner (1883).

» 23. Melilite, Villa Senni, Italy. From nepheline melilitite lava. Published by Washington (1927).

» 24. Melilite, Turja, Kola, USSR. From turjaite. Published by Ramsay (1921).

» 25. Melilite, Oka, Quebec, Canada. Analysis No. 7 of Table V published by Edgar (1965).

» 26. Melilite, Oka, Quebec, Canada. Analysis No. 8 of Table V published by Edgar (1965).

» 27. Melilite, Oka, Quebec, Canada. Analysis No. 9 of Table V published by Edgar (1965).

No. 28. Melilite, Oka, Quebec, Canada. Analysis No. 10 of Table V published by Edgar (1965).

» 29. Melilite, Mt. Nyiragongo (specimen VM 611), Congo. Microprobe analysis by the author of a groudmass grain: SiO_2 42.4, Al_2O_3 6.2, FeO (total iron) 9.7, MgO 5.5, CaO 33.7, Na_2O 3.2, K_2O 0.3, total 101.0. From melilite nephelinite.

Microprobe determination of the ratio Al : Fe : Mg in the core and in the margin of a melilite phenocryst from the following lavas:

No. 30. Mt. Nyiragongo (specimen VM 611), Congo. Melilite nephelinite.

» 31. Tantalus Flow, Pauoa Valley, Honolulu, Hawaii. Melilitite.

» 32. Katunga Flow (specimen FEAE 39), Uganda. Katungite.

» 33. Baruta crater (specimen VM 362), Mt. Nyiragongo, Congo. Melilite nephelinite.

» 34. Mt. Nyiragongo (specimen VM 701), Congo. Melilite nephelinite.

» 35. Mt. Nyiragongo (specimen VM 707), Congo. Melilite nephelinite.

REFERENCES

BERMAN, HARRY (1929) Composition of the melilite group. Amer. Miner., vol. 14, p. 389.

BODLÄNDER, G. (1893) Die Zusammensetzung des Meliliths. N. Jahrb. f. Min. etc., Bd. I, S. 15.

BOWEN, N. L., SCHAIRER, J. F. and POSNJAK, E. (1933) The system, CaO—FeO—SiO_2. Am. Jour. Sci., vol. 26, p. 193.

CHRISTIE, OLAV H. J. (1961a) On sub-solidus relations of silicates. I. The lower breakdown temperature of the åkermanite gehlenite mixed crystal series at moderate water pressure. Norsk Geol. Tidskr., Bd. 41, p. 255.

CHRISTIE, OLAV H. J. (1961b) On sub-solidus relations of silicates. II. Preliminary note on the chemistry of melilites. Norsk Geol. Tidskr., Bd. 41, p. 322.

—»— (1962a) On sub-solidus relations of silicates. III. A contribution to the chemistry of melilites. Norsk Geol. Tidskr., Bd. 42, p. 1.

—»— (1962b) On sub-solidus relations of silicates. IV. The systems åkermanite-sodium gehlenite and gehlenite-sodium gehlenite. Norsk Geol. Tidskr., Bd. 42, p. 31.

EDGAR, A. D. (1965) Lattice parameters of melilite solid solutions and a reconnaissance of phase relations in the system $Ca_2Al_2SiO_7$ (gehlenite)-$Ca_2MgSi_2O_7$ (åkermanite)-$NaCaAlSi_2O_7$ (soda melilite) at 1 000 kg/cm^2 water vapor pressure. Canadian Jour. of Earth Sciences, vol. 2, p. 596.

LARSEN, ESPER S. (1942) Alkalic rocks of Iron Hill, Gunnison County, Colorado. U. S. Geol. Surv. Prof. Paper, 197 A.

MITTEMPERGHER, MARIO (1965) Vulcanismo e petrogenesi nella zona di San Venanzo (Umbria). Atti della Soc. Tosc. Sc. Nat., Serie A, vol. LXXII, p. 437.

NEUVONEN, K. J. (1952) Thermochemical investigation of the åkermanite-gehlenite seiries. Bull. Comm. géol. Finlande, No. 158.

NEUVONEN, K. J. (1955) On the composition of natural melilites. C. R. Soc. géol. Finlande. No. 28, p. 13.

NEUVONEN, K. J. (1956) Minerals of the katungite flow. C. R. Soc. géol. Finlande, No. 29, p. 1.

NURSE, R. W. and MIDGLEY, H. G. (1953) Studies on the melilite solid solutions. Jour. Iron Steel Inst., vol. 174, p. 121.

RAMSAY, W. (1921) En melilitförande djupbergart från Turja på sydsidan av Kolahalvön. Geol. För. Stockholm Förh., Bd. 48, p. 488.

SAHAMA, TH. G. and MEYER, A. (1958) Study of the volcano Nyiragongo, A progress report. Inst. des Parcs Nationaux du Congo Belge, Mission d'Etudes Vulcanologiques, Fasc. 2.

SAHAMA, TH. G. (1959) Detection of zoning in orthorhombic and uniaxial colorless minerals. Amer. Miner., vol. 44, p. 1303.

SAHAMA, TH. G. (1961) Thermal metamorphism of the volcanic rocks of Mt. Nyiragongo (Eastern Congo). C. R. Soc. géol. Finlande. No. 33, p. 151.

SCHAIRER, J. F., YODER, H. S. and TILLEY, C. E. (1965) Behavior of melilites in the join gehlenite-soda melilite-åkermanite. Carnegie Inst. Wash. Year Book 64, p. 95.

SHANNON, EARL V. (1922) Velardenite from a new locality in Tulare County, California. Proc. U. S. National Museum, vol. 60, No. 2417.

SMITH, J. V. (1953) Reexamination of the crystal structure of melilite. Amer. Miner., vol. 38, p. 643.

Stelzner, Alfred (1883) Melilith und Melilithbasalte. N. Jahr. f. Min. etc., B.-B., II, S. 399.

Tilley, C. E. (1929) On melilite as a product of interaction of limestone and basaltic liquid. Geol. Mag., vol. 66, p. 347.

Tilley, C. E. and Henry, N. F. M. (1953) Latiumite (sulphatic potassium-calcium-aluminium silicate), a new mineral from Albano, Latium, Italy. Min. Mag., vol. 30, p. 39.

Washington, H. S. (1927) The italite locality of Villa Senni. Am. Jour. Sci., vol. 14, p. 173.

Winchell, A. N. (1924) The composition of melilite. Am. Jour. Sci. Fifth Series, vol. VIII, p. 375.

Yoder, H. S. (1964) Soda melilite. Carnegie Inst. Wash. Year Book 63, p. 86.

Zambonini, F. (1910). Mineralogia Vesuviana. Napoli 1910.

Comptes Rendus de la Société géologique de Finlande
N:o XXXIX (1967), pp. 29—40

INFRARED ABSORPTION OF MELILITE

BY

TH. G. SAHAMA and MARTTI LEHTINEN

University of Helsinki, Finland

ABSTRACT

Infrared absorption spectra of a number of synthetic and analyzed natural melilite samples were recorded with a Leitz spectrophotometer in the wavelength range from 1 to 24 microns and illustrated in the range from 8 to 24 microns in Figs. 1—3. The absorption spectra of the pure crystalline end members åkermanite, soda melilite and gehlenite are compared with each other. With respect to their chemical composition the specimens of natural melilite studied are subdivided into two groups. In the first group (two specimens) the content of the gehlenite component is high whereas in the second group (eleven specimens) the content of the gehlenite component is low and that of the alkali melilite component is considerable. The infrared absorption shown by these two melilite groups differs from each other. In accordance with the chemical composition calculable from the analysis, it is concluded that, in the second melilite group, Al substitutes mainly for Mg in the tetrahedral sites No. 1 of Smith's notation. No evidence for an order-disorder transition in the occupation of the tetrahedral sites of the structure could be traced.

INTRODUCTION*

The determination of the crystal structure of melilite dates back to relatively early days. The crystal structure of a natural melilite from Capo di Bove was published by Warren (1930) and, simultaneously, that of a synthetic gehlenite by Raaz (1930). Since then, these two studies have served as standards for the crystal structure of rock forming melilite until Smith (1953) carried out a refinement on the Capo di Bove material using more accurate modern methods.

On the basis of chemical data for the composition of natural rock forming melilite, the melilite group has been taken as a representative of the silicates with Si_2O_7 or $(Al,Si)_2O_7$ groups (sorosilicates). However, the melilite structure consists of sheets of MgO_4 and SiO_4 tetrahedra in åkermanite and of AlO_4 and SiO_4 tetrahedra in

---

* Many of the references mentioned in a previous paper (Sahama, 1967) will not be repeated here. The reader is referred to that paper.

gehlenite. These sheets, lying parallel to 001, contain 5-sided rings of tetrahedra and are held together by calcium atoms in an 8-fold coordination, approximating the square Archimedean antiprism. Accordingly, there are no separate Si_2O_7 (åkermanite) nor $(Al,Si)_2O_7$ (gehlenite) groups in the structure but, as pointed out by Smith *(op. cit.)*, the distribution of Mg, Al and Si among the tetrahedral sites in the åkermanite and gehlenite structures are better regarded as a phenomenon of ordering. The melilite structure is essentially a sheet structure and can be classified as belonging to the phyllosilicates. This was actually done by Hugo Strunz in the first (1941) and second (1949) editions of his »Mineralogische Tabellen».

According to Smith *(op. cit.)*, the six tetrahedra contained in the melilite unit cell are not equivalent. Two of the tetrahedra (numbered 1) are large with a metal-oxygen distance $1.87_6 \pm 0.01_5$ Å whereas the four remaining tetrahedra (numbered 2 and 3) are equivalent and show an average metal-oxygen distance of $1.63_3 \pm 0.01_1$ Å. If extreme ordering is considered, the following occupations of the tetrahedral sites are possible:

	In åkermanite	In gehlenite	
		a)	b)
Tetrahedron No. 1	Mg	Al	Si
No. 2	Si	Al	Al
No. 3	Si	Si	Al

Because a substitution of Al for Si is known in many silicates and, on the other hand, the substitution of Si for Mg or *vice versa* in tetrahedral coordination is not known in other silicates, the alternative marked *a)* seems more probable for gehlenite. Considering the fact that the Capo di Bave melilite, served as material for crystal structure determination, in respect of its chemical composition, represents a complex solid solution, it is evident that a part of the Al atoms must occupy the tetrahedral positions No. 1 substituting for Mg. If extreme ordering is assumed, only a smaller part of Al will substitute for Si in tetrahedral positions Nos. 2—3.

The crystal structure of the soda melilite component $CaNaAlSi_2O_7$ has not been studied so far. This component is not stable at pressures below 4 kb and, consequently, studies of solid solutions of soda melilite with åkermanite and gehlenite have not been extended to compositions of more than 50 % by weight of the soda melilite component (Edgar, 1965). In view of the fact that, in the composition ranges $Åk_{100}SM_0$-$Åk_{50}SM_{50}$ and $Ge_{100}SM_0$-$Ge_{50}SM_{50}$, the unit cell dimensions vary linearly with the Åk/SM and Ge/SM ratios, respectively, it is most probable that, again assuming ordering, Al in soda melilite occupies tetrahedral positions No. 1 substituting for Mg of åkermanite, and Si occupies tetrahedral positions Nos. 2—3 as in åkermanite.

Published chemical analyses of melilite from volcanic rocks show constantly significant amounts of alkalies indicating that the alkali melilite component plays an important role. The atomic ratio of Al to the alkalies is for the most part nearly 1 : 1

or exceeds this ratio only slightly. Accordingly, in volcanic melilite, the content of the gehlenite component proper is low or negligible. In contact metamorphic melilite, on the other hand, the alkali contents are often low and the Al contents high, indicating that the gehlenite component is quantitatively important or even predominating.

The actual existence of a possible order-disorder transition in melilite has not been tested by X-ray crystal structure analysis. The fact that the structure of the Capo di Bove melilite contains tetrahedra of two different sizes, indicates a high order in the distribution of Mg, Al and Si among the tetrahedral sites. The Capo di Bove melilite which occurs in a leucite melilite lava is the only one of which accurate single crystal X-ray data are available.

The considerable content of alkali melilite in all analyzed volcanic melilite specimens makes the problem of ordering complicated. In addition to the Mg-Si order-disorder, there arises the question of the distribution of Al among the tetrahedral sites. Theoretically, it should be possible to bring some evidence to the problem by means of infrared absorption spectroscopy. Therefore, the infrared absorption of a number of natural and synthetic melilite specimens was studied. The results obtained are reported in this paper.

Unfortunately, at the present stage of knowledge, most of the frequences of the absorption bands found cannot be assigned to vibrations of specific bonds in the structure. For that reason, the absorption spectra recorded were interpreted in an entirely empirical way. The interpretation was greatly facilitated by the fact that pure synthetic preparations of the åkermanite, gehlenite and soda melilite components were available.

MATERIALS

For this investigation both synthetic and natural melilite materials were available.

The synthetic materials consist of the pure åkermanite and gehlenite end members and, in addition, of solid solutions of these end members with the molecular compositions $\text{Åk}_{74}\text{Ge}_{26}$, $\text{Åk}_{50}\text{Ge}_{50}$ and $\text{Åk}_{25}\text{Ge}_{75}$, all in both crystalline and glassy states. These materials represent batches of original samples prepared and used by Neuvonen (1952). Because the preparation of these samples has been fully described by him, the reader is referred to that paper. The synthetic soda melilite end member used in this paper was kindly prepared by Hatten S. Yoder, of the Geophysical Laboratory. According to personal communication delivered by him, the material was prepared by devitrifying glass of soda melilite composition at 10 kb pressure and at a temperature of 1 150°C. The annealing time was 70 hours. The crystalline soda melilite content of the sample was ca. 95 %, the rest consisting of some residual glass and wollastonite.

TABLE I.

List of the melilite specimens used in this paper

No	Locality	Mode of occurrence	Åkermanite	Iron åkermanite	Gehlenite	Iron gehlenite	Alkali melilite
			Molecular percent				
2	Iron Hill, Colorado	Uncompahgrite	54	10	1	2	33
4	Fassathal, Tyrol	Contact metamorphic	27	8	55	2	8
5	Luna County, New Mexico	Contact metamorphic	46	3	46	2	3
10	Katunga Flow, Uganda	Lava	69	9	2	—	20
11	Sugar Loaf Series, Honolulu, Hawaii	Lava	50	12	—	3	35
12	Elgon, Uganda	Lava	60	11	—	—	29
13	Kabfumu Flow, (FEAE 83), Nyiragongo, Congo	Lava	56	12	3	1	28
14	Nyiragongo, (VM 569), Congo	Lava	60	9	3	2	26
15	Nyiragongo, (FEAE 93), Congo	Lava	52	14	4	1	29
16	Baruta crater, (S 96 = VM 355), Nyiragongo, Congo	Lava	58	2	2	7	31
17	Baruta crater, (VM 372), Nyiragongo, Congo	Lava	48	14	1	2	35
19	Nyiragongo, (RG 22778), Congo	Vesicles in lava	35	31	3	—	31
20	Nyiragongo, (VS 217), Congo	Lava	34	5	3	16	42

The natural melilite samples used in this paper are listed in Table I. All samples represent batches of the purified mineral powders which have been chemically analyzed. The numbering of the specimens indicated in the first column of the table is the same as used by Sahama (1967, Table I). Table I of this paper lists also the mode of occurrence and the molecular composition calculated from the analysis.

EXPERIMENTAL PROCEDURE

For recording the infrared absorption spectrum the KBr pressed pellet technique was employed. The preparation of the samples was done in the way described by Sahama (1965) except that the grain size of the melilite materials used in the pellet was less than 1 micron. The spectra were recorded with a Leitz double beam infrared spectrophotometer with both sodium chloride and potassium bromide optics. Thus, the wavelength range covered by the spectra extends from 1 micron to 24 microns. However, because no significant bands were found in the range below 8 microns, the figures presented in this paper illustrate the tracings obtained in the range from 8 to 24 microns (1 250—417 cm^{-1}). The instrumental settings were the same as those

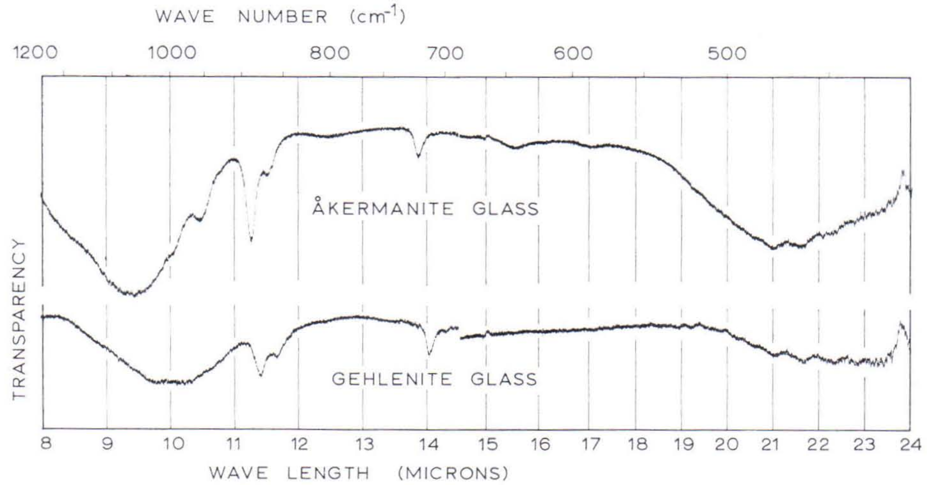

FIG. 1. Spectrophotometer tracings illustrating the infrared absorption of synthetic åkermanite and gehlenite glasses.

given earlier (Sahama, *op. cit.*) except that the slit program 3 was used instead of 5. This somewhat wider slit was found to give a satisfactory resolution. The wavelength range of highest transparency, *viz.*, around 4 microns, was adjusted to correspond approximately to 95 % on the chart.

Because most of the bands recorded are more or less broad, their wavelengths cannot be given with an accuracy better than ± 0.05 microns. For the very broad bands the accuracy will be ± 0.1—0.2 microns.

SYNTHETIC GLASSES

The spectrophotometer tracings illustrating the infrared absorption of synthetic åkermanite and gehlenite glasses are reproduced in Fig. 1. The glassy solid solutions Åk$_{74}$Ge$_{26}$, Åk$_{50}$Ge$_{50}$ and Åk$_{25}$Ge$_{75}$ were also recorded. The tracings are, however, not included in the figure.

A comparison of the tracings of the pure åkermanite and gehlenite glasses with those of the glassy solid solutions reveals the fact that the åkermanite glass bands shift regularly with the glass composition to the positions of the gehlenite glass bands. The broad åkermanite glass band centered at 9.4 μ shifts to the broad gehlenite glass band centered at 10.0 μ; the weak Åk$_{\rm gl}$ band at 10.4_5 μ is not produced by any of the glassy solid solutions nor by the pure gehlenite glass; Åk$_{\rm gl}$ band at 11.2_6 μ shifts to Ge$_{\rm gl}$ band at 11.40 μ; Åk$_{\rm gl}$ band at 13.8_7 μ shifts to Ge$_{\rm gl}$ band at 14.0_3 μ; the tracing of the broad band group of Åk$_{\rm gl}$ at 21—24 μ attains gradually that of

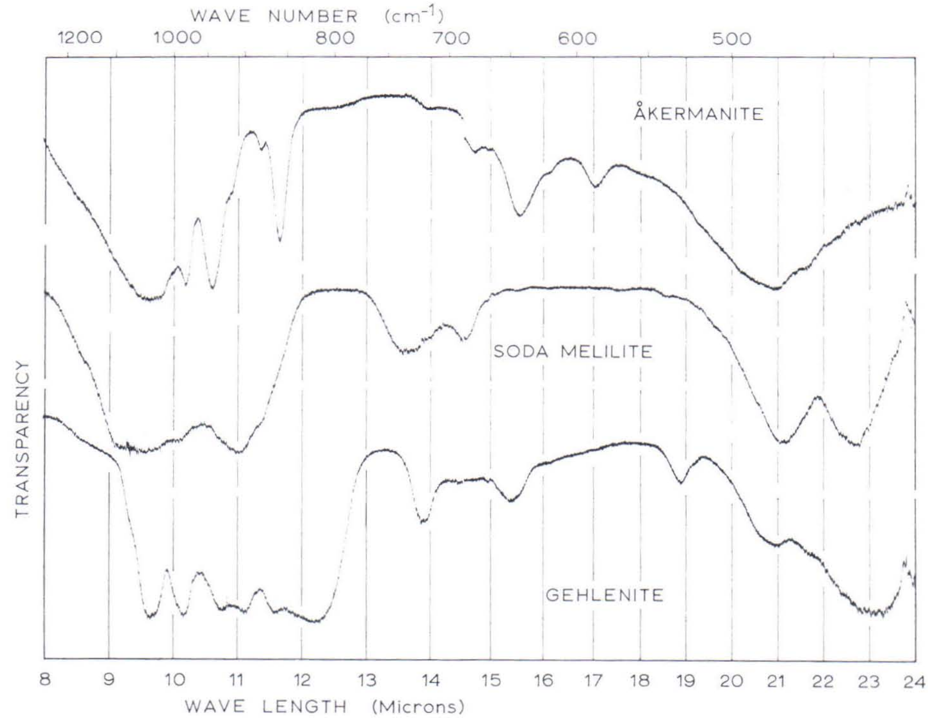

FIG. 2. Spectrophotometer tracings illustrating the infrared absorption of the synthetic crystalline åkermanite, soda melilite and gehlenite end members.

Ge_{gl}. This relationship between the bands of the åkermanite and gehlenite glasses, evidenced by the absorption of the intermediate solid solutions, is apparently a result of an environmental influence upon the vibration frequency of a particular bond.

SYNTHETIC CRYSTALLINE MELILITES

The spectrophotometer tracings illustrating the infrared absorption of the åkermanite, soda melilite and gehlenite end members are reproduced in Fig. 2. The infrared absorption spectra of the crystalline solid solutions $Åk_{74}Ge_{26}$, $Åk_{50}Ge_{50}$ and $Åk_{25}Ge_{75}$ were also recorded. However, the tracings of these solid solutions are not included in the figure.

The infrared absorption spectra of the pure melilite end members as indicated in Fig. 2 have not been previously given in literature. Keller *et al.* (1952) illustrate the infrared absorption of a number of different minerals including a melilite from Iron Hill, Colorado. A melilite specimen from the same locality was studied by Neuvonen (1955) and its molecular composition, calculated from the chemical analysis, is indicated in Table I, No. 2. In his extensive collection of data for infrared absorption of minerals, Moenke (1962—1966) * includes a »melilite» from Vesuvius and a »gehlenite» from Monzoni. He indicates the melilite from Vesuvius as representing a solid solution. The gehlenite from Monzoni comes from the locality in Fassathal described originally by Weinschenk (1897). A melilite specimen from the same locality has also been studied by Neuvonen (1955). The molecular composition of the mineral, on the basis of Neuvonen's analysis, is listed in Table I, No. 4. Although the gehlenite component predominates in the mineral, its composition is not near to that of the gehlenite end member. Because no melilites with a composition of any of the pure end members are known in Nature, the following discussion will be based entirely on the infrared absorption of the synthetic materials available to this study.

Because it is not possible to reproduce the original spectrometer tracings in such a way as to permit accurate wavelength measurements on the printed figure, the wavelengths and the rough intensities of the bands appearing in Fig. 2 are listed in Table II **. As is seen from the table, the absorption bands of åkermanite, soda melilite and gehlenite, marked with the same number, differ slightly in their wavelengths from each other. The correlation of the åkermanite bands with those of gehlenite was made on the basis of the infrared spectra obtained for the crystalline solid solutions. In the spectra of these solid solutions a regular shift from the positions of the åkermanite bands to those of the gehlenite bands was observed. The slight differences in wavelengths, found between the bands of the three melilite components marked with the same numbers in Table II, are apparently caused by environmental influence upon the vibration frequency of a particular bond.

The infrared absorption spectra of all silicates show a strong band group in the wavelength range from approximately 8 to 12 microns. It is generally inferred that this band group corresponds to stretching vibrations of the silicon-oxygen bonds. In the absorption spectra of the three melilite components of Fig. 2 this band group is represented by Nos. 1—6 of Table II. The complex character of the band group is well understood on the basis of the discussion presented by Lazarev (1960) concerning the possibilities of band splitting when passing over from single SiO_4 tetrahedra to

---

* The first part of Moenke's data sheets was published in 1962 and the second part, representing an extension of the data, in 1966. Because the two parts form a coherent collection, they are cited together in this paper.

** As was remarked in connection with the description of the materials used in this study, the material for the synthetic soda melilite contains some 5 % residual glass and wollastonite. To test whether wollastonite absorption bands produced by this impurity have affected the infrared absorption spectrum of soda melilite shown in Fig. 2, the infrared spectrum of the original wollastonite material from Lammala, Westanfjärd in Finland, studied by Simonen (1953) was recorded. The tracing obtained shows a very strong absorption band at ca. 10.9 microns coinciding with the very strong soda melilite band No. 4 (Table II) and another very strong wollastonite band at 21.0—21.1 microns coinciding with the very strong soda melilite band No. 13 (Table II). Therefore, another potassium bromide pellet was made that contained only 0.3 mg of the same wollastonite instead of 3.0 mg as normally used. The infrared spectrum obtained from this highly diluted wollastonite pellet showed only very weakly the two wollastonite absorption bands mentioned. Accordingly, it is concluded that the wollastonite bands produced by the impurity are too weak to have affected significantly the shape of the tracing obtained from the soda melilite.

TABLE II.

Principal infrared absorption bands of the crystalline synthetic melilite materials. Wavelengths given in microns; vs = very strong; s = strong; m = medium; w = weak; vw = very weak

Band No	Åkermanite		Soda melilite		Gehlenite	
1	9.5—9.8	vs	9.1—9.8	vs	9.6_5	vs
2	10.1_8	vs	10.1	vs	10.1_6	vs
3	10.6_0	vs	—		10.7_5	vs
4	—		11.0	vs	11.1_3	vs
5	11.6_4	s	—		11.5_7	vs
6	—		—		12.1—12.3	vs
7	—		13.6—13.7	m	—	
8	13.9_5	vw	—		13.9_0	m
9	14.7	vw	14.5_5	w	—	
10	15.5_5	m	—		15.4	w
11	17.0_4	w	—		—	
12	—		—		18.9_0	w
13	20.8—21.1	vs	21.0—21.2	vs	20.9—21.1	w
14	—		22.6—22.8	vs	22.9—23.3	vs

Si_2O_7 groups. A further reason for the complexity is evidently the fact that the tetrahedral positions in the melilite structure are partly occupied by atoms other than Si and, in addition, possibly because the oxygen atoms occupying the apexes of the tetrahedra show three non-equivalent positions. With respect to this band group, the three melilite components of Fig. 2 are distinctly different from each other. The most striking difference is the occurrence of the strong band No. 6 (Table II) in the gehlenite spectrum. This band is absent in the spectra of åkermanite and soda melilite. If ordering is assumed, gehlenite is the only one of the three melilite components in which half of the Al atoms occupy tetrahedral sites Nos. 2—3. It is a well established fact that the substitution of Al for Si in tectosilicates shifts the strong absorption band centered about 9.0 to 9.5 microns toward slightly longer wavelengths. This fact, mentioned by Keller *et al.* (1952), has been discussed particularly by Milkey (1960). Using the expression for the force constant of tetrahedral AB_4 groups derived by Gorky (1946), the wavelength shift resulting from an Al-Si substitution was calculated by Milkey and was found to correspond to the order of magnitude of the shift actually observed in tectosilicates. If the same principle is extended to the $AlSiO_7$ groups of the ordered gehlenite structure (tetrahedra Nos. 2—3 in Smith's notation), a shift similar to that for tectosilicates can be expected. Band No. 6 (Table II), reflecting the presence of the gehlenite component proper, could thus be regarded as an indication of an Al-Si substitution in the tetrahedral positions Nos. 2—3. * In the synthetic åkermanite-gehlenite solid solutions studied

---

* In the infrared absorption spectra of some aluminum-bearing silicates (not including any of the melilite components) Kolesova (1959) has constantly found a band in the wavelength range of 12.8—13.9 microns (780—720 cm^{-1}) and has drawn the general conclusion that this band arises from vibration of the covalent Al-O bond irrespective of the coordination of aluminum. Actually, the soda melilite and gehlenite spectra do contain a band of medium intensity within that range (No. 7 and No. 8 in Table II, respectively). In åkermanite, with no aluminum content, the band No. 8 is also present although its intensity is very low.

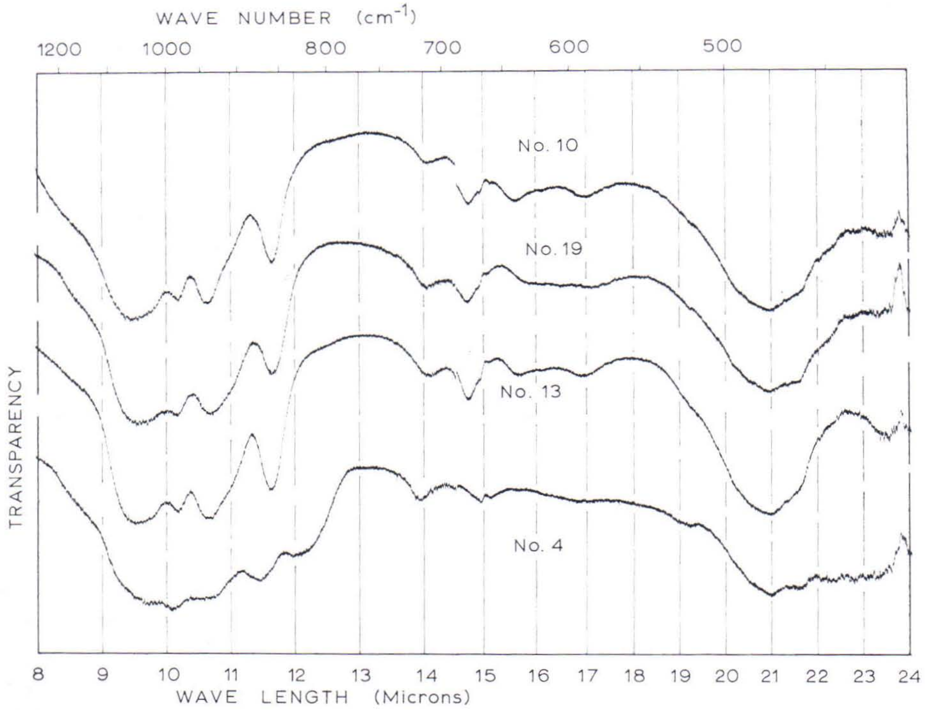

FIG. 3. Spectrophotometer tracings illustrating the infrared absorption of natural melilite. The numbers indicated in the figure correspond to the numbering of specimens in Table I.

the band No. 6 is still clearly but weakly visible in the preparation $Åk_{74}Ge_{26}$. Accordingly, the lower limit of detection of the gehlenite component by means of band No. 6 is roughly 20 mol. % gehlenite.

In the spectra of the three melilite components of Fig. 2 another strong group of bands occurs in the wavelength range from 21 to 23 microns, represented by Nos. 13—14 in Table II. This band group is distinctive for each of the three melilite components. The same applies to the weaker bands in the range between 13 and 20 microns (Nos. 7—12 in Table II).

NATURAL MELILITES

The infrared absorption spectra of all natural melilite specimens listed in Table I were recorded with the spectrophotometer. Four examples of the tracings obtained are illustrated in Fig. 3. The numbering of the tracings in the figure corresponds to the specimen numbers mentioned in Table I.

As is revealed by the data of Table I, all natural melilite specimens studied represent solid solutions. Expectedly, the absorption spectrum of such a solid solution will be intermediate between those of the pure end members. The bands which are common to the end members will retain their intensity in the spectrum of the solid solution. Those bands, on the other hand, which are specific to only one of the end members will appear weak or will vanish entirely depending on the content of that end member. As a consequence, the medium to weak bands appearing in the wavelength range from 13 to 20 microns of the melilite spectrum (Nos. 7—12 in Table II) are less suitable even for a rough qualitative estimation of the melilite composition. The judgement must be based mainly on the band groups Nos. 1—6 and Nos. 13—14 of Table II.

According to the molecular composition, the specimens of natural melilite listed in Table I can be divided into two groups. The one group is represented by specimens Nos. 4 and 5 and is characterized by a predominance of the gehlenite component whereas the content of the alkali melilite component is low. The infrared absorption spectrum of melilite No. 4 is illustrated in Fig. 3. The spectra of both these specimens show clearly band No. 6 (Table II), however, with an intensity lower than that of the same band in the spectrum of pure gehlenite in Fig. 2. The shapes of the tracings of these two natural melilite specimens are intermediate between those of pure åkermanite and pure gehlenite. The other group is represented by the rest of the specimens studied. In this group the åkermanite (plus iron åkermanite) component predominates, the content of the alkali melilite component is considerable and the content of the gehlenite component is low. The content of gehlenite (plus iron gehlenite) is in all specimens of this group below the lower limit of detection by means of the band No. 6. The absorption spectra of specimens Nos. 10, 19 and 13 are included in Fig. 3. Actually, band No. 6 could not be traced in any of the spectra of specimens belonging to this group. The shapes of the tracings in the range 9—12 microns approximate that of pure åkermanite. Due to the content of the alkali melilite component for which the tracing of this band group is more continuous, the single bands are, however, less sharply separated from each other. In the range 21—23 microns, the soda melilite band No. 14 (Table II) makes the slope of the tracing to differ slightly from that of the tracing of pure åkermanite. It is to be expected that, because the gehlenite band No. 6 was absent, the gehlenite band No. 14 will also be negligible.

The difference in infrared absorption between the two groups of natural melilite specimens is in accordance with the difference found in chemical composition. The same difference in infrared absorption is detectable between the »melilite» and »gehlenite» absorption spectra published by Moenke (1962—1966). It is concluded that in a natural melilite solid solution, the chemical analysis of which shows a low content of the gehlenite component, aluminum occupies (mainly) the tetrahedral position No. 1 in Smith's notation. Because pure soda melilite has no bands which do not coincide with those of either åkermanite or gehlenite, the direct detection of the alkali melilite component in a natural melilite specimen becomes difficult. The possible presence of alkali melilite can only be judged by comparing the entire tracing with those of the three pure end members in Fig. 2.

The effect of the Fe^{2+}-Mg substitution upon the infrared absorption can best be studied by comparing tracings No. 19 and No. 13 with each other. These two melilite specimens are of virtually identical composition except for the ratio of åkermanite to iron åkermanite. Melilite No. 13 shows a content of iron åkermanite which is fairly common in ordinary volcanic melilite. Melilite No. 19, on the other hand, is extremely rich in iron. The infrared absorptions of these two melilite specimens, as illustrated in Fig. 3, are very similar to each other. This observation is in accordance with the results obtained by White and Roy (1964) on the effect of polymorphic transition upon infrared absorption. These authors have found that the spectra of polymorphs with the same structure type are nearly identical except for slight shifts in the wavelengths of certain bands. Such shifts can be correlated to the composition of a solid solution as has actually been done, *e. g.*, by Thompson and Wadsworth (1957) for plagioclase feldspars, by Duke and Stephens (1964) for the olivine group minerals and by Sahama (1965) for nepheline solid solutions. The effect of the iron content upon the wavelengths of infrared absorption bands for melilite is probably too slight to be used for estimating the ratio of ferrous iron to magnesium.

As was described by Neuvonen (1952), the synthetic crystalline samples of the åkermanite-gehlenite series used in this work were prepared by devitrifying glass at a temperature ca. 30°C below the corresponding solidus temperature. The annealing time was one or more hours. Accordingly, if any definite order-disorder transition occurs in the occupation of the tetrahedral sites of the melilite structure, the synthetic preparations should represent expectedly a more or less highly disordered state. In addition, the specimens of natural melilite Nos. 10—17 and 19—20 come from volcanic rocks. If any analogy with the feldspars is applicable to melilite, these specimens of natural melilite should also be disordered to some extent. However, as has already been remarked, the crystal structure of the Capo di Bove melilite indicates no high disorder. Neither does the infrared absorption of the synthetic crystalline preparations nor of the natural melilite specimens disclose any order-disorder transition. The two natural melilite specimens Nos. 4 and 5 are of a contact metamorphic origin and, accordingly, are likely to represent a highly ordered state. For that reason, batches of the specimens No. 5 were heated at a temperature of ca 1 150°C for 22 and 71 hours, respectively. The spectra of the heated materials were recorded. No notable change in the infrared absorption of the heated materials as compared with that of the original mineral was detected. In conclusion it may be stated that no evidence is so far at hand indicating a more pronounced order-disorder transition in rock forming melilite.

Acknowledgments — The authors are indebted to professor K. J. Neuvonen, Dept. of Geology, University of Turku, Finland, for placing available the synthetic preparations of the åkermanite-gehlenite series and to Dr. Hatten S. Yoder, of the Geophysical Laboratory, Washington, D. C., for the synthetic soda melilite.

Manuscript received, December 15, 1966

REFERENCES

Duke, David A. and Stephens, James D. (1964) Infrared investigation of the olivine group minerals. Amer. Miner., vol. 49, p. 1388.

Edgar, A. D. (1965) Lattice parameters of melilite solid solutions and a reconnaissance of phase relations in the system $Ca_2Al_2SiO_7$ (gehlenite) — $Ca_2MgSi_2O_7$ (åkermanite) — $NaCaAlSi_2O_7$ (soda melilite) at 1 000 kg/cm^2 water vapor pressure. Canadian Jour. Earth Sci., vol. 2, p. 596.

Gordy, Walter J. (1946) A relation between bond force constants, bond orders, bond lengths, and the electronegativities of the bonded atoms. Jour. Chem. Phys., vol. 14, p. 305.

Keller, W. D., Spotts, John H. and Biggs, Donald L. (1952) Infrared spectra of some rock-forming minerals. Am. Jour. Sci., vol. 250, p. 453.

Kolesova, V. A. (1959) Infrared absorption spectra of the silicates containing aluminum and of certain crystalline aluminates. Optics and Spectroscopy, vol. VI, p. 20.

Lazarev, A. N. (1960) Vibration spectra of the silicates. I. Infrared spectra of silicates with anions of the type $(Si_2O_7)^{-6}$. Optics and Spectroscopy, vol. IX, p. 103.

Milkey, Robert G. (1960) Infrared spectra of some tectosilicates. Amer. Miner., vol. 45, p. 990.

Moenke, Horst (1962—1966) Mineralspektren. Akademie-Verlag, Berlin.

Neuvonen, K. J. (1952) Thermochemical investigation of the åkermanite-gehlenite series. Bull. Comm. géol. Finlande, No. 158.

—»— (1955) On the composition of natural melilites. C. R. Soc. géol. Finlande, vol. 28, p. 13.

Raaz, Franz (1930) Über den Feinbau des Gehlenit. Sitzungsber. Akad. Wiss. Wien, Bd. 139, S. 645.

Sahama, Th. G. (1965) Infrared absorption of nepheline. C. R. Soc. géol. Finlande, vol. 37, p. 107.

—»— (1967) Iron content of melilite. C. R. Soc. géol. Finlande, vol. 39, p. 17.

Simonen, Ahti (1953) Mineralogy of the wollastonites found in Finland. C. R. Soc. géol. Finlande, vol. 26, p. 9.

Smith, J. V. (1953) Reexamination of the crystal structure of melilite. Amer. Miner., vol. 38, p. 643.

Thompson, C. S. and Wadsworth, M. E. (1957) Determination of the composition of plagioclase feldspars by means of infrared spectroscopy. Amer. Miner., vol. 42, p. 334.

Warren, B. E. (1930) The structure of melilite $(Ca,Na)_2$ $(Mg,Al)_1$ $(Si,Al)_2O_7$, Zeitschr. Krist., Bd. 74, S. 131.

Weinschenk, E. (1897) Fuggerit, ein neues Mineral aus dem Fassathal. Zeitschr. Krist., Bd. 27, S. 577.

White, William B. and Roy, Rustum (1964) Infrared spectral-crystal correlations: II: Comparison of simple polymorphic minerals. Amer. Miner., vol. 49, p. 1670.

Comptes Rendus de la Sosiété géologique de Finlande
N:o XXXIX (1967), pp. 41—43

PERRIERITE FROM MÄNTYHARJU, FINLAND

Mineralogical communication

BY

PEKKA KALLIO

Geological Survey of Finland

A few metamict perrierite grains were found in the heavy fraction of a gabro-anorthosite from Mäntyharju. The heavy fraction consists of grains which have a specific gravity greater than that of bromoform (2.8), the grain diameter being less than 0.25 mm. The principal minerals of the heavy fraction are pyroxenes. Apatite and ilmenite are abundant, olivine, amphibole and zircon minor, and pyrite and perrierite very rare constituents of the fraction. A mode of the rock is presented in table 1. Savolahti (1956) has described the petrology of this gabro-anorthosite in detail.

TABLE 1.

Mode of the gabro-anorthosite from Mäntyharju (sample A-118)

Plagioclase	82.0
Quartz	0.8
Amphibole	0.4
Pyroxenes	9.5
Biotite	0.8
Chlorite Epidote	1.3
Apatite	2.9
Others	2.3
	100.0

The perrierite grains are red-brown, and have a conchoidal fracture. The refractive index is 1.90. The main elements determined by microprobe are Ce, La, Ca, Ti, Fe and Si. These agree well with the chemical formula of perrierite which according to Galli (1965) is: $Ce_8Fe^{2+}_2Me^{3+}_4Ti_4[O_4 | (Si, Al)_2O_7]_4$

where $Ce = RE, Th^{4+}, Ca^{2+}Na^{+}$

$Fe^{2+} = Fe^{2+}, Ca^{2+}$

$Me^{3+} = Ti^{4+}, Fe^{3+}, Mg^{2+}$.

The perrierite grains are coated with a white bastnäsite powder which is obviously an alteration product of perrierite.

Perrierite was identified after heat-treatment. The metamict grains were heated at 700°C for three hours and at 1 000°C for one hour; both heatings were done in air. The X-ray powder photographs of the unheated and heated materials were taken with a Debye-Scherrer camera of 57.3 mm diameter using Cu-radiation and Ni-filter. After heating at 700°C the sample was still in the metamict state. At 1 000°C the perrierite phase crystallized. Very similar thermal behaviour of two perrierites from India were observed by Lima de Faria (1964) (Table 2, Nos. 2 and 3). Also some chevkinites behaved fairly similarly (Table 2, Nos. 5, 6 and 7). But all three chevkinites, when heated in air at 1 000°C for one hour, showed a well developed cubic phase and only a poorly developed perrierite phase, while the two perrierites as well as the grains used in this study showed a well developed perrierite phase. For this reason these grains are regarded as perrierites and not as chevkinites.

TABLE 2.
Thermal behaviour of some perrierites and chevkinites, as shown by X-ray powder photographs

No	Locality and reference	Heat treatment			Mineral
		Unheated	700°C 3h	1 000°C 1h	
1	Mäntyharju, Finland GSF A 118	—	—	Pe	Perrierite
2	Bangalore, India S.I. 106630	—	—	Pe + c	Perrierite
3	Kanjamalai, India B.M. 34167	*Pe*	—	Pe	Perrierite
4	Bedford Ca, USA B.M. 86189	*Pe*	Pe	Pe	Perrierite
5	Ilmen, Urals, USSR B.M. 39244	—	—	c + *Pe*	Chevkinite
6	Urals USSR B.M. 39244	—	—	c + *Pe*	Chevkinite
7	W. Ambatofinandrahana Madagascar	—	—	c + *Pe*	Chevkinite

GSF = Geological Survey of Finland
S. I. = Smithsonian Institution U.S. National Museum
B. M. = British Museum, Department of Mineralogy
Pe = Perrierite c = CeO_2 (cupic a_0 = 5.44 Å)
Pe = Poorly developed perrierite phase — no diffraction lines
2—7 Lima de Faria (1964)

According to some research workers (Jaffe, Evans and Chapman 1956) chevkinite and perrierite are the same mineral species, others (Bonatti 1959, Gottardi 1960) assume that they are separate species. According to Lima de Faria (1962) perrierite is an oxidized form of chevkinite.

Until now chevkinites and perrierites have been reported only from alkali and granite pegmatites and fayalite-quartzsyenite, but never before from rocks belonging to the gabro family.

Acknowledgement — The author wishes to express his thanks to Dr. Olavi Kouvo for providing the heavy fraction used in this study and to Mr. Jaakko Siivola, Mag. Phil., for the microprobe analysis.

Manuscript received, February 14, 1967

REFERENCES

Bonatti, S. (1959) Chevkinite, perrierite and epidote. Amer. Mineral., **44**, 115—137.

Galli, Ermanno (1965) Affinamento della struttura della perrierite. Miner. Petrogr. Acta **11**, 39—48.

Gottardi, G.: (1960) The crystal structure of perrierite. Amer. Mineral., **45**, 1—14.

Jaffe, H. W., Evans, H. T. Jr., and Chapman, R. W. (1956) Occurrence and age of chevkinite from Devil's Slide fayalite-quartz syenite near Stark, New Hampshire. Amer. Mineral., **41**, 474—487.

Lima de Faria (1962) Heat-treatment of chevkinite and perrierite. Mineral. Mag., **33**, 42—47.

—»— (1964) Identification of metamict minerals by X-ray powder photographs. Junta de investigacoes do ultramar. Estudos ensoios e documentos **112**. Lisboa, Portugal.

Savolahti, A. (1956) The Ahvenisto massif in Finland. Bull. Comm. géol. Finlande **174**.

Comptes Rendus de la Société géologique de Finlande
N:o XXXIX (1967), pp. 45—69

ON THE BARYTES OF FINLAND

BY

HEIKKI PAPUNEN

Institute of geology, University of Turku, Finland

ABSTRACT

Twenty baryte specimens from seven localities in Finland have been described and analyzed chemically. Also variations of the lattice constants have been determined by using the d_{410}-spacing as the indicator of the cell constants. Ca-diadochy in baryte has been studied from several synthetic $BaSO_4$—$CaSO_4$ mix crystals. The Ca-content of the baryte is proved to be principally dependent on the Ca to Ba ratio of mineral forming fluids. Also the fluid inclusions and twinning of barytes at inversion point have been represented. The paragenetic and genetic aspects of the baryte deposits have been discussed.

CONTENTS

INTRODUCTION

Among the baryte deposits of the world the most usual are the hydrotermal vein deposits and the baryte-bearing sedimentary formations. For example Central European baryte-bearing veins (type Freiberg) and baryte-bearing sedimentary rocks in North America (Missouri) are well known. Baryte deposits in the Pre-Cambrian are not as common as in some younger formations.

This study presents seven baryte deposits in Finland and neighbouring areas:

— The limestone quarries of Illo and Lammala in Vestanfjärd commune, SW-Finland, contain cavities filled with idiomorphic crystal druses in which also baryte crystals are found.

— Small baryte-bearing carbonatite veins occur in Panjavaara, Juuka commune, E-Finland. One baryte-sample is analyzed from these veins.

— In the coastal area of Petsamo, USSR, there are numerous brecciated quartz-baryte-carbonate veins from which some specimens have also been studied.

— In the Taporova iron ore deposit in the Kolari district, N-Finland, baryte occurs together with iron oxide minerals.

— Vihanti and Pyhäsalmi sulfide deposits have baryte as gangue mineral of the ores.

— In the mineralogically very interesting sulfide deposit of Korsnäs, baryte exists as gangue mineral of the lead ores and also in cavities as idiomorphic crystals.

Barytes have been found also in some other localities in Finland, but as they are similar to those of the type localities presented here, they have not been described in this study.

As baryte forms complete solid solutions with anglesite ($PbSO_4$) and celestine ($SrSO_4$) and uncomplete solid solution with $CaSO_4$ one can suppose, that the chemical composition of the natural barytes gives valuable information concerning the composition of the deposition forming fluids and also concerning the temperature and other factors of crystallization. Therefore the variations of chemical composition and cell edge of natural barytes have been measured. Some syntheric $CaSO_4$-$BaSO_4$ mix crystals have also been studied to explain the Ca-Ba diadochy in baryte.

In the last part of the study the paragenetic and genetic conclusions have been represented.

DESCRIPTION OF THE ANALYZED SPECIMENS

Vestanfjärd

The limestone deposit of Vestanfjärd and its cavities have been described by Eskola (1913 and 1919), Pehrman (1947), Ahlfors (1954) and Neuvonen (1960). According to them cavities of limestone were formed by the dissolution of limestone by acid solutions. Cavities were filled with sand or clayey material in such places where they were open to the surface of the earth. At deeper levels the holes were filled by crystal druses.

According to Pehrman (1947) the following minerals are found in the cavities: calcite in three generations, which have been named after Kalb (1928, 1929) as calcite III, IV and V, baryte, fluorite, pyrite and rarely, marcasite, adular, chalcopyrite, malachite, limonite and kaolin minerals. Taking into consideration the mineral species of the druses, one can suppose that the cavity forming and mineralizing fluids were originally hydrothermal.

Specimen no 1 was taken in the quarry of Illo and it consists of white coarse-crystalline calcite coated with platy baryte crystals. They are from 1.5 to 0.2 cm in size and from 2 to 0.5 mm in thickness. Baryte is light yellow in colour and often the crystals have a thin white zone at the border parallel to the face {210}. The thickness of this zone is only 0.1 mm and there is no marked difference in composition between the outer zone and the inner part of the crystal. Baryte crystals have the faces of the zone [010] and thus they belong to type III a of Kalb and Koch (1931).

Another analyzed specimen no 2 from Illo quarry contains baryte crystals together with fluorite and coarse-crystalline calcite. Immediately on the calcite-base there is a brown cluster of limonite upon which are the platy baryte crystals, which always have the forms {001} {210} and occasionally also {101} and {102}. Sometimes a thin pyrite layer exists between baryte and the limonite cluster. Fluorite occurs as greenish-yellow cubes.

Juuka

In Panjavaara, western part of Juuka commune, some carbonatite veins have been found. They are only a few centimeters broad and occur in the Karelian mica gneiss cutting the strike of schistosity.

In the marginal part of the vein the chief minerals are bastnäsite and calcite, which occur together as a fine-grained brown-coloured mass. Some quartz and potash feldspar grains also occur among them. Parallel to the vein-contacts there are light coloured bands, which consist of apatite prisms and idiomorphic, zoned tourmaline crystals. As accessory minerals there is some tremolite, oligoclase and baryte. Pyrite and galena are the most common sulfide minerals in the marginal parts of the vein. Pyrite occurs as cataclastic grains and galena fills its cracks and margins. Galena

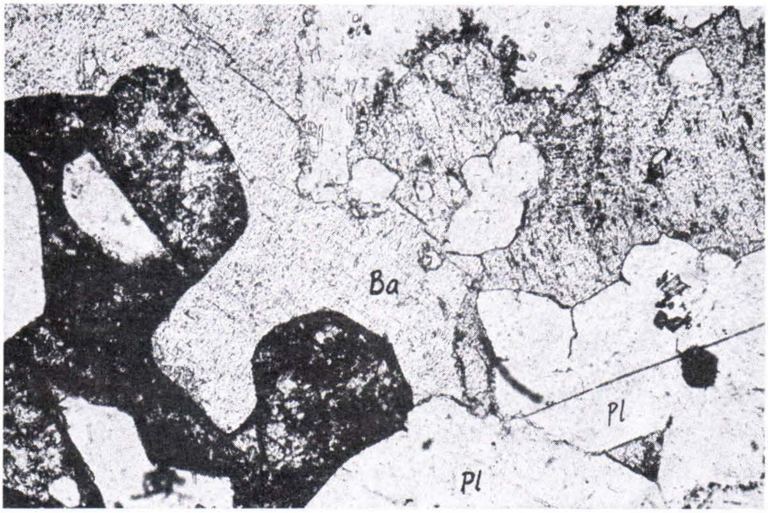

FIG. 1. A fine grained carbonate mass replaces baryte. (Ba = baryte, Pl = plagioclase, carbonate mass is almost black). Parallel nicols, magn. 30 ×. Panjavaara, Juuka.

occurs also as small veins and disseminated irregular grains. Chalcopyrite is less usual than pyrite and galena and is found together with pyrite as crackfillings and inclusions in the pyrite and galena. Covellite appears as secondary mineral at the margins of chalcopyrite. Sphalerite grains are very rare. Some marcasite has been found between pyrite crystals and small pyrrhotite inclusions occur in the pyrite. In some places the skeletal texture of marcasite has been formed by the inversion of pyrrhotite into marcasite.

The specimen taken from the middle part of the vein is coarser in crystal size than the specimen from the marginal parts. Chief minerals are baryte, carbonates, oligoclase and tremolite. Baryte occurs as big, light-yellow crystals. The characteristic feature of the specimen is the porphyric texture: oligoclase and occasionally also microcline occur as idiomorphic crystals in a fine-grained brownish carbonate mass. This mass consists of two carbonates, one of which is limonite-pigmented calcite ($d_{1012} = 3.02$ Å) and the other colourless dolomite ($d_{1012} = 2.89$ Å). The carbonate mass replaces baryte (Fig. 1) and galena. The amphibole mineral occurs as long thin prisms, which have Z (greenish) = 1.634, $2V_x$ c.a. 80°, $c \wedge Z = 21°$ and Z-X = 0.013. The cell constants measured with single-crystal Weissenberg photographs are $a_0 = 9.99 \pm 0.08$ Å, $b_0 = 17.94 \pm 0.20$ Å, $c_0 = 5.28 \pm 0.02$ Å and $\beta = 105.7°$. Optical and cell constants indicate that the mineral is tremolite. Blue abnormal interference colours are probably due to the abnormally high sodium-content of the mineral. Galena is almost the only sulfide mineral occurring in the middle part of the vein.

Some single chalcopyrite grains are met with, but pyrite is absent. The analyzed baryte, specimen no 8, is from the middle part of the vein.

Radioactive age measurements of the galena of Panjavaara and also a sulphur-isotope determination have been made by Kouvo (1958) and Kouvo and Kulp (1961).

Petsamo

Some baryte-bearing quartz veins occur in the coastal area of Petsamo. They have been described by Hausen (1926 and 1932). These veins are mineralized dislocation zones and most of them occur at the contacts of metamorphozed dolerite veins (trapp). Owing to dislocation the brecciated textures of the veins are very numerous. Quartz, baryte, calcite and sulfides, galena and sphalerite are the chief vein minerals. As a peculiar feature the cell-texture (»zellige struktur» by Hausen) of quartz is to be mentioned. This has been formed by the replacement of baryte by quartz. The curved crystal faces of baryte and galena often show deformation, which took place after mineral deposition. According to Hausen (1932, p. 14) the formation of mineralized dislocation zones is associated with the downthrowing of the graben of Varanger-fjord. According to him (1932, p. 37) the sequence of vein filling has been as follows: 1) opening of the joints by the action of tectonic movements 2) filling with silica and bariumsulfate-bearing solutions; quartz, baryte and cell-quartz crystallized, 3) dislocation and crystallization of sphalerite 4) dislocation; the sphalerite-grains cracked and quartz crystallized in cavities 5) dislocation, galena and quartz crystallized 6) calcite, pyrite and chalcopyrite crystallized as final minerals. 7) Mineralized veins weathered by the action of descendent solutions.

The analyzed specimens are taken from the collection of Turku University and were collected by prof. A. Laitakari. Specimen no 3 is from the Samuel vein and consists only of baryte, which is 1—10 cm broad, platy grains. The (001)-faces of crystals are curved and prove thus tectonic deformation after deposition. Specimen no 4 is from Peuravuono, Petsamo. In addition to the white, platy baryte there is also quartz and sphalerite, which is brown in colour and brecciated. Specimen no 5 is from the Suolavuono vein group. Baryte occurs here as big, platy, radial crystals. There are idiomorphic quartz prisms in small cavities between them. A fine-grained mass consisting of galena, brown sphalerite and quartz, has crystallized after baryte.

Kolari, Toporova

Both magnetite and hematite iron ores occur in the Kolari district. Juvakaisenmaa, Sivakkalehto, Rautavaara and Rytivaara are mainly magnetite deposits whereas Taporova, Suuvaara and Suuoja are characterized by hematite-rich ores. Taporova hematite ore contains baryte in marked amounts, in other hematite ores it is only accessory and in magnetite ores fully absent. The Kolari district has been described

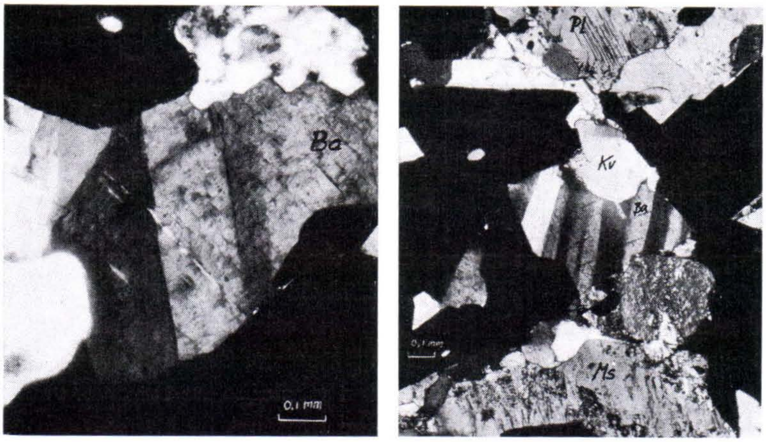

FIG. 2. Twinned and laminated baryte grains in the ore of Taporova, Kolari. Ba = baryte, Kv = quartz, Ms = potash feldspar, Pl = plagioclase, black is hematite. Crossed nicols.

by Toivo Mikkola (1960). According to him the Taporova iron ore is sedimentogenous as all the other iron deposits in the Kolari district. It belongs to Karelian formations and is connected to the same sediment facies as black shists and marbles. Taporova ore lies between mica gneiss and quartzite and is in a syncline the axis of which plunges steeply to the north-east. A pegmatite granite penetrates the syncline and cuts the ore into several pieces.

The chief ore mineral in the Taporova deposit is hematite, but also magnetite occurs. Gangue minerlas are quartz, muscovite microcline and baryte. Blagioclase, apatite, sphene, green tourmaline and zircon are accessory minerals. The rock is shistose and banded, but it does not, however, belong to the group of so-called »banded ironstones», which are well known from other Precambrian localities.

The baryte content of the Taporova deposit is remarkable, according to Toivo Mikkola (1960) the BaO-content varies from 3 to 10 wt-%. Baryte occurs as xenomorphic grains which occasionally have muscovite inclusions. Baryte is not evenly distributed in the rock but occurs as small flakes and lenses parallel to the schistosity. In connection with microcline the baryte grains are very irregular and small. They show clear indications of deformation: grains have lamellar texture and twins (Fig. 2.). Only one baryte, specimen no 7 was analyzed from the Taporova deposit.

Vihanti

The Vihanti deposit has been described in detail by Isokangas (1954), Laatio and A. Mikkola (1957) and A. Mikkola (1963). From the standpoint of the occurrence of baryte the characteristic features of the deposit are as follows. There are two principal

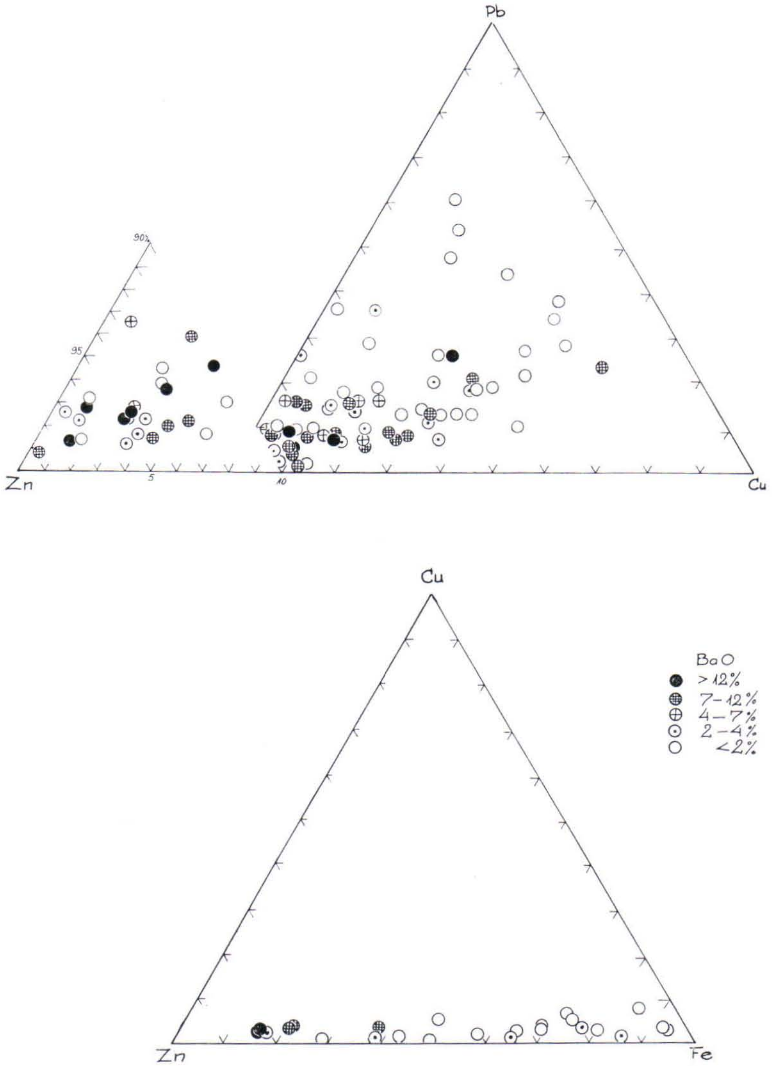

FIG. 3. Triangle diagrams representing the compositions of sulfides and BaO-content of the Vihanti ore. The Zn-corner of the Zn-Cu-Pb-triangle is enlarged because there are plenty of spots in this part.

types of ore mineralizations: zinc-copper ores and pyrite ores. Baryte occurs only in the zinc-copper ores, in pyrite mineralizations it is fully absent. On the basis of gangue minerals the carbonate-skarn type and the quartzite type zinc-ores can be distinguished. Baryte occurs in both types. The zinc ore has the following paragenetic types: 1) chalcopyrite-rich ore 2) compact sphalerite ore 3) galena-sphalerite ore

TABLE 1.

The correlation coefficients between the percentages of the elements in the Vihanti ore deposit

	Zn	Cu	Pb	Fe	BaO	S
Zn	—	+0.1861	+0.1389	—0.1248	+0.09136	+0.28072
Cu	+0.1861	—	—0.0560	—0.5417	—0.05029	+0.12201
Pb	+0.1380	—0.0560	—	—0.4586	—0.04954	—0.00099
Fe	—0.1248	—0.5417	—0.4586	—	—0.52061	+0.24677
BaO	+0.0914	—0.0503	—0.0495	—0.5206	—	+0.19751
S	+0.2807	+0.1220	—0.0010	+0.2468	+0.1975	—

4) baryte- and/or carbonate-rich sphalerite ore, which is often banded or brecciated. Occasionally idiomorphic baryte crystals have also been found in cavities formed by jointing or faulting. The idiomorphic baryte crystals found in U-quarry, + 175 m level, have distinct forms {011}, {101} and {001} and occasionally also forms {211}, {210} and {201}.

The triangle diagrams in Figure 3 have been drawn on the basis of 118 analyses of the ore. Analyses were made of the diamond drilling cores from different parts of the ore doposit. The diagrams represent variations in the composition of sulfides and the BaO-content of the rock. From the darkness of the analysis-marks one can observe that the BaO-content of the rock is parallel to the Zn-content of the sulfides. Correlation is not, however, unambigous owing to the paragenetic types of the zinc ore (compact sphalerite ore on the one hand and baryte-bearing zinc ores on the other).

Also correlation coefficients between different metals and BaO have been determined on the basis of the chemical drill-core analyses using the method described by Fisher (1958). Coefficients are listed in Table 1. (The number of analyses was 118). From Table 1 one can see that a slightly significant positive correlation exists between sulfidic sulfur and the BaO-content of the rock. The correlation is significant at the 0.05 level of significance. This is explained by the fact that baryte occurs together with sulfides and not in the host rocks of the ore. The strong negative correlation between sulfidic iron and BaO proves that baryte does not occur in the pyrite ore bodies.

The effect of the wall rock on the barium content is represented in Figure 4. One can observe that the ores with quartzite base possibly have more baryte than ores with skarn and carbonate rock base.

Three samples from Vihanti were analyzed. One of them, specimen no 11, is a zinc-ore in quartzitic rock abundant in baryte. It is taken from the crosscut RKp 8, + 165 m level. The rock is unhomogenous, banded and its chief ore minerals are sphalerite and galena; some chalcopyrite, pyrrhotite, berthierite, boulangerite and stannite grains have also been found. As gangue minerals baryte, quartz and minor diopside and tremolite grains occur. The texture is granoblastic. Carbonate minerals do not occur in this rock. In the hand specimen the baryte is yellow but colourless in the thin section, only yellow pleochroic halos around small zircon crystals being then visible. The yellow colour of baryte disappears when heated up to 350°C and the mineral becomes white.

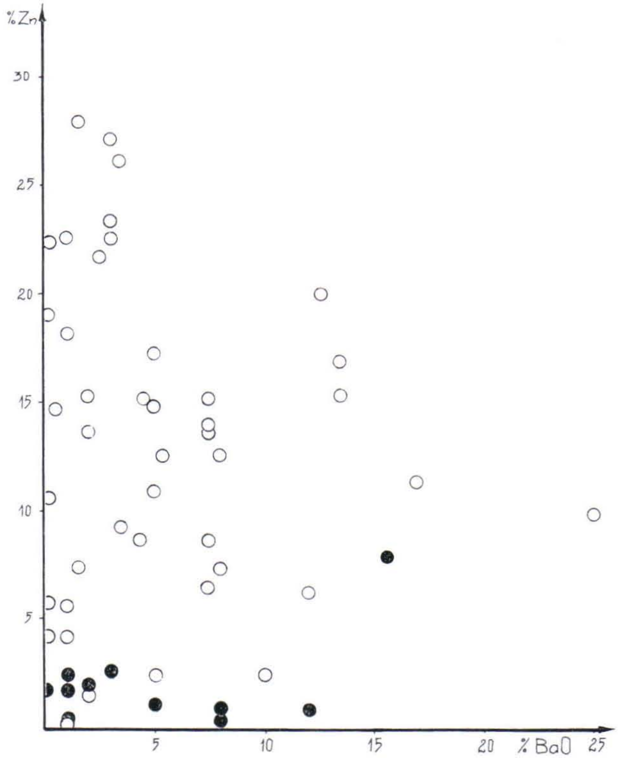

FIG. 4. The effect of the wall rock on the BaO- and Zn-contents of the Vihanti ore. Open circles are ores with carbonate or skarn rock base, black spots are quartzites.

Specimen no 12 (crosscut RP 6, + 200 m level) is a zinc-ore whose ore minerals are sphalerite, chalcopyrite and galena. The main gangue mineral is calcite ($d_{1012} = 2.03$ Å). In addition plenty of baryte, tremolite and diopside also occur. Chlorite, sphene and zircon are accessory minerals. Baryte grains are xenomorphic and often twinned parallel to {210}.

The third analyzed sample from Vihanti is an idiomorphic baryte crystal from U-quarry. It was found in a cavity and occurs together with idiomorphic calcite, pyrite and laumontite crystals. Most of the baryte crystals are large, and the analyzed crystal is shaped like a thick plate parallel to (001). The baryte crystal seems zonal, which is due to the zonal distribution of small inclusions. In the middle part of the crystal the inclusions are roundish and consist of a soft hydrogoethite mass, but close to the crystal surface they are composed of a soft pyrite mass and on the surface the inclusions change into small pyrite octahedrons. The analyses nos 9 and 10 are of idiomorphic baryte.

TABLE 2.

The correlation coefficients between the percentages of the elements in the Pyhäsalmi ore deposit

	Cu	Fe	S	Zn	Pb	Ba	Ag	Au
Cu ...	—	+0.1260	+0.0524	—0.2915	—0.0439	—0.2267	+0.6026	+0.2249
Fe ...	+0.1260	—	+0.8934	+0.0609	—0.2916	+0.0775	—0.1732	—0.3101
S ...	+0.0524	+0.8934	—	+0.2025	—0.2990	+0.2430	—0.2276	—0.3524
Zn ...	—0.2915	+0.0609	+0.2025	—	+0.1926	+0.6542	—0.0762	—0.2095
Pb ...	—0.0439	—0.2916	—0.2990	+0.1926	—	—0.1449	+0.7740	+0.0052
Ba ...	—0.2267	+0.0775	+0.2430	+0.6542	—0.1449	—	—0.2780	—0.2318
Ag ...	+0.6026	—0.1732	—0.2276	—0.0762	+0.7740	—0.2780	—	+0.2135
Au ...	+0.2249	—0.3101	—0.3524	—0.2095	+0.0052	—0.2318	+0.2135	—

Pyhäsalmi

The pyrite ore of Pyhäsalmi contains abundant baryte as gangue mineral. According to Helovuori (1965) the main ore minerals in the deposit are pyrite, chalcopyrite and sphalerite. Occasionally also pyrrhotite, galena, magnetite, arsenopyrite, molybdenite, tennantite, andorite, hessite, electrum and native gold have been met with. Quartz, baryte, mica and carbonates are chief gangue minerals. The ore is coarse-crystalline, compact, and the gangue minerals play an unimportant role in the mass. As the mineral associations in the ore seem to vary indefinitely, the correlation coefficients between the main metals, sulphur and barium, have been calculated from 119 analyses of drill cores according to the method described by Fisher (1958). The correlation coefficients are represented in Table 2. By reason of the numerical values of the coefficients, the following mineral associations can be established:

1. Iron sulfide association: very definite positive correlation between iron and sulphur. As iron has not any other positive correlation, pyrite is the only mineral in this association. The definite negative correlation between iron and lead means that pyrite and galena have been localized separately.

2. The strong positive correlation between Zn and Ba is due to the coexistence of sphalerite with baryte. As the correlation between zinc and iron is not positive, the coexistence of the sphalerite-baryte association with pyrite mineralization is only occasional.

3. According to Helovuori (1965) copper-precious metal association often occurs at the contacts of the ore. It is characterized by the significant positive correlation between Cu and Ag on the one hand and between Cu and Au on the other. The coefficients are significant at a level lower than 0.01.

4. The lead-silver association is due to the coexistence of galena with low-temperature silver minerals. The negative correlation between iron and lead is explained by the occurrence of galena and its mineral-association principally in the host rock fragments.

5. Gold-association: gold has a significant positive correlation coefficient with copper and silver at the 0.05 level of significance. The correlations are not significant with other elements. This proves that, even in this ore, gold occurs as a separate association, the significant correlations with copper and silver are due to diadochy of gold and silver in the minerals of copper-precious metal association.

The observations in the deposit and the the study of sections confirm the foregoing opinion of the mineral associations. There is no reason in discussing here whether or not these mineral associations have a genetic significance. It is self-evident, however, that the correlation coefficients show which minerals occur together and have been localized in the same place.

The two analyzed specimens were collected by the author from the outcrop of the ore in the year 1961. Specimen no 13 represents ore rich in baryte. The ore minerals are pyrite, sphalerite and minor chalcopyrite. In addition to baryte, carbonates occur as gangue minerals, one of which is colourless dolomite (d_{1014} = 2.88 Å and d_{3030} = 1.387 Å) and the other brownish siderite (d_{1012} = 3.617 and d_{1014} = 2.812 Å).

The other analyzed specimen no 14, is pyrite ore, which also contains minor sphalerite and chalcopyrite grains. Baryte is the only gangue mineral.

Korsnäs

The lead deposit of Korsnäs is characterized by unhomogenous pegmatite or carbonatite-like formations in wide fractured zones. Further, the breccias and also the large cavities with their beautiful mineral druses are typical of the deposit. Galena is economically the most important mineral. In addition to it sulfide minerals such as pyrite, pyrrhotite and chalcopyrite also occur. The gangue minerals are numerous; the common are calcite, quartz, apatite, potash-feldspar, green chlorite-like sheet silicate and less common baryte, monazite, allanite, U-minerals, amorphic carbon, celestine, apophyllite and zeolites, of which the idiomorphic Ba-zeolite, harmotome, is the most remarkable. Baryte occurs in Korsnäs both as a massive gangue mineral in galena-ore breccias and also as idiomorphic crystals in the walls of cavities. One of the analyzed baryte specimens was a massive baryte in galena ore, all the others were idiomorphic crystals from cavities.

Specimen no 15. On a coarse-crystalline calcite there is a thin layer of green chlorite-like mineral. Water-clear calcite crystals and baryte prisms occur in the sheet silicate. On the surfaces of calcite and especially of baryte there are plenty of minute pyrite cubes.

Baryte crystals are elongated in the direction of the a-axis, zone [100] is well developed and the crystals have forms {101} and {011} and occasionally {210}. The green sheet silicate has been studied by X-ray diffraction by using preparates suspended in glycol and water and also by heating to 600°C. This determination proved that the mineral belongs to the montmorillonite group (McEwan 1961). However, its largest interplanar spacing was 30 Å, which makes one suppose that the mineral has a super structure with $c_0 = 30$ Å. The crystallization sequence has been as follows: calcite-base — montmorillonite and sulfides — calcite II and baryte — small pyrite cubes.

Specimen no 16 is almost entirely small-grained light-yellow baryte. In addition galena and water-clear calcite crystals also occur. There is also a platy baryte crystal about 3 cm long and 0.5 cm thick, which is dark brown and idiomorphic having the forms {001}, {210}, {101} and {011}. Small pyrite cubes occur as inclusions in the baryte. They have been arranged in zones parallel to {101} and {011}. This dark brown baryte crystal has been analyzed. A pink, coarse-crystalline calcite is the base in specimen 17. Immediately on the surface of the calcite, idiomorphic pyrite cubes have crystallized or in some other places idiomorphic baryte crystals, which are platy parallel to {001} and also have the form {210}. Generally however baryte-crystals occur on the pyrite crystal layer. In some places calcite crystals with thick prisms have crystallized immediately on the pyrite. Calcite has the forms {1010} and {0110} and occasionally also a small {1012}-rhombohedron. A 0.2—0.5 mm thick pyrite layer occurs on the surfaces of the baryte crystals, which is thus pyrite of the second generation. Between these pyrite druses needle-like pinkish calcite crystals occur. The crystallization sequence is as follows: calcite I (base) — pyrite I — calcite II and baryte — pyrite II — calcite III.

Specimen no 18 was taken at the + 190-level of the mine. It is a platy baryte crystal, 11 mm thick and 20 × 25 mm broad. The colour is light brown in the middle part of the crystal and white near the surface. On the (001)-face of the crystal there are numerous small grooves in the direction of the b-axis. The walls of the grooves are crystal faces: (101), $(\bar{1}01)$ and (201). The basal cleavage of this baryte is excellent due to numerous liquid-inclusions parallel to the face (001).

Specimen no 19 represents the baryte of the ore. Calcite, galena and baryte are the chief minerals and chalcopyrite occurs accessorily. Calcite is very coarse-crystalline.

Specimen no 20 consists of two baryte crystals taken from the + 190-level. These crystals are light brownish and prismatic parallel to the b-axes. Crystal forms {011} and {101} are distinct and {210} and {001} are small.

CLASSIFICATION OF BARYTE DEPOSITS

On the basis of mineral paragenesis and conditions of crystallization the Finnish baryte deposits have been classified as follows:

1. Barytes which have crystallized in cavities. The idiomorphic crystals and clear sequence of crystallization characterize this type of deposition. Barytes of Vestanfjärd and Korsnäs and idiomorphic crystals of Vihanti belong to this type.

2. Deposits of Juuka and Petsamo are barytebearing veins. They are characterized by brecciated textures and by zonality of the veins.

3. Baryte is one of the main gangue minerals in the sulfide deposits of Vihanti, Pyhäsalmi and partly Korsnäs. The most striking features of this type are the sulfide minerals associated with baryte and the indefinite mineral associations.

4. The deposit of Taporova is peculiar because the baryte occurs together with oxidic iron minerals and sulfides are totally lacking. This deposit has been considered of sedimentary origin (Toivo Mikkola, 1960).

CHEMICAL COMPOSITION OF THE BARYTES

$BaSO_4$ forms a complete solid solution with $SrSO_4$ and $PbSO_4$. With $CaSO_4$ the substitution is not complete because anhydrite, $CaSO_4$, has a different crystal structure. Since Ba, Sr, Pb and Ca are the cations of natural barytes, the analyzing of these elements gives the variation in composition of the barytes.

As $BaSO_4$ is almost completely insoluble in water, acids and other solvents, it must first be brought into soluble form for an ordinary gravimetric or volumetric analysis. This is not, however, an easy task.

In this study the barytes have been analyzed by X-ray fluorecence analysis. The apparatus was a Philips vacuum X-ray fluorecence spectrometer with an automatic Norelco recorder. Sr and Pb were analyzed with a LiF-crystal and scintillation counter, whereas an EDDT-crystal and methane flow-counter were used for Ca. Ba-content can be determined by calculation from the stoichiometric formula after analyzing Ca, Pb and Sr.

Mixtures made from the measured amounts of pure $CaSO_4$, $PbSO_4$, $SrSO_4$ and $BaSO_4$-powders were homogenized and used as standards. From the several measurements of standards the relative analytical errors can be calculated as 2.5 % for Pb, 5.5 % for Sr and Ca 3.2 % when the content of every cation is about one weight per cent.

The baryte samples were separated by means of Clerici solution and Franz isodynamic separator and finally purified by nitric acid treatment. The purity of every sample was over 99.5 %.

The $CaSO_4$, $PbSO_4$ and $SrSO_4$-contents of the samples are represented in Table 3. The $SrSO_4$-content varies from 0.2 to 1.8 wt-% and distinct variations occur even in the samples of the same deposit as well as in those of Korsnäs (samples 15—20). (Fig. 5.) Starke (1963, p. 404) has calculated the frequency distribution of the $SrSO_4$-content of 2 293 baryte analyses and has shown that the barytes with 0.1—3.0 mol-% $SrSO_4$ are the most usual, those with 3—5 mol-% and under 0.1 mol-% are scarce and barytes with $SrSO_4$-content over 3 mol-% are very exceptional.

TABLE 3.

Chemical composition of the barytes

No	Sample	$PbSO_4$ wt-%	$CaSO_4$ wt-%	$SrSO_4$ wt-%
1	Vestanfjärd, Illo	0.000	0.048	1.24
2	Vestanfjärd, Illo	0.028	0.067	0.68
3	Petsamo, Samuel	0.011	0.067	1.63
4	Petsamo, Peuravuono	0.011	0.042	1.78
5	Petsamo, Suolavuono	0.066	0.060	1.34
6	Petsamo, Suolavuono	0.011	0.048	1.44
7	Kolari, Taporova	0.017	0.206	1.58
8	Juuka, Panjavaara	0.060	0.060	1.62
9	Vihanti, core of the idiomorphic baryte crystal	0.000	0.048	0.21
10	Vihanti, rim of the crystal	0.010	0.036	0.18
11	Vihanti, zinc ore in quartzite	0.050	0.060	0.28
12	Vihanti, zinc ore in dolomite	0.011	0.157	0.28
13	Pyhäsalmi, carbonate-rich ore	0.017	0.121	0.60
14	Pyhäsalmi, pyrite ore	0.028	0.109	0.56
15	Korsnäs, prismatic baryte crystals	0.017	0.042	0.24
16	Korsnäs, dark-brown crystals	0.050	0.060	0.40
17	Korsnäs, baryte together with pyrite	0.022	0.054	0.91
18	Korsnäs, platy baryte crystal	0.030	0.048	1.00
19	Korsnäs, baryte in lead ore	0.000	0.036	0.84
20	Korsnäs, clear baryte crystals	0.006	0.054	0.36

In the idiomorphic baryte crystals of Vihanti (analyses 9 and 10) one can observe a slight zonality of the $SrSO_4$-content. Starke (1963, p. 407) has described in his study variations of 1—2 % in the $SrSO_4$-content of the same baryte crystal. Barytes, which have crystallized in cavities, have the most distinct variations of Sr-content whereas the Sr-content of barytes in sulfide ores is constant.

The amounts of $CaSO_4$ are between 0.05—0.2 wt-% and the $PbSO_4$-contents are very small, not more than 0.066 wt-%.

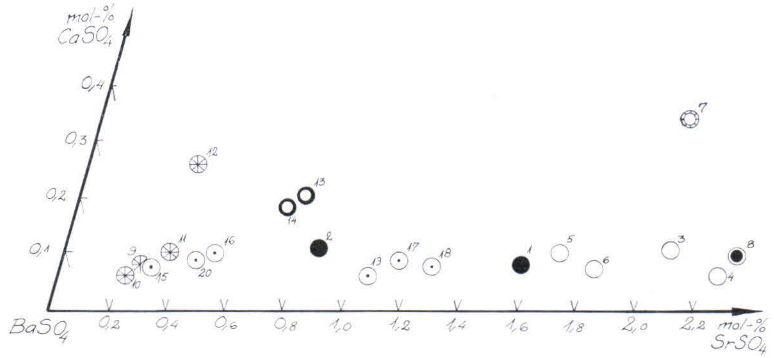

FIG. 5. The $BaSO_4$-corner of the triangle diagram $BaSO_4$-$CaSO_4$-$SrSO_4$. Numbers refer to the specimens. Different symbols indicate samples from different localities.

TABLE 4.

d_{410} Determinations of the barytes

Sample no	$2\Theta_{220}$ of Si-standard			$\triangle$	$2\Theta_{410}$ of Baryte		d_{410} of baryte
	$CuK\alpha_1$	$CuK\alpha_2$	$CuK\overline{\alpha}$		$K\overline{\alpha}_{meas.}$	$K\overline{\alpha}_{corr.}$	
1	47.373	47.472	47.406	—0.062	44.102	44.060	2.05520
2	47.316	47.490	47.374	—0.030	44.071	44.041	2.05600
3	47.403	47.463	47.483	—0.079	44.165	44.086	2.05405
4	47.365	47.470	47.400	—0.056	44.146	44.090	2.05387
5	47.301	47.511	47.371	—0.027	44.137	44.110	2.05299
6	47.351	47.482	47.395	—0.051	44.110	44.059	2.05529
7	47.432	47.504	47.456	—0.112	44.218	44.106	2.05317
8	47.329	47.455	47.371	—0.027	44.136	44.109	2.05299
9	47.361	47.484	47.402	—0.058	44.092	44.034	2.05636
10	47.333	47.489	47.385	—0.041	44.081	44.040	2.05609
11	47.368	47.491	47.409	—0.065	44.096	44.031	2.05644
12	47.362	47.461	47.395	—0.051	44.105	44.054	2.05547
13	47.401	47.473	47.425	—0.081	44.132	44.051	2.05556
14	47.343	47.468	47.384	—0.040	44.089	44.049	2.05565
15	47.354	47.579	47.389	—0.045	44.066	44.021	2.05689
16	47.365	47.469	47.400	—0.056	44.080	44.024	2.05680
17	47.336	47.477	47.383	—0.039	44.087	44.048	2.05573
18	47.367	47.469	47.401	—0.057	44.102	44.045	2.05556
19	47.303	47.483	47.363	—0.019	44.063	44.044	2.05591
20	47.317	47.494	47.376	—0.032	44.069	44.037	2.05618

X-RAY STUDY

Single crystal Weissenberg- and rotation photographs were taken of several samples of different composition. This method, however, was found not to be as precise as was needed for the determination of the relation between cell parameters and chemical composition. Therefore diffraction measurements with a wide-angle Philips goniometer were used for the precies determination of interplanar spacings. A silicon powder was used as internal standard. The 410 reflection ($2\theta = 44.020°$ for $CuK\alpha_1$) was used for the measurement of cell parameters. Also the reflections 004 and 006 were measured, but they turned out to be too weak for precise determinations. Table 4 gives the measured 2θ-angles corrected by means of silicon reflections and the calculated d-spacings.

If one supposes, that the change of d_{410}-spacing is linear in the $BaSO_4$-$SrSO_4$ solid solution, 1 mol-% $SrSO_4$ in baryte causes a decrease of 0.00126 Å in d_{410}. From the synthetic barytes the present author has established that 1 mol-% $CaSO_4$ in baryte corresponds to the change of 0.00196 Å in d_{410}. Thus one can get the equation $d_{410} = 2.05699—0.00126.\ Sr—0.00196.\ Ca$ for d_{410}-spacing of the baryte, where Sr and Ca are Sr-mol-% and Ca mol-% of the mineral.

Figure 6. presents the relation between measured and calculated d_{410}-values. The effect of $PbSO_4$ was not observed in calculations because the amonts of $PbSO_4$ in the analyzed samples were very small.

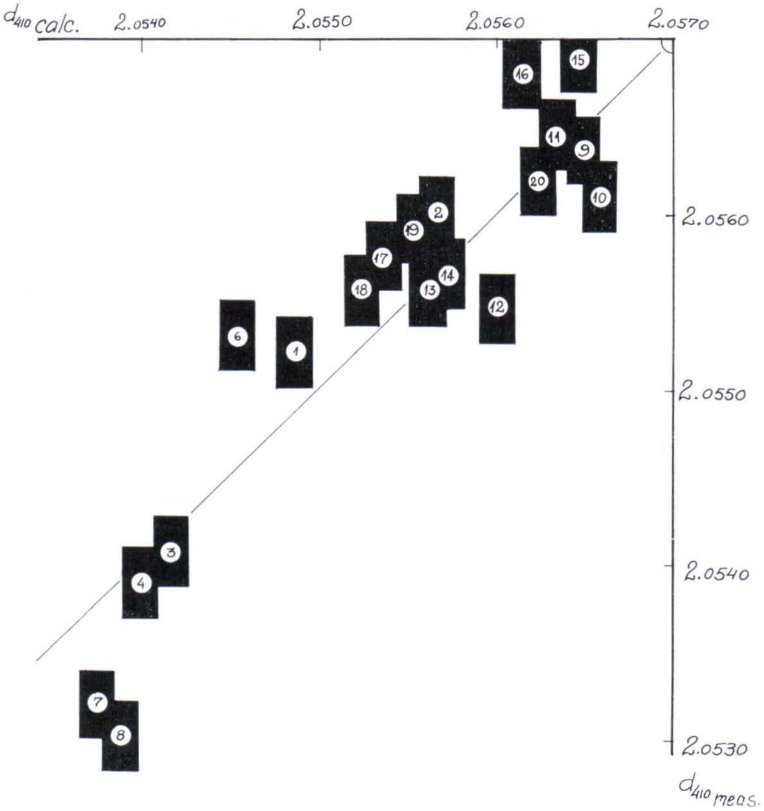

FIG. 6. Relation between measured and calculated d_{410}-spacings. Rectangular figures are the error boxes.

THE DIADOCHY OF CA IN THE BARYTE AND ITS SIGNIFICANCE

Contrary to $SrSO_4$ and $PbSO_4$, which form complete solid solutions with baryte, Ba in $BaSO_4$ is only partially substituted by Ca. Some experiments were arranged to study the limits of the substitution.

The effect of the ionic concentrations of the solutions was studied by precipitating sulfate with H_2SO_4 from water solutions containing different amounts of Ba and Ca. The precipitation process has been described previously by Starke and Rühlicke (1961). The cation percentage compositions of the solutions were 0.8 %, 2.84 %, 8.88 % and 22.63 cation-% Ba (Ba + Ca = 100 %). The precipitation was carried out at a temperature of 80°C. The d_{410}-reflection was measured from every precipitate using the X-ray diffraction technique described on the foregoing pages. The measured d-spacings are in Table 5. It is clearly seen that the d-spacings of the precipitates depend

TABLE 5.

Determination of d_{410} of the precipitated $BaSO_4$

Catione-% Ba in solution	$2\Theta_{220}$ of Si-standard			△	$2\Theta_{410}$ of $BaSO_4$		d_{410} of $BaSO_4$
	$CuK\alpha_1$	$CuK\alpha_2$	$CuK\overline{\alpha}$		$CuK\overline{\alpha}$ meas.	$CuK\overline{\alpha}$ corr.	
100.00	47.341	47.463	47.382	—0.038	44.058	44.020	2.05699
22.63	47.384	47.500	47.423	—0.079	44.108	44.029	2.05663
8.88	47.341	47.467	47.383	—0.039	44.078	44.039	2.05618
2.84	47.342	47.462	47.385	—0.041	44.088	44.047	2.05583
0.80	47.312	47.439	47.354	—0.010	44.078	44.068	2.05538

TABLE 6.

Determination of the relation between d_{410}-spacing and Ca-content of the $CaSO_4$-$BaSO_4$ mix crystals

$CaSO_4$ wt-%	$CaSO_4$ mol-%	$BaSO_4$ $2\Theta_{(410)}$	d_{410}	D	R	△
0	0	44.020	2.05699			
3	5.04	44.223	2.0480	90	17.67	—1.95
6	9.86	44.487	2.0366	204	20.58	0.96
9	14.50	44.700	2.0272	298	20.49	0.86
12	18.95	44.828	2.0220	350	18.42	—1.21
15	23.23	45.146	2.0082	488	20.97	1.34
				mean	19.62	

D = difference between the d_{410}-value of $CaSO_4$-$BaSO_4$ mix crystal and that of pure $BaSO_4$ ($\times 10^{-4}$ Å)
R = relation between difference (D) and percentage content of $CaSO_4$
Δ = error of R from the mean value

on the primary Ba to Ca-proportions of the solutions. Thus the Ca-content of the $BaSO_4$ precipitate evidently increases according to the Ca to Ba-proportion of the primary solution. These d-spacings do not, however, give the exact Ca-content of the precipitate. To determine the relation between d-spacings and Ca-content of the baryte, Ca-rich synthetic barytes were prepared by mixing measured amounts of $CaSO_4$ and $BaSO_4$, which were then homogenized by heating at almost the melting point of baryte. The homogenity of the mix-crystals was verified under the microscope. From the mix-crystals the d_{410}-spacings were measured. The results are represented in Table 6 and in Fig. 7. From the d-values in Table 6 one can calculate that one mol-% $CaSO_4$ in $BaSO_4$ reduces the d_{410}-value by 0.00196 Å, with the standard deviation of 0.000126 Å. By means of this value the compositions of the precipitated sulfates can be determined. Calculations are given in Table 7.

On the basis of the relative contents of the Ca-cations in primary solutions and in precipitated sulfates, diagram 8 can be drawn. From the form of the curve it is estimated that the cation-relation Ca : Ba = 125 : 1 leads to the maximum Ca-content of the baryte precipitated at 80°C.

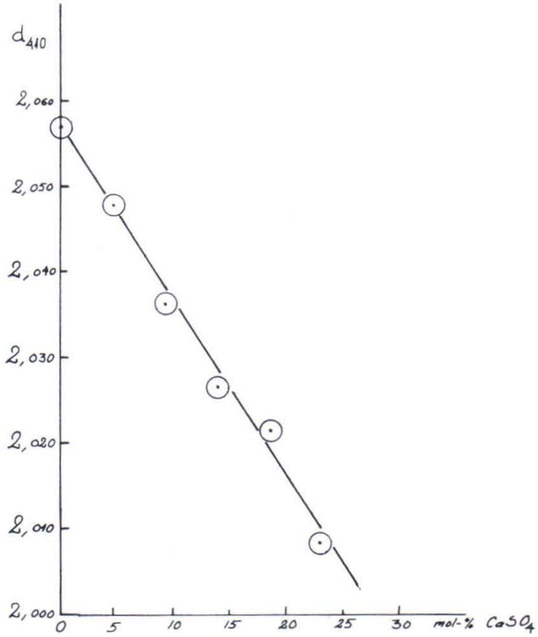

FIG. 7. Dependence of the d_{410}-spacing of $CaSO_4$-$BaSO_4$ mix crystal on the composition.

TABLE 7.

Determination of the composition of the precipitated $CaSO_4$-$BaSO_4$ mix crystals

Catione-% Ba in solution	$2\Theta_{410}$ of the precipitate	d_{410}	D	mol-% $CaSO_4$
22.63	44.029	2.05663	36	0.18
8.88	44.039	2.05618	81	0.41
2.84	44.047	2.05583	116	0.59
0.80	44.068	2.05538	161	0.82

D = difference of the value of d_{410} from that of pure $BaSO_4$ ($\times 10^{-5}$ Å)

As the $CaSO_4$-content of about 0.2 wt-% was maximum in the natural barytes analyzed here, the Ca-contents over 0.2 wt-% are, from the viewpoint of this study, of theoretical interest only. It is also most probable that the barytes described here have crystallized at temperatures far exceeding 80°C. Thus it is obvious that the $CaSO_4$-$BaSO_4$ mix crystals cannot be used as a mineralogical thermometer without $CaSO_4$ in the paragenesis. Variations of Ca-contents in the barytes described here are principally dependent on the concentrations of the primary solutions.

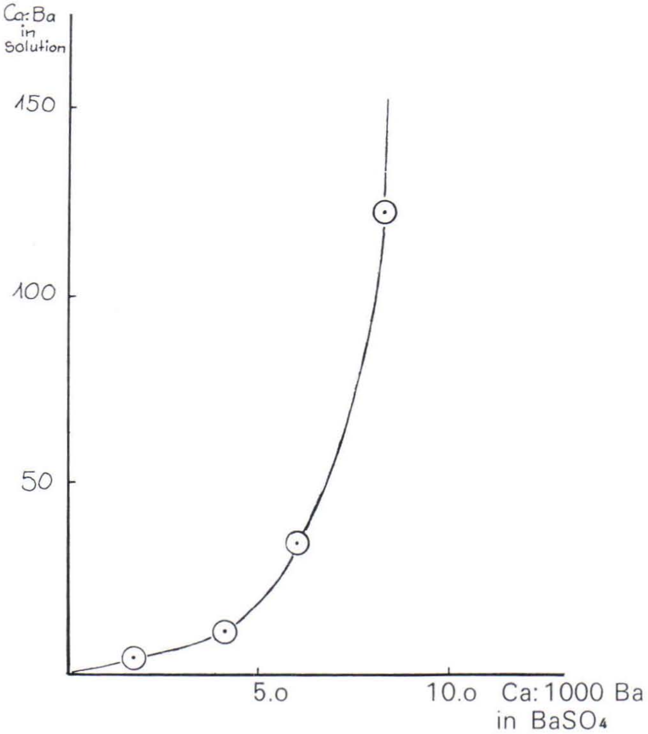

FIG. 8. Relation between the concentration of the solution and the composition of the mix crystal, which have precipitated at 80°C.

TWINNING OF BARYTES AT INVERSION

Palache et al. (1951) denotes that baryte inverts at 1 149°C to the high temperature form, which is monoclinic and isostructural with high-anhydrite and high-celestine. Though it is inconceivable how these minerals could have symmetry-rich low temperature forms and symmetry-poor high temperature forms, this could not be studied here, because the high temperature forms are not stable under a temperature of 1 149°C. The inversion of the baryte lattice leaves its mark, however, in the form of lamellar twinning of the grains. This twinning does not appear in the pure $BaSO_4$, but lamellae form very clearly as soon as a little $CaSO_4$ or some other strange cation is present. Thus it can be supposed that the irrelevant cation in the lattice of baryte forwards the development of the lamellae. In the natural barytes heated above the inversion point the beautiful lamellar texture is also formed (Fig. 9).

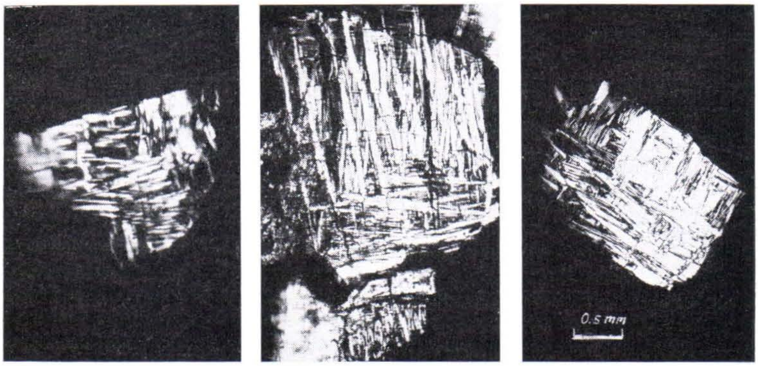

FIG. 9. Twinning of the baryte (specimen 18, Korsnäs), which has been heated over the inversion point.

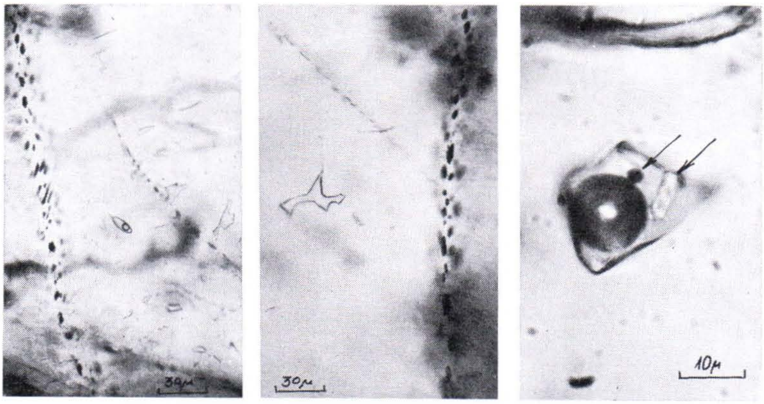

FIG. 10. Fluid inclusions of barytes. In Figs. A and B both zonal and single inclusions occur. In Fig. C there is a three-phase inclusion, which contains two small crystals (arrows).

INCLUSIONS

Tiny inclusions occur in almost every baryte grain. Most of them are minute mineral grains, but also irregular fluid inclusions can be seen. Fluid inclusions occur mostly as zones but also separate inclusions are met with. Some of them also contain small crystals floating in the fluid with a gas bubble (Fig. 10. C). Crystals are either transparent or opaque. The latter are, however, very sparse. The gas bubbles of the inclusions are generally mobile, sometimes the smallest bubbles are in Brownian motion, but also some jelly-like inclusions have been seen in the barytes of Juuka.

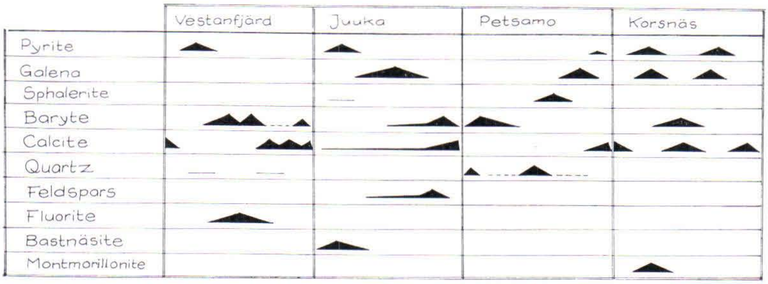

FIG. 11. Schematic crystallization diagram of the minerals which occur together with baryte.

These inclusions may be oversaturated. As the jelly-like and also the three phase inclusions occur only accidentally it is most probable that the primary fluids from which the barytes have crystallized have been generally very diluted.

ON THE PARAGENESIS OF THE BARYTES:

Since the paragenesis of the baryte is examined in different classes of deposits, the deposits of the first and second type must be regarded as the most distinct, because in these the conditions of crystallization best correspond to the precipitation of $BaSO_4$ from aqueous solutions.

Fig. 11. represents the schematic crystallization sequence of the Vestanfjärd, Korsnäs, Panjavaara and Petsamo baryte bearing paragenesis. From that it can be seen that calcite crystallizes together with baryte, but quartz and baryte are incompatible, which is possibly due to water-soluble barium-metasilicate $BaSiO_3$ formed by the reaction between SiO_2 and $BaSO_4$. The crystallization of sulfides and barytes has not generally taken place at the same time in deposits of this type. Only the galena of Panjavaara has cocrystallized with baryte; the pyrite occurring as inclusions in the barytes of Korsnäs is very sparse. In the mineral associations of the third deposit type the baryte occurs together with sphalerite. This is most evident in the Pyhäsalmi deposit.

BARYTE AS THE INDICATOR OF THE CONDITIONS OF CRYSTALLIZATION:

Being a very insoluble sulfate, baryte is an indicator of the existence of sulfate ions in the deposition forming fluids. In the system containing different ions of sulphur, the existence of sulfate-ion generally depends on the redox-potential (Eh) of the solution. The Eh-pH-diagram of different sulfur ions has been presented *e.g.*

by Barnes and Kullerud (1961). According to crystallization products the hydrothermal solutions often contain chalcophile cations and sulfidic ions. As the solubility products of most sulfides are very small, it is probable that the chalcophile cations must exist in solutions as complex compounds, for example as polysulfide complexes. Polysulfide complexes of this type have been described by Cloke (1963). According to him the stability field of polysulfides in the Eh-pH-system is very limited and thus small changes in Eh or pH cause variations in equilibrium in the polysulfide — sulfide system, and can increase the activity of sulfide or sulfate ions. The increase in pH of the system containing polysulfides due to reaction with carbonate rocks for example, can thus cause the precipitation of baryte, since the activity of sulfate ion increases so much that the solubility product of baryte is exceeded.

The mineral association of the Vestanfjärd baryte is the only one that contains fluorite in significant amounts. Fluorite has been regarded as a typical hydrothermal mineral. The mineral forming fluids have been acid, as they have dissolved the carbonate rock and formed the cavities for the mineral druses. These hydrothermal solutions contained polysulfide anions and fluoride ions and as cations Ba and Fe. By reaction with the carbonate rock the pH of the fluid increased, the polysulfide complexes decomposed and the activity of the sulfate-ion increased so much that baryte precipitated. When $CaCO_3$ dissoved, the activity of Ca^{2+} increased until the solubility product of CaF_2 was reached and fluorite precipitated. The crystallization of calcite depends on the activity of CO_3^{2-} and thus on the pressure of CO_2 and total pressure. The variations of pressure and/or pH of the solution can cause the crystallization of calcite as a new generation.

The mineral associations of the Korsnäs cavity barytes prove that calcite can crystallize together with pyrite, but baryte and sulfides do not crystallize together. This can be explained by the constant sum of sulfur ions in mineral-forming fluids. As the activity of sulfate ions increases for any reason, for example by oxidation of the system, this causes a decrease in the sulfide ion activity. This sequence is seen *e.g.* in specimen no 17, where pyrite has crystallized before and after baryte but not at the same time. It is probable that variation in the activity of SO_4^{2-} ion has caused alterations in the crystallization of sulfides and sulfates.

In Juuka, the sulfides principally occur near the walls of the veins and baryte in the core. Thus sulfides crystallized at the first stage and the sulfate minerals at the last. The primary solutions were carbonatic fluids at high pressure and moderate temperature and contained Ba, Pb, Fe and Ce as cations in addition to Ca, Mg and alkalies and sulfides and polysulfides as anions. At the beginning of the deposition the activity of SO_4^{2-} ion was very small but increased by oxidation during the filling of the vein and thus at the end reached the solubility product of baryte.

The substances of the Petsamo veins have been less complicated than those of Panjavaara. Tectonic events have played an important role in the formation of veins, which is proved by the numerous breccias. It is obvious that baryte has crystallized at a very early stage and sulfides, galena and sphalerite and chalcopyrite later.

The deposition forming solutions have thus been oxidized at the beginning and later changed into the reduced form.

On the basis of the total mineralogical and chemical composition the similarity of the Vihanti and Pyhäsalmi deposits is obvious. Differences occur, however, in the form and structure, and also in the host rocks of the deposits. The main differences are the carbonatic and skarn host rocks of Vihanti which do not occur in Pyhäsalmi and also the localization of iron sulfide and zinc-ores separately in Vihanti, whereas in Pyhäsalmi they have been localized in the same place. Investigations on correlation prove however, that even here separate pyrite mineral association and sphalerite-baryte associations exist and they occur together only accidentally.

In the Vihanti deposit, according to A. Mikkola (1963, p. 40), even though »Many features point to an epigenetic origin and some of these are hydrothermal» also a sedimentary origin, somewhat similar to that of Rammelsberg and Meggen, is possible (A. Mikkola, 1963, p. 41). By reason of the structural, textural and compositional features of the ores of Vihanti and Pyhäsalmi it is most probable that both deposits are either epigenetic or have been almost remobilized by metamorphic events. It seems likely that the materials have been similar, but that various tectonic events and unequal host rocks have caused differences of the ore deposits. In view of the baryte deposition the ideas concerning the role of polysulfides as described by Cloke (1963) are worthy of consideration. According to him (Cloke 1963, p. 1314) the reactions with carbonate rocks, such as in Vihanti can cause decomposition of polysulfides. This increases the activity of sulfide and also sulfate ions and thus sulfidic and sulfatic minerals form. The fact that sphalerite and pyrite occur separately is possibly due to their deposition at different acidity of the system; or pyrite ores may have been formed by the reaction of sulfide ion with iron silicates. In that case the pyrite ores occur near the rocks from which they have received the iron. This sulfurization has caused the Mg-enrichment of the wall rocks.

The reaction with carbonate rocks and the change of pH were, however, the primary reaction to cause the deposition of the Vihanti ore.

As carbonate and skarn rocks are almost fully lacking in Pyhäsalmi, the change of pH cannot have caused the deposition of the ore. According to Cloke (1963, p. 1316) the reaction of sulfide ion with iron silicates in the polysulfide-sulfide system can change the equilibrium of the system and cause the decomposition of polysulfides to sulfide and sulfate ions. This may be the reason for the deposition of the Pyhäsalmi baryte. The iron of the deposit thus originates from the wall rocks: The breccias and the banded structure of the ore prove that tectonic movements have played an important role in the deposition of both the Pyhäsalmi and the Vihanti ore.

The Taporova iron ore has been considered as sedimentary. The absence of sulfides and the occurrence of ferric iron minerals (hematite) prove the high state of oxidation in the system. Such a state can best be explained by oxidated sedimentic environments. Also the deformed texture of the baryte (lamellae, twins) proves that it belongs to the primary mineral association of the rock and has been deformed in metamorphosis as all the other minerals of the rock.

CONCLUSIONS

The barytes of Finland have been classified into four groups: 1) cavity barytes, 2) vein barytes, 3) baryte as a gangue mineral of the massive sulfide ores and 4) sedimentary baryte. Compositions of the barytes vary within narrow limits and differences of the compositions are due to variations in cation concentrations of the fluid. The effect of temperature on the composition has not yet been determined totally and numerically. In $CaSO_4$-$BaSO_4$ mix crystals this effect is much smaller than that of cationic concentrations. The Ca-content of the baryte cannot be used as a mineralogical thermometer without $CaSO_4$ as a separate phase in the system. The occurrence of baryte proves the existence of sulfate ions in the mineralizing solutions. Variations in the concentrations of anions can cause the precipitation of the baryte if Ba is present in sufficient amounts. The sulfate ion activity of the system can increase due to oxidation or an increase of pH, if polysulfide complexes exist in the system together with other ions of sulphur. As the solubility product of the baryte increases together with the temperature, so also a decrease in temperature can cause the crystallization of baryte. There is no unambigous evidence as to whether the baryte in a deposit has precipitated by an increase in the activity and concentration of the sulfate ions or by a decrease in the temperature, because they usually occur together. The effects of both of them must be explained in accordance with the facts characterizing the case.

Acknowledgements — Prof. K. J. Neuvonen of the university of Turku has inspired me in this study. For this I am deeply grateful. I should like to thank the geologists of the Outokumpu Co who gave me valuable aid by collecting and analyzing the samples. I also thank the foundation »Outokumpu Oy:n Säätiö» for the grants which made this work possible.

Manuscript received, March 2, 1967

REFERENCES

Ahlfors, B. (1954) The limestone quarries of the firm of Karl Forsström Aktiebolag in »The mines and quarries of Finland» by E. Aurola, Geotekn. julk. no 55, p. 81, Helsinki.

Barnes, H. L. and Kullerud, G. (1961) Equilibria in sulfur-containing aqueous solutions, in the system Fe—S—O and their correlation during ore deposition. Econ. Geology 56, pp. 648—688.

Cloke, Paul L. (1963) The geologic role of polysulfides — Part II Geoch. Cosmoch. Acta vol. 27, pp. 1299—1319.

Eskola, P., — Hackman, W. — Laitakari, A. — Wilkman, W. W. (1919) Suomen kalkkikivi, Geotekn. julk. No. 21, Helsinki.

Fisher, R. A. (1958) Statistical methods for research workers, London.

Hausen, H. (1926) Über die prequartäre Geologie des Petsamogebietes am Eismeere. Bull. Comm. Geol. Finlande No. 76.

—»— (1932) Die Bleiglanz—Zinkblende—Lagerstätten an der Küste von Petsamo, Fennia 57, No. 2.

Helovuori, O. (1964) Malmiesiintymän geologia in »Kurppa — Helovuori — Myyryläinen: Outokumpu Oy Pyhäsalmen kaivos». Vuoriteollisuus — Bergshanteringen No. 1. Helsinki (Finnish, with an English summary).

Isokangas, P. (1954) The Vihanti zinc deposit. Geotekn. julk. No. 55, p. 29, Helsinki.

Kalb, G. (1928) Die Kristalltracht des Kalkspates in minerogenetischer Betrachtung, Zentralblatt für Mineralogie A, p. 337.

—»— (1929) Bemerkungen zu den minerogenetischen Kristalltrachttypen des Kalkspates, Zentralblatt für Mineralogie A. p. 137.

—»— — Koch, L. (1931) Die Kristalltracht des Baryt in minerogenetischer Betracht. Groth' Zeitschr. Kristallogr. 78, p. 169.

Kouvo, O. (1958) Radioactive age of some Finnish Pre-Cambrian minerals. Bull. Comm. geol. Finlande 182.

—»— — Kulp, L. (1961) Isotopic composition of Finnish galenas, Ann. New York Academy of Sci. Vol. 91, pp. 476—491.

Laatio, G. — Mikkola, A. (1957) Outokumpu Oy, Vihannin kavos, Vuoriteollisuus — Bergshanteringen No. 1, Helsinki.

McEwan, D. M. C. (1961) Montmorillonite minerals in »The X-ray identification and crystal structures of clay minerals» Min. Soc. London.

Mikkola, A. (1963) On the sulphide mineralization in the Vihanti zinc deposit, Finland. Bull. Comm. geol. Finlande No. 205.

Mikkola, Toivo (1960) Kolarin rautamalmeista, Geologi No. 8, pp. 89—90, Helsinki.

Neuvonen, K. J. (1960) The crystal cavities of Illo, in »Aurola — Neuvonen: Nonmetallic mineral deposits, Finland». Int. Geol. Congr. XXI, Guide to Excursions, Copenhagen.

Palache, C. — Berman, H. — Frondel, C. (1951) The system of mineralogy of J. D. Dana and E. S. Dana. Vol. II, 7th ed. New York.

Pehrman, G. (1947) Om mineraldrusen i Vestanfjärd. Acta Acad. Aboensis, Mat. & Phys. XV. 11.

Starke, R. — Rühlicke, D. (1961) Eine Methode zur flammenphotometrischen und röntgenographischen Bestimmung von Strontium und Kalzium im Baryt. Bergakademie 7—8, pp. 505—511.

Starke, R. (1963) Die Strontiumgehalte der Baryte. Bergakademie 15. Jg. pp. 404—408.

Comptes Rendus de la Société géologique de Finlande
N:o XXXIX (1967), pp. 71—86

ON DATING THE GENESIS OF PEAT BANKS AND HOLLOWS IN THE RAISED BOGS OF SOUTHWESTERN FINLAND

BY

TOIVE AARTOLAHTI

Department of Geography, University of Helsinki

ABSTRACT

The purpose of the present study is to determine the time of origin of the peat banks and bog hollows in the raised bogs of southwestern Finland. According to the C 14 datings their development started already 3 200—3 100 years ago. Two periods of accelerated growth could be distinguished, the first one 3 200—3 100 years ago, and the second one 2 100 years ago. The palsas and aapabog ridges in northern Finland and the peat banks and bog hollows on the Swedish raised bogs have arised simultaneously. This is due to general deterioration of climate in vast areas during the time in question.

INTRODUCTION

In an earlier paper (Aartolahti 1965, pp. 164, 248) I have expounded the time of origin of certain small formations situated in raised bogs, formations like *Sphagnum* banks (in Finnish »*kermi*»), or »strings», hollows (in Finnish »*kulju*») and pools. It was brought out that in the regions of southwestern Häme and northern Satakunta — that is, in southwestern Finland in general — these formations originated not long after the general spread of the spruce tree. The evidence indicates that they appeared during the deterioration of the climate around the turn of the Sub-Boreal and Sub-Atlantic periods, possibly at the beginning of the Sub-Atlantic period. It was subsequently perceived (Aartolahti 1966) that the spruce became common in different parts of Finland at different times. This raised the question as to whether the formations might not likewise have appeared in different parts of the country at different times. The purpose of the present study, then, is to determine, by means of C14 datings, the time of origin of certain small formations in southwestern Finnish bogs toward the end of ascertaining whether they originated at different times in different areas.

METHODS and FIELD STUDIES

In dating the origin of peat banks and hollows, I have used the *Sphagnum*-leaf method (Aartolahti 1965, pp. 132—134). This involves ascertaining what species of *Sphagnum* have formed the banks and what species, on the other hand, have formed the peat underlying the hollows. The peat in both cases consists of species of *Sphagnum* of its own. The method is aimed to differentiate the peat varieties of adjacent banks and hollows in bogs. At any level where the difference between species of *Sphagnum* vanishes and the same species of *Sphagnum* are found to exist in by and large the same proportions in both the peat banks and at the bottom of adjacent hollows, or where, to judge by the species represented, the same kind of vegetation may in general be deemed to have prevailed, the differentiation of the surface of the bog into banks and hollows must have started.

Efforts were made to locate the oldest banks and hollows of each bog during the field investigations. In each bog the formations that extended to the greatest depth were naturally considered to be the oldest. And these were the ones from which series of samples were taken for laboratory study. In the search for deep hollows, open pools have greatly facilitated matters. As a large proportion of the banks and hollows reaches to the same depth, roughly speaking, the probability is that by and large they originated at about the same time. In dating, age differences of a few hundred years are liable, however, to result easily, depending on the choice of drilling site. This is a likelihood even in the same bog, let alone different bogs, where any comparison of levels of differentiation is more difficult on the basis of pollen diagrams alone.

Moreover, local circumstances may have prevented the formation of banks and hollows in some bog for one reason or another (most often dryness) at a stage during climatic deterioration when they have started to develop in other bogs where conditions have favored the process. Accordingly, field investigations involving bogs of the former type are often apt to prove fruitless. In certain cases, the pollen diagrams alone make it plain that, in spite of considerable depths, the process of differentiation into banks and hollows had started at a later date in some bogs than others. However, this circumstance is not always brought out by pollen diagrams, though readily revealed by the C14 dating method. The surest way is to look for ancient banks and hollows in bogs which research has already proved to have been sufficiently wet and convex at the time the climate turned colder (cf., Aartolahti 1965, pp. 250—251). Bogs of this kind are to be found with the least trouble in the interior of the country. On the other hand, most of the bogs situated near the coast evolved into raised bogs with a convex surface considerably after the spruce had become generally established (cf. Aartolahti 1965, p. 217, appendix 4). Thus, banks and hollows could not form in them at the stage when climatic conditions would have made it possible.

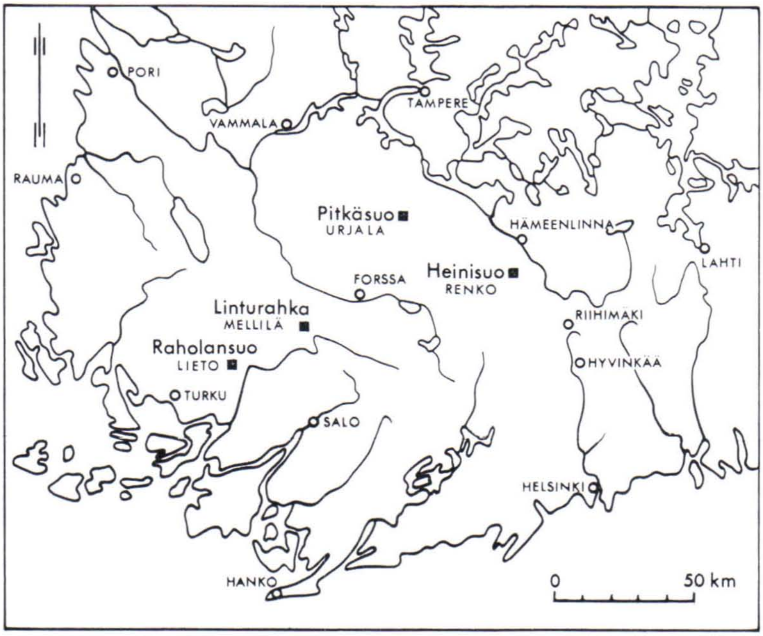

FIG. 1. Map of area investigated. Black squares = bogs investigated.

BOGS and C14 DATINGS

The investigation concentrated on four bogs: Raholansuo, at Lieto; Linturahka, at Mellilä; Pitkäsuo, at Urjala; and Heinisuo, at Renko (Figure 1). In the selection of bogs, a factor kept in view was whether there were differences between coast and interior with respect to the time of differentiation. In the case of each bog, the level of differentiation is presented by means of a *Sphagnum*-leaf table (Tables 1—4). In addition, a pollen diagram of each bog is given to enable the C14 datings obtained to be applied in connection with subsequent investigations embracing these areas.

Raholansuo (Fig. 2, Table 1), in the northern part of the commune of Lieto. After the deposition of the mud, the area turned into a treeless *Carex* bog. The *Sphagnum* is identifiable from a depth of 3.3 meters. Judging from the macrosubfossils, the bog was then distinguished by the prevalence of *Sphagnum apiculatum* and birch trees, soon after which it became more barren, though still supporting trees, with *Sphagnum parvifolium* the dominant species of moss. At a depth of 3.2—3.1 meters, ther is a stratum of *Eriophorum-Sphagnum* peat, whereas at 3.0 meters the peat has become rich in *Sphagnum fuscum*. The differentiation of the bog surface into strung-out banks and hollows took place at the 2.5 m-level, as shown in Table 1. The spruce had by that time achieved its maximum and was already on the wane. The dating of

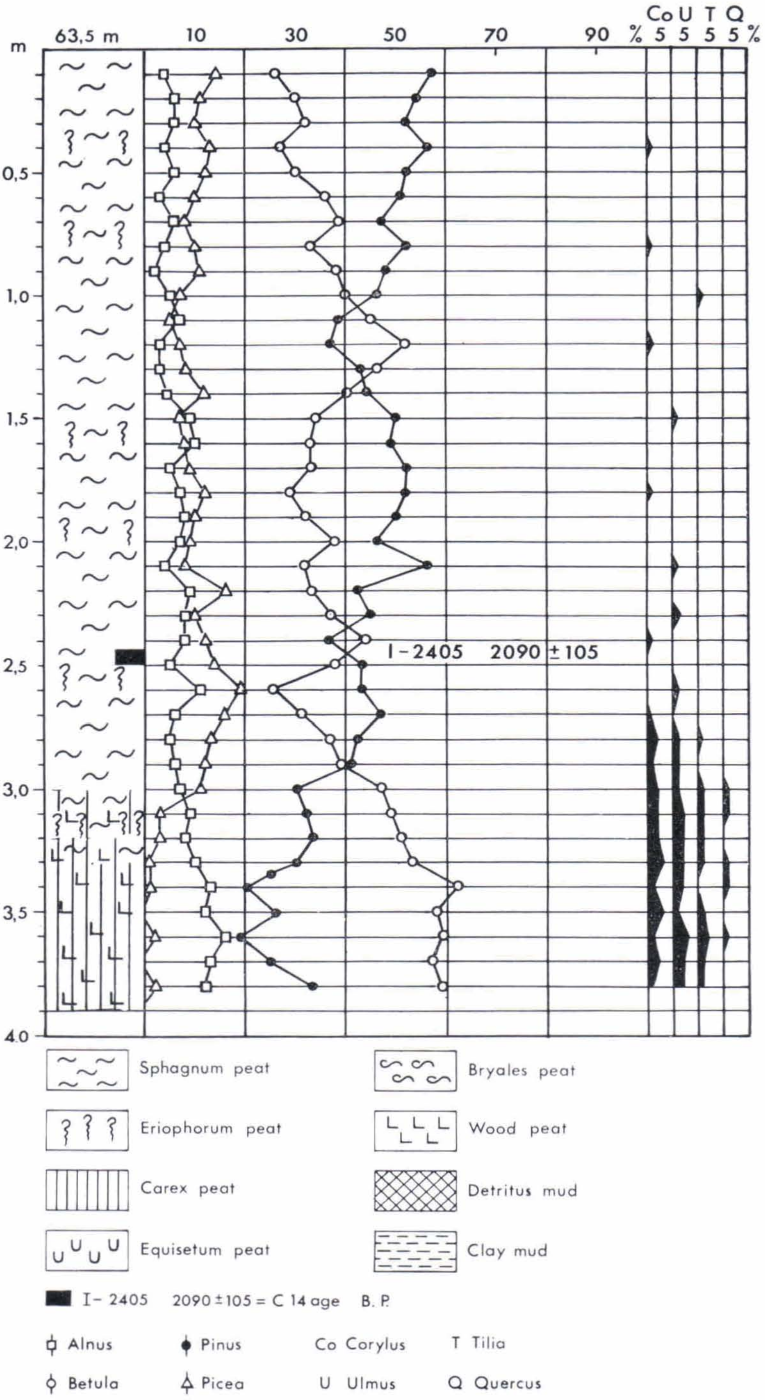

FIG. 2. Pollen diagram from Raholansuo, Lieto.

TABLE 1.

Sphagnum-leaf analyses from Raholansuo

Dehpt	Peat Bank							Bog Hollow									
	S. fuscum	*S. rubellum*	*S. parvifolium*	*S. magellanicum*	*S. balticum*	*S. papillosum*	*S. apiculatum*	*S. fuscum*	*S. rubellum*	*S. parvifolium*	*S. magellanicum*	*S. balticum*	*S. Duseni*	*S. cuspidatum*	*S. papillosum*	*S. apiculatum*
0.1	94	—	1	5	—	—	—									
0.2	95	—	2	3	—	—	—									
0.3	100	—	—	—	—	—	—	—	5	—	2	54	—	39	—	—
0.4	100	—	—	—	—	—	—	2	—	—	—	13	10	75	—	—
0.5	98	2	—	—	—	—	—	—	—	—	—	9	—	91	—	—
0.6	100	—	—	—	—	—	—	—	7	—	—	8	—	85	—	—
0.7	98	—	2	—	—	—	—	6	—	—	—	60	—	34	—	—
0.8	95	—	5	—	—	—	—	14	—	—	—	77	—	9	—	—
0.9	93	—	4	3	—	—	—	3	—	—	—	86	—	21	—	—
1.0	96	—	4	—	—	—	—	5	1	—	9	59	30	6	—	—
1.1	98	—	2	—	—	—	—	8	5	—	—	87	—	—	—	—
1.2	95	—	3	2	—	—	—	11	—	—	—	89	—	—	—	—
1.3	100	—	—	—	—	—	—	—	9	—	3	88	—	—	—	—
1.4	96	—	3	1	—	—	—	2	—	5	—	84	—	9	—	—
1.5	96	3	1	—	—	—	—	—	4	—	—	96	—	—	—	—
1.6	100	—	—	—	—	—	—	11	—	—	—	89	—	—	—	—
1.7	98	—	2	—	—	—	—	—	—	—	3	41	—	56	—	—
1.8	96	1	—	3	—	—	—	—	—	—	1	15	—	84	—	—
1.9	93	4	3	—	—	—	—	12	—	—	—	6	—	82	—	—
2.0	98	—	2	—	—	—	—	6	—	—	—	18	—	73	—	—
2.1	100	—	—	—	—	—	—	13	2	—	—	44	—	41	—	—
2.2	100	—	—	—	—	—	—	8	—	2	3	79	—	9	—	—
2.3	97	—	—	3	—	—	—	42	10	—	—	48	—	—	—	—
2.4	84	—	4	12	—	—	—	27	—	—	4	64	—	—	—	—
2.5	96	—	3	1	—	—	—	17	4	4	—	75	—	—	—	—
2.6	100	—	—	—	—	—	—	83	—	15	—	2	—	—	—	—
2.7	93	—	7	—	—	—	—	96	—	4	—	—	—	—	—	—
2.8	9	2	89	—	—	—	—	71	—	5	14	—	—	—	—	—
2.9	21	—	71	3	—	—	—	32	—	65	—	3	—	—	—	—
3.0	3	—	85	12	—	—	—	15	—	79	6	—	—	—	—	—
3.1		—	78	22	—	—	—	4	—	81	15	—	—	—	—	—
3.2		—	67	—	10	4	19	—	—	54	—	7	—	—	8	31
3.3		—	23	—	—	6	71	—	—	3	—	—	—	—	8	89

the sample (I—2 405) taken from this differentiation level gives an age of 2 090 ± 105 years.

Linturahka (Fig. 3, Table 2), along the southern boundary of the commune of Mellilä. Overlying the thin layer of mud on top of the clay, there is a stratum of *Carex-Equisetum* peat, which transformed the area into a treeless *Carex* bog. Thanks to ample drainage conditions, the surface of the bog became dry, turning it into a *Sphagnum parvifolium* bog with trees. During the period marked by the general spread of the spruce, the bog produced a layer of *Eriphorum-Sphagnum* peat. Judging by the small number of hyphae, the bog would still appear to have been fairly wet. The first signs of the differentiation of the surface of the bog into banks and hollows are

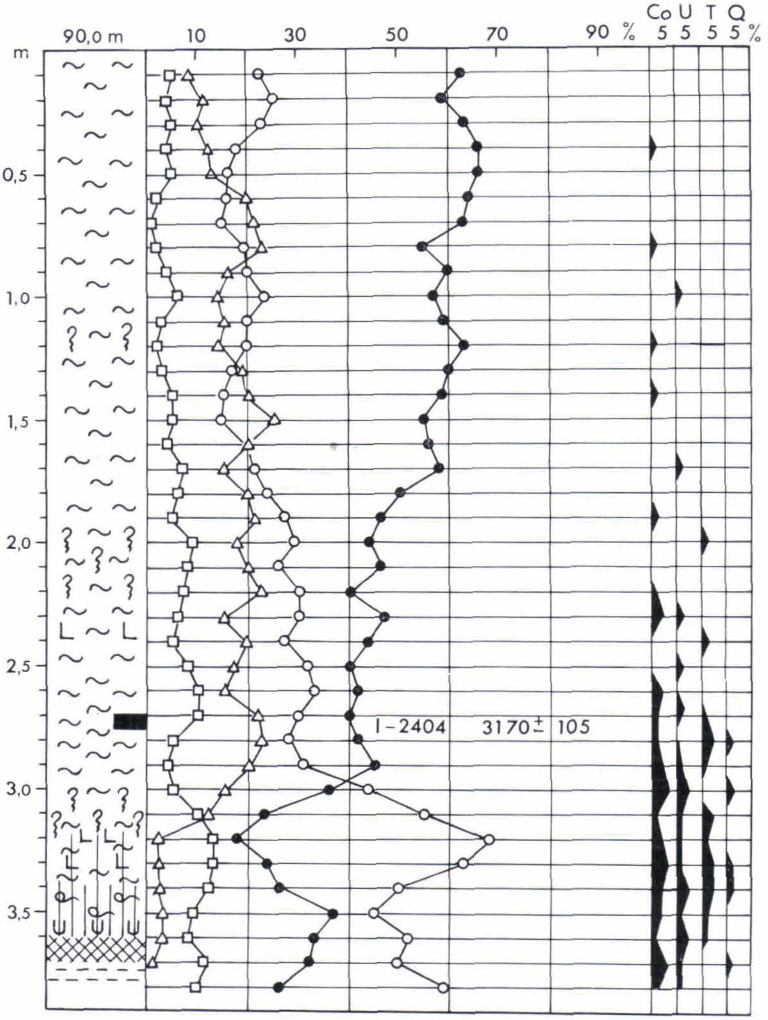

FIG. 3. Pollen diagram from Linturahka, Mellilä.

to be seen at the 2.7—2.8-m level, as shown in Table 2. After that the hollows reveal alternate stages distinguished by a rich content of *Sphagnum balticum* or of *Sphagnum cuspidatum*, while the stringy banks remain dominated by *Sphagnum fuscum* peat. The age of the specimen (I—2 404) extracted from the differentiation stage is 3 170 ± 105 years.

Pitkäsuo (Fig. 4, Table 3), situated in the commune of Urjala alongside the road leading from the church to Toijala. Overlying the thick stratum of clay mud, there is a thin layer of mud and *Equisetum* peat saturated with mud, which in turn is

TABLE 2.
From Linturahka

Depht	Peat Bank						Bog Hollow							
	S. fuscum	*S. rubellum*	*S. parvifolium*	*S. magellanicum*	*S. papillosum*	*S. apiculatum*	*S. fuscum*	*S. rubellum*	*S. parvifolium*	*S. magellanicum*	*S. balticum*	*S. Duseni*	*S. cuspidatum*	*S. apiculatum*
0.1	92	—	8	—	—	—								
0.2	96	—	3	1	—	—								
0.3	96	2	2	—	—	—	7	6	—	5	79	—	—	—
0.4	100	—	—	—	—	—	5	—	—	—	36	12	47	—
0.5	100	—	—	—	—	—	7	—	2	—	68	—	23	—
0.6	94	—	4	3	—	—	—	—	—	—	15	14	71	—
0.7	97	—	—	3	—	—	—	—	—	2	26	—	70	—
0.8	100	—	—	—	—	—	4	—	5	4	84	—	3	—
0.9	96	—	—	4	—	—	—	—	—	7	62	—	31	—
1.0	87	—	13	—	—	—	—	—	—	3	11	—	82	—
1.1	94	—	3	3	—	—	—	1	—	—	12	—	87	—
1.2	100	—	—	—	—	—	24	—	—	—	13	—	63	—
1.3	96	—	3	1	—	—	12	—	—	—	10	—	78	—
1.4	87	2	11	—	—	—	3	3	—	—	7	—	82	—
1.5	93	4	3	—	—	—	18	—	4	7	3	—	68	—
1.6	96	—	—	4	—	—	6	—	2	4	12	—	76	—
1.7	100	—	—	—	—	—	—	4	—	5	71	—	20	—
1.8	100	—	—	—	—	—	6	7	—	—	87	—	—	—
1.9	95	1	4	—	—	—	—	2	—	6	92	—	—	—
2.0	100	—	—	—	—	—	—	—	—	—	93	7	—	—
2.1	100	—	—	—	—	—	—	—	—	3	11	—	82	—
2.2	97	—	3	—	—	—	—	2	—	—	7	—	91	—
2.3	97	—	3	—	—	—	—	—	—	1	9	13	77	—
2.4	94	—	2	4	—	—	2	—	—	—	64	7	27	—
2.5	83	1	14	2	—	—	3	12	—	5	80	—	—	—
2.6	100	—	—	—	—	—	—	5	17	—	78	—	—	—
2.7	95	—	5	—	—	—	7	—	11	—	82	—	—	—
2.8	71	—	26	3	—	—	63	—	31	6	—	—	—	—
2.9	73	—	25	2	—	—	61	—	36	3	—	—	—	—
3.0	41	—	47	12	—	—	12	—	84	4	—	—	—	—
3.1	15	—	39	46	—	—	—	—	81	13	6	—	—	—
3.2	10	—	88	2	—	—	3	—	89	—	—	—	—	8
3.3	—	—	19	—	13	68	—	—	17	—	4	—	—	79
3.4	—	—	3	—	14	83	—	—	5	—	—	—	—	95

overlain by *Bryales*-rich sedge peat. Upwards from the depth of 3.5 m, the peat has undergone so little humification that the *Sphagnum* species can still be readily identified. At this stage the bog was covered with *Sphagnum apiculatum* and rich sedge growths as well as trees. At the 3.2-m level *Sphagnum parvifolium* became the prevailing species of moss and the trees persisted. Just before the general spread of the spruce, the bog was covered with a bed of *Eriophorum* peat. It was at the present 2.6-m level that the peat banks and hollows appeared in the bog, as shown in Table 3. The table further reveals that the bog had not prior to that been exclusively covered with *Sphagnum fuscum* — and thus dry — but probably fairly moist, judging also by the

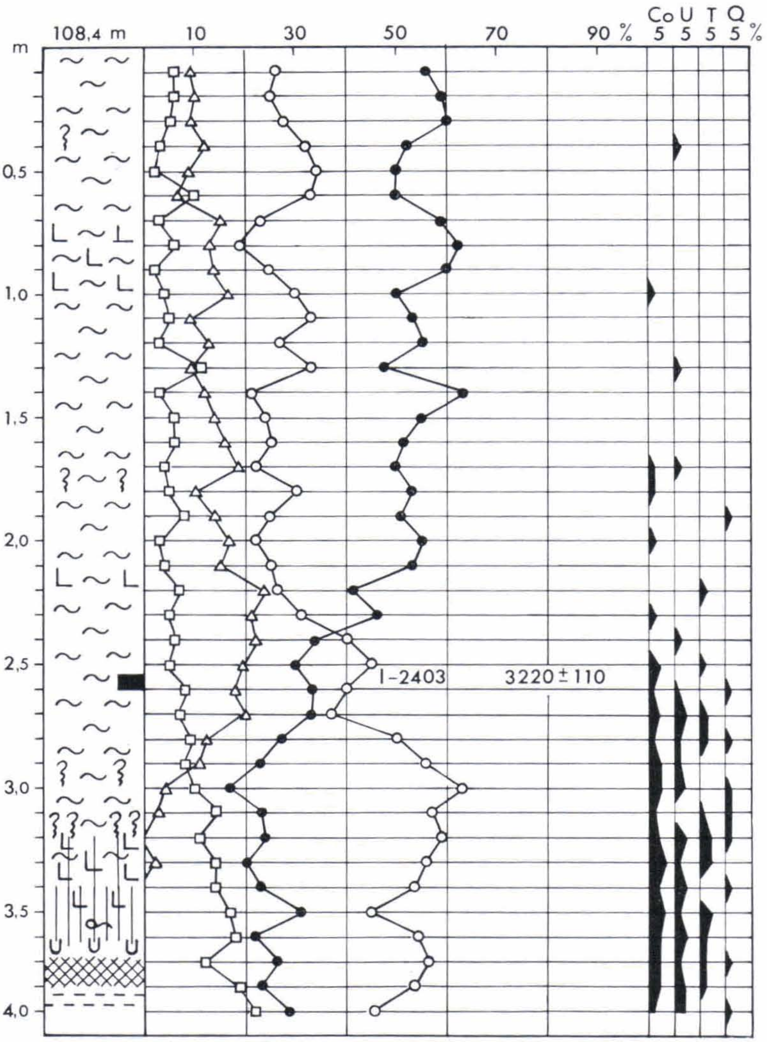

FIG. 4. Pollen diagram from Pitkäsuo, Urjala.

slight occurrence of hyphae. The moisture content of the hollows has varied from time to time, whereas the banks have remained continuously covered with *Sphagnum fuscum* and thus dry. The age of the differentiation stage, according to sample I—2 403, is 3 220 ± 110 years.

Heinisuo (Fig. 5, Table 4), at the boundary of Renko and Hämeenlinna. Overlying the thin layer of mud is a bed of *Carex* peat 0.8 m thick. The first indentifiable *Sphagnums* in this layer occur at a depth of 2.8 m. The subfossils indicate that the area at this time had been a treeless *Carex* bog with an abundant growth of

TABLE 3.
From Pitkäsuo

Depht	Peat Bank						Bog Hollow								
	S. fuscum	*S. rubellum*	*S. parvifolium*	*S. magellanicum*	*S. papillosum*	*S. apiculatum*	*S. fuscum*	*S. rubellum*	*S. parvifolium*	*S. magellanicum*	*S. balticum*	*S. Duseni*	*S. cuspidatum*	*S. papillosum*	*S. apiculatum*
0.1	98	—	2	—	—	—	—								
0.2	100	—	—	—	—	—	—								
0.3	97	—	3	—	—	—	—	—	—	—	84	5	11	—	—
0.4	100	—	—	—	—	—	—	—	—	5	42	—	53	—	—
0.5	100	—	—	—	—	—	9	—	—	—	11	—	80	—	—
0.6	96	—	3	1	—	—	—	—	—	—	23	1	76	—	—
0.7	99	—	1	—	—	—	—	—	—	—	86	11	3	—	—
0.8	89	—	11	—	—	—	—	—	—	—	74	26	—	—	—
0.9	100	—	—	—	—	—	—	1	—	—	15	84	—	—	—
1.0	100	—	—	—	—	—	—	—	—	—	11	86	3	—	—
1.1	98	—	2	—	—	—	—	—	—	—	22	10	68	—	—
1.2	97	—	2	1	—	—	10	—	—	—	4	—	86	—	—
1.3	96	1	3	—	—	—	7	—	—	—	19	—	74	—	—
1.4	100	—	—	—	—	—	—	2	—	—	16	—	82	—	—
1.5	100	—	—	—	—	—	9	—	2	—	74	—	15	—	—
1.6	100	—	—	—	—	—	—	21	—	5	74	—	—	—	—
1.7	94	—	6	—	—	—	9	2	—	—	89	—	—	—	—
1.8	83	—	17	—	—	—	—	—	—	4	96	—	—	—	—
1.9	100	—	—	—	—	—	5	—	—	—	32	—	63	—	—
2.0	100	—	—	—	—	—	1	—	—	—	4	—	95	—	—
2.1	89	—	9	2	—	—	—	—	—	—	14	3	83	—	—
2.2	100	—	—	—	—	—	—	—	—	—	13	—	87	—	—
2.3	100	—	—	—	—	—	—	—	—	—	38	47	15	—	—
2.4	97	—	3	—	—	—	—	—	—	—	36	64	—	—	—
2.5	83	—	15	2	—	—	2	—	—	—	98	—	—	—	—
2.6	100	—	—	—	—	—	32	14	—	—	54	—	—	—	—
2.7	79	—	10	11	—	—	63	—	21	16	—	—	—	—	—
2.8	86	2	12	—	—	—	52	—	44	4	—	—	—	—	—
2.9	42	—	56	2	—	—	21	—	72	7	—	—	—	—	—
3.0	15	—	74	11	—	—	9	—	82	9	—	—	—	—	—
3.1	27	—	35	38	—	—	4	—	48	48	—	—	—	—	—
3.2	—	—	89	11	—	—	—	—	97	3	—	—	—	—	—
3.3	—	—	21	15	—	64	—	—	16	2	—	—	—	—	82
3.4	—	—	16	2	—	82	—	—	5	1	—	—	—	—	94
3.5	—	—			8	92	—	—	—	—		—	—	15	85
3.6															

Sphagnum apiculatum. Next there followed a stage marked by the appearance of trees out of the *Sphagnum apiculatum*, which was later replaced by *Sphagnum parvifolium*, and, then, at the 2.5-m level, a stage characterized by the prevalence of *Sphagnum-Eriophorum* peat. Subsequently, the area developed into a raised bog overgrown with *Sphagnum fuscum* and, at least in the beginning, with many pine trees. The differentiation stage occurred at the 1.7-m level (Table 4). The hollows were quite watery, except for a brief transitional period, throughout the stage of their formation. The age of the sample (I—2 402) taken from the differentiation level is 2 090 ± 105 years.

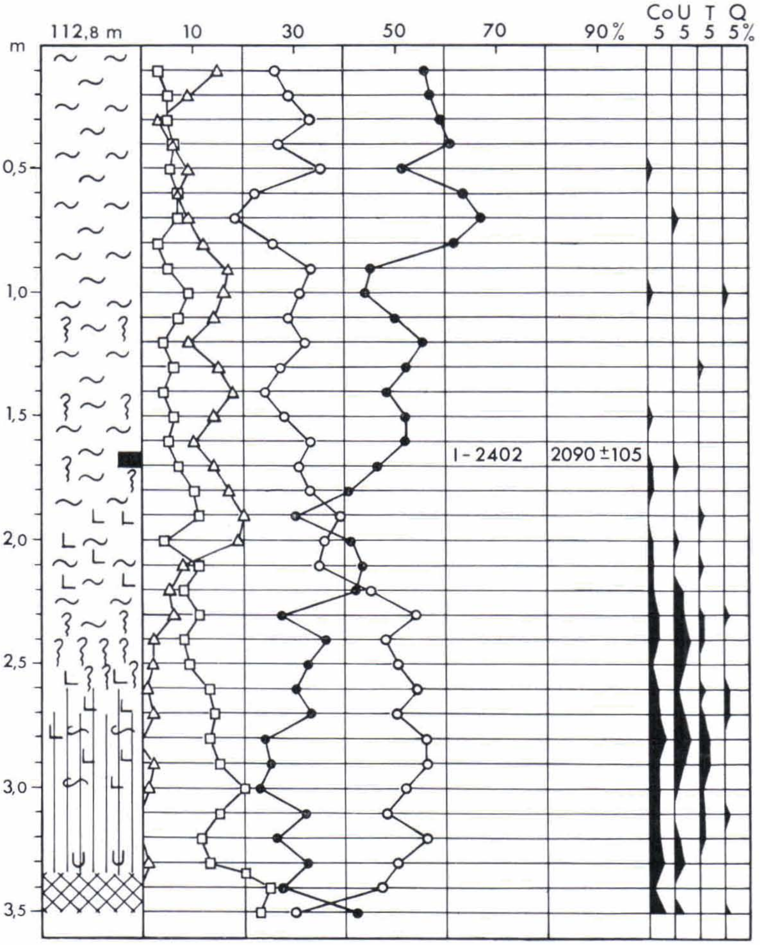

FIG. 5. Pollen diagram from Heinisuo, Renko.

DISCUSSION

The samples studied and their ages are thus as follows:

I—2 405	2 090 ± 105	years	Lieto
I—2 404	3 170 ± 105	»	Mellilä
I—2 403	3 220 ± 110	»	Urjala
I—2 402	2 090 ± 105	»	Renko

At first glance, the process of differentiation seems to have taken place at markedly different periods. The age difference between these periods in the bogs of Lieto and

TABLE 4.

From Heinisuo

Depht	Peat Bank							Bog Hollow							
	S. fuscum	*S. nemoreum*	*S. rubellum*	*S. parvifolium*	*S. magellanicum*	*S. balticum*	*S. apiculatum*	*S. fuscum*	*S. rubellum*	*S. parvifolium*	*S. magellanicum*	*S. balticum*	*S. Duseni*	*S. cuspidatum*	*S. apiculatum*
0.1	100	—	—	—	—	—	—								
0.2	96	—	—	4	—	—	—								
0.3	97	—	—	3	—	—	—	2	—	—	—	51	5	42	—
0.4	100	—	—	—	—	—	—	—	—	—	—	9	13	78	—
0.5	91	—	—	9	—	—	—	—	—	—	4	27	—	69	—
0.6	95	2	3	—	—	—	—	8	5	—	—	87	—	—	—
0.7	100	—	—	—	—	—	—	20	2	—	—	63	—	15	—
0.8	85	—	7	8	—	—	—	3	—	—	—	6	—	91	—
0.9	97	—	3	—	—	—	—	—	2	—	—	25	—	73	—
1.0	94	—	2	6	—	—	—	5	—	—	—	7	—	88	—
1.1	91	—	—	6	3	—	—	21	—	—	3	15	49	12	—
1.2	67	—	—	27	6	—	—	19	—	—	—	27	—	54	—
1.3	93	—	—	3	2	2	—	8	—	—	10	8	—	74	—
1.4	100	—	—	—	—	—	—	8	—	—	—	21	13	58	—
1.5	89	—	—	11	—	—	—	12	—	—	9	58	—	21	—
1.6	100	—	—	—	—	—	—	16	—	14	27	43	—	—	—
1.7	97	2	—	—	1	—	—	13	—	17	—	70	—	—	—
1.8	95	—	—	4	1	—	—	94	—	4	2	—	—	—	—
1.9	98	—	—	2	—	—	—	100	—	—	—	—	—	—	—
2.0	100	—	—	—	—	—	—	100	—	—	—	—	—	—	—
2.1	94	—	—	6	—	—	—	96	—	3	1	—	—	—	—
2.2	92	—	—	8	—	—	—	89	—	7	4	—	—	—	—
2.3	87	—	2	11	—	—	—	63	—	25	9	—	—	—	—
2.4	83	—	—	7	10	—	—	74	—	18	6	—	—	—	—
2.5	18	—	—	57	25	—	—	31	—	46	21	—	—	—	—
2.6	11	—	3	72	10	—	4	16	—	69	15	—	—	—	—
2.7	—	—	—	42	22	—	36	—	—	39	17	—	—	—	44
2.8	—	—	—	12	—	4	84	—	—	5	3	—	—	—	92

Mellilä is over a thousand years. On the other hand, the bogs at the opposite ends of the series, which are situated at a distance of 100 kilometers from each other, have yielded precisely the same age, 2 090 ± 105 years. There is very little difference between the samples from the bogs of Mellilä and Urjala, either — only 50 ± 110 years. Surely, it is no accident that peat banks and hollows should have started to form in two widely separated bogs simultaneously.

In a previous study, I made the observation that several banks and hollows in the same bog appear to begin from two different levels. Set against the pollen diagram, the lower level falls just before the first maximum of the spruce and the upper one shortly afterwards. Following the formation of the upper level, banks and hollows formed at various stages, and they have continued to develop until the present day. The C14 datings indicate the first period of their formation to have occurred some 3 100—3 200 years ago and the second approximately 2 100 years ago.

At the initial stage, differentiation occurred in places where the surface of the bog had been sufficiently wet and had had the necessary slope (cf., Aartolahti 1965, p. 74—78). As previously pointed out, on p. 75—79, the Linturahka bog at Mellilä and the Pitkäsuo area at Urjala had been wet in the formations making up their small relief (Tables 2 and 3). Thus, banks and hollows could form in these bogs as a consequence either of increasing cold or temporary dryness, or, most probably, of a combination of both circumstances. Evidence of a cooling down of the climate during this period, notably in northern Finland, is plentiful. According to Sorsa (1965, pp. 404—405), the boundary of both the birch and conifer forests retreated in the Arctic hills at the end of the Sub-Boreal period. The bald areas extending from the summits of the fells had thus expanded. Similar signs of a colder climate have also been observed by Aario (1943) in the Petsamo region, by Kanerva (1956) in the Hyrynsalmi region and by Vasari (1962) in the Kuusamo region. Toward the end of the Sub-Boreal period, the winters in particular became colder, and this circumstance played a decisive part in promoting differentiation in the bogs. Sauramo (1940, p. 254) remarked that the climate took a decisive turn for the worse (mainly by getting colder) in approximately 1 000 B. C.

The probability is that certain other phenomena, such as the appearance of ridges in *aapa* bogs and the formation of *palsas* (relatively high frost mounds of peat), were synchronous with the genesis of banks and hollows of raised bogs (cf. Ruuhijärvi 1962, p. 68, 1963, p. 35). According to G. Lundqvist (1951 a, p. 223), the formation of the *palsas* started slightly before 1 000 B. C., that is, fully 3 000 years ago. Ruuhijärvi (1963, p. 30) has noted that the increase of the birch took place at the end of his IV stage; and his conclusion was that the increase in the share of the birch at the expense of the pine was a consequence of the increase in humidity and the cooling down of the climate (cf., Ruuhijärvi 1962, p. 66). He has further observed (1963, p. 35) that it is no matter of chance that hollows should have formed in northern raised bogs in conjunction with the increase of the birch toward the end of his IV stage. In his view, the ground frost began at that time to remain in peat ridges in *aapa* bog even during the season of growth and to thrust them upward. This event was probably synchronous with the formation of the *palsas*. Later on, Ruuhijärvi dated the beginning of the youngest birch stage from two *palsas* (Radiocarbon 7, pp. 3—4). In the Inari region, the age of the youngest birch stage, according to sample B — 415, is 3 120 ± 120 years, and according to another sample, B — 511, 4 100 ± 200 years. Thus, the formation of the *palsas*, ridges and banks would appear to have started about the same time in Lapland, to some extent even earlier than the peat banks and hollows of the raised bogs of Mellilä and Urjala.

G. Lundqvist (1951 b, pp. 99, 129, 146, 171, 177) has investigated a number of bogs situated in the province of Kopparsberg, northern Sweden, and concluded that the ridges, banks, hummocks and hollows there had formed between 1 000 and 600 B. C. J. Lundqvist (1958, pp. 172—174) has described a certain bog pool from the ocality of Råda Stormoss, which is situated in the area covered by the map sheet of

Uddeholm (sheet 80), Värmland province; the pool dates back to before the beginning of the Sub-Atlantic period. As the Sub-Atlantic period is believed to have begun 2 700—2 500 years ago (Sauramo 1958, p. 44; Sorsa 1965, pp. 405, 409; Donner 1964, p. 17), the formation of peat banks and hollows in this Swedish locality started at about the same time as at Mellilä and Urjala.

Several investigators (e.g., Auer 1927, Ruuhijärvi 1962, Lundqvist 1963 and Tolonen 1966) have explained that the formation of peat banks, hollows, ridges and *palsas* has been promoted by the drying up of the surface of bogs. In the view of Auer (1927, p. 45), *palsas* developed in two stages during dry periods. Such dry periods have been observed to have occurred despite the generally increasing humidity of the Sub-Boreal period (Ruuhijärvi 1963, p. 31; Sorsa 1965, pp. 323, 325, 343, 405). During each dry period, certain parts of the surface of bogs dried more than others, and in such parts the ice lasted longer in the spring, eventually causing hummocks to form. And during these dry periods the vertical growth of the bogs slowed down and, in places, even halted, especially if the weather was cold (Aario 1941, p. 64). During the ensuing humid periods, the differences in moisture content increased further, promoting the formation of small relief in the bogs. Among others, G. Lundqvist (1963, pp. 116—117) and Tolonen (1966, p. 164) have described the formation of small relief on such dried-out surfaces. It is possible that peat banks and hollows did not yet evolve in connection with the drying up and subsequent recurrence of wet conditions in the bogs toward the end of the Sub-Boreal period but only hummocks separated by watery stretches. The peat banks and hollows would then have developed later as the climate grew colder.

Tolonen (1966, p. 164) takes the position that at Varrassuo, in the commune of Hollola, stages marked by the formation of hummocks and of depressions alternated during the late Atlantic period. These formations, however, probably do not fit into the category of peat banks and hollows as understood in the light of the Finnish designations, namely, *kermi* and *kulju;* rather do they represent the kind of hummock-interspace pattern that prevails at the present day in the southwesternmost part of Finland (Eurola 1962). In Germany vestiges of the hummock-interspace pattern have been met with also in strata dating back to the Atlantic period in ancient raised bogs (Rudolph & Firbas 1927, pp. 131, 136; Schneekloth 1963, p. 57; Woldstedt 1950, pp. 388—389).

A second significant period conducive to the formation of bog hollows in the area involved in my study thus occurred 2 100 years ago. This result fits in very nicely with the view that the coldest period of the Sub-Atlantic period happened at the beginning of the stage, shortly before the Christian era began (cf., Sorsa 1965, p. 404; Kalela 1961, p. 96). On the basis of C14 datings, Nilsson (1964, pp. 26, 32) calculated the beginning of the Sub-Atlantic period as having occurred in Sweden 2 300 years ago. It was as a consequence of the deterioration of the climate at this time that the second-stage peat banks and hollows referred to formed. As the diagram of Heinisuo shows (Fig. 5), trees grew abundantly in the area of the bog just before the formation of the hollows, which indicates the existence of dry ground. Accordingly, it was impossible for hollows to develop immediately. It was only after the climate progressively worsened that the growth of *Sphagnum* increased, the trees died and conditions in the previously dry bog began to favor the formation of hollows. The same developmental trend took place at Raholansuo, in the commune of Lieto.

In the area of the Ockelbo map sheet of surficial deposits (sheet 105), Gävleborg province, Sweden, G. Lundqvist (1963, pp. 116—117) has carried out the dating of the recurrence surface at the level of the bottom of several bog pools. Lundqvist explains the formation of the pools as having started from the level of this surface. Near the pools the recurrence surface developed 40 ± 75 years before the Christian era, and at a greater distance 225 ± 70 B. C., or 2 000—2 200 years ago. The age of these bog pools by and large corresponds to that of the hollows at Raholansuo and Heinisuo. In both Sweden and Finland, the bogs are situated in largely the same latitudes. The likelihood is that the same change of climate caused the formation of peat banks and hollows in these bogs.

Peat banks and hollows evolved also during periods between the stages mentioned (3 200 and 2 100 years ago), though to a distinctly lesser extent, as well as from aforementioned times up to the present day. Accordingly, the formation of all banks and hollows of raised bogs as well as of ridges and *rimpis* of *aapa* bogs was by no means a synchronous process (cf., G. Lundqvist 1951 b, p. 99). The probability is, however, that during the aforementioned periods the climate was more conducive to the development of small relief forms than in intervening periods. Auer (1927, p. 45) has observed that *palsas* evolved at two stages. The evidence indicates that at certain periods peat banks and hollows formed in greater numbers than usual.

The aim of the present study has been to determine whether the differentiation of bog surfaces into peat banks and hollows took place in different parts of the area investigated — and, possibly, of the country as a whole — at different times. In the light of the C14 datings carried out up to the moment, no definitive conclusion can be reached. In comparing the datings arrived at with respect to the bogs of Lieto, Mellilä and Urjala, one will note that the differentiation process took place earlier in the interior of the country than near the coast. The Renko area, however, represents a marked exception to this rule. As I have already pointed out (p. 72), peat banks and hollows could not evolve in coastal bogs at the time they began to evolve elsewhere. Accordingly, only the datings arrived at from Mellilä and Urjala are mutually comparable. The age difference between these localities with respect to the event of differentiation is 50 ± 110 years. However, it should be borne in mind that the magnitude of the age difference also depends on the care with which the dated samples were taken. Purely from the standpoint of the technical factors involved in the taking of samples, the age difference could be even greater or smaller, or, then, the result obtained at Mellilä might indicate a greater age than at Urjala. On the other hand, furthermore, the datings from the bogs of Lieto and Renko are comparable. These bogs were dry at the time peat banks and hollows began to form elsewhere, meaning that relief patterns could not develop in them until later. According to the datings, this eventually happened some 2 100 years ago.

The evidence thus indicates that the formation of peat banks and hollows occurred in different parts of southwestern Finland over extensive areas simultaneously in response to changes in the climate favoring the process.

It was pointed out in the foregoing (p. 84) that a climatic change some 2 100 years ago caused peat banks and hollows to form in bogs in corresponging geographic latitudes in both Finland and Sweden. If we compare the datings of the oldest peat banks and hollows arrived at in southern Finland with the datings of ridges and *palsas* in the north, we will note that there are no great differences between the times of origin of the various formations. The bog ridges, *rimpis* and *palsas* began to form only slightly earlier than did the peat banks and hollows. This is only natural. After all, the average annual temperature in northern Finland differs markedly from that prevailing in southern Finland to this day. Still, the climatic change for the worse has been conspicuous and its effects have been rapidly felt over a wide area.

Manuscript received, February 28, 1967

REFERENCES

AARIO, LEO (1941) Napapaholainen ja ilmaston paraneminen. (Referat: Polardämon und Klimaverbesserung). — Terra 53 (57—69).

—»— (1943) Über die Wald- und Klimaentwicklung an der lappländischen Eismeerküste in Petsamo, mit einem Beitrag zur nord- und mitteleuropäischen Klimageschichte. — Ann. Bot. Soc. »Vanamo». 19 : 1 (1—158).

AARTOLAHTI, TOIVE (1965) Oberflächenformen von Hochmooren und ihre Entwicklung in Südwest-Häme und Nord-Satakunta. — Fennia 93 : 1 (1—268).

—»— (1966) Über die Einwanderung und die Verhäufigung der Fichte in Finnland. — Ann. Bot. Fenn. 3 (368—379).

AUER, VÄINÖ (1927) Untersuchungen über die Waldgrenzen und Torfböden in Lappland. — Comm. Inst. Quest. Forest. Finl. 12 : 4 (1—52).

DONNER, J. (1964) The late-glacial and post-glacial emergence of south-western Finland. — Soc. Sci. Fenn., Comm. Phys. — Math., 30 : 5 (1—47).

EUROLA, SEPPO (1962) Über die regionale Einteilung der südfinnischen Moore. — Ann. Bot. Soc. »Vanamo» 33 : 2 (1—243).

KALELA, AARNO (1961) Kasvillisuutemme ja kasvistomme historiaa. — Oma Maa IX, 3 Aufl. (85—97). Porvoo.

KANERVA, REINO (1956) Pollenanalytische Studien über die spätquartäre Wald- und Klimageschichte von Hyrynsalmi in NO-Finnland. — Ann. Acad. Sci. Fenn. Ser. A III, 46 (1—108).

LUNDQVIST, G. (1951 a) En palsmyr sydost om Kebnekaise. — Geol. Fören. Förhandl. 73 : 2 (209—225).

—»— (1951 b) Beskrivning till jordartskarta över Kopparbergs län. — Sv. Geol. Unders. Ser. Ca 21.

—»— (1963) Beskrivning till jordartskarta över Gävleborgs län. — Ibid. 42.

LUNDQVIST, J. (1958) Beskrivning till jordartskarta över Värmlands län. — Ibid. 38.

NILSSON, TAGE (1964) Entwicklunggeschichtliche Studien im Ageröds Mosse, Schonen. — Lunds Univ. Årsskr. N. F. Avd. 2, 59 : 8 (1—34).

RUDOLPH, KARL & FRANZ FIRBAS (1927) Die Moore des Riesengebirges. Paläofloristische und stratigraphische Untersuchungen bömischer Moore III. — Beih. Bot. Centralbl. Abt. II 43 : 2 — 3 (69—144).

RUUHIJÄRVI, RAUNO (1962) Palsoista ja niiden morfologiasta siitepölyanalyysin valossa (Zusammenfassung: Über die Palsamoore und deren Morphologie im Lichte der Pollenanalyse). — Terra 74 : 2 (58—68).

—»— (1963) Zur Entwicklungsgeschichte der nordfinnischen Hochmoore. — Ann. Bot. Soc. »Vanamo» 34 : 2 (1—40).

SAURAMO, MATTI (1940) Suomen luonnon kehitys jääkaudesta nykyaikaan. Porvoo—Helsinki.

SCHNEEKLOTH, HEINRICH (1963) Beiträge zur Kenntnis niedersächsischer Torflagerstätten. I und II. — Beih. Geol. Jahrb. 55 (1—104, 105—137).

SORSA, PENTTI (1965) Pollenanalytische Untersuchungen zur spätquartären Vegetations- und Klimaentwicklung im östlichen Nordfinnland. — Ann. Bot. Fenn. 2 : 4 (301—413).

VALOVIRTA, VEIKKO (1965) Zur spätquartären Entwicklung Südost-Finnlands. — Bull. Comm. géol. Finlande 220 (1—101).

VASARI, YRJÖ (1962) A study of the vegetational history of the Kuusamo district (NE-Finland) during the late-Quaternary period. — Ann. Bot. Soc. »Vanamo» 33 : 1 (1—140).

WOLDSTEDT, PAUL (1950) Norddeutschland und angrenzende Gebiete im Eiszeitalter. (464 p). Stuttgart.

Comptes Rendus de la Société géologique de Finlande
N:o XXXIX (1967), pp. 87—94

PALEOMAGNETISM OF THE DIKE SYSTEMS IN FINLAND III. REMANENT MAGNETIZATION OF DIABASE DIKES IN HÄME, FINLAND

BY

K. J. NEUVONEN

Institute of Geology, University of Turku, Finland

ABSTRACT

The strength and direction of the remanent magnetization of a diabase dike system in southern central Finland is measured. The magnetization is unstable and only a small percentage is left after demagnetization in AC-field. The origin of the magnetization is discussed.

CONTENTS

INTRODUCTION

Ilkka Laitakari (1965 and 1966) has recently described a suite of diabase dikes occuring in the Heinola—Orivesi area in the southwestern part of central Finland. More than 60 dikes are found to occur in the area, all running subparallel in a diretion N 55°W between Lakes Näsijärvi and Päijänne (Fig. 1).

According to Laitakari (1966) the dimensions of the dikes vary greatly. The largest, presumably almost continuous dike recently described in detail by Savolahti (1964), is about 16 km in length and more than 100 meters in breadth. Usually, the rock in the dikes has plagioclase, olivine, and augite as the principal constituents. The texture is ophitic. A fine-grained chilled margin is common at the contacts of

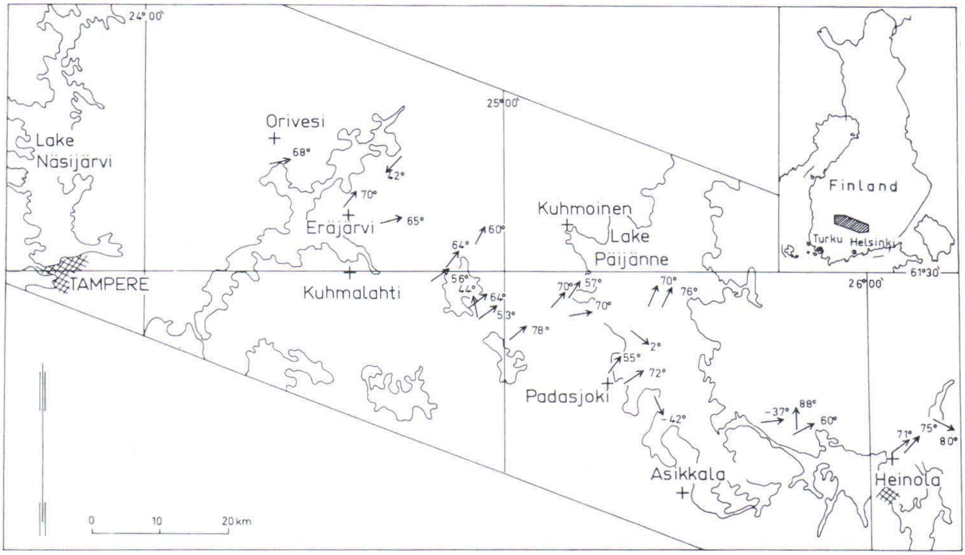

FIG. 1. Directions of remanent magnetization of diabase dikes in Häme, Finland.

the smaller dikes. A large number of the dikes have a coarse, breccia like central part with large, broken plagioclase (An_{55-60}) xenolites up to 30 cm in diameter. The mineral composition of some diabase dikes of the area is given in Table 1. As accessory minerals apatite, biotite, hornblende and serpentine are most common. Ilmenite is the most abundant opaque mineral. It occurs as individual grains as well as fine lamella in magnetite. Table 3 gives the magnetite and ilmenite contents of the magnetically measured samples. In some rocks, however, opaque minerals occur as lathy skeletons so fine-grained that modal analysis is not possible. Both ilmenite and magnetite appear well-preserved and primary.

The age of the dikes is not known. The dikes cut the Svecofennian (Precambrian) basement and occur spatically in close connection with the gabro anorthosite intrusions in the Heinola—Mäntyharju region (Savolahti 1956). A relation to the rapakivi intrusion further southeast is also possible. The age of the dikes could, therefore, be considerably less than that of the surroundings (i.e. 1.800 m.y.) and possibly somewhat more than that of rapakivi granite (1.640 m.y., Kouvo and Tilton, 1966). Radiometric determinations of the age of the dike system will be performed in the near future by the age group of the Geological Survey of Finland.

SAMPLES AND MEASUREMENTS

Oriented sample cores were drilled from the dikes of the area during the summers 1965 and 1966. The drilling and orientation were made using the same equipment

TABLE 1.

Mineral composition (mode) of some diabase dikes from the Heinola—Orivesi area. Determined with a point counter (Chayes, 1949).

	1.	2.	3.	4.	5.
Plagioclase (An~58)	59.5	56.8	70.4	65.4	62.0
Olivine (Fa 55)	6.3	31.5	13.3	11.6	27.5
Augite	21.3	7.2	7.5	10.4	3.7
Opaque minerals	10.4	1.5	5.6	6.9	3.0
Accessories	2.5	3.0	3.2	5.7	3.8
	100.0	100.0	100.0	100.0	100.0

1. Diabase, Pääskylä, Längelmäki (Laitakari, 1966, diagram 1c)
2. Main dike, Torittu, Padasjoki (Laitakari, 1966, diagram 1g)
3. Diabase dike, Linnasaari, Padasjoki (Laitakari, 1966, diagram 1i)
4. Diabase, Huppionvuori, Orivesi, sample No. 126.1
5. Diabase, Ansio, Padasjoki (Savolahti, 1964)

and same technique described in connection with the work on the Satakunta region (Neuvonen, 1965). The direction and intensity of the remanent magnetization of specimens cut from the samples collected were measured with an astatic magnetometer. Altogether 30 samples cut into 190 specimens were measured. Table 2 lists the collection sites, measured directions and intensities of the remanent magnetization. The observed directions are also marked on the map in Fig. 1 and shown in the equal area (Lambert-Schmidt) projection in Fig. 2a.

The declination of the measured magnetic orientation of the dikes varied considerably as does also the angle of inclination. Most dikes show, however, remanent magnetization pointing northeast and having positive (downward) inclination. Four dikes have magnetic orientation towards the south and two dikes show negative inclination. Some of the greatest deviations from the mean direction might have been caused by lightning (Graham, 1961). In the samples from these localities, the intensity of magnetization is about 100 times higher than in the rest of the samples and the intensity decreases rapidly with depth.

It is also possible that some of the samples included in the study do not belong to the same set of dikes but are of a different origin and age. Especially the samples 359.1 and 359.2 are from a dike which differs from the others both pertographically and in type of occurrence. All the samples measured are, however, included in the average value calculated, utilizing the statistical method of Fisher (1953).

The paleomagnetic North Pole calculated on the basis of the average direction of magnetization lies in Siberia at latitude 57.5° north and longitude 100.5° east.

DEMAGNETIZATION

The investigation of the magnetic orientation of Satakunta and Vaasa dolerites (Neuvonen, 1965 and 1966) revealed a secondary magnetization formed in connec-

TABLE 2.

Remanent magnetization of diabase rocks in Häme, Finland before demagnetization

Sample No	Locality			Magnetic direction					Intensity emu/cm³	Remarks
	Name	Lat.	Long.	Decl.	Incl.	N	k	95		
124.1	Tuomasvuori Padasjoki	61.3°	25.3°	36°	+55°	7	57	8°	1.6 10^{-4}	
125.1	Iilivuori Eräjärvi	61.6°	24.8°	75°	+65°	7	337	4°	2.3 »	
126.1	Huppionvuori Orivesi	61.7°	24.3°	79°	+68°	7	48	9°	3.2 »	
127.1	Ansio Padasjoki	61.4°	24.9°	350°	+44°	4	1 154	3°	8.1 »	
127.2	Ansio Padasjoki	»	»	54°	+53°	7	47	9°	1.4 »	
128.1	Hirtniemi Padasjoki	61.3°	25.4°	158°	—42°	5	59	8°	17.4 »	
219.1	Virmaila Padasjoki	61.4°	25.3°	129°	+ 2°	9	37	9°	9.3 »	
220.1	Munuajärvi Padasjoki	61.4°	25.2°	43°	+70°	6	625	3°	123.5 »	Lightning?
221.1	Koukkujärvi Padasjoki	61.4°	25.3°	81°	+70°	6	154	5°	7.6 »	
222.1	Myllylahti Kuhmoinen ..	61.5°	25.2°	24°	+76°	6	307	4°	8.4 »	
222.2	Myllylahti Kuhmoinen ..	»	»	45°	+78°	5	133	7°	0 6 »	
223.1	Linnasaari Padasjoki	61.5°	25.4°	27°	+76°	9	200	4°	6.4 »	
223.2	Linnasaari Padasjoki	»	»	25°	+73°	7	870	3°	5.6 »	
223.3	Linnasaari Padasjoki	»	»	23°	+67°	7	225	4°	4.2 »	
224.1	Saksala Padasjoki	61.3°	25.3°	56°	+72°	6	204	4°	2.8 »	
225.1	Romo Padasjoki	61.3°	25.0°	53°	+78°	9	240	4°	4.6 »	
226.1	Ansio Padasjoki	61.4°	24.8°	54°	+68°	6	99	7°	0.9 »	
226.2	Ansio Padasjoki	»	»	50°	+60°	4	84	10°	0.8 »	
227.1	Liehu Kuhmalahti ..	61.6°	24.9°	31°	+60°	6	233	4°	4.8 »	
228.1	Vehkajärvi Kuhmalahti ..	61.5°	24.8°	39°	+64°	7	140	5°	5.6 »	
229.1	Karivuori Kuhmalahti ..	61.5°	24.8°	57°	+56°	8	154	4°	2.0 »	
230.1	Pääskylä Längelmäki ...	61.7°	24.7°	223°	+42°	8	72	6°	91.0 »	Lightning?
231.1	Maijaanvuori Eräjärvi	61.6°	24.5°	41°	+70°	5	488	4°	7.5 »	
248.1	Church-village Heinola county	61.3°	26.1°	61°	+71°	5	417	4°	3.5 »	
356.1	Polkjärvi Asikkala	61.3°	25.8°	62°	+60°	5	109	7°	21.8 »	
357.1	Polkjärvi Heinola county	61.3°	25.8°	358°	+88°	7	205	4°	10.5 »	
358.1	Hepomäki Asikkala	61.3°	25.7°	85°	—37°	7	9	21°	7.6 »	
359.1	Imjärvi Heinola county	61.3°	26.2°	107°	+78°	1	—	—	23.4 »	
359.2	Imjärvi Heinola county	»	»	119°	+81°	7	163	4°	22.9 »	
361.1	Church-village Heinola county	»	26.0°	49°	+75°	7	250	4°	1.7 »	
	Mean of all samples	61.4°	24.8°	61°	+70°	30	5.57	12.3°	$\delta m = 21.1°$	$\delta p = 185°$

N = number of specimens measured (or samples compiled)
k = precision parameter (N-1/N-R)
α_{95} = circle of conficence with a probability of 95 per cent

TABLE 3.

Remanent magnetization of diabase rocks in Häme, Finland after demagnetization in alternating magnetic field (300 Oersteds peak)

No Sample	Locality	Magnetic direction					Intensity		Contents of opaque minerals	
		Decl.	Incl.	N	k	α 95	emu/cm³	% of original	Magnetite %	Ilmenite %
124.1	Tuomasvuori Padasjoki	44°	+55°	4	9	32°	2.3 10^{-5}	14	0.9	2.8
125.1	Iilivuori Eräjärvi	100°	+48°	4	38	15°	1.2 »	5	0.6	4.2
126.1	Huppionvuori Orivesi	49°	+75°	4	109	9°	3.9 »	12	0.3	2.5
127.1	Ansio Padasjoki	74°	+76°	2	—	—	3.9 »	5	0.2	3.5
127.2	Ansio Padasjoki	118°	+10°	4	10	30°	2.0 »	12	0.3	2.2
128.1	Hirtniemi Padasjoki	89°	+59°	3	10	26°	1.9 »	1	1.2	3.4
219.1	Virmaila Padasjoki	177°	+49°	9	3	35°	0.1 »	1	0.8	3.5
220.1	Munuajärvi ..... Padasjoki	163°	+32°	6	6	31°	3.1 »	0.3	unmeasurable	lathy skeletons
221.1	Koukkujärvi Padasjoki	79°	+50°	6	2	66°	3.1 »	4	1.1	4.0
222.1	Myllylahti Kuhmoinen ..	56°	+73°	6	9	24°	3.5 »	4	1.3	3.3
222.2	Myllylahti Kuhmoinen ..	329°	+82°	5	20	17°	1.7 »	28	unmeasurable	lathy skeletons
223.1	Linnasaari Padasjoki	308°	+84°	9	52	7°	5.3 »	8	2.4	3.0
223.2	Linnasaari Padasjoki	10°	+81°	7	6	26°	2.0 »	4	1.6	2.9
223.3	Linnasaari Padasjoki	9°	+72°	7	29	11°	3.0 »	7	1.0	3.5
224.1	Saksala Padasjoki	134°	+81°	6	9	24°	0.9 »	3	0.4	1.6
225.1	Romo Padasjoki	16°	+82°	9	113	5°	2.5 »	5	0.5	2.3
226.1	Amsio Padasjoki	125°	+24°	6	8	25°	0.7 »	8	0.1	1.9
226.2	Ansio Padasjoki	136°	+17°	4	9	32°	0.8 »	10	0.2	2.4
227.1	Liehu Kuhmalahti ..	348°	+80°	6	43	10°	3.4 »	7	unmeasurable	lathy skeletons
228.1	Vehkajärvi Kuhmalahti ..	94°	+75°	7	33	11°	3.4 »	6	unmeasurable	lathy skeletons
229.1	Karivuori Kuhmalahti ..	219°	+78°	8	16	14°	1.4 »	7	0.3	2.4
230.1	Pääskylä Längelmäki ...	297°	+79°	8	104	6°	5.1 »	0.5	1.4	4.2
231.1	Maijaanvuori Eräjärvi	8°	+79°	5	35	13°	13.1 »	18	0.7	2.5
248.1	Church-village Heinola county	12°	+15°	5	2	79°	0.8 »	2	0.3	2.2
356.1	Polkjärvi Asikkala	61°	+41°	5	22	17°	2.2 »	1	unmeasurable	impregnation
357.1	Polkjärvi Heinola county	34°	+54°	7	26	12°	2.5 »	2	1.8	2.5
358.1	Hepomäki Asikkala	9°	+73°	7	78	7°	5.7 »	8	1.0	3.6
359.1	Imjärvi Heinola county	108°	+81°	1	—	—	5.6 »	2	unmeasurable	impregnation
359.2	Imjärvi Heinola county	109°	+87°	7	7	24°	3.9 »	2	unmeasurable	impregnation
361.1	Church-village Heinola county	23°	+45°	7	4	38°	0.9 »	5	0.2	1.3
Mean of the samples α95 < 25°		48°	+78°	19	23.2	7.2°	δm = 13.4° δp = 13.8°			

Paleomagnetic North pole: Latitude 67.3° north Longitude 72.2° east

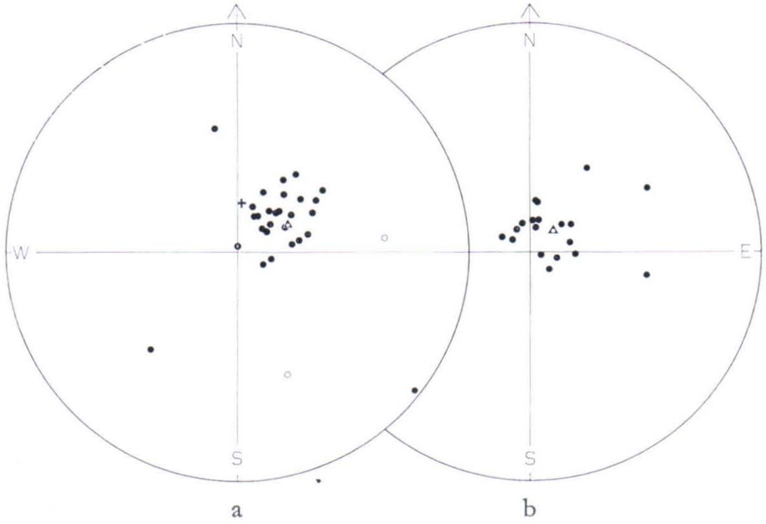

FIG. 2. Directions of remanent magnetization of diabase dikes in Häme, Finland, in equal area (Schmidt) projection. a) before demagnetization b) after demagnetization with 300 Oersteds alternating field.

● = north seeking pole lower hemisphere
○ = north seeking pole upper hemisphere
+ = Present geomagnetic field direction
△ = average

tion with surface weathering. This caused a gradual variation in the magnetic direction along the depth. No such systematic change of magnetic orientation can be observed in the rocks now studied. A secondary magnetization was, however, thought to be present and attempts to remove it were made.

AC-demagnetization experiments with a stepwise increased field showed systematic changes in magnetic orientation up to nearly 300 Oersteds. The natural remanent magnetization of the samples investigated was found to be very unstable and only a small portion of the original stregth of magnetization remained in the samples after demagnetization. Heat treatment, on the other hand, gave no systematic variation in the magnetic orientation and caused an increase in the circle of confidence (α_{95}). This was possibly produced by the small remnant of incompletely compensated geomagnetic field inside the Helmholz coil where the specimens were heated in random orientation.

Demagnetization of the specimens was performed after these experiments with an alternating magnetic field of 300 Oersteds. The technique and instrumentation used were essentially the same as described earlier (Neuvonen, 1965). After this treatment the magnetization of the specimens was so weak that it could be hardly measured with the magnetometer available. The direction of the magnetization after

AC-demagnetization is given in Table 3 and shown in projection in Fig. 2b. This table also lists the ilmenite and magnetite contents of the samples measured.

The circle of confidence (α_{95}) calculated for the individual core samples is quite large, mainly because of the insufficient sensitivity of the instrument used. Therefore, when calculating the average direction, the weakest samples with α_{95} larger than 25° were omitted. This means that only 19 samples are included in the average. The average direction does not differ greatly from the direction initially determined on the samples. The corresponding paleomagnetic pole is located at longitude 67.2° north and latitude 72.2° east.

DISCUSSION OF THE RESULTS

The interpretation of the magnetic directions found for the diabase dikes studied is difficult, since no direct test is available to prove the origin of the orientation. Magnetite in the dike rock looks as if it is a primary mineral of the rock except for the small amount found as an exolution product in ilmenite. Consequently, the magnetization measured could well be natural thermoremanent magnetization (TRM) developed in the rock during the crystallization and cooling period of the diabase magma. The directions measured differ greatly, however, from the direction measured for the dolerites in the Satakunta and Vaasa areas (Neuvonen, 1965 and 1966). The calculated magnetic north pole position lies in northern Siberia and does not come close to any pole site measured on Precambrian rocks in Europe (Irving, 1964).

The declination of the present geomagnetic field in the sampling area is on an average about + 5° and the inclination about + 75°. The direction of the remanent magnetization measured on the diabase dikes does not differ much from the direction of this present field. Therefore, the possibility has to be emphasized that the remanent magnetization of the diabase dikes studied can be viscous magnetization caused by the present geomagnetic field. This reasoning is justified by the low coersive force observed in these rocks in connection with the AC and thermal demagnetization.

The small fraction of natural remanent magnetization found in the samples after demagnetization evidently has components of different origin. The initial thermoremanent magnetization is obviously one of those. The chemical remanent magnetization and the residum of viscous magnetization superpose the original magnetization created under the crystallization period. No method so far is known to be able to reveal its direction in the rock.

Acknowledgments — I am sincerely grateful to many who assisted my work in the field and in the laboratory. Mrs. Ritva Ääri, Mr. Leo Grundström (B. Sc), Mr. Aimo Hiltunen (M. Sc.) and Mr Ilkka Laitakari (Lic. Ph.) deserve special mention as does Mrs. Leena Kiiskilä who did the drawings. The National Research Council for Science made the work possible through the financial aid given. The English of the manuscript was kindly corrected by Mrs. Gillian Häkli.

Manuscript received, March 3, 1967

REFERENCES

Chayes, F. (1949) A simple point counter for thin-section analysis. Amer. Min., Vol. 34, pp. 1—11.

Fisher, R. A. (1953) Dispersion on a sphere. Royal Soc. London Proc., ser. A, Vol. 217, pp. 295—305.

Graham, K. W. T. (1961) The re-magnetization of a surface outcrop by lightning currents. Geophys. J., Vol. 6, pp. 85—105.

Irving, E. (1964) Paleomagnetism and its application to geological and geophysical problems. John Wiley and Sons, inc., New York/Sydney.

Kouvo, Olavi and Tilton, G. R. (1966) Mineral ages from the Finnish Precambrian. Jour. Geol., Vol. 74, pp. 421—442.

Laitakari, Ilkka (1965) Padasjoen—Oriveden seudun oliviinidiabaaseista. Summary: On olivine diabases of the Padasjoki — Orivesi area, Finland. Geologi No. 5, pp. 3—7.

—»— (1966) Heinolan—Padasjoen—Oriveden Seudun diabaasijuoniparvi. Thesis for Phil.lic. in the archive of the geological institute, University of Turku.

Neuvonen, K. J. (1965) Paleomagnetism of the dike systems in Finland I. Remanent magnetization of Jotnian dolerites in southwestern Finland. Compt. Rend. Soc. géol. Finlande, Vol. 37, pp. 153—168.

—»— (1966) Paleomagnetism of the dike systems in Finland II. Remanent magnetization of dolerites in the Vaasa archipelago. Compt. Rend. Soc. géol. Finlande, Vol. 38, pp. 275—281.

Savolahti, A. (1956) The Ahvenisto massif in Finland. Bull. Comm. géol. Finlande 174.

Savolahti, Antti (1964) Olivine diabase dike of Ansio in Padasjoki, Finland. Compt. Rend. Soc. géol. Finlande, Vol. 36, pp. 99—112.

Comptes Rendus de la Société géologique de Finlande
N:o XXXIX (1967), pp. 95—100

ON THE HAAPALUOMA Sc-BEARING COLUMBITE AND ITS INCLUSIONS

BY

ILMARI HAAPALA, JAAKKO SIIVOLA and ARVO LÖFGREN

Geological Survey of Finland, Otaniemi

ABSTRACT

Columbite occurs in the Haapaluoma pegmatite in two mineral assemblages. Columbite$_I$ contains as inclusions zircon, thorite, brockite, cassiterite, löllingite, two unidentified Nb-Ta minerals, quartz and feldspars. Recalculation of the unit cell contents of columbite$_I$ gave $(Mn_{2\cdot 426}, Fe_{1\cdot 181}, Sc_{0\cdot 180}, Ca_{0\cdot 074}, Sn_{0\cdot 047}, Mg_{0\cdot 010}, U_{0\cdot 006}, Pb_{0\cdot 006}, Cu_{0\cdot 002})_{3\cdot 93}(Nb_{7\cdot 168}, Ta_{0\cdot 491}, Ti_{0\cdot 336}, Al_{0\cdot 054}, W_{0\cdot 011})_{8\cdot 06} O_{24\cdot 01}$. The Sc_2O_3 content (0.90 wt %) of this columbite is evidently the greatest published in the literature. According to spectrographic analyses the scandium content of the older columbite generation is greater than that of the younger one.

INTRODUCTION

In connection with the study of the granitic pegmatites of the Peräseinäjoki—Alavus area one of the writers also described briefly the columbite from the Haapaluoma pegmatite (Haapala, 1966). In this pegmatite columbite is met with in two mineral assemblages. Columbite$_I$ occurs usually with albite, quarz, black tourmaline, cassiterite, monazite-cheralite and brockite in replacement bodies and fracture fillings. The biggest columbite$_I$ crystals measure about 10 cm × 5 cm × 2 cm. Columbite$_{II}$ occurs as a rarity in association with cleavelandite, lepidolite, cheralite, quartz and red tourmaline as thin, needlelike crystals or sometimes as {010} tables.

A chemical analysis, made by Pentti Ojanperä, of the Haapaluoma columbite$_I$ showed an especially large Sc_2O_3 content, 0.90 %. Electron microprobe analysis showed that the columbite contains zirconium-rich silicate inclusions in which also scandium, calsium and aluminium were concentrated. Therefore these constituents were omitted as non-essential in calculating the unit cell contents (Haapala, *op.cit.*) Later the writers made further studies of the Haapaluoma columbite and its inclusions. The columbite$_I$ used in this study is from the same sample from which the chemical analysis was made. Four polished sections of this columbite were studied by means of ore microscope, electron microprobe and powder X-ray methods. The X-ray diffraction studies and the compilation of the manuscript were made by Ilmari Haapala. The microprobe analyses were performed by Jaakko Siivola and the spectrochemical analyses by Arvo Löfgren.

COLUMBITE

According to X-ray studies, both the columbite$_I$ and columbite$_{II}$ of the Haapaluoma pegmatite are in a very disordered structural state (see Nickel *et al.*, 1963) Single-crystal photographs showed only extremely weak columbite 020 and 040 reflections. In order to clarify the changes in structure *a*- and *c*-axis zero-level precession photographs were taken from a crystal fragment of columbite$_I$. Then the same crystal fragment was heated in air at 900°C for three hours and a new set of precession photographs was taken. The unit cell dimensions of the unheated material were $a_0 = 5.72$, $b_0 = 14.22$ ($= 3 \times 4.74$) and $c_0 = 5.13$ Å, and those of the heated material $a_0 = 5.73$, $b_0 = 14.35$ and $c_0 = 5.06$ Å. The heat treatment also made the reflections clearly visible that distinquish the columbite structure from the ixiolite structure, *i.e.*, ordering took place. No reflections indicating the presence of the monoclinic $FeNbO_4$-like phase could be detected (*cf.* Vorma, 1965).

According to the wet chemical analysis columbite$_I$ contains 0.90 % Sc_2O_3. For spectrochemical study, material was drilled from places without any inclusions in two polished sections of columbite$_I$. Spectrographic analyses of these materials gave 0.77 and 0.75 % Sc_2O_3. Similar analyses of two columbite$_{II}$ samples gave 0.43 and 0.31 % Sc_2O_3. Spectrographic analysis of columbite$_I$ showed also 0.23 % Al_2O_3. Zirconium was not detected.

THE INCLUSIONS

Zircon is by far the most common of the inclusions in the Haapaluoma columbite. The mineral usually occurs in columbite$_I$ at the junction of cracks as euhedral crystals 0.02—0.2 mm in diameter. The inclusions are not equally distributed throughout the columbite, but there are areas in which inclusions are concentrated. Zircon is partially metamict giving broad, diffuse reflections in a powder photograph. Microprobe analysis showed that the zircon inclusions contain calcium, aluminium, hafnium and varying amounts of scandium as minor constituents. Some zircon inclusions contain considerably more scandium than the columbite. Figs. 1 a and b present the distribution of zirconium and scandium in such a grain. In other zircon inclusions the scandium content is of the same magnitude as in the columbite, or even lower.

Owing to the small grain size of the zircon inclusions it was not possible to separate it for chemical analysis. From two samples containing albite, quartz and

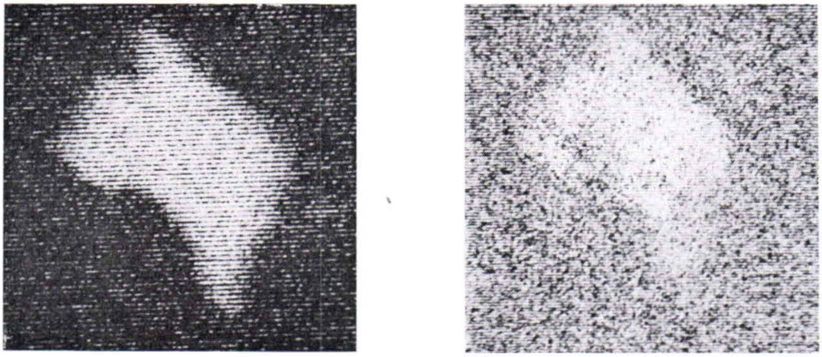

a b

FIG. 1. X-ray images showing the distribution of zirconium and scandium between a zircon inclusion and columbite$_I$. Magn. 780 ×. a) Zr $L\alpha_1$, b) Sc $K\alpha$.

lithium minerals — a typical mineral assemblage of the Haapaluoma zircon — it was, however, possible to get enough zircon for spectrographic analysis. The analysis of this zircon gave 0.46 % Sc_2O_3 and 2.08 % Al_2O_3.

Thorite inclusion are very rare in the Haapaluoma columbite. In the four polished sections made from columbite$_I$ only three thorite inclusions were noticed. The spindle-shaped inclusions were 0.03—0.1 mm in diameter (Fig. 2). The unheated material was X-ray amorphous. Heated in air at 700°C for three hours the mineral gave weak cubic phase and thorite reflections. Heating at 1 000°C for one hour produced distinct thorite and huttonite reflections in a powder photograph. This behaviour during heating is typical of thorite (Lima de Faria, 1964). In the heat treatment the whole polished section was heated, and then material was separated from the inclusions with a sharpened needle.

According to an electron microprobe analysis the thorite contains about 60 % ThO_2, 10 % ZrO_2 and 20 % SiO_2. Rare earths, phosphorus, calcium and uranium were not detected.

Brockite occurs usually as very fine-grained, equididimensional aggregates on the faces of columbite$_I$. The largest aggregates are 1—2 cm in diameter. Sometimes brockite is met with also as anhedral inclusions in columbite$_I$, measuring 0.2—3 mm in diameter. One fresh looking, very finegrained aggregate gave a diffuse powder pattern in which weak reflection at 4.49 Å suggests orthohombic (pseudohexagonal) symmetry (*cf.* Muto *et al.*, 1959). Possibly this mineral is grayite, a mineral very closely related to brockite. Generally the aggregates give brockite powder patterns. A semiquantitative microprobe analysis of brockite is given in Haapala (1966).

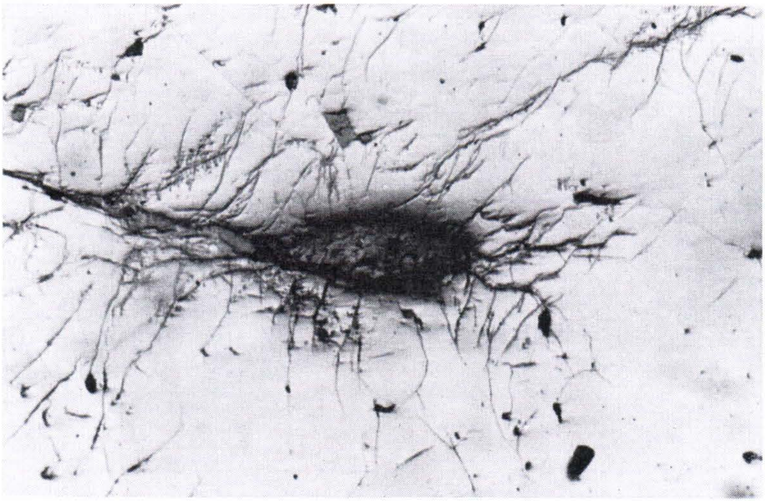

FIG. 2. A thorite inclusion in columbite$_I$. Polished section, one nicol. Magn. 150 ×. Photo Ilmari Haapala.

Cassiterite occurs as inclusions 0.02—0.1 mm in diameter or as overgrowths on the {010} faces of columbite$_I$ crystals. These overgrowths are generally oriented forming thin ridges parallel to the columbite *a* axis. A Weissenberg photograph of such a columbite-cassiterite intergrowth showed that the cassiterite *a* axis is parallel with the columbite *b* axis (*cf.* Ramdohr, 1961, p. 478) and the cassiterite [011] direction is parallel with the columbite *a* axis. A spectrographic analysis of a cassiterite crystal occurring in the same mineral assemblage as columbite$_I$ gave 0.09 % Sc_2O_3.

Löllingite is met with as very small inclusions in columbite$_I$. The grains are 0.01 mm in diameter at the most. The mineral was identified by means of electron microprobe.

Along the borders of fissures and around inclusions there are in columbite$_I$ irregular patches of lower reflecting mineral replacing columbite. These patches are 0.05 mm in diameter at the most. The polishing hardness is nearly the same as that of columbite. An electron microprobe analysis showed that this mineral contains 5.1 % Fe_2O_3*, 2.1 % MnO_2*, 2.8 % CaO, 68.5 % Nb_2O_5, 7.1 % Ta_2O_5 and 2.9 % TiO_2 as well as 2—5 % SiO_2 and some minor uranium. Owing to the small grain size and hardness of the mineral it was not possible to get pure material for X-ray study. Obviously similar alteration products in columbite have been described by Heinrich (1962, p. 1371). He suggests that they represent columbite-tantalite in which bivalent iron and manganese have been oxidized.

In one polished section of columbite$_I$ still two inclusions 0.02—0.05 mm in diameter were detected. According to an electron microprobe analysis these inclusions

---

* Oxydation state unknown.

contain about 40 % Nb_2O_5, 15 % Ta_2O_5, 10 % SiO_2 and 2% TiO_2 as well as some potassium and barium. Uranium and rare earths were not detected. Unheated material of these inclusions gave no measurable X-ray reflections. When heated in air at 1 000°C for one hour the mineral gave a set of reflections which were largely similar to those of ignited samarskite and betafite. For lack of more exact data, the mineral must be regarded as unidentified.

In addition to the minerals described above also inclusions of quartz and feldspars occur as rarities in the columbite.

CONCLUSIONS

The columbite$_I$ from the Haapaluoma pegmatite contains as inclusions zircon, brockite, thorite, cassiterite, löllingite, an unidentified Fe-Ca-Mn-Nb-Ta-Ti mineral, an unidentified Ba-K-Nb-Ta-Si mineral, quartz and feldspars. Of these inclusions only zircon occurs in a manner that could cause an error in the columbite analysis. Therefore ZrO_2 (0.24 %) and SiO_2 (0.08 %) occurring in the analysis of columbite$_I$ must be regarded as impurities. On the contrary, Sc_2O_3, CaO and Al_2O_3 belong essentially to the columbite structure. In view of the similar ionic radii (Sc_3^{3+} 0.81, Mn^{2+} 0.80, Fe^{2+} 0.74 Å) it is evident that the scandium in the columbite structure takes the place of bivalent manganese and iron (see Neumann, 1961 and Borisenko, 1963).

The chemical analysis of columbite$_I$, made by Pentti Ojanperä, gave MnO 12.49, FeO 6.16, Sc_2O_3 0.90, MgO 0.03, CaO 0.30, SnO_2 0.51, U_3O_8 0.13, PbO 0.09, CuO 0.01, Nb_2O_5 69.14, Ta_2O_5 7.88, TiO_2 1.95, Al_2O_3 0.20, WO_3 0.19, ZrO_2 0.24, SiO_2 0.08, H_2O + 0.05, H_2O — 0.05, sum 100.40 % (see Haapala, 1966). The unit cell contents were recalculated from the analysis using the cell dimensions obtained from powder diffraction data (a_0 = 5.740, b_0 = 14.243, c_0 = 5.133 Å) and the specific gravity 5.45 (values given *in* Haapala, *op. cit.*). ZrO_2, SiO_2 and water were omitted as non-essential. The calculation gave $(Mn_{2.426}, Fe_{1.181}, Sc_{0.180}, Ca_{0.074}, Sn_{0.047}, Mg_{0.010}, U_{0.006}, Pb_{0.006}, Cu_{0.002})_{3.93} (Nb_{7.168}, Ta_{0.491}, Ti_{0.336}, Al_{0.054}, W_{0.011})_{8.06} O_{24.01}$, which corresponds very closely to the ideal formula of columbite.

The scandium content of the Haapaluoma columbite$_I$ is evidently the largest published so far in the literature. Neumann (1961) has detected in the columbites of Norway scandium contents as great as 2 000 ppm (0.2 % Sc, 0.3 % Sc_2O_3). According to Borisenko (1963) the Sc_2O_3 content of columbite-tantalite varies between 0 and 0.15 %. In the Haapaluoma pegmatite the Sc_2O_3 content of the older columbite generation is greater than that of the younger one.

Acknowledgements — The writers wish to express their sincere thanks to Mr. Pentti Ojanperä, Mag. Phil., for making the chemical analysis of columbite$_I$ and to Dr. Atso Vorma for critically reading the manuscript.

Manuscript received, March 4, 1967

REFERENCES

Borisenko, L. F. (1963) Scandium, its geochemistry and mineralogy. Authorized translation from the Russian. Consultants Bureau, New York.

Haapala, Ilmari (1966) On the granitic pegmatites in the Peräseinäjoki — Alavus area, South Pohjanmaa, Finland. Bull. Comm. géol. Finlande 224.

Heinrich, E. Wm. (1962) Radioactive columbite. Am. Mineral. 47, pp. 1363—1379.

Lima de Faria, J. (1964) Identification of metamict minerals by X-ray powder photographs. Estudos, Ensaios e Documentos No. 112, Junta de Investigações do Ultramar, Lisboa.

Muto, T., Meyrowitz, R., Pommer, A. M., and Murano, T. (1959) Ningyoite, a new uranous phosphate mineral from Japan. Am. Mineral. 44, pp. 633—650.

Neumann, Heinrich (1961) The scandium content of some Norwegian minerals and the formation of thortweitite, a reconnaissance survey. Norsk geol. tidskr. 41, pp. 197—210.

Nickel, E. H., Rowland, J. F., and McAdam, R. C. (1963) Ixiolite — a columbite substructure. Am. Mineral. 48, pp. 961—979.

Ramdohr, Paul (1961) Magnetische Cassiterite. C. R. Soc. géol. Finlande 33, Bull. Comm. géol. Finlande 196, pp. 473—480.

Vorma, Atso (1965) Notes on columbite and tapiolite from the pegmatite area of Tammela and Somero in SW Finland. C. R. Soc. géol. Finlande 37, Bull. Comm. géol. Finlande 218, pp. 169—176.

Comptes Rendus de la Société géologique de Finlande
N:o XXXIX (1967), pp. 101—104

ON THE ORIGIN OF PRIMARY SKARN IRON ORES

BY

TAUNO PIIRAINEN AND RISTO PIISPANEN

Department of Geology, University of Oulu, Finland

ABSTRACT

A suggestion is made to explain the formation of primary skarn iron ores as results of liquid immiscibility caused by the reaction of parent magma with dolomitic carbonate rock. The chief factor causing the unmixing of silicate and iron oxide phases is considered to be carbon dioxide, which is produced by various skarn forming reactions.

The skarn iron ores, by which is meant the occurrences of magnetite with or without hematite in association with carbonate rocks connected with vast amounts of Ca-, Mg-, Fe-silicates such as e.g. diopside, tremolite, andradite, forsterite, serpentine etc., are well known all over the world. They have been divided by Magnusson (1953) into two groups: the primary ones, in which the skarn rock and the iron ore probably formed in the same magmatic process, and the reaction skarn ores, in which the skarn minerals are considered as having resulted from the metamorphic reaction of carbonate rock with its siliceous impurities, the ore mineral being of sedimentary origin. The scope of this paper is restricted to the first-mentioned group.

Representative examples of the primary iron ore group are the Banat iron ore in Rumania, Iron Springs and Hanover in the U.S.A. The Finnish ores of this type are those of Juvakaisenmaa and Sillböle (Saksela 1965).

The primary skarn iron ores are generally tacitly accepted as results of pneumatolytic halogen gas action carrying the iron as halogen compounds and precipitating iron as oxides after reaction with limestone. The classical point of view of these phenomena has been stated by e.g. Schneiderhöhn (1955). The ores are thought to be associated with intrusions of intermediate acidity such as monzonites, syenites and granodiorites etc. . The formation of iron oxides is considered to have taken place according to the following kind of reactions (Magnusson 1953, p. 24):

$$(1)\ 2\,FeF_3 + 3\,CaCO_3 \rightleftharpoons Fe_2O_3 + 3\,CaF_2 + 3\,CO_2$$

$$(2)\ 2\,FeCl_3 + 3\,CaCO_3 \rightleftharpoons Fe_2O_3 + 3\,CaCl_2 + 3\,CO_2$$

However, the scarcity and even the occasional lack of fluorspar and other halogen bearing minerals on the one hand and the enormous quantities of iron oxides on the other have caused some writers to look for other mechanisms to explain the origin of these ores. Therefore, the role played by liquid emanations from the parent magma has been taken into consideration when interpreting the mode of formation of the skarn iron ores (Hickok and Graton in Bateman 1956). Ovchinnikov (1960) has recently put forward an idea starting from the liquation caused by interaction of the ore-bearing magma with limestone. As opposed to us Ovchinnikov emphasizes the role of Ca^{2+} in »displacing iron from its magmatic silicate compounds». Thus Ovchinnikov concludes that even other rocks rich in calcium could cause the separation of iron from silicate magma (Ovchinnikov 1958).

It is not the purpose of the present writers to deny the entire significance of halogen compounds in this connection. Especially Zn, Pb and Sn are likely to be transported as halogenids according to the calculations made by Krauskopf (1964) and certainly some of the iron, too, is carried into the surrounding limestone as halogen compounds.

The factors that have led us to doubt the correctness of the classical pneumatolytic point of view may be summarized as follows:

— The relative amounts of iron oxides and halogen-bearing minerals do not support the idea of halogen gases carrying such enormous quantities of iron. This has been emphasized also by Eastwood (1965).

— The calculations presented by Krauskopf (1954) do not support the large-scale role of $FeCl_3$ or FeF_3 as an iron carrier.

— The brecciating nature of iron ore in relation to the skarn reported by Borgström (1928, fig. 3, p. 9).

— The ideas presented by R. Fischer (1950) upon the effect of volatiles in general, causing the immiscibility of iron oxide and silicate melts.

— The experiences from blast furnaces in iron metallurgy. The unmixing of oxide and silicate melts is achieved by adding limestone or dolomite to the iron ore.

— The mode of occurrence of the primary skarn iron ores as massive lenses and pipes along the contacts of an intrusive and skarn rock.

Furthermore, Park's recent discovery (1961) of a magnetite »flow» in Chile strongly suggests the existence of a magnetite magma at least in some special cases. Thermodynamic relations do not rule out the possibility of liquid immiscibility (Barth and Rosenqvist 1949).

On the above stated grounds we are putting forward the following suggestions concerning the sequence of events in the skarn iron ore formation. Because some of the skarn iron ores are known to be associated with basic intrusives (Bateman 1956, p. 87) the parent magma may have been in principle of any composition. It is perhaps due to the different distribution of basic and silicic intrusives in orogenic belts that the skarn iron ores are generally associated with more acid intrusives. In any case the parent magma begins to react with the carbonate rock with which it has been brought into contact. The common skarn mineral associations indicate that following kinds of reactions took place:

$$(3)\quad CaMg(CO_3)_2 + 2\ SiO_2 \rightleftharpoons CaMg(SiO_3)_2 + 2\ CO_2$$

and

$$(4)\quad 2\ CaMg(CO_3)_2 + SiO_2 \rightleftharpoons Mg_2SiO_4 + 2\ CaCO_3 + 2\ CO_2$$

Likewise, tremolite and sometimes wollastonite are generated in reactions producing carbon dioxide. The rarity of wollastonite indicates moderate to high pressure during the reactions forming the skarn rock. The above-mentioned reactions make easily understood the purification of originally dolomitic carbonate into pure calcite. Even the occasional abundance of serpentine rock is explained easily as a hydrated alteration product of forsterite.

The surrounding limestone is thus destroyed and CO_2 is produced until an equilibrium is reached corresponding to the prevailing pressure and temperature conditions. Some of the CO_2 can be said to be forced to go into the reacting mother intrusive. The present writers assume this to cause the separation of two immiscible liquids, the iron oxide and the silicate phases.

Manuscript received, March 9, 1967

REFERENCES

BARTH, T. F. W. and ROSENQVIST, T., (1949): Thermodynamic relations of immiscibility and crystallization of molten silicates. Am. J. Sc., Vol. 247, pp. 316—323.

BATEMAN, A. M., (1956): Economic Mineral Deposits. John Wiley & Sons.

BORGSTRÖM, L. H., (1928): The iron ore of Juvakaisenmaa. Fennia 50, no. 20, pp. 1—20.

EASTWOOD, G. E. P., (1965): Replacement magnetite on Vancouver Island, British Columbia. Econ. Geol., vol. 60, pp. 124—148.

FISCHER, R., (1950): Entmischungen in Schmelzen aus Schwermetalloxyden, Silikaten und Phosphaten. N. Jb. f. Min. Abh., Bd. 81, S. 315—364.

KRAUSKOPF, K. B., (1964): The possible role of volatile metal compounds in ore genesis. Econ. Geol., v. 59, pp. 22—45.

MAGNUSSON, N. H., (1953): Malmgeologi. Jernkontoret—Stockholm.

OVCHINNIKOV, L. N., (1958): Experimental Study of the Processes of Ore Genesis. Acta Geologica Acad. Sci. Hungaricæ, Tom. V, fasc. 3—4, pp. 337—350.

OVCHINNIKOV, L. N., (1960): Some regular phenomena in the magmatogene ore genesis. Int. Geol. Congr., Report of the 21st Session Norden, Part XVI, pp. 7—16.

PARK, C. F., Jr., (1961): A magnetite »flow» in Northern Chile. Econ. Geol., vol. 56, pp. 431—6.

SAKSELA, M., (1965): Chapter »Malmit» in Suomen Geologia, (ed. K. Rankama). Kirjayhtymä, Helsinki.

SCHNEIDERHÖHN, H., (1955): Erzlagerstätten. Kurzorlesungen zur Einführung und zur Wiederholung. Gustav Fischer Verlag, Stuttgart.

Comptes Rendus de la Société géologique de Finlande
N:o XXXIX (1967), pp. 105—121

ÜBER DIE DÜNEN VON URJALA

VON

TOIVE AARTOLAHTI

Institut für Geographie, Universität Helsinki

ZUSAMMENFASSUNG

Der Verfasser behandelt in der vorliegenden Arbeit die in der Südostecke von Urjala gelegenen fossilen Dünen. Sie liegen teils in supraaquatischem, teils in subaquatischem Gebiet. Ihr Material stammt aus der Moräne der Umgebung und ist vom Wellengang und vom Wind sortiert worden. Die Körner sind deutlich abgerundet, obschon wegen der kurzen Transportstrecke und infolge der Verwitterung auch kantige Körner darunter sind. Aus der Richtung und Struktur der Dünen zu schliessen sind sie in der Hauptsache durch die Tätigkeit von Nordwestwinden aufgehäuft worden. Die Entstehung der Dünen hat eingesetzt, als das Inlandeis in der Zeit des Y I-Meerstadiums aus dem Gebiet zurückwich, und sie hat nur ein paar hundert Jahre in Anspruch genommen. Die Dünen unterscheiden sich von der Umgebung ausser durch ihre Oberflächenformen auch deutlich hinsichtlich der Vegetation.

EINLEITUNG

Es ist allgemein bekannt, dass Flugsand und Dünen an Küsten von Finnland vorkommen. Freilich sind auch schon die Flugsandstrände in unserem Lande ziemlich selten, denn für die aufhäufende Tätigkeit des Windes günstige Voraussetzungen sind nur an einigen Stellen von geringer Ausdehnung gegeben. In Ostbottnien, wo die Küste offen und flach ist, und wo es viel in der Eiszeit angehäuften und von den Flüssen angeschwemmten Sand und Schluff gibt, sind die Flugsandfelder am häufigsten. Wie aber aus der von Lumme (1934) gesammelten Übersicht und der von Okko (1964 s. 296) ausgearbeiteten Karte hervorgeht, gibt es Flugsand und Dünen auch im Binnenland. Da sie heute bewaldet sind, lassen sie sich von den anderen Anhöhen der Umgebung oftmals nicht unterscheiden. Im Lauf der letzten Jahrzehnte sind beim Strassenbau diese Erhebungen angeschnitten worden, so dass ihre Struktur ans Licht kam. Wenn eine fossile Düne angeschnitten wird, setzt der Wind den Sand von neuem in Bewegung, und an der Schnittstelle entstehen kleine Sandfelder mit Windrippelmarken. Eben ein solcher Durchschnitt hat auch das Dünenfeld enthüllt, dessen Formen, Struktur und Entstehung in der vorliegenden Arbeit behandelt wird.

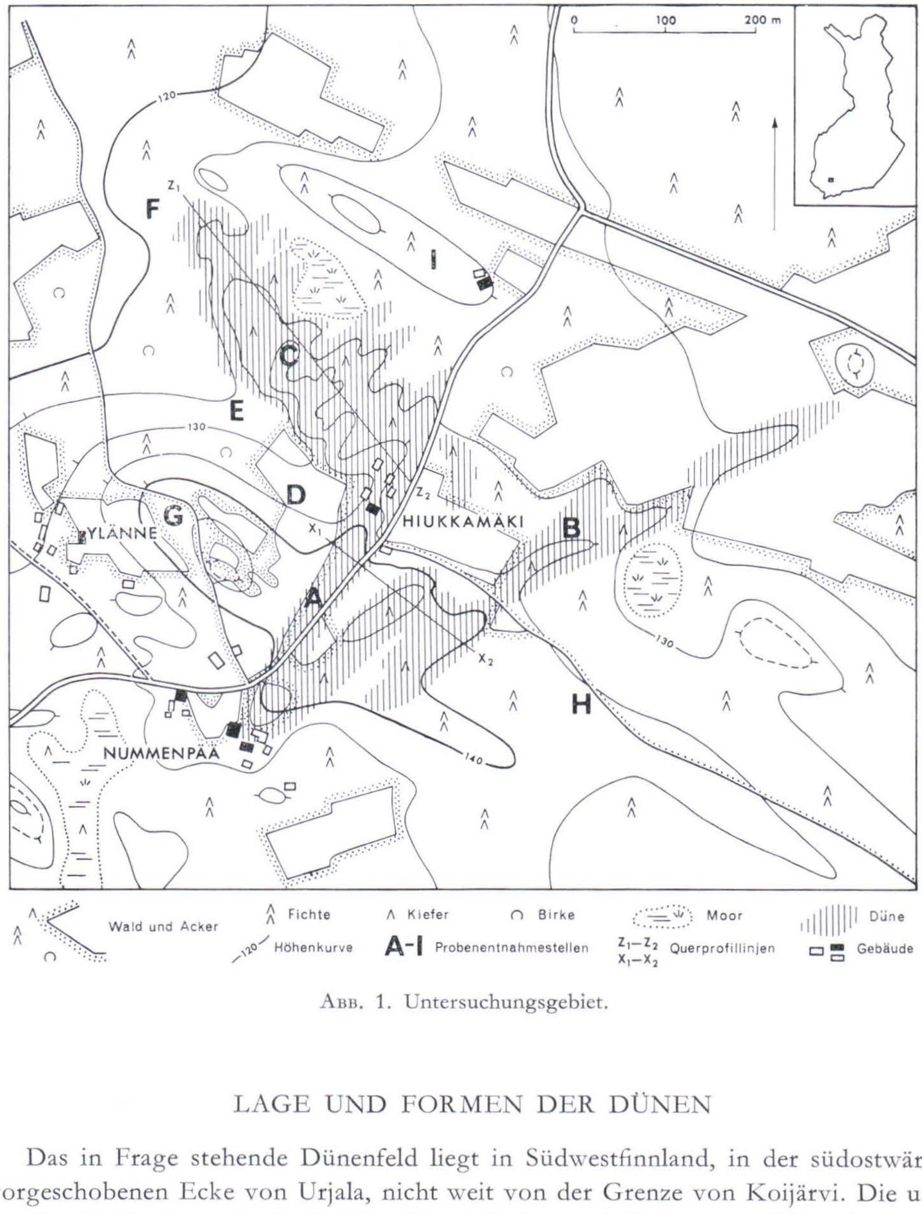

ABB. 1. Untersuchungsgebiet.

LAGE UND FORMEN DER DÜNEN

Das in Frage stehende Dünenfeld liegt in Südwestfinnland, in der südostwärts vorgeschobenen Ecke von Urjala, nicht weit von der Grenze von Koijärvi. Die um den See Kokko herumlaufende, über Rämsänkulma nach Lautaporras führende Landstrasse läuft hindurch. In dem Dünenfeld lassen sich drei hinsichtlich Höhe und Aufbau unterschiedliche Teile unterscheiden (Abb. 1). Zwischen den Gehöften Nummenpää und Hiukkamäki liegt ein 10—15 m hoher, von Nordwest nach Südost gerichteter Drumlin. Auf seinem Scheitel, quer zur Längsachse des Drumlins, liegen drei grosse und zwei kleine Dünen, die eine über das übrige Feld deutlich hinausra-

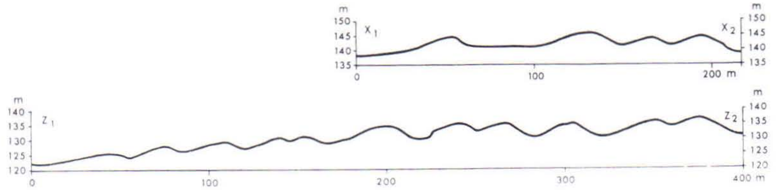

Abb. 2. Querprofilen von Dünen.

gende Gruppe bilden. Die grössten von den Dünen dieser Gruppe sind 150—200 m lang, 30—40 m breit und 2—5 m hoch. Die kleineren sind 30—40 m lang und 1.5—2 m hoch und teilweise miteinander verschmolzen. Die vom Gehöft Nummenpää nordostwärts verlaufende, südöstlich von der Landstrasse gelegene Düne ist von dieser Gruppe und auch von dem ganzen Feld die grösste. Die Seitenhänge haben eine Neigung von 10—20°, stellenweise sogar 30°. Der Südosthang ist deutlich steiler als der nordwestliche, obschon auch der letztgenannte steile Stellen hat (Abb. 2, Profil x_1-X_2). Im Längsprofil sind die Dünen konvex, wozu in gewissem Grade auch die Konvexität des Querprofils des Drumlins beiträgt. An den Böschungen des Drumlins, an den Enden der Dünen liegt der Sand 3—5 m hoch, auf dem Scheitel des Drumlins dagegen, in den Mittelpartien der Dünen nur 1.5—3 m. Infolgedessen ist der Kamm der Dünen ebener, als die Wölbung der Unterlage voraussetzen könnte.

Die Dünen sind von dem Drumlin recht scharf abgesetzt. Sie rufen an der Oberfläche des Drumlins Formen hervor, die sich von dessen Stromlinienformen deutlich abheben. Die Böschungen der Dünen steigen steil aus der Oberfläche des Drumlins empor. Ausserdem geht am Fuss der Dünen der Sand in die deutlich abgegrenzte, mit Steinen durchsetzte Sandmoräne des Drumlins über. Die genannten fünf Dünen liegen grösstenteils oberhalb der Höhenkurve von 140 m, und nur die Enden der drei grössten an den Hängen des Drumlins liegen in 137—138 m Höhe.

Der Hauptteil des Dünenfeldes liegt zwischen dem oben beschriebenen Drumlin und einem anderen, kleineren, 5—6 m hohen Drumlin etwa 300 m nordostwärts vom Gehöft Hiukkamäki. In diesem Gebiet sind die Dünen auf einem leicht nordwestwärts geneigten Untergrund entstanden, dessen Höhe über dem Meeresspiegel 123—130 m beträgt (Abb. 2, Profil z_1-z_2). Während die Dünen in der erstgenannten Partie des Feldes deutlich voneinander abgesetzte Gebilde sind, schliessen sie im letzteren Teil des Feldes ziemlich eng aneinander an. Am weitesten im Nordwesten liegen aus 123—124 m Höhe aufsteigende kleine Dünen, die teils über- und zwischeneinander gedrängt sind, so dass sich die Höhe der einzelnen Dünen nicht genau bestimmen lässt. Sie sind grösstenteils kurz, nur 40—50 m lang. Ihre Nordwestseite ist deutlich flacher (5—10°) als die Südostseite (10—20°). Am weitesten im Nordwesten haben die Dünen eine Höhe von ca. 2 m. Südostwärts nehmen sie an Höhe zu, so dass die 6. und 7. Düne schon eine Höhe von 5 m erreichen. Während der Scheitel der ersten Düne in 125.5 m Höhe liegt, erhebt sich der Kamm der 6. bis zu 135 m Höhe. Von hier südostwärts bleibt die Scheitelhöhe ungefähr gleich, 136—137 m ü.d.M. Zwischen dem in der Karte eingetragenen kleinen Moor und der Landstrasse sind die Dünen deutlicher abgegrenzt und stehen weiter auseinander als die vorn genannten kleinen Dünen, und stellenweise sieht man zwischen ihnen Steine des Moränenbodens. Am südwestlichen Ende sind auch diese Dünen miteinander verbunden und bilden einen gewundenen, nach Südwest steil abfallenden (30°, stellenweise auch mehr) Zug, dessen Kamm etwa 5—6 m höher liegt als die benachbarte Bachniederung. Am Nordostende dagegen laufen die Dünen sehr flach aus (3—5°) und gehen ohne klare Grenze in das umgebende Moränengelände über, nicht selten durch Vermittlung eines ebenen Flugsandfeldes. Auch an den Dünen dieser Gruppe sind die Nordwesthänge durchschnittlich flacher als die Südosthänge, obschon auch die Nordwesthänge steile Stellen aufweisen. Grössere Differenzen in der Neigung der Böschungen bestehen jedoch nicht.

Zum dritten Teil des Dünenfeldes zählen die vier Dünen, die östlich vom Gehöft Hiukkamäki liegen. Drei davon steigen aus einem Niveau von 130—128 m empor, die vierte tiefer, aus etwa 125 m. Auch in diesem Teil des Feldes sieht man, wie die Dünen von Nordwest nach Südost an Höhe zunehmen. Unmittelbar an der Landstrasse liegt eine nur gut 1 m hohe, aus zwei Hügeln bestehende Düne. Die dahinter in einer Waldecke gelegene Düne ist schon höher, etwa 2 m. Unmittelbar hinter dieser erhebt sich die höchste (3—5 m) Düne, die am besten ausgebildet ist. Auch hier sieht man, dass der Südosthang steiler ist als der Nordwesthang. In Längsrichtung fällt diese Düne fast durchweg nordostwärts ab und endet ziemlich steil am Ackerrand. Ihren Fortsätz bildet eine durch das Ackerland laufende, schmale und nur 0.5—1 m hohe Düne, die seinerzeit gerodet, dann aber nicht mehr bebaut worden ist. Während der Zeit der Bebauung ist sie wahrscheinlich etwas abgeflacht worden. In diesem Teil des Feldes sind die Dünen deutlich voneinander getrennt.

Die Dünen des Gebiets sind ziemlich gerade, nicht bogenförmig wie auf vielen anderen Feldern (vgl. Hörner 1927). Da die Dünen relativ kurz sind, hat sich keine Bogenform herausgebildet, oder diese ist kaum wahrnehmbar. Stellenweise besteht freilich eine schwache Biegung am Nordwestrand der Düne, der also nicht so grade verläuft wie der Südostrand. Auch weisen die Dünen keine Anzeichen davon auf, dass der Wind sie erodiert oder zerrissen hätte, sie sind vielmehr unversehrt und haben ebene Oberfläche (vgl. Högbom 1923 s. 150, Hörner 1927 s. 106). Die Richtung der Längsachse wechselt bei den einzelnen Dünen. Im Südosten haben sie die Richtung N 50°E—N 60°E, aber weiter im Nordwesten N 30°E. Vergleicht man die Längsrichtung der Dünen mit den Richtungen der Höhenkurven und somit also mit den Richtungen der vormaligen Uferlinien, so sieht man, dass sie im südöstlichen Teil des Gebiets beträchtlich von der Richtung der ehemaligen Uferlinie abgewichen sind, während sie im nordwestlichen Teil ungefähr die gleiche Richtung einhielten (vgl. Okko 1949 s. 63, Flint 1957).

STRUKTUR DER DÜNEN

Die Aufklärung der Struktur der Dünen erwies sich als eine schwierige Aufgabe. Für die Untersuchung geeignete Durchschnitte gab es nur zwei. Ausserdem ist die Schichtung in diesen Dünen sehr schwach ausgbildet, und an den frischen Grabungen war sie überhaupt nicht wahrzunehmen. Erst nachdem die Wände der Gräben eine zeitlang getrocknet waren, liess sich eine gewisse Schichtung feststellen. Am ausgeprägtesten war die Schichtung am Landstrassengraben zu sehen sowie ferner an den Rainen der an den Dünenböschungen ausgetretenen Pfade, wo die Wand getrocknet und teilweise auch erodiert war. Die aus gröberem Sand bestehenden Schichten waren schneller ausgetrocknet und erodiert worden, so dass sich hier schwache Streifen in die Wand eingefressen hatten. Die aus feinerem Material bestehenden Schichten waren länger feucht geblieben und hielten daher besser zusammen, so dass die Erosion nicht so gut angreifen und Material herausnagen konnte wie in den vorgenannten Schichten. Infolgedessen waren diese feuchteren Lager in dem Wall etwas erhoben. An dem frischen Durchschnitt sahen nach dem Trocknen die aus gröberem Material bestehenden Schichten heller aus als die feuchteren, aus feinerem Material zusammengesetzten. Anhäufung von dunklen Mineralien in gewissen Schichten konnte dagegen nicht beobachtet werden (vgl. Hörner 1927 s. 115, Okko 1949 s. 65). Grössere Unterschiede in der Korngrösse der einzelnen Schichten bestehen nicht (vgl. s. 111), sondern das Material ist ziemlich homogen und die Schichtung daher schwer nachzuweisen. In den oberflächlichen Partien der Dünen ist die Schichtung sehr schwach, in den tieferen hingegen besser ausgeprägt. Deutlich wahrnehmbare Schichten findet man nicht selten erst in etwa 1 m Tiefe.

Die Durchschnitte sind in der Düne zwischen den Gehöften Hiukkamäki und Nummenpää. Die Düne ist an dem angeschnittenen Ende flach, und die Schnitte sind daher für die Untersuchung nicht gerade am vorteilhaftesten. Man sieht an ihnen nur die Struktur der niedrigen Düne. Am Nordwesthang haben die Schichten eine Neigung von 5—10° nach Nordwest, am Südosthang von 10—15° nach Südost. In den Mittelpartien der Düne sind die Schichten gewunden, im ganzen aber nur leicht konvex oder fast waagrecht. Die untersten Schichten liegen waagrecht. Am Südostrand der Düne, wo der Durchschnitt in Längsrichtung läuft, sind die Schichten nahezu waagrecht, aber an manchen Stellen sind sie zum Ende der Dünen hin geneigt und verlieren sich ohne deutliche Grenze. An den Wänden der senkrecht zu diesen Schichten gegrabenen Grube haben die Schichten eine Neigung von 15° südostwärts.

Die übrigen Dünen habe ich nur anhand von mir selbst gegrabenen Gruben untersucht, und dort konnten die Schichten nur kurze Strecken weit verfolgt werden. In den dem Drumlin aufgelagerten Dünen sind die Schichten am Südosthang ziemlich steil (20—25°) südostwärts geneigt. Am Nordosthang liegt zuoberst etwa 1 m ungeschichteter Sand, aber weiter in der Tiefe sind die Schichten südostwärts geneigt (15—20°). Im grossen und ganzen gleiche Struktur haben die nördlich vom Gehöft Hiukkamäki gelegenen Dünen, aber weiter nordwestwärts in den eng zusammen-

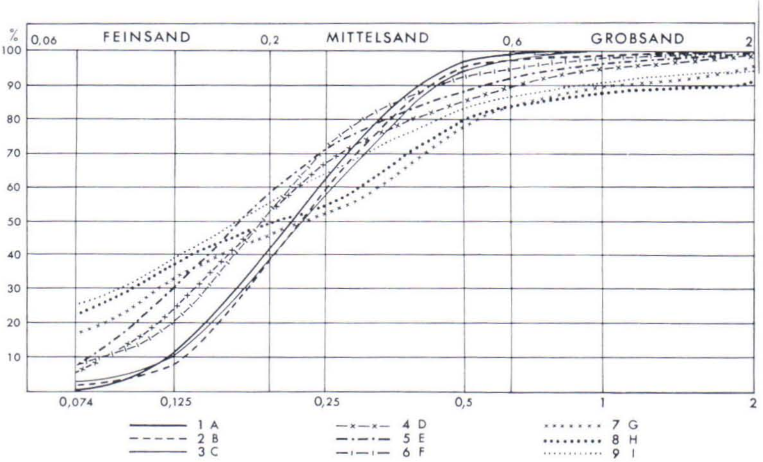

ABB. 3. Summenkurven der Korngrössen von Flugsand (1—3), Strandsand (4—6) und Moräne (7—9). A-I = Probenentnahmestellen (vgl. Abb. 1).

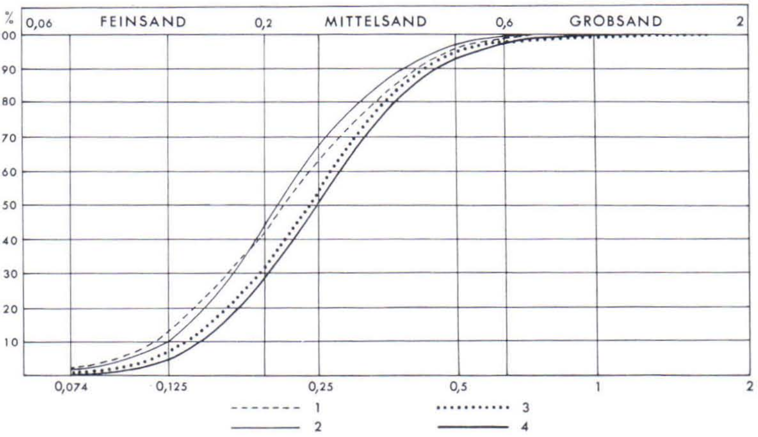

ABB. 4. Summenkurven der Korngrössen von Material in den verschiedenen Schichten einer Düne. 1—2 = feines Material, 3—4 = grobes Material.

gedrängten Dünen, fallen die Schichten am Nordwesthang 5—10° nach Nordwest hin ab. In den niedrigsten Dünen dagegen sind die Schichten fast waagrecht und flach geschlängelt. Besonders steil geneigt sind die Schichten in den Oberflächenpartien am südwestlichen Ende der im Nordwesten gelegenen Dünen. Die Neigung der Schichten beträgt 25—30° nach SW. Diskordanzen haben die Dünen wenig.

Oben sind nur einige vereinzelte Beobachtungen über den Aufbau der Dünen wiedergegeben. Um ein verlässlicheres Bild zu gewinnen, müssten einige von den höchsten Dünen angeschnitten werden, aber z.Zt. ist hierzu keine Möglichkeit gegeben.

MATERIAL

Das Material der untersuchten Dünen ist Mittelsand und Feinsand, deren gemeinsamer Anteil über 90 % beträgt. Der Mittelsand ist vorherrschend, und zwar macht er 57—61 % aus (vgl. Okko 1949 s. 64, M. Okko 1962 s. 111). Das Material ist im ganzen Feld ungefähr gleich, was gut auch aus den Summenkurven vom Material der verschiedenen Dünen hervorgeht (Abb. 3, Kurven 1, 2 und 3). Die Sortierung des Materials ist schon aus den Kurven schön ersichtlich, man kann den Sortierungsgrad aber auch mit einer gewissen Zahl angeben. Sindowksi (1938) hat für die Bestimmung des Sortierungsgrads folgende Formel ausgearbeitet:

$$S = \frac{H + A - R}{100}$$

In der Formel bedeutet S = Sortierungsgrad, H = Anteil der Hauptfraktion in Prozent, A = H + Anteil der vorhergehenden + Anteil der darauffolgenden Fraktion in Prozent, R = 100 — H. Wenn H = 100 ist, beträgt S = 2.

Dieser Formel gemäss ist der Sortierungsgrad des an der Stelle A entnommenen Materials 1.12, von der Stelle B 1.20 und von der Stelle C 1.13.

Die Korngrössenanalysen zeigen ferner, dass die Korngrösse in den verschiedenen Schichten der gleichen Düne keine grossen Unterschiede aufweist, wie u.a. aus Abb. 4 hevorgeht (vgl. Hörner 1927, s. 114—115). Da die Differenzen in der Korngrösse so geringfügig sind, ist es wohlverständlich, dass die einzelnen Schichten nicht besonders klar hervortreten.

Zum Vergleich machte ich noch eine Korngrössenanalyse von den Strandablagerungen des vormaligen Ufers sowie zwei Analysen vom Material aus dem Sandfeld, das sich an den Seiten und im Vordergrund des Dünengebiets ausbreitet (Stellen D, E und F, Abb. 1). Wie die Kurven 4—6 in Abb. 3 zeigen, ist das Material hier anders beschaffen als in den Dünen. Es handelt sich um Material, das vom Wellenschlag sortiert ist. Im Vergleich zu rezenten Ufersanden ist dieses Material schwächer sortiert, was mit der Kürze der Tätigkeit des Wellenschlags zusammenhängt.

Petrographisch ist der Dünensand ziemlich gut sortiert. Die mikroskopische Analyse zeigte, dass die hellen Mineralien, wie Quarz und Feldspat, vorherrschen und die helle Farbe des Sandes verursachen. Ferner enthält der Sand etwas Biotit, Hornblende und einige andere dunkle Mineralien. Gewöhnlich bestehen die Sandkörner aus nur einem Mineral, es sind durchschnittlich aber zwei Prozent Körner darunter, die aus zwei oder mehr Mineralien bestehen. Die petrographische Zusammensetzung ist aus der folgenden Tabelle ersichtlich. Das Material für die Analysen stammt von den Stellen A—F.

Stelle	A	B	C	D	E	F
Helle Mineralien	94	93	94	91	81	83 %
Dunkle Mineralien	5	6	6	8	14	15 %
Steinsplitter	1	1	—	1	5	2 %

Im Flugsand des Untersuchungsgebiets (Proben A—C) machen die hellen Mineralien 90 % aus. Sie sind z.T. Feldspat, in der Hauptsache aber Quarz. Dass der Dünensand so reichlich andere Mineralien enthält und nicht nur Quarz wie die alten, lang in Bewegung gewesenen Dünen, hängt mit der kurzen Transportstrecke zusammen.

Für den Flugsand ist es im allgemeinen charakteristisch, dass die Körner rundgeschliffen sind. Je länger der Sand in Bewegung gewesen ist, umso besser sind die Körner abgerundet. Der Sand von den untersuchten Dünen ist ziemlich wenig rundgeschliffen (vgl. Högbom 1923 s. 137, Hörner 1927 s. 108, Okko 1964 s. 295), aber Zurundung ist doch deutlich wahrzunehmen. Die nahezu runden Körner mit durchweg matter Oberfläche machen 10—15 % aus. Etwa 40—50 % der Körner haben deutlich abgerundete Ecken, aber ihre ursprüngliche Eckigkeit ist noch teilweise zu sehen, und manche Flächen sind glatte Bruchflächen. An diesen Körnern sind erst die Ecken abgeschliffen und matt. Die restlichen Körner sind ziemlich kantig und glatt oder erst wenig abgeschliffen, so dass die Kanten noch deutlich hervortreten. Es sind auch Körner darunter, bei denen eine Fläche deutlich konvex und matt ist, die übrigen aber glatt und glänzend. Sie sind dadurch entstanden, dass abgerundete Körner zerbrochen sind. Die grossen Körner sind deutlicher gerundet als die kleinen. In der Zurundung des Materials bestehen stellenweise beträchtliche Unterschiede. An manchen Stellen sind fast alle Körner rundgeschliffen, an anderen wiederum weitgehend eckig. In den Schichten mit kleinen Körnchen scheint die Zurundung geringer zu sein als in Schichten mit grossen Körnern. Wahrscheinlich ist bei der Windverwehung ein Teil der Körner zerbrochen, und die kleinen, eckigen Körnchen haben eine Schicht für sich gebildet, über die hinaus die grösseren Körner auf der Leeseite weitergerollt sind. In der von der Oberfläche der Düne genommenen Probe waren die Körner deutlich eckiger, geradezu scharfkantiger als mehr in der Tiefe. Hier spielt wahrscheinlich der Umstand mit, dass das Material an der Oberfläche stärker verwittert und deswegen kantiger ist als in den tieferen Lagen.

Zum Vergleich habe ich auch die Zurundung der Körner in den benachbarten Strandablagerungen und in der Moräne des Gebiets untersucht. In den Strandablagerungen ist das Material fast ebenso rundgeschliffen wie auch in den Dünen. Dies kann daher kommen, dass am Ufer äolisches Material angeweht worden ist, entweder direkt oder zuerst ins Wasser, von wo es der Wellenschlag dann aufgeschüttet hat (vgl. Okko 1964 s. 297). Wahrscheinlicher ist es jedoch, dass das Material schon ziemlich weitgehend durch die Tätigkeit der Wellen abgerundet wird, und da der Wind diesen Ufersand nur eine kurze Strecke weit fortgeblasen hat, ehe er ihn zu Dünen anhäufte, sind die Körner kaum wesentlich weitergeschliffen worden. Die Differenz in der Zurundung des Ufersandes und des Dünensandes ist so gering, dass man diese Sande längst nicht immer bloss aufgrund der Zurundung sicher voneinander unterscheiden kann (vgl. Högbom 1923 s. 137, Holtedahl 1924 s. 34, Hörner 1927 s. 108). Dagegen ist der Unterschied in der Zurundung der Körner zwischen dem Ufersand und dem aus der Moräne ausgesiebten (Korngrösse 0.075—0.5) Fein- und Mittelsand unverkennbar. Die Körner der Moräne sind deutlich eckiger, wennschon sich auch manche weitgehend rundgeschliffenen darunter befinden.

Vergleichende Untersuchungen haben gezeigt, dass in den rezenten Flugsandfeldern das Material mehr abgerundet ist als in den untersuchten fossilen Dünen. Als Vergleichsmaterial diente Sand von den Flugsandfeldern in Kalajoki, Yyteri und Höytiäinen. Abgesehen von der grösseren Zurundung war dieses Material auch etwas gröber, indem es grösstenteils aus Mittelsand bestand. Der Sortierungsgrad war höher, nämlich 1.3—1.5 (vgl. Okko 1949 s. 65, Ohlson 1957 s. 134). Die Ursache für die grössere Zurundung und Sortierung des Materials dürfte darin liegen, dass die Strandverschiebung heutzutage langsamer vor sich geht als früher (Okko 1964 s. 298), weshalb der Sand länger dem Wellenschlag ausgesetzt ist, ehe er vom Wind fortgetragen wird. Andererseits hat die Verwitterung den rezenten Flugsand noch nicht angegriffen, und selbst wenn Verwitterung stattfinden sollte, sortiert der Wind das feinste, zerbrochene und eckige Material aus dem eigentlichen Flugsand heraus.

Im Vergleich zum rezenten Flugsand ist der Sand der untersuchten Dünen deutlich brauner gefärbt. Dies kommt von dem feinen, aus Eisenocker bestehenden Überzug der Körner. Die braune Schale ist in den oberflächlichen Schichten der Düne stärker als in den tieferen, wo der Sand heller ist. Dies wiederum hängt damit zusammen, dass das vom Wasser mitgespülte Eisen sich in den oberen Schichten angereichert hat. Die Anreicherung ist jedoch auf einer ziemlich langen Strecke vor sich gegangen, denn eine ausgesprochene Anreicherungsschicht ist in den Dünen kaum zu sehen. Überhaupt scheint die Bodenbildung in den Dünen schwach zu sein (vgl. Okko 1964 s. 297).

Abgesehen von den Dünen kommt Flugsand in dem Gebiet an ziemlich begrenzten Stellen vor. Am proximalen Ende des Drumlins zwischen den Gehöften Nummenpää und Hiukkamäki erheben sich steile, kahle Felsen. Hinter diesem und teilweise auch an seinen Flanken liegt in 137—145 m Höhe ü.d.M. ein 10—100 cm starkes Sandlager. Es ist völlig frei von Steinen, und die Korngrösse ist die gleiche wie beim Dünensand. Südostwärts, gegen die Dünen hin, wird das Sandlager dünner, und kurz vor der ersten Düne kommt die Moräne zum Vorschein. Der Sand ist hier nicht wallartig aufgeschüttet, sondern bildet ein ebenmässiges, den Formen des Drumlins folgendes Feld. Das Gebiet ist gerodet und bestellt, und die früher eventuell vorhanden gewesenen Erhebungen sind infolgedessen eingeebnet. Auch in der Bachniederung zwischen dem genannten Drumlin und dem Dünenfeld liegt ziemlich viel Sand. Es ist jedoch nicht alles Flugsand, da sogar kleine Steinchen darunter sind, die der Wind nicht fortzutragen vermocht hat. Dieses Material besteht wahrscheinlich zum Teil aus Flugsand, zum Teil wieder aus Material, das der Wellengang vom Drumlin heruntergeschwemmt hat (vgl. Hörner 1957 s. 21—22, M. Okko 1962 s. 112).

Im Ostteil des Untersuchungsgebiets liegt rings um die am weitesten nordostwärts vorstossende Düne ein weites, ebenes Sandfeld, das wahrscheinlich aus auf der flachen Strandterrasse angehäuftem Flugsand besteht (vgl. Lundqvist 1943 s. 135). Zwischen dem Sand der Düne und dem des umliegenden Feldes besteht kein wesentlicher Unterschied. Die sanften Wellen des Ackerlandes rühren wahrscheinlich eben von Flugsandanhäufungen her. Eine für die Dünen ungewöhnliche Besonderheit ist es, dass die Bodenbildung dort stellenweise sehr ausgeprägt ist.

HERKUNFT DES MATERIALS

In Finnland ist früher festgestellt worden, dass die Dünen meistens im Zusammenhang mit Oszügen und Randbildungen vorkommen (Tanner 1915 s. 372, 380, 529—533, Okko 1949 s. 65, 1964 s. 295, M. Okko 1962 s. 109). Auch anderwärts scheinen die Dünen ihr Material aus glazifluvialen Ablagerungen bezogen zu haben (Hörner 1929 s. 112—113, Lundqvist 1943 s. 136, Flint 1957 s. 176—177, Wright 1961 s. 948). Andererseits kann das Material auch aus anderen als glazifluvialen Sedimenten herausgeschwemmt sein, sofern nur die geeignete Korngrösse gegeben war (Lundqvist 1943 s. 136—141).

Die Herkunft des Dünenmaterials in dem Untersuchungsgebiet liess sich gar nicht so leicht aufklären. Das nächstgelegene Vorkommen von glazifluvialen Material ist ein kleiner Oszug gut 1 km nordöstlich vom Dünenfeld. Ein weiterer, ähnlicher Oszug liegt südwestlich von dem Feld, 1.7—2 km weit entfernt. Ausserdem liegt zwischen dem letzteren und dem Dünenfeld ein weites Moränenhügelgebiet, wo keine Spur von glazifluvialem oder äolischem Material zu sehen ist. Auch zwischen dem Dünenfeld und dem nordöstlichen Os liegen ein paar flache Moränenrücken. Beide Oszüge sind so niedrig und flach, dass sie in der Hauptsache erst dem Meer entstiegen sein können, als das Gebiet von Dünenfeld sich schon gehoben hatte und wenigstens ein Teil von den Dünen bereits entstanden war. Diejenigen Teile des auf der Nordostseite verlaufenden Oses, die ungefähr zur gleichen Zeit dem Meer entstiegen sind wie auch das Dünenfeld, liegen 2—2.5 km nordnordwestwärts vom letzteren. Ausserdem befand sich damals zwischen dem Os und dem Dünenfeld ein weites Wasserbereich. Das oben Gesagte spricht also ganz offenbar dafür, dass das Material des Dünenfeldes nicht aus glazifluvialen Ablagerungen herstammt.

Die Herkunft des Materials wurde mit Hilfe der oben schon erwähnten Korngrössenanalysen geklärt. Ausserdem ist auch Moräne des Untersuchungsgebiets gesiebt worden. Die Moräne wurde vom Scheitel der früher beschriebenen Drumlins in 0.5 m Tiefe genommen. Die Summenkurven sind auf Abb. 3 zu sehen, Kurven 7—9. Aus Kurve 9 geht hervor, dass es sich um eine Feinsandmoräne mit wenig Steinen handelt, die reichlich auch Mittelsand enthält. Das Material des grösseren Drumlins ist etwas gröber, wie die Kurven 7 und 8 zeigen. Die Sandproben der Strandablagerung wurden an den gleichen Stellen genommen, wie vorn auf S. 111

beschrieben, und die Kurven 4—6 auf Abb. 3 zeigen die Korngrösse des Materials. Wie ein Vergleich zwischen den oben genannten Kurven zeigt, ist das Material der Strandablagerung so entstanden, dass die Wellen aus der Moräne die feineren Bestandteile (Ton und Schluff) ausgewaschen und tiefer ins Wasser hineingetragen haben. Entsprechend sind die Steine der Moräne am Fuss des Uferabhang zurückgeblieben. In dem vom Wellenschlag sortierten und aufgeschütteten Material befinden sich noch 10—20 % Schluff, eventuell auch etwas tonige Bestandteile. Der Unterschied zwischen den Kurven 1—3 und 4—6 lässt sich folgendermassen erklären. Als der Wind anfing, das am Ufer angehäufte oder zu einem Strandwall aufgeschüttete Material fortzutragen, wurden die feineren Bestandteile, die ja leichter waren, aus dem Dünenfeld fortgeblasen (vgl. Hörner 1927 s. 112). Entsprechend war der grobe Sand zu schwer, um vom Wind verweht zu werden, er blieb daher am Strande liegen und wurde später, als das Dünenfeld nordwestwärts vordrang, vom Dünensand begraben. Derartiges grobes Material ist heute unter den Dünen anzutreffen. Der Wind hat nur Körner von gewisser Grösse, Mittelsand und Feinsand, zu Dünen zusammenzutragen vermocht. Andererseits ist es möglich, dass der Wellenschlag den Ufersand in den oberflächlichen Partien noch weitgehender sortiert hat, und dass die feinen Bestandteile dann weggeschwemmt worden sind, wonach der Wind das zurückgebliebene Material zu Dünen aufgehäuft hat.

Aufgrund des oben Gesagten hat es also den Anschein, dass das Material der Dünen in dem Untersuchungsgebiet aus der benachbarten Moräne herstammt. Das Wasser hat es zunächst zu Strandablagerungen ausgeschwemmt, wonach der Wind es erneut sortiert und zu Dünen zusammengeweht hat.

In dem Gebiet findet man viele Spuren von der Tätigkeit des Wellenschlags. An den Hängen des zwischen Nummenpää und Hiukkamäki gelegenen Drumlins, insbesondere an seinem Nordwestende, ist 135—136 m ü.d.M. ein gut ausgebildetes Ufer zu sehen. Das entsprechende Ufer sieht man auch an anderen genügend hohen Erhebungen in der Nachbarschaft, an der 1 km ostwärts gelegenen Anhöhe Rakuunavuori in 134 m und auf dem Scheitel der etwa 2.5 km nordnordwestwärts gelegenen Deltas in 136—137 m Höhe (vgl. Sauramo 1958 s. 234—248). Weiter oben sind keine Spuren des Wellenschlags mehr wahrzunehmen. Reichlich findet man sie dagegen in der Höhe von 125—130 m, insbesondere an dem kleinen Drumlin nordöstlich vom Dünenfeld (vor allem an seinem nordwestlichen Ende) sowie an dem hohen Waldrücken, der sich auf der Südwestseite des Untersuchungsgebiet nordwestwärts hinzieht. In diesem Niveau hat der Wellengang den Moränenboden stark ausgewaschen und einen steinigen Ufergürtel hinterlassen. Unterhalb von 120 m wird das Gelände ebenmässiger, und die Ufermarken sind nicht mehr so deutlich zu sehen. Von den ausgewaschenen Stellen, wo nun noch Steinhaufen liegen, haben die Wogen viel Material fortgetragen. Ein Teil davon liegt nun weiter unten als Schluff- und Tonboden, einen Teil hat der Wellengang am Ufer zur Strandablagerung angehäuft, und ein Teil ist von dem damaligen Strand vom Wind verweht und zu Dünen aufgeschüttet worden.

ENTSTEHUNG DER DÜNEN

Nachdem das Inlandeis zurückgewichen war, ragte das Untersuchungsgebiet teilweise als supraaquatische Inseln aus dem Yoldiameer hervor. Die bedeutendste Insel war der Drumlin zwischen den Gehöften Nummenpää und Hiukkamäki. Dort haben die Wellen einen deutlichen Uferabhang ausgewaschen (135—136 m ü.d.M.) und Material als Strandablagerung angehäuft. Nach Sauramo (1958 s. 234—237) handelt es sich um ein Y I -Ufer (Sauramos jüngeres Y I). Als der Meeresspiegel absank, begann der Wind Mittelsand und Feinsand auf dem Scheitel des Drumlins zu Dünen zusammenzuwehen. Bald stieg auch der kleinere Drumling (133 m ü.d.M.) aus dem Meer und wurde zugleich ausgewaschen. Das feine Material wurde mindestens teilweise zwischen diesen beiden Drumlins abgelagert. Als der Meeresspiegel auf das heutige Niveau von 130—129 m abgesunken war, ragte aus dem Wasser ein Landstreifen hervor, der in Richtung der jetzigen Landstrasse die beiden Drumlins miteinander verband. So hatte sich zwischen den beiden Erhebungen eine nordwestwärts offene Bucht gebildet. Am Innenrand dieser Bucht ging Akkumulation vor sich, wie sie auch heute noch in vielen geschützten Buchten stattfindet. Dieses Material nahm der Wind nun auf und häufte es anfänglich in dem östlich von Hiukkamäki gelegenen Gebiet, später in der Nähe der jetzigen Landstrasse zu gleichgerichteten Dünen an. Die Dünenbildung auf dem Scheitel des Drumlins dürfte in diesem Stadium zum Stillstand gekommen sein. Da der Sand in niedrigerem Niveau liegenblieb, gelangte er nicht mehr bis zum Scheitel des Drumlins. Ausserdem hatte dort in diesem Stadien mindestens Tundravegetation schon Fuss gefasst, die den Sand festhielt und die Wanderung der Dünen zum Stehen brachte. Als der Wasserspiegel weiterhin sank, wurde die Bucht weiter, und der Wellengang griff die Landzungen an, die die Bucht schützten, insbesondere den proximalen Teil des Nordostdrumlins, der heutzutage aus lauter Steinen besteht. Nachdem der Wasserspiegel von 130 auf 125 gesunken war, wuchs die im Südwest das Dünengebiet schützende Landzunge auf fast 1 km Länge an; die Halbinsel auf der Nordwestseite blieb etwas kürzer und niedriger, setzte sich aber unter dem Wasser noch eine Strecke weit als unterseeischer Wellenbrecher fort. Das Dünenfeld blieb also im Innern der immer länger werdenden Bucht liegen. Die Bucht war in diesem Stadium schon ziemlich seicht, und durch das eingeschwemmte Material wurde sie ständig noch flacher. Das Meeresufer wich ziemlich rasch zurück, und die Dünen konnten nicht so hoch anwachsen wie früher. Sie wurden immer niedriger, und schliesslich kam ihre Bildung zum Stillstand (vgl. Solger 1910 s. 43, Granlund 1943 s. 87, Okko 1964 s. 295). Dass die Dünenbildung aufhörte, hatte ausser mit dem raschen Zurückweichen der Strandlinie auch damit zu tun, dass die die Bucht einschliessenden Landzungen immer länger wurden, und dass aus dem Meer immer zahlreichere und grössere Inseln emportauchten, wodurch die Windwirkung abgeschwächt wurde. Auch die Pflanzendecke war dichter geworden, wofür die reichlichen organischen Stoffe in dem unter den letzten Dünen hervorgegrabenen Strandsand ein Zeichen sind.

Als die letzten Dünen in der Nordwestpartie des Dünenfeldes aufgeweht wurden, entstand auf der Ostseite der heutigen Landstrasse ein weites, ebenes Strand- und Flugsandfeld. Zur Bildung von hohen Dünen ist es in diesem Gebiet nicht gekommen, denn der flache, ebene Strand wurde weit landeinwärts von den Wellen überspült, so dass eventuelle Flugsandanhäufungen bald wieder eingeebnet wurden. Weil das Gelände so flach war, wich auch das Ufer rasch zurück, und da die schützende Bucht nun fehlte, wurde kein Sand mehr abgelagert; ferner hielten die Pflanzen den Sand fest, und wahrscheinlich spielten auch die Winde eine Rolle.

DIE AN DER ENTSTEHUNG DER DÜNEN BETEILIGTEN WINDE

Im allgemeinen sind die Dünen quer zur Richtung des vorherrschenden Windes gestellt, seltener verlaufen sie in der gleichen Richtung wie dieser. Längsdünen, die auf die letztere Art angeordnet sind, kommen nur in genügend grossen Sandfeldern und gewöhnlich in extrem trockenen Verhältnissen vor (Flint 1957 s. 177). In dem untersuchten Gebiet sind die Dünen quer zur Richtung der stärksten Winde gestellt (vgl. Solger, Graebner u.a. 1910 s. 34).

Die Struktur der Dünen von Urjala weist Eigenschaften auf, die davon zeugen, dass das Material hauptsächlich unter Mitwirkung des Nordwestwindes aufgeschüttet worden ist. Dies zeigen die Schichten der Dünen, die auf der Nordwestseite sanft südostwärts ansteigen, und auf der Südostseite deutlich steiler in gleicher Richtung abfallen (vgl. s. 109). Für die gleiche Auffassung sprechen auch die Querprofile der Dünen: der Nordwesthang oder die Luvseite ist im allgemeinen flacher als der Südosthang oder die Leeseite. Die Einwirkung des Nordwestwindes macht sich auch im Verhältnis der Dünen zueinander geltend, insbesondere gerade an der Nordwestspitze des Feldes. Jede von diesen kleinen Dünen liegt teilweise auf der nächsten, südostwärts von ihr gelegenen Düne, und muss demgemäss also später entstanden sein. Zugleich nimmt die Höhe der Dünen nordwestwärts ab, ein Zeichen dafür, dass die Dünenbildung in dieser Richtung nachgelassen hat.

Die Entstehung der Dünen unter der Einwirkung von Nordwestwinden ist gut verständlich. Zu Beginn der Dünenbildung lag das Inlandeis noch ziemlich nahe, und aus dem dortigen Hochdruckgebiet bliesen die Winde nach Südost in das eisfreie Tiefdruckgebiet (vgl. Högbom 1923 s. 140—170, Hörner 1927 s. 170—173, M. Okko 1962 s. 113). Die Dünen auf dem Rücken des Drumlins sind gerade in dieser Zeit entstanden, als die Wirkung des Eises noch ziemlich stark war. Als der untere Teil des Dünenfeldes gebildet wurde, hatte das Eis sich schon etwas weiter zurückgezogen, aber sein Einfluss machte sich immer noch geltend. Ausserdem ist diese Partie des Dünenfeldes im Innern einer nordwestwärts offenen Bucht aufgehäuft worden, wo es vor anderen Winden gut geschützt war. Dass die letzten Dünen mehr in Nord-Südrichtung verlaufen, lässt sich, was den Wind betrifft, so erklären, dass das Eis schon in diesem Stadium weiter zurückgewichen war und die nordwestlichen Winde nicht mehr so stark beeinflusste wie früher. Andererseits wäre auch denkbar, dass der

Strand mehr die Richtung Nord-Süd angenommen hätte, und die Dünen dementsprechend angeordnet wären.

Die Nordwestwinde sind jedoch nicht allein herrschend gewesen (vgl. Högbom 1923 s. 223, Hörner 1927 s. 170—173, Lundqvist 1943 s. 142, M. Okko 1962 s. 113), obschon sie am stärksten waren oder unter dem Einfluss der Umgebung am stärksten zur Geltung kamen. Den Nordwestwinden stand kein Hindernis im Weg, während die Wirkung der Süd-, Südwest- und Westwinde durch den südwestlichen Drumlin und das dahinter gelegene Hügelland abgeschwächt wurde. Die Südostwinde konnten unbehindert blasen, und es ist nicht ausgeschlossen, dass sie wenigstens auf dem Scheitel des Drumlins den Sand etwas zurückgeweht haben (vgl. Solger usw. 1910 s. 169). Der nördliche Drumlin hat die Dünen bis zu einem gewissen Masse vor den Nordwinden geschützt. Die Nordostwinde dagegen wurden vom Gelände nicht abgehalten, und ihre Einwirkung auf die Dünen ist auch ganz offenbar, insbesondere bei den nordwestlich von der Landstrasse gelegenen. Dort hat der Wind zwischen den Dünen hindurchgeblasen, und infolgedessen tritt am Nordostende zwischen den Dünen stellenweise die Moräne des Untergrundes zutage. Zugleich hat er Material südwestwärts getragen und stellenweise an den Flanken der Dünen steile Böschungen ausgehobelt (vgl. Abb. 2, Profil z_1-z_2, Düne bei 240 m). Das Nordostende der Dünen ist etwas abgeflacht worden, während das Südwestende etwas angestiegen ist. Deswegen ist die Struktur der Dünen am Südwestende weniger deutlich als am Nordostende. Der Nordostwind musste auf der Südwestseite des Dünenfeldes wegen des im Wege stehenden Drumlins aufsteigen, wobei er das mitgeführte Material rasch fallen liess. Der Südwesthang des Dünenfeldes an dem Drumlin wurde infolgedessen steil (vgl. Mattila 1938 s. 277—278).

Auf dem Sandfeld, das den Ostteil des Dünenfeldes umgibt, konnten mit Ausnahme der Süd- und Westwinde alle anderen Winde unbehindert wehen. Vielleicht ist gerade dies der Grund dafür gewesen, dass in diesem Gebiet überhaupt keine regelrechten Dünen zustandegekommen sind, obwohl Material vorhanden gewesen wäre. Wahrscheinlich ist der Nordwestwind in diesem Stadium jedoch noch vorherrschend gewesen, denn die einzige ausgeprägte, wennschon niedrige Düne steht quer zu dieser Richtung. Das Gleiche zeigen auch einige andere geringere Erhebungen.

ENTSTEHUNGSZEIT DER DÜNEN

Um die Entstehungszeit der Dünen zu klären, untersuchte ich das Moor, das in dem Dünenfeld liegt. Sein Boden besteht aus Sand, wahrscheinlich eben Flugsand. Die Pollenanalyse zeigte, dass das Moor in einer Zeit entstanden sein muss, wo reichlich Betulapollen abgelagert worden ist. Der Kiefernpollen ist deutlich spärlicher vertreten. Erle ist an der Stelle reichlich gewachsen. Pollen von edlen Laubhölzern findet man relativ viel. Der Pollenbestand zeigt also, dass das Moor im Atlantikum entstanden sein muss. Wahrscheinlich hat sich das Moor jedoch erheblich nach der Entstehung der Dünen gebildet.

Unter der am weitesten nordwestlich gelegenen Düne stiess ich auf eine aussergewöhnlich dunkle Sandschicht. Die mikroskopische Untersuchung ergab, dass die dunkle Färbung von organischen Stoffen herrührte. Diese etwa 5 cm dicke Schicht ist wahrscheinlich so zustandegekommen, dass sich im Endstadium der Dünenbildung am Innenrand der Bucht etwas organisches Material angehäuft hat, das dann von den Wellen mit dem Strandsand vermischt und in diesem vergraben wurde. Später, als das Land sich hob, wurde die Ablagerung von der Düne zugeschüttet. Die Pollenanalyse zeigte, dass in der oberen Partie der Schicht die Birkenpollen 81 % ausmachten und die Kiefernpollen 19 %. Im unteren Abschnitt waren die entsprechenden Zahlen 86 und 14. Beide Partien enthielten auch reichlich NBP und Sporen. Demgemäss wuchs in dem Gebiet zur Zeit der Entstehung der letzten Dünen Birke und Kiefer. Höchstwahrscheinlich sind die letzten Dünen eingangs des Präboreals entstanden, wovon der grosse Anteil der NBP Zeugnis ablegt. Freilich kann das reiche Vorkommen dieser Pollen auch mit der Nähe des Strandes zu tun haben.

Die Entstehungszeit der Dünen kann man auch mit Hilfe der Uferbildungen im Gelände aufzuklären versuchen. Nach den Untersuchungen von Hyyppä (1963 s. 44—46) stand der Rand des Inlandeises zu der Zeit, als der Baltische Eissee auf das Niveau des Yoldiameeres abzusinken begann (8213 v.Chr.), auf der Proximalseite des III Salpausselkä (Nach Sauramo (1958) auf der Proksimalseite des II Salpausselkä). Mein Untersuchungsgebiet liegt ca. 15 km nordwestlich vom III Salpausselkä und war in diesem Stadium also noch vom Eis zugedeckt. Erst nach der Befreiung vom Eise konnte es dort zu Uferbildungen kommen, was frühestens erst eingangs des Y I-Stadiums geschehen sein kann (ca. 8200 v.Chr., Hyyppä op.cit.). Das höchste Ufer, das in meinem Untersuchungsgebiet ca. 136 ü.d.M. liegt, ist auch nach Sauramo (1958 s. 234—248) ein Y I-Ufer (Sauramos jüngeres Y I, das nach Sauramo 7858 v. Chr. enstanden ist). Die ersten Dünen konnten erst aufgeweht werden, als die Wellen genügend Material aus der Moräne ausgewaschen hatten, also erst gegen Ende des Y I-Stadiums.

Gut 5 m unterhalb vom höchsten Ufer liegt in meinem Untersuchungsgebiet ein zweites Ufer. Sauramo (1958 s. 245—247) hat in der Nähe meines Gebiets zwei Moore (Likolampi, Lahmajärvi) untersucht. Aufgrund seiner diesbezüglichen Diagramme hat Hyyppä (1963 s. 38, 45, Beilagen 1 und 2) die Höhe des Y II-Stadiums in diesem Gebiet bestimmt. Das vorn genannte Ufer ist im Laufe dieses Stadiums entstanden, d.h. ca. 8000 v.Chr nach Hyypä (ca. 7750 v.Chr. nach Sauramo). Als der Meeresspiegel in diesem Niveau lag, begann der östlich vom Gehöft Hiukkamäki gelegene Teil des Dünenfeldes aus dem Meer emporzusteigen, und die Dünenbildung setzte dort ein. Auf dem Rücken des Drumlins dürfte die Dünenbildung damals aufgehört haben.

Die untersten Dünen steigen aus dem Niveau von 123—124 m auf. Das damalige Ufer lag ein paar Meter tiefer, wahrscheinlich in ca. 120 m Höhe. Nach Hyyppäs (1966, Beilage 2) Diagramm ist das fragliche Ufer während des Stadiums Y II_2 entstanden, reichlich hundert Jahre später als das vorige Ufer. Der Nordwestteil des Dünenfeldes ist in der genannten kurzen Zeit entstanden.

Wie grob die obigen Datierungen auch sein mögen, so zeigen sie doch, dass die Dünen um die Wende der jüngeren Dryaszeit zum Präboreal gebildet worden sind, und zwar gleich eingangs des Yoldiameer-Stadiums, bald nachdem das Gebiet vom Eis befreit war. Die Entstehung des ganzen Dünenfeldes hat nur 200—300 Jahre in Anspruch genommen (vgl. Högbom 1923 s. 159, Hörner 1927 s. 167).

VEGETATION DER DÜNEN

Die Dünen weichen von der Ungebung auch hinsichtlich ihrer Vegetation deutlich ab. Von den Baumarten ist die Kiefer fast allein herrschend. Ferner wächst auf den Dünen auch viel Wacholder. Zwischen den Dünen hingegen und auch sonst in der Umgebung überhaupt ist der dominante Baum die Fichte.

Aufgrund seiner Bodenvegetation gehört der Wald auf den Dünen zum *Vaccinium*-Typ. Der Boden trägt eine dichte, ziemlich starke Moosdecke, worin *Pleurozium Schreberi*, *Hylocomium splendens* und *Dicranum undulatum* vorherrschen. An ein paar Stellen, zuvörderst auf dem Scheitel und an den Südhängen der Dünen, findet man fleckenweise Flechten, zuvörderst *Cladonia rangiferina* und *Cl. silvatica.* Von den übrigen Flechten ist *Cetraria islandica* am bedeutsamsten.

Von den Zwergsträuchern dominiert *Vaccinium vitis-ideaea* fast allein, obschon seine Bestände im allgemeinen sehr schütter sind. *Calluna vulgaris* wächst auf den Dünen nur stellenweise, desgleichen *Vaccinium myrtillus* und ganz spärlich *Arctostaphylos uva-ursi.* Auf der dicken Moosdecke wächst allgemein, aber verstreut, grösstenteils sterile *Deschampsia flexuosa.* Da und dort seht man einige Büschel von *Calamagrostis arundinaceae.* Von den übrigen Pflanzen sind *Equisetum hiemale* und *Lycopodium complanatum* ziemlich verbreitet, obwohl sie nirgends ausgedehnte oder dichte Bestände bilden. Stellenweise wächst etwas *Pirola secunda*, *P. rotundifolia*, *Linnea borealis*, *Luzula pilosa* und *Trientalis europaea.* Im Vergleich zu dem Moränengebiet der Umgebung sind die Dünen durch ihre Artenarmut charakterisiert. Die Dünen des Untersuchungsgebiets sind jedoch längst nicht so karg wie viele andere mit Flechten bewachsenen Dünen des Binnenlandes. Die Ursache hierfür liegt teilweise in der Feinheit des Dünenmaterials, dank deren die Feuchtigkeitsverhältnisse günstig sind.

Manuskript eingegangen am 29, März, 1967

LITERATUR

GRANLUND, ERIK (1943) Beskrivning till jordartskarta över Västerbottens län nedanför odlingsgränsen. Sv. Geol. Unders. Ser. Ca 26. 1—165.

FLINT, RICHARD (1957) Glacial and pleistocene geology. New York 1—553.

HOLTEDAHL, O. (1924) Studier over israndterassene syd for de store østlandske sjøer. Videnskapsselsskapets Skrifter I. Mat. — naturv. klasse, no 14. 1—110.

HYYPPÄ, ESA (1963) On the late-Quaternary history of the Baltic Sea. Fennia 89 : 1. 37—50.

—»— (1966) The late-Quaternary uplift in the Baltic Sphere and the relation diagram of the raisen and tilted shore levels. Ann. Acad. Sci. Fenn. Ser. A III 90. 153—168.

HÖGBOM, A. G. (1923) Ancient inland dunes of Northern and Middle Europe. Geogr. Ann. 5. 113—243.

HÖRNER, N. G. (1927) Brattforsheden. Ett värmländskt randdeltekomplex och dess dyner. Sv. Geol. Unders. Ser. C. 342. 1—243.

LUMME, ESTER (1934) Die Flugsandfelder und Dünengebiete Finnlands. Nach Literaturbelegen zusammengestellt. Fennia 59 : 2. 1—77.

LUNDQVIST, G. (1943) Norrlands jordarter. Sv. Geol. Unders. Ser. C. 457. 1—165.

MATTILA, JORMA (1938) Lohtajan lentohietikko. Vanhaa Lohtajaa. Kyrönmaa IV. Helsinki. 263—281.

OHLSON, BIRGER (1957) Om flygsandfälten på Hietatievat i östra Enontekiö. Terra 69 : 4. 129—137.

OKKO, MARJATTA (1962) The development of the First Salpausselkä, west of Lahti. Bull. Comm. géol. Finlande. 202. 1—162.

OKKO, VEIKKO (1949) Suomen geologinen yleiskartta. Lehti B 4. Kokkola. Maalajikartan selitys. Geologinen tutkimuslaitos. The general geological map of Finland. Sheet B 4 Kokkola. Explanation to the map of surficial deposits. The geological survey of Finland.

—»— (1957) On the thermal behaviour of some finnish eskers. Fennia 81 : 5. 1—37.

—»— (1964) Maaperä. — Rankama, Kalervo: Suomen geologia. Helsinki. 239—331.

SAURAMO, MATTI (1958) Die Geschichte der Ostsee. Ann. Acad. Sci. Fenn. Ser. A III 51. 1—522.

SINDOWSKI, K.-H. (1938) Sedimentpetrographische Methoden zur Untersuchung sandiger Sedimente. — Geologische Rundschau 29.

SOLGER, F., P. GRAEBNER, J. THIERMANN, P. SPEILER, F. W. SCHULZE (1910) Dünenbuch. Stuttgart.

TANNER, V. (1915) Studier öfver kvartärsystemet i Fennoskandias nordliga delar. III. Bull. Comm. géol. Finlande. 38. 1—815.

WRIGHT, H. E. JR. (1961) Late-pleistocene climate of Europe; a review. Geol. Soc. America Bull. 72. 933—983.

Comptes Rendus de la Société géologique de Finlande
N:o XXXIX (1967), pp. 123—131

CONVOLUTE LAMINATION IN A LATE PLEISTOCENE DEPOSIT AT PANNUJÄRVI, TUULOS, FINLAND

BY

MARJATTA OKKO

Geological Survey of Finland, Otaniemi

ABSTRACT

Convolute lamination is reported for the first time from the Late Pleistocene glaciofluvial deposits of Finland. The metadepositional structure is considered to be the result of gravity-induced thixotropic behaviour during compaction under water. Glaciofluvial deposition in a shallow sea is the sedimentary environment of the convoluted bed.

INTRODUCTION

Deformational structures in glaciofluvial and glaciolacustrine beds have been described from various parts of Finland by several authors. The descriptions are mostly included in regional reports (*e.g.*, V. Okko 1949). Van Straaten (1949) and Aurola (1960) have reported deformational structures that developed through subaqueous folding by sliding movements. Some of the structures attributed by Virkkala (1959) to frost phenomena include features of plastic deformation.

During the last ten or fifteen years sedimentary structures have been studied extensively. This has resulted in the introduction of many new structural concepts, including convolute lamination. Several hypotheses have been proposed for the origin of convolute lamination (see, *e.g.*, Einsele 1963, pp.184—189;Potter and Pettijohn 1963, pp. 152—155; Davies 1965, p. 308). Convoluted beds are most common in flysch sequences dating from the Precambrian onwards, but they occur also in shallow-sea environments. Not all the authors recognize them in recent sediments (*e.g.*, Potter and Pettijohn 1963, p. 154). Convolute lamination or closely related structures have been produced, however, also in laboratory experiments (*e.g.*, Stewart 1956, Selley and Shearman 1962). Convolute lamination is found in some Pleistocene glaciolacustrine varved silts (*e.g.*, Emery 1950). The purpose of the present paper is to add to the knowledge of convolute lamination in Pleistocene glaciofluvial beds.

GEOLOGICAL SETTING

In the Pannujärvi area (Long 24°49′ E, Lat 61°06′ N) there is a cone-shaped glaciofluvial accumulation that occupies a depression between two elevated blocks of bedrock covered with ground moraine. Pitted topography strewn with boulders occurs at the neck of the accumulation, where it reaches its maximum altitude, about 145 m above sea level. The pitted surface of the accumulation slopes evenly towards E and SE, about 3 m to each kilometer. In the middle, the remnants of an esker can be distinguished. The esker has a distal continuation as it extends outside the accumulation and can be followed southeastward to the Mataramäki delta (V. Okko 1957) of the Second Salpausselkä belt, which lies 12 km SE of the neck of the accumulation and 8.5 km SE of its southeastern border at Pannujärvi (lake).

Field relationships indicate that during and after the Second Salpausselkä stage, deposition of an esker took place along a radial zone extending from the Mataramäki delta to the Pannujärvi area. The deposition of the cone-shaped glaciofluvial accumulation represents a standstill in the retreat of the ice margin, probably caused by the topography of the bedrock underlying the thinned glacier. The accumulation is superposed in relation to the original esker. Similar relationships have been described from the Evo area (M. Okko 1965), 25 km NE of Pannujärvi.

In the Jylisjärvi section of the Second Salpausselkä belt, SE of Pannujärvi, the ice margin had retreated to a distance of 3 km from the end moraine when the Baltic Ice Lake was discharged into the ocean and the Yoldia Sea phase began (V. Okko 1957) in about 8300 B. C. Along the esker extending from the Mataramäki delta to the Pannujärvi area, this drop in level is marked by the difference in altitude of the truncated tops of the heavily pitted esker 5 km beyond the delta. From there onwards the esker and the cone-shaped glaciofluvial accumulation were controlled by the Yoldia Sea.

Judging by V. Okko's (1957) observation of the altitude of the Yoldia shore to be 132—133 m above present sea level in the Jylisjärvi area and by the tilt of that shore surface between Jylisjärvi and Lahti, estimated to be 0.75 m/l km (M. Okko 1962, p. 119), the Yoldia level should have stood at about 141—142 m at the neck of the accumulation and at 138—139 m at Pannujärvi. These figures are in accord with Hyyppä's (1963, 1966) relation diagram of the Baltic shore levels.

At Pannujärvi a gravel pit has been opened close to the southeastern border of the cone-shaped glaciofluvial accumulation and 700 m SW of the original esker. The top of the gravel pit lies at 135 m above sea level or 3 m to 4 m below the calculated Yoldia level.

DESCRIPTION OF THE GRAVEL PIT AT PANNUJÄRVI

On the horizontal plane the gravel pit is roundish, and about 120 m in diameter. Only the topmost layer, 4 m to 5 m thick and comprising pebbly gravels rich in cobble material, has been removed. In the southwestern part of the pit, two diggings have been made below the lower limit of the top layer. Both reveal fine and medium sands in graded beds with ripple marks. There is a distinct unconformity between the coarse top layer and the underlying current-bedded material. The unconformity occurs at an altitude of 130 m above sea level, or 8 m to 9 m below the calculated Yoldia level. The underlying sediments were deposited from the meltwater stream that produced the esker in the Pannujärvi area. The overlying coarse bed belongs to the subaqueous part of the cone-shaped glaciofluvial accumulation. Redeposition of its material has taken place in the shore zone.

At the eastern digging the following sequence is to be seen in the pit:

Top at	134 m	above sea level
A	4 m	pebbly gravel with cobbles; topmost layer horizontal, deeper structure unknown
unconformity		
B	0.5 m	graded fine sands
slight structural unconformity		
C	0.1 m	convoluted bed composed of silty fine sand and fine sand
D	0.3 m	graded fine sands with ripple marks
E	0.05 m	thin laminae of sandy coarse silt intercalated with fine sand
below	129 m	fine sands

The structures below the unconformity between beds A and B are shown in Fig. 1.

The distorted bed C exhibits all the diagnostic features ascribed to convolute lamination (see Davies 1965, p. 306). The basic elements are a series of anticlinal folds separated by broad »synclines». The »anticlines» are mostly sharp-crested. Only one bed is affected and it is quite regular in thickness. The height of the bed and of the convolutions, 10 cm, is typical of convolute lamination. The deformation is most conspicuous in the lower half of the bed and ceases at the upper limit, showing that the original bed has not been eroded. Individual lamination planes can be traced through a number of undulations. Furthermore, the deformation is strong in two perpendicular sections. On the upper surface of the convoluted bed the »anticlines» form variants between ridges and cones (Fig. 2). In a cross section parallel to the bedding, the anticlinal ridges show a subparallel arrangement (Fig. 3). The fault seen in the horizontal section is distinctly younger than the distortion as the convolutions have not been observed to be controlled by faulting. The absence of contemporaneous faulting is also a criterion for convolute lamination.

DISTRIBUTION OF GRAIN SIZES

The results of the grain-size analyses made of the four beds of the eastern digging are shown in Fig. 4. In order to avoid mixing of the matter from the various beds, the samples were taken when the ground was frozen.

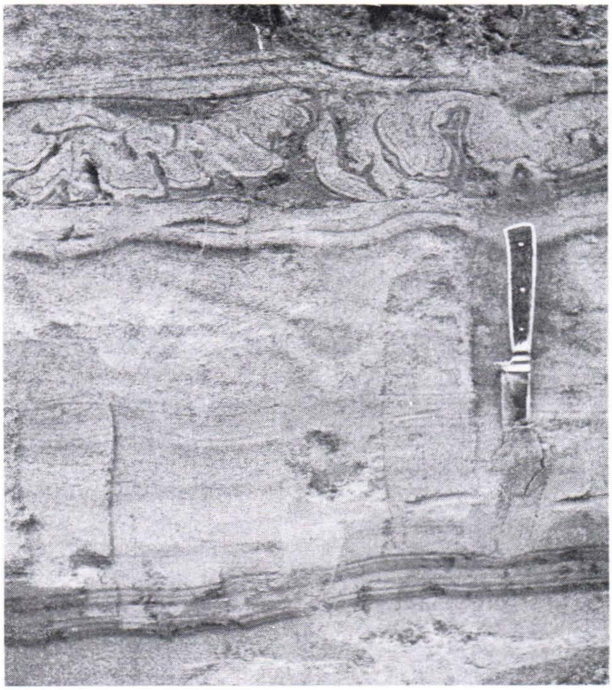

FIG. 1. Vertical section of the digging in the gravel pit at Pannujärvi. In the upper right corner secondary debris. Note the unconformity on top of the convoluted bed. Ripples occur throughout the bed underlying the convoluted bed. Length of knife-handle is 10 cm.

Bed B is distinctly arenaceous and well sorted. No ripples occur in this bed. It overlies bed C unconformably.

The sample taken from bed C represents the finer-grained laminae of the convoluted bed. The poor sorting of the sample suggests that coarser-grained material intermingled with the silty laminae is included in the sample, although this effect was reduced to a minimum by picking the sample carefully from a frozen surface.

Bed D comprises rather well-sorted fine sands. Ripple marks occur throughout the bed. They are best seen on the weathered surface. The amplitude of the ripples increases upwards. They show transportation from NNW or from the esker in the middle of the cone-shaped accumulation.

Bed E consists of fine sand intercalated with thin silty laminae. The sample represents the latter. Sample E is better sorted than sample C, indicating that sampling was more successful from the undistorted bed.

According to ten Haaf (1956), convolute lamination is most common in graded beds, where the light-coloured laminae consist of silty fine sand — the largest grain

FIG. 2. Oblique view of the convoluted bed. The vertical section is parallel to the section seen in Fig. 1 at a distance of 10 cm from the latter. The convoluted structure varies markedly from section to section. The top of the convoluted bed shows both conical (right) and subparallel (left) arrangement of the »anticlines».

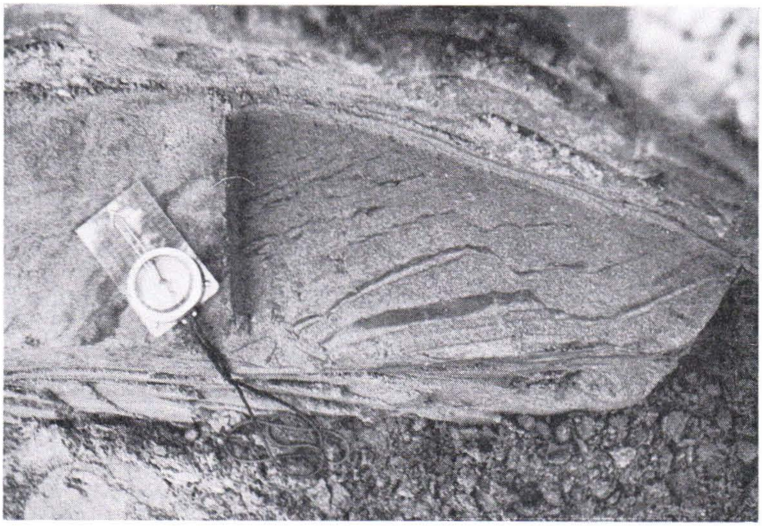

FIG. 3. Horizontal section, parallel to bedding, of the convoluted bed. The »anticlines» show a subparallel arrangement below the conical pattern of the top of the bed seen in Fig. 2. Under the compass — length of plate is 10 cm — the dark pattern on top of the bed is identical with the pattern between compass and edge of vertical section in Fig. 2. The fault seen on the horizontal plane is younger than the plastic deformation.

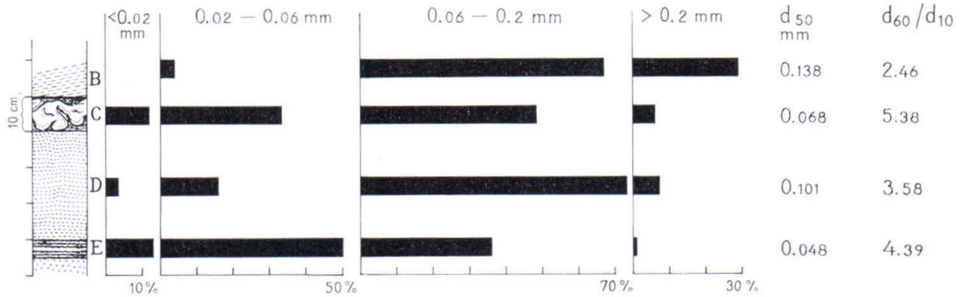

FIG. 4. Distribution of grain sizes in the different beds of the digging in the Pannujärvi gravel pit. The letters to the right of the stratigraphic column refer to the stratigraphic listing on p. 125. Median grain size and sorting are shown to the right. For description of the samples see text.

diameter being 0.05 mm—0.10 mm — and the dark bands contain, in addition, flat-lying clay and mica flakes of slightly larger dimensions. The sieves used in the grain-size analysis do not enable recognition of the upper grain limit given by ten Haaf. A microscopic investigation of the 0.06 mm—0.2 mm fraction of sample C showed, however, that the majority of the light-coloured grains are close to the minimum size of this fraction. The median grain size d_{50} of sample C falls within the limits given by ten Haaf. Under the microscope the corresponding fraction of sample E is very similar to sample C. Also its median grain size is close to the grain limits referred to. Convolute lamination is restricted to the grain-size range from silty clay to silty fine sands (Einsele 1963). The grain properties of bed E were certainly no obstacle to its becoming convoluted. For some reason this did not happen.

ORIGIN OF THE CONVOLUTE LAMINATION

The term »convolute lamination» is used in this paper in a purely morphological sense. Dott and Howard (1962) demonstrated that convolute lamination is a typical mixed-origin structure (see also Dzulynski and Smith 1963). Thus, each sedimentary environment may have processes operating which are capable of producing convolute lamination (Davies 1965).

The overburden of pebbly gravel, 4 m thick, can scarcely be thought to be responsible for the convolute lamination in bed C. Although relatively thin to become convoluted, bed E with its grain-size properties ought to have become affected by that load as well. Possibly the weight of bed A induced the small postdeformational faults when the sea regressed from the Pannujärvi area and the sediments dried up. Also the melting of buried dead ice in the vicinity may have caused small differential movements in the sediments.

Ten Haaf (1956) noted in the Apennine convoluted beds a systematic heeling of the anticlinal crests in the same direction. This he considered an indication of a downstream component in the depositing current. In places the Pannujärvi convolutions show a downstream heeling of the »anticlines», but this feature is not systematic and has not been encountered in all the sections cut. If this criterion is used in explaining the origin of the convolute lamination, a syndepositional origin related to current deformation (see also Einsele 1963, Davies 1965) must be ruled out. Kuenen (1953) described syndepositional convolutions that occur in connection with ripples. Because the »anticlines» of bed C do not show any systematic relationship to the crests of the ripples of bed D, the Pannujärvi convolutions seem to belong to non-current convolute laminations as defined by Dzulynski and Smith (1963).

The relationships between beds E and D, on the one hand, and between beds C and B, on the other hand, suggest that the unconformity between C and B can serve as a clue to explain the origin of the convolute lamination at Pannujärvi. In contrast to bed E, which is conformably overlain by the fine sands of bed D, bed C was not immediately buried. Although the convoluted bed C appears practically flat, it slopes quite gently towards SSE. Because even on such surfaces gravity always is a factor (Dott and Howard 1962), it is suggested that the convolutions at Pannujärvi originated during the compaction of bed C under water through a gravity-induced rearrangement within the bed, leading to thixotropic behaviour (*cf.* Emery 1950, Dott and Howard 1962, Nagtegaal 1963, Davies 1965). After its metadepositional deformation, bed C was buried under the arenaceous bed B.

As far as the writer is aware, convolute laminae have not been described from strictly glaciofluvial environments. At Pannujärvi the convoluted bed C, together with beds D and E, represents the end phase of sedimentation by the meltwater stream that produced the esker north of the gravel pit. Probably bed B and certainly A derive from the glaciofluvial cycle that produced the funnel-shaped accumulation. Redeposition in the shore zone has affected bed A but it is improbable that the entire bed would consist of redeposited material. Einsele (1963) surmised that convolute lamination may occur also in a fluviatile environment. At Pannujärvi the convolute lamination represents an environment where shallow-sea conditions and glaciofluvial sedimentation combine.

DISCUSSION

In Finnish geological literature structures have been described that either can be designated as convolute lamination or closely resemble it. Thus, the deformed bed of varved clay described by Sauramo (1958, pp. 259—260) from Hämeenlinna strongly resembles the simple convolutions described by ten Haaf (1956, p. 191) and Nagtegaal (1963, p. 372). Sauramo thought that the deformation was caused by a local advance of the ice margin. This advance has been questioned by M. Okko (1965).

Virkkala (1959) described distorted structures confined to a single bed: from Järvenpää, from Vuorentaka near Hämeenlinna, and from Villilä near Tampere. In the published photographs showing the deformations, one is able to trace some of the diagnostic features of convolute lamination (see p. 125). The concentric structure described by Virkkala from Pälkäne resembles convolutional balls (ten Haaf 1956, Plate 1, C) or roll-up structures (Dott and Howard 1962, Plate 3, A), whereas the structure from Kuru bears a resemblance to the corrugated lamination in Davies' (1965) classification of deformational structures. Virkkala's (1959) term for these structures is involutions and he explained them as late-glacial frost phenomena.

Convolute lamination is a polygenetic structure (Dott and Howard 1962) and so is patterned ground (Washburn 1956). The confinement of the deformation at Pannujärvi within a single bed — if a frost structure, at least some of the »anticlines» should inject the overlying arenaceous bed — and the age relationship between the deformation and the deposition of the overlying bed rule out the possibility of interpreting the deformation as a frost phenomenon. It seems that the sites listed in the foregoing chapter should be reinvestigated. In the event that the structures can be ascribed to frost-generated movements, an important contribution to the knowledge of convolute lamination and related structures will have been achieved.

Acknowledgments — The field work was done in connection with the mapping operations of the Geological Survey's Department of Surficial Deposits. Mr. Heikki Peura, field assistant in the summer of 1965, found the described structures and reported them to the writer. Miss Annikki Parkkonen is responsible for the grain-size analyses. Mrs. Elsa Järvimäki drew the graph.

Manuscript received, March 3, 1967

REFERENCES

AUROLA, ERKKI (1960) Poimurakenteista Piispanristin sorakuopan seinämässä lähellä Turkua. Summary [Folded structures in the wall of the gravel pit at Piispanristi near Turku]. Geologi, 12. vsk., pp. 34—37. Helsinki.

DAVIES, HUW G. (1965) Convolute lamination and other structures from the Lower Coal Measures of Yorkshire. Sedimentology, Vol. 5, pp. 305—325.

DOTT, R. H., and HOWARD, JOHN K. (1962) Convolute lamination in non-graded sequences. J. Geol., Vol. 70, pp. 114—121.

DZULYNSKI, STANISLAW, and SMITH, ALEC J. (1963) Convolute lamination, its origin, preservation, and directional significance. J. Sediment. Petrol., Vol. 33, pp. 616—627.

EINSELE, GERHARD (1963) »Convolute bedding» und ähnliche Sedimentstrukturen im rheinischen Oberdevon und anderen Ablagerungen. N. Jb. Geol. Paläont., Abh., Bd. 116, pp. 162—198.

EMERY, K. O. (1950) Contorted Pleistocene strata at Newport Beach, California. J. Sediment. Petrol., Vol. 20, pp. 111—115.

TEN HAAF, E. (1956) Significance of convolute lamination. Geol. en Mijnb., Jg. 18, pp. 188—194.

HYYPPÄ, ESA (1963) On the late-Quaternary history of the Baltic Sea. Fennia 89, No. 1, pp. 37—48.

—»— (1966) The late-Quaternary land uplift in the Baltic sphere and the relation diagram of the raised and tilted shore levels. Ann. Acad. Scient. Fennicae, Ser. A, III, 90, pp. 153—168.

KUENEN, PH. H. (1953) Graded bedding, with observations on Lower Palaeozoic rocks of Britain. Verh. Kon. Nederlandsch Akad. Wetensch., Amsterdam, Afd. Nat., Vol. 20, pp. 1—47.

NAGTEGAAL, P. J. C. (1963) Convolute lamination, metadepositional ruptures and slumping in an exposure near Pobla de Segur (Spain). Geol. en Mijnb., Jg. 42, pp. 363—374.

OKKO, MARJATTA (1962) On the development of the First Salpausselkä, West of Lahti. Bull. Comm. géol. Finlande No. 202. 162 p.

—»— (1965) M. Sauramo's Baltic Ice Lake BIV — BV — BVI; a re-evaluation. Ann. Acad. Scient. Fennicae, Ser. A, III, 84. 36 p.

OKKO, VEIKKO (1949) Explanation to the map of surficial deposits, Sheet B 4, Kokkola. General Geological Map of Finland, 1 : 400 000. 55 p.

—»— (1957) The Second Salpausselkä at Jylisjärvi, East of Hämeenlinna. Fennia 81, No. 4. 46 p.

POTTER, PAUL EDWIN and PETTIJOHN, F. J. (1963) Paleocurrents and basin analysis. Springer-Verlag. 296 p.

SAURAMO, MATTI (1958) Die Geschichte der Ostsee. Ann. Acad. Scient. Fennicae, Ser. A, III, 51. 522 p.

SELLEY, R. C. and SHEARMAN, D. J. (1962) Experimental production of sedimentary structures in quicksands. Proc. Geol. Soc. London, Session 1961—62, No. 1599, pp. 101—102.

STEWART, H. B. (1956) Contorted sediments in modern coastal lagoon explained by laboratory experiments. Bull. Am. Assoc. Petroleum Geologists, Vol. 40, pp. 153—179.

VAN STRAATEN, L. M. J. U. (1949) Occurrence in Finland of structures due to subaqueous sliding of sediments. C. R. Soc. Géol. Finlande 22, pp. 9—18. — Bull. Comm. géol. Finlande No. 144, pp. 9—18.

VIRKKALA, K. (1959) On the Lateglacial frost phenomena in Southwestern Finland. C. R. Soc. Géol. Finlande 31, pp. 21—40. — Bull. Comm. géol. Finlande No. 184, pp. 21—40.

WASHBURN, A. L. (1956) Classification of patterned ground and review of suggested origins. Bull. Geol. Soc. America, Vol. 67, pp. 823—866.

Comptes Rendus de la Société géologique de Finlande
N:o XXXIX (1967), pp. 133—159

ZUR SPÄT- UND POSTGLAZIALEN ENTWICKLUNG IM OSTTEIL DES ERSTEN SALPAUSSELKÄ

REINO REPO und RISTO TYNNI

Geologische Forschungsanstalt in Finnland, Otaniemi

ABSTRACT

In the present study concerning the late and postglacial development of the eastern region of the 1st Salpausselkä special emphasis has been placed on the vegetation history and the desplacement of shore lines based on the stratigraphy of pollen and diatom successions. The pollen dating is supported by the C^{14}-age of 8 110 ± 140 B. C. determined from the oldest limmic deposits of the Mustalampi bog situated on the distal side of the 1st Salpausselkä at an altitude of 155 meters above sea level. The dated horizon corresponds to the latter part of the rather high NAP-maximum and to a diatom flora consisting of fresh small-water forms.

The elevations in the region investigated varies from 67 meters to about 200 meters above sea level. The major part of the area remained after the retreat of the ice margin covered by the Baltic Ice Lake (possibly also by the late-glacial Yoldia Sea). Only the highest hills formed islands at that time. The lowest parts of the terrain emerged from the sea during the preboreal Yoldia Sea.

INHALT

EINLEITUNG

Das Untersuchungsgebiet liegt in Nordkarelien und umfasst zuvörderst das Nordostende des 1. Salpausselkä in der Gegend von Tohmajärvi—Värtsilä. Es erstreckt sich vom Kirchspiel Kitee im Südwesten bis zum südlichen Teil von Ilomantsi im Nordosten. Die Skizzierung der Salpausselkäs und die Bodenkartierung in diesen Gebieten haben schon Berghell (1903) im südlichen Teil sowie Frosterus und Wilkman (1910) im nördlichen Teil vorgenommen. Wilkmans (1917) Erklärung zum Kartenblatt der Gegend von Joensuu behandelt schon vielseitig die östliche Partie des Salpausselkä. Ende des 19. Jahrhunderts hatte u.a. Ramsay (1891) den Ostteil des Salpausselkä untersucht. Später veröffentlichte Ramsay (1931) in erster Linie Beobachtungen vormaliger Ufer aus dieser Gegend.

Von den zahlreichen Untersuchungen, die sich dann mit dem östlichen Gebiet des Salpausselkä oder mit benachbarten Gegenden befasst haben, sind vom Gesichtspunkt der quartärzeitlichen Uferverschiebung und der weiteren Entwicklungsgeschichte die Forschungen von Sauramo (1921), Sauramo und Auer (1928) sowie Sauramo (1928) am bedeutsamsten. Die Entwicklung des nördlichsten Gebiets von Pielis-Karelien wird in der Untersuchung von Hyvärinen (1966) besprochen, und die spätere Publikation des gleichen Autors (1967) behandelt ausführlich die Uferverschiebung in dem Untersuchungsgebiet, wobei von Ramsays Beobachtungen vormaliger Ufer ausgegangen wird. Donners (1951) Untersuchung berührt auch die spät- und postglaziale Pollensukzession in den Moorablagerungen des Untersuchungsgebiets.

Unsere vorliegende Arbeit dient dem Zweck, weiteren Aufschluss zu gewinnen über die Richtung des Eisstroms, über den Zeitpunkt des Eisrückzuges und die Uferverschiebung der nachfolgenden Ostseestadien sowie noch aufgrund von Pollen- und Diatomeenanalysen über die Entwicklung der Vegetation. Zur Wahl des Untersuchungsgebiets hat seine Lage in Beziehung zum 1. Salpausselkä beigetragen sowie ferner die Höhenverhältnisse, welche die Bildung relativ alter und wenig bekannter organogener Ablagerungen ermöglicht haben. Die hier veröffentlichte C^{14}-Datierung repräsentiert bis auf weiteres die älteste Datierung von Seesedimenten in der südlichen Partie unseres Landes.

RÜCKZUG DES EISRANDES IN DEM UNTERSUCHUNGSGEBIET

Die von Berghell (1904) sowie Frosterus und Wilkman (1917) veröffentlichten Karten über die Erosionsspuren des Eises, die Schrammen, und über die Verbreitung glazifluvialer Aufschüttungen tragen auch zur Klärung der Vorgänge im Rückzugsstadium des Inlandeises in dem Untersuchungsgebiet bei. Die Strömungen des Eises im Untersuchungsgebiet sind auch in den Publikationen von Aurola (1955) und Repo (1957) berührt. Aus Abb. 1 gehen die in dem Gebiet gemachten Schrammenbeobachtungen hervor, inbegriffen auch die Beobachtungen der oben genannten Forscher.

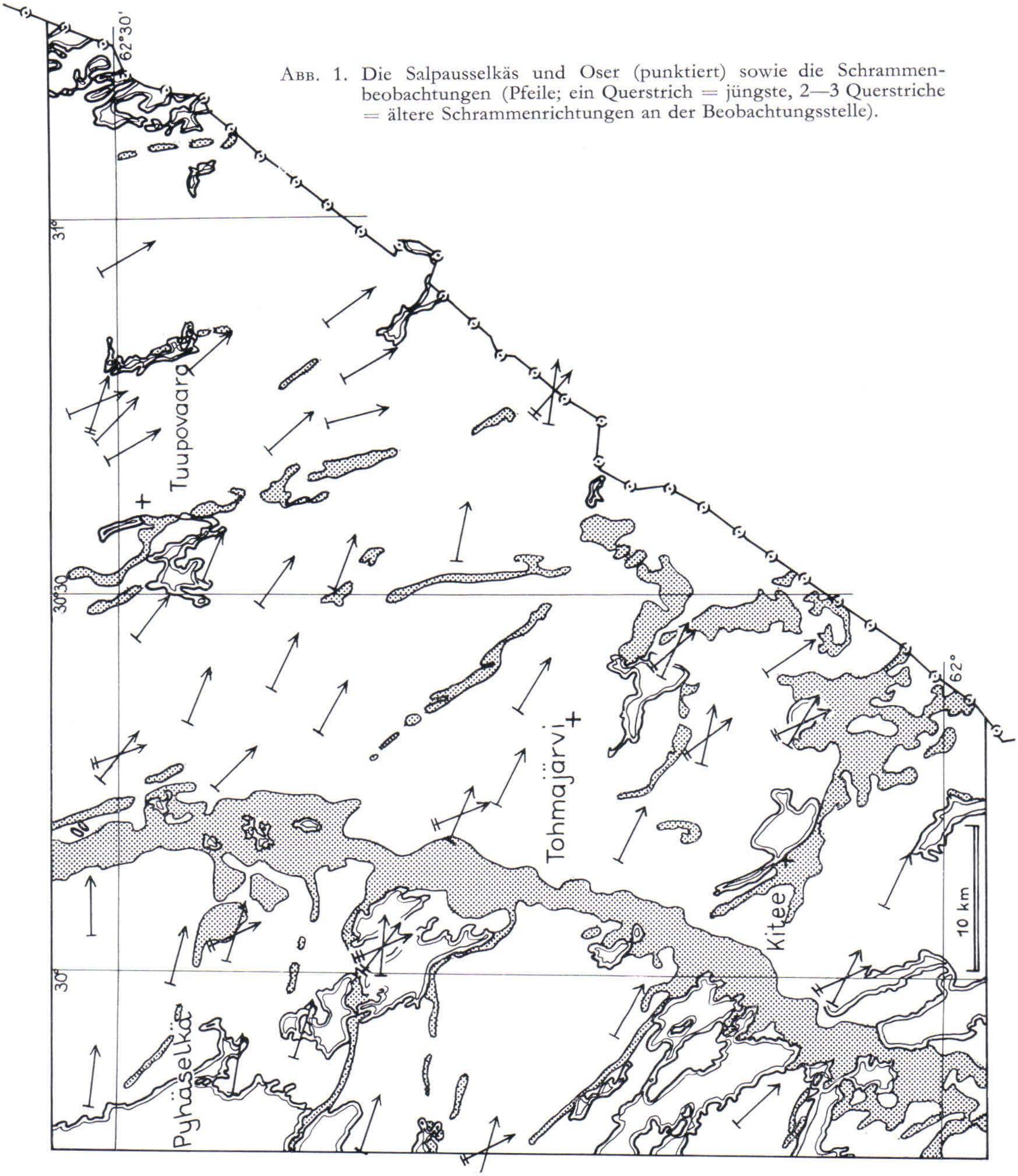

Abb. 1. Die Salpausselkäs und Oser (punktiert) sowie die Schrammenbeobachtungen (Pfeile; ein Querstrich = jüngste, 2—3 Querstriche = ältere Schrammenrichtungen an der Beobachtungsstelle).

Den Schrammen gemäss hat die Stromrichtung des Eises in dem Gebiet beträchtlich gewechselt. Bestimmend für die Richtung sind offenbar nicht nur die von den Vereisungsstadien bedingten verschiedenen Strömungen gewesen, die u.a. von der Lage der Eisscheide oder sonst einem die allgemeine Strömung ausschlaggebend beeinflussenden Faktor abhängig waren, sondern auch topographische Umstände haben mitgespielt. Das benachbarte tiefe Becken des Ladogasees hat höchstwahrscheinlich die Eisströmung auf sich gelenkt, als das Untersuchungsgebiet noch vereist war. In der Eisrandzone sind insbesondere während der langen Haltestadien, in denen der 1. und 2. Salpausselkä abgelagert worden sind, die lokalen Strömungen senkrecht zum Proximalteil der Aufschüttung verlaufen.

Der 1. Salpausselkä erstreckt sich im Norden bis in die Gegend des Sees Sääperijärvi, während dagegen der 2. Salpausselkä noch über 50 km nordnordwestwärts bis nach Jaamankangas weiterzieht und einen ziemlich einheitlichen, bogenförmigen Höhenzug bildet. An den Salpausselkäs, und insbesondere am 1. Salpausselkä gibt es in dem Untersuchungsgebiet nur spärlich Durchschnitte, an denen die Struktur der Aufschüttung zu sehen wäre. Aufgrund der bisherigen Schnitte scheinen beide Randbildungen zum weitaus grössten Teil aus glazifluvialen Ablagerungen zu bestehen.

Dass der Bogen des 1. Salpausselkä in der Gegend vom Sääperijärvi endigt, hat vielleicht damit zu tun, dass am Übergang zum Vaara-Gebiet ein mächtigerer, zusammenhängender Eisrand fehlte. Da in Nordkarelien vor dem Eisrand die Topographie und die Tiefenverhältnisse des Wassers beträchtlicher schwankten als weiter westlich, wurde die Randbildung nicht so einheitlich oder kam dort, wo kein Gleichgewicht zwischen dem Eisstrom und dem Abschmelzen erreicht wurde, überhaupt nicht zustande.

Nach dem Zurückweichen des Eisrandes überflutete ein Eissee oder Eismeer den grössten Teil des Gebiets, u.a. den 1. Salpausselkä, und nur die Kuppen der höchsten Erhebungen, die heutzutage in ca. 160—200 m Höhe liegen, ragten als Inseln aus dem spätglazialen Baltischen Eissee (Eismeer?) hervor. Auf diesen Inseln hat die vorwiegend krautige Vegetation in relativ frühem Stadium Fuss gefasst.

ZUR POLLEN- UND DIATOMEENSTRATIGRAPHIE DES GEBIETS

Schichtenfolge vom Weiher Mustalampi

Der Weiher Mustalampi liegt in Ilomantsi unweit der Grenze von Tuupovaara distalwärts vom 1. Salpausselkä (Abb. 2, Punkt 1) in ca. 155 m Höhe. Die am Ufer des Weihers erbohrte Schichtenfolge enthält die Moorablagerungen in 4—2.5 m Tiefe (Abb. 3.)

Pollenflora

Nach der Pollenzoneneinteilung (Sauramo 1958) entspricht die Schichtenfolge, die von unten nach oben Feinsandschluff, Feinsand, *Bryales*-Gyttja und Diatomeengyttja enthält, lückenlos der Sedimentation von der Jüngeren Dryaszeit (z III) bis zum Spätatlantikum (z VII).

Im unteren Abschnitt des Feinsandes, des Schluffs und der *Bryales*-Gyttja befindet sich ein beträchtliches NBP-Maximum, das hauptsächlich aus *Artemisia*-, *Chenopodiaceae*- und *Ranunculaceae*-Pollen besteht. *Salix*-Pollen ist relativ reichlich vorhanden, aber als Seltenheit tritt *Helianthemum* auf. *Helianthemum*-Pollen ist u.a. in Schweden und England in spätglazialen Ablagerungen angetroffen worden (Erdtman 1949, Godwin 1956). Heutzutage wächst *Helianthemum nummularium* spärlich ca. 30 km südlich vom Mustalampi, an einer nordwestwärts vorstossenden Bucht des Sees Jänisjärvi. In der Gegend des Jänisjärvi kommt im Felsgrund Kalkstein und Dolomit vor. *Helianthemum nummularium* erfordert einen kalkreichen und trockenen Boden. In der Jüngeren Dryaszeit sind diese Wachstumsbedingungen auch wahrscheinlich vorhanden gewesen, und *Helianthemum* dürfte damals in dem Gebiet besser gediehen sein als jetzt (Abb 4).

Das beträchtliche NBP-Maximum vom Mustalampi ist im Feinsandschluff ähnlich geartet wie in der *Bryales*-Gyttja. Dieser Umstand beweist, dass der Pollenbestand des anorganischen Sediments in der Hauptsache primär ist. Er spiegelt die Pollenverhältnisse einer baumlosen Gegend wider, wie sie in der Jüngeren Dryaszeit herrschten. Die im Isotopes Inc., New Jersey, durchgeführte C^{14}-Datierung bestätigt ausserdem die obige Pollenzoneneinteilung.

Die nördlich von dem Untersuchungsgebiet in der bisher nächstgelegenen Gegend durchgeführten C^{14}-Datierungen stammen vom Moor Puhtiinsuo in Ilomantsi (Tolonen 1963) und aus Pielis-Karelien (Hyvärinen 1966). Die erstere betrifft u.a. eine präboreale Moorablagerung mit einem Alter von ca. 7 190 ± 250 v.Chr., die letztere wiederum mehrere Datierungen, von denen die älteste auf ca. 7 500 v.Chr. fällt.

Nach den Untersuchungen von Fromm (1963) und E. Nilsson (1964) hat der Durchbruch des Baltischen Eissees und sein Abfliessen ins Yoldiameer etwa 8 300 oder 8 200 v.Chr. stattgefunden. Die Datierung des Gyttjasediments vom Mustalampi auf. ca. 8 110 v.Chr. entspricht dieser (± 140) oder einer etwas jüngeren Zeit, als das B III-Stadium schon abgeschlossen war. Auch im Vergleich zum 2. Salpausselkä dürfte die Schichtenfolge vom Mustalampi das entsprechende Alter haben. Das Feinsandschluff-Sediment ist wahrscheinlich zur Zeit des Abflusses des Baltischen Eissees oder vorher abgelagert worden.

Die obere Partie der *Bryales*-Gyttja und der untere Teil der Diatomeengyttja gehören zuvörderst aufgrund des grossen Maximums der *Betula*-Pollen ins Präboreal. Der Pollenbestand der Borealablagerung ist in diesem Falle nicht charakteristisch, denn das *Pinus*-Maximum fehlt. Auch das Früh- und Spätatlantikum reflektieren sich in der Pollenflora nicht so klar wie in den südfinnischen Diagrammen, wie ja auch zu erwarten war, da es sich um ein nördlicheres Gebiet handelt.

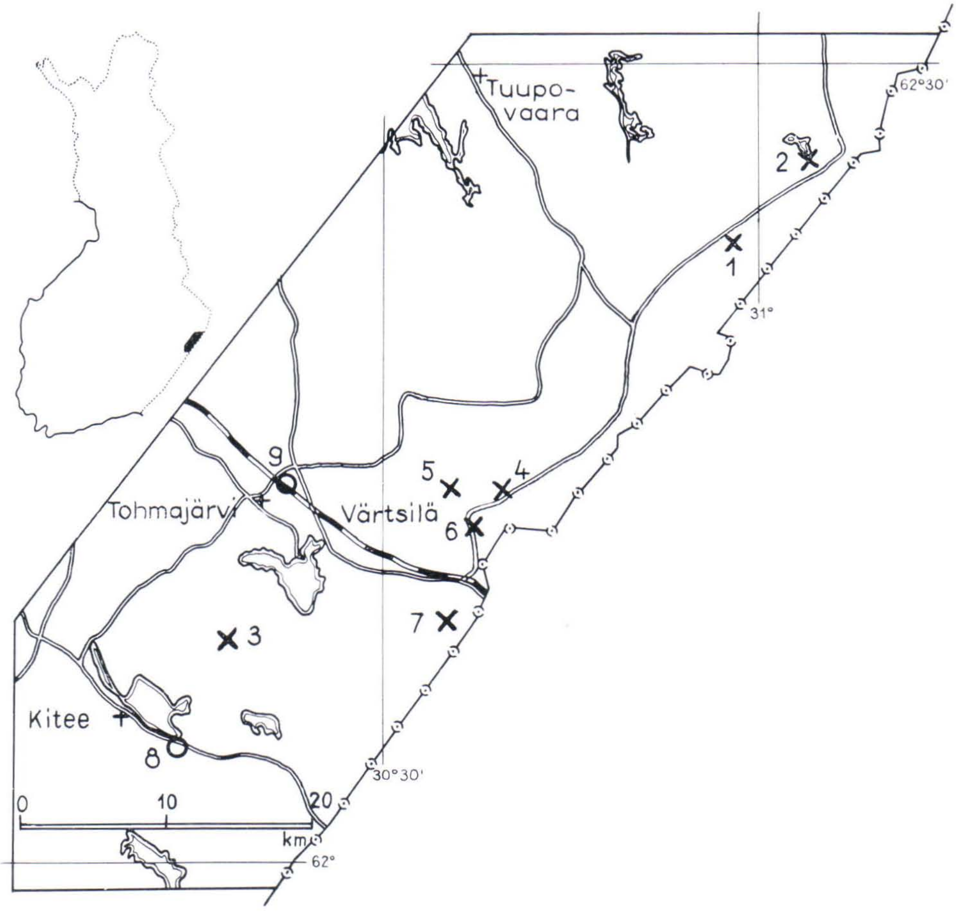

Abb. 2. Lage der untersuchten Schichtenfolgen (1—7) und der Bändertonvorkommen (8—9).

Diatomeenflora

Die Schichtenfolge vom Weiher Mustalampi enthält reichlich Kieselalgen; das Sediment ist auch schon von der Präborealzeit an Diatomeengyttja. Aus Tabelle 1 sind die Diatomeenarten ersichtlich. Die Formen süsser Kleingewässer dominieren in der Schichtenfolge. Die Mehrzahl der Arten sind im allgemeinen Litoralformen. Anzeichen für eine grössere Wasserfläche in der Jüngeren Dryaszeit sieht man nur in den zwei untersten Diatomeenanalysen, wo *Melosira islandica* ssp. *helvetica* spärlich vorkommt.

Der Diatomeenflora gemäss ist das Ablagerungsbecken schon in der Jüngeren Dryaszeit vom Baltischen Eissee oder vom spätglazialen Yoldiameer abgeschnürt gewesen.

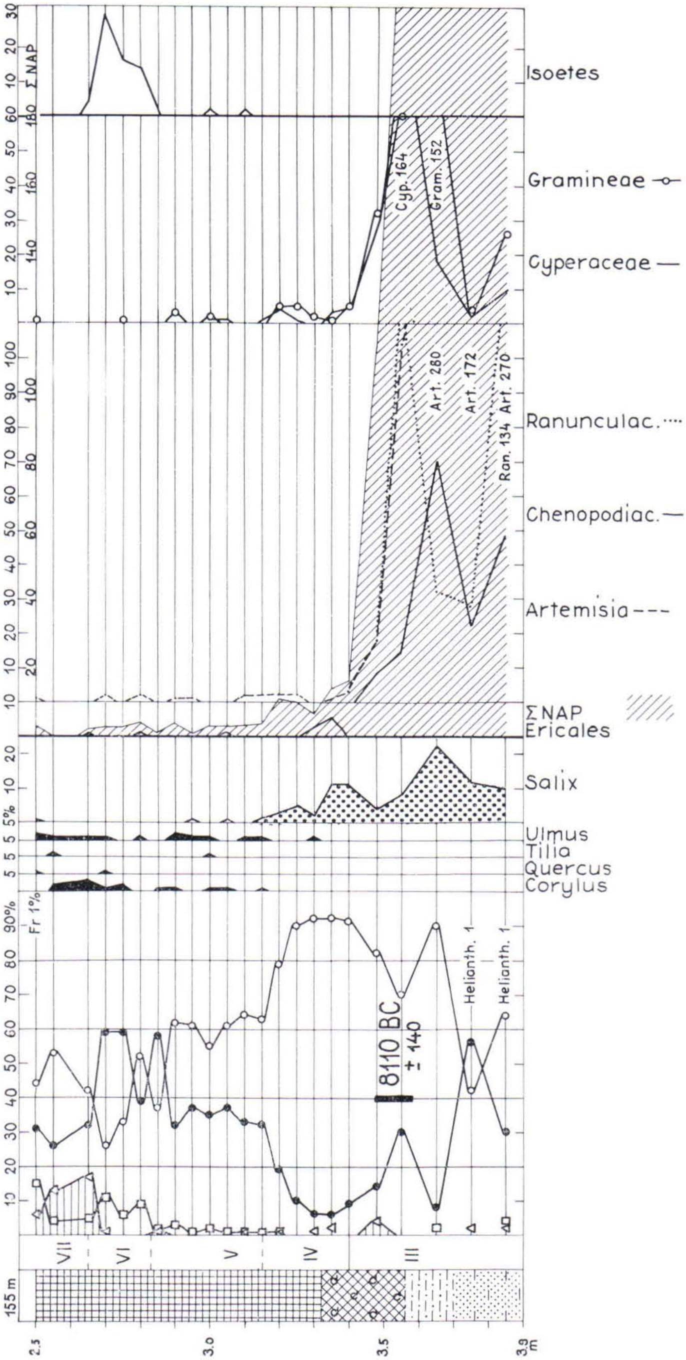

ABB. 3. Pollendiagramm der Schichtenfolge vom Weiher Mustalampi. — Erklärungen der Zeichen in Abb 5, Fr = *Fraxinus*.

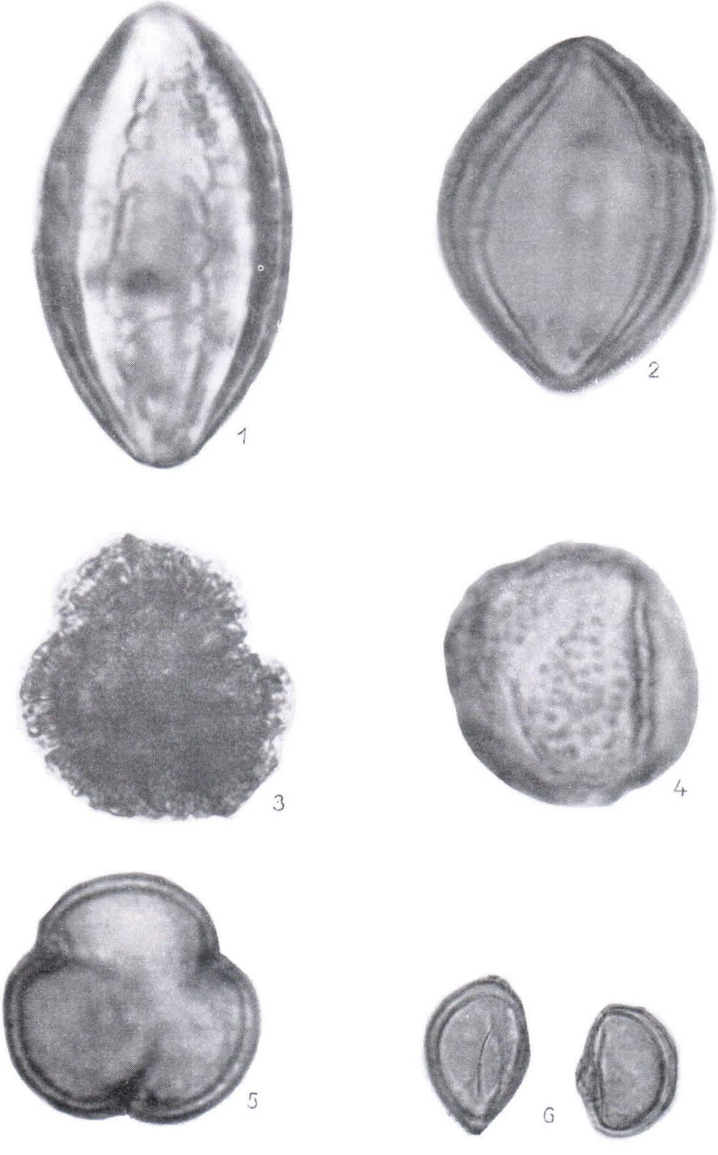

Abb. 4. In den Schichtenfolgen gefundene Mikrofossilien: 1. *Ephedra distachya*-Pollenkorn, 2. *Helianthemum*-Pollenkorn, 3. *Armeria*-Pollenkorn, 4. *Ranunculaceae*-Pollenkorn, 5. *Papilionaceae*-Pollenkorn, 6. *Isoetes*-Spore. Photo E. Halme.

Schichtenfolge vom Moor Umpijärvi

Der See Umpijärvi liegt in Ilomantsi ost- und distalwärts vom 1. Salpausselkä (Abb. 2, Punkt 2) in ca. 145 m Höhe. Die Probeserie ist in dem südlich an den See anschliessenden Aapamoor erbohrt worden (Abb. 5).

Pollenflora

Die Schichtenfolge enthält zuunterst ca. 10 cm Gyttja sowie Torfablagerungen mit vorwiegend *Equisetum*, *Carex* und *Sphagnum*. Die Gyttja und der *Equisetum*-Torf sind im Präboreal entstanden, der *Carex*-Torf im Boreal und im Früh-Atlantikum und der vorwiegend aus *Sphagnum* bestehende Torf später in der postglazialen Wärmezeit und in dem darauf folgenden Subatlantikum.

Das Pollenspektrum weist eine ziemlich reguläre Artenverteilung auf, ausser im superfiziellen Teil der Lagerfolge, wo *Pinus*-Pollen ausserordentlich reichlich, nämlich mit 93 % vertreten ist. Der in der Gyttja angetroffene *Myriophyllum spicatum-verticillatum*-Pollen-Typ zeigt an, dass die erstere Art, eventuell auch die letztere, in der Präborealzeit in dem See gewachsen ist. Gegenwärtig wächst *M. spicatum* u.a. in dem Untersuchungsgebiet im See Sääperijärvi.

Diatomeenflora

Der Diatomeenbestand der im Präboreal abgelagerten Gyttja setzt sich hauptsächlich aus Kleinsee-Epiphytenarten zusammen. Am gewöhnlichsten sind die *Epithemia*-, *Cymbella*- und *Gomphonema*-Arten. Die Kieselalgen der Lagerfolge zeigen, dass das Yoldiameer zur Zeit der Ablagerung nicht bis zur Höhe von 145 m hinaufgereicht hat.

Schichtenfolge vom Moor Suksilampi

Im Kirchspiel Tohmajärvi ca. 5 km proximalwärts vom 1. Salpausselkä liegt in ca 125 m Höhe der Suksilampi (Abb. 2, Punkt 3), ein kleiner, dys-eutropher See, dessen Ufer fast ringsum vermoort ist. In der Nähe der Bohrstelle wächst u.a. *Typha latifolia* und *Phragmites communis*. Die erbohrte Schichtenfolge umfasst die Bodenschichten des Moors in 3.3—1.3 m Tiefe (Abb 6).

Pollenflora

Die tiefsten Sedimente, Feinsand und der Hauptteil vom Schluff, müssen dem grossen NBP-Maximum gemäss in der Jüngeren Dryaszeit abgelagert worden sein. Von den Kraut- und Graspollen sind *Artemisia*, *Ranunculaceae*, *Gramineae*, *Cyperaceae* und *Chenopodiaceae* am gewöhnlichsten, während wieder als Seltenheiten u.a. *Armeria* sp. und *Helianthemum* vorkommen. Die Menge des *Ericales*- und *Salix*-Pollens ist verhältnismässig gross, insbesondere an der Zonengrenze III/IV.

TABELLE 1.

Diatomeen der Schichtenfolge vom Weiher Mustalampi

Zone	VII		VI	V			IV			III					
Tiefe cm	255	265	275	285	295	305	315	325	335	345	355	365	375	385	395
Achnanthes flexella .... %	2	1	5	1	5	3	4								
A. kryophila		1			2										
A. linearis							1		1						
— var. *pusilla*			1												
A. microcephala					1				2						
A. minutissima									2						
Amphora ovalis									1	1	2	4	1	3	6
Anomoeoneis follis	1	2	4	1	6	1									
A. serians											1	2			1
— var. *brachysira*	7	4	4		10	2		1							
Caloneis bacillum												1			
C. silicula												1			
— var. *truncatula*											1				
Cyclotella antiqua										1	1	4	1		
C. comta				1			1								
C. meneghiniana						1									
C. stelligera					3	4	4				1				
Cymbella affinis												1		1	
C. amphicephala		2	1				1		1						
C. aspera								1							
C. cesati	1					3	1	1							
C. cistula								1			1				
C. cuspidata			1	1	1	1									
C. cymbiformis										2				1	
C. gracilis	3	2	7	1	3	3	2						1		
C. hustedtii									1					1	
C. naviculiformis				1	1			1			1	3			
C. tumida											2		1		
C. turgida									2			1	3	2	1
C. ventricosa	2	1	1	2	5	4				1	1	1		2	
Denticula tenuis							1		1	1	1	1		1	
Diatoma hiemale											1				
Diploneis finnica						1	1	2		2					
D. ovalis										1					
Epithemia sorex										1					
Eunotia arcus	2		1		2	1	3			1					
— var. *bidens*	1	1			1										
E. diodon	1														
E. faba	6	1		1										1	
E. flexuosa			1												
E. formica		1		1	2	1		1							
E. gracilis				1											
E. lapponica	1														
E. paludosa	1														
E. pectinalis			1			1									
— var. *minor*		1			1						1	1		1	
— — f. *impressa*			1												
— var. *undulata*			1											1	
E. polyglyphis	1			1											
E. praerupta							1		1	3				1	
E. robusta	1		2	1	1	1		1				1		1	
— var. *tetraodon*	2	2	3	3			2								
E. sudetica	1	9													
— var. *bidens*						1									
E. tenella	3														
E. veneris	1	5	14	1	3	3	2	1		3		1		1	
Fragilaria angustata										5		3		4	
F. brevistriata		1			2	2			3	6		1			
F. construens				1			5	20	40	19	15	9	1	4	
— var. *binodis*		1													
— var. *venter*									1				5	9	
F. pinnata						1		5	15	30	48	29	71	21	
F. sp. fragm.						2					1		1	2	

Tabelle 1. (Fortsetzung)

Zone	VII		VI	V			IV			III					
Tiefe cm	255	265	275	285	295	305	315	325	335	345	355	365	375	385	395
Fragilaria virescens							4								
— var. *mesolepta*														1	
Frustulia rhomboides	10	2	3	1		1								1	2
— var. *saxonica*						2									
Gomphonema acuminatum var. *brebissonii*											1				
G. acuminatum var. *coronata*		1	1		2	4	2	1		1		1			
G. angustatum						3					1				
— var. *undulata*						1									
G. bohemicum					3			1							
G. constrictum			1	1					2						
— var. *capitata*										1					
G. gracile										1					
G. longiceps var. *sagitta*			2												
G. parvulum	2	2	2		6	3	1	1					1		
Hantzschia amphioxys												1			
H. elongata				1	1			1							
Melosira ambigua	4	1	2			1								1	1
M. distans	16	32	11	34	6	15	13	3	2	1	1	1	1	9	6
M. islandica ssp. *helvetica*														3	5
M. italica	5	8	8	20	8	11	34	48				1	1		4
Navicula americana						1									
N. cryptocephala									1	1					
N. cuspidata															4
N. pseudoscutiformis									1	1					
N. pupula			1									1			
— var. *capitata*							1		1						
— var. *rectangularis*	2	1				1	1			1	1		1		1
N. radiosa			2				1		5	1	2	7	1	3	1
N. scutiformis											1				
N. subtilissima								1							
N. viridula											1	7		1	1
Neidium bisulcatum f. *undulata*													1		
N. dilatatum	1														
N. iridis	5	1	1	1		1	1		1		1			1	
Nitzschia angustata							1								
N. fonticola					2			1	4						
N. kützingiana									2	1					
Pinnularia appendiculata	3	2		1	1			1							
P. borealis													1		
P. braunii var. *amphicephala*		1	2												
P. brevicostata				1		1		1							
P. divergens												1			
P. gentilis								1							1
P. gibba	2	2	2	5	2	3	1	1	1				1		
— var. *linearis*	5	3	2	2	3	3					1	1			
— var. *mesogongyla*			1	2											
P. interrupta	2		2					1			1			2	
P. maior	1	1	1		1	1	3	1		1					2
P. mesolepta			1	1	2				2	1					
P. molaris														1	
P. nobilis						1						1			
P. sp. fragm.						1	2			1					4
P. subsolaris															1
P. undulata				1											
P. viridis				1	1		1	1	1		1				9
Stauroneis anceps			1	1	1	1	1		3			1		1	5
S. phoenicenteron		1		1	2		1	1			1	1	1	2	43
S. smithii	2		1	1		2				2					
Synedra ulna									1						
Tabellaria fenestrata	1	3	3	1	5	4	2			1	1			1	2
T. flocculosa	2	2	1	2	4	2	1		2	8	8	12	6	16	
Tetracyclus lacustris		2	1	4	1	1									

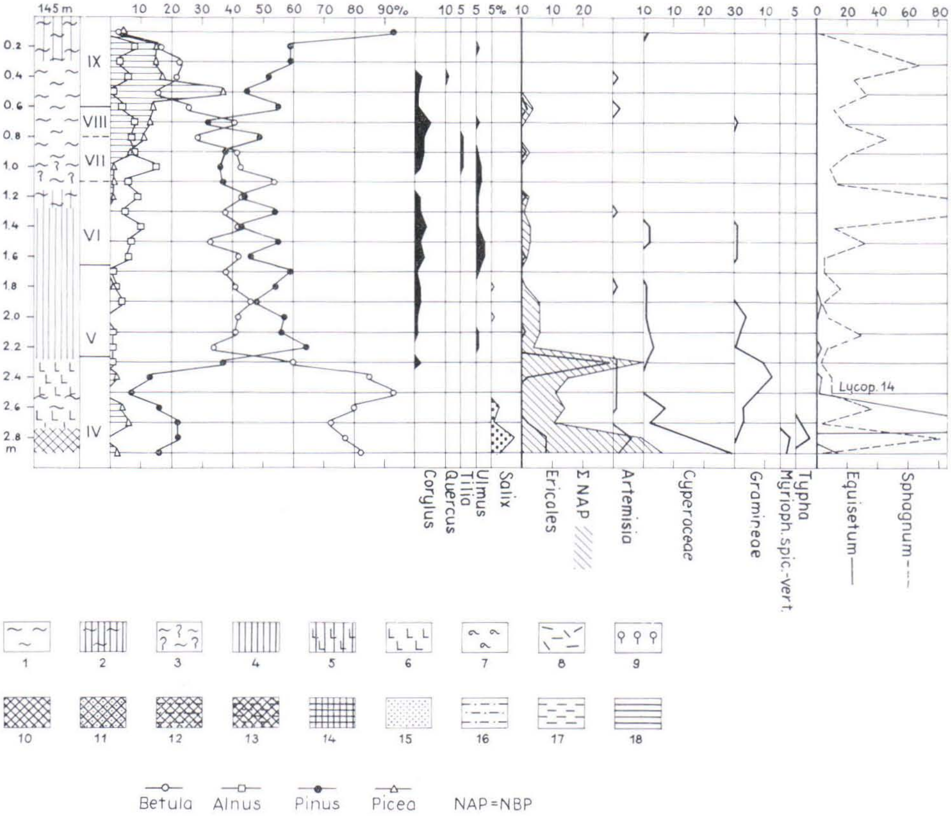

ABB. 5. Plolendiagramm der Schichtenfolge vom Moor Umpijärvi.

Erklärung der Zeichen. 1. *Sphagnum*-Torf, 2. *Carex-Sphagnum*-Torf, 3. *Eriophorum-Sphagnum*-Torf, 4. *Carex*-Torf, 5. *Carex-Equisetum*-Torf, 6. *Equisetum*-Torf, 7. *Bryales*-Torf, 8. Akkumulationstorf, 9. Laubholztorf, 10. Detritusgyttja, 11. Feinsandgyttja, 12. Schluffgyttja, 13. Tongyttja, 14. *Diatomaceae*-Gyttja, 15. Feinsand, 16. Schluff, 17. Ton, 18. Bänderton.

Die Ablagerung der Gyttja hat im Präboreal eingesetzt. Der Anteil des NBP ist hier noch relativ hoch, wahrscheinlich wegen der Nähe des Eisrandes (vgl. Donner 1958, 1967).

Die prozentualen Verhältnisse des Pollendiagramms variieren in den Sedimenten vom Boreal, Frühatlantikum und Atlantikum in gleicher Weise wie in den Lagerfolgen aus Südfinnland. Weil keine C^{14}-Datierungen vorliegen, lässt sich über den Synchronismus dieser Pollenzonen nichts Sicheres sagen. Höchstwahrscheinlich sind jedoch die fraglichen Zonen in dem Untersuchungsgebiet nicht wesentlich jünger als die entsprechenden Zonen in Südfinnland. Die C^{14}-Datierungen, die weiter nördlich in der Gegend des Pielisjärvi gemacht worden sind (Hyvärinen 1966), weisen auf eine gewisse Verjüngung der Zonen hin.

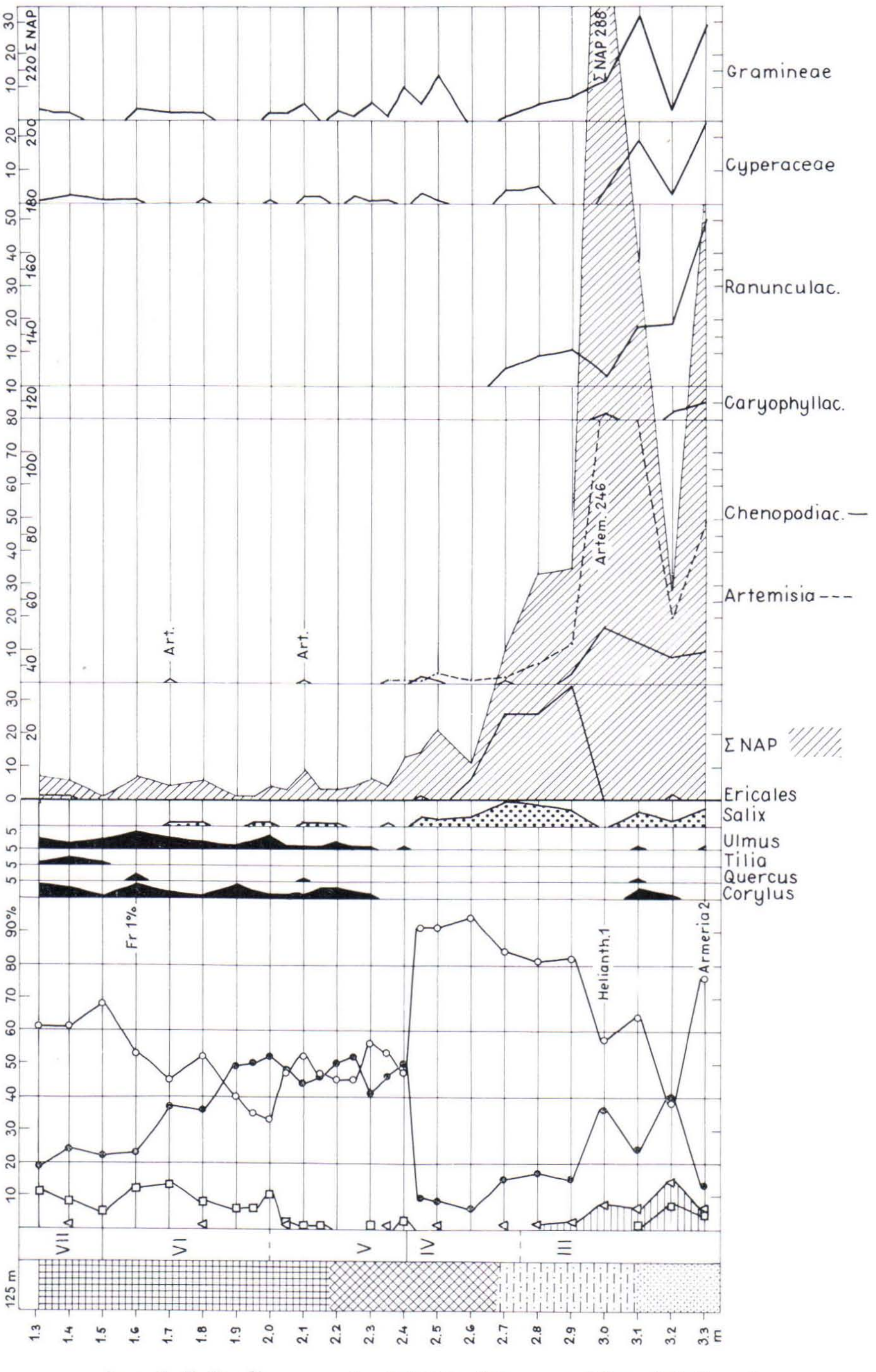

ABB. 6. Pollendiagramm der Schichtenfolge vom Moor Suksilampi.

TABELLE 2.

Diatomeen der Schichtenfolge vom Weiher Suksilampi

Zone	IV				III					
Tiefe cm	240	250	260	270	280	290	300	310	320	330
Achnanthes calcar %		1			2	1				
A. coarctata									1	
A. flexella								1		2
A. lanceolata		1		1						
— var. *elliptica*	1	4								
A. linearis var. *pusilla*						1	1			3
Amphora ovalis		1		1	2	1	1		2	2
Anomoeoneis serians var. *brachysira*	1									
Caloneis bacillum							2			
C. schumanniana			1							
C. silicula					2	1	2		2	2
Campylodiscus noricus var. *hibernica*				2	1					
Cocconeis diminuta				2	5	1				1
C. placentula					2					
Cyclotella antiqua									1	4
C. comta					2					
C. meneghiniana	1									
C. stelligera	1	1								
Cymatopleura elliptica				1						
C. solea					3					
Cymbella affinis						2				
C. amphicephala							2	2		2
C. aspera		1			1			5		2
C. cistula								2		
C. cuspidata						1		1		
C. cymbiformis					3	2	2	2		
C. ehrenbergii				4						
C. lanceolata								1		
C. naviculiformis				1	1	1	1	2		2
C. tumida							1		1	1
C. turgida		1		1	1	1		3	1	
C. ventricosa				1	2	4	3	3	1	2
Diploneis elliptica					1				1	
D. finnica				1						
D. puella				1						
Epithemia argus				1						
E. hyndmanni			1	1						
E. sorex			2		3	2	1			
E. turgida	1		1	1	2					
— var. *granulata*					1					
E. zebra					2					
Eunotia arcus				1				1		
E. flexuosa							1			
E. formica			1						1	
E. praerupta									1	
E. robusta									1	
Fragilaria angustata	1					2	1			
F. brevistriata	2	2	7	3	3	1	1		3	1
F. construens	24	28	29	23	9	16	19	13	22	23
— var. *venter*	11	11	24	5	2	1	10	14	1	3
F. leptosoma var. *dubia*	5	12							1	
F. pinnata	9	7	20	32	23	13	1	5	20	3
F. virescens	1									
Frustulia rhomboides		1								1

TABELLE 2. (Fortsetzung)

Zone	IV				III					
Tiefe cm	240	250	260	270	280	290	300	310	320	330
Gomphonema acuminatum var. *coronata*	1					1		1		1
G. angustatum										1
G. constrictum					1	3	1	3		
G. lanceolatum							1			
Gyrosigma attenuatum				3						
Hantzschia amphioxys				1						
Melosira ambigua	2									
M. distans	4	9	2	1	1	5	1	1	5	2
— var. *lirata*	13	9	4		1			3	7	9
M. italica	12	2	5			1			1	1
— var. *valida*			1							
Navicula americana	1									
N. amphibola				1						
N. bacillum				1					1	
N. cuspidata				1		1	1			
N. laterostrata	3	4								
N. menisculus					1					
N. pseudoscutiformis	2			1	1	1	2			1
N. pupula								1		
N. radiosa					4	2	10	15	3	9
N. viridula				1			1			
Neidium hitchcockii					1	1				
N. iridis					2	1		2	1	
Nitzschia dissipata									1	
N. fonticola						3	1	1		1
N. sigmoidea						1				
Opephora martyi					1					
Pinnularia borealis									1	
P. dactylus			1			2				
P. gentilis		1								
P. gibba	1					1				
— var. *linearis*					1					
— var. *mesogongyla*					1					
P. interrupta						1	2			
P. maior		1		2	1					
P. mesolepta					2	1			1	1
P. nodosa	1									
P. semicruciata						1			2	
P. viridis			1	1	1		1	1		1
Rhopalodia gibba					4	1	1	1	2	
— var. *ventricosa*				1		4				
Stauroneis acuta		1		1						
S. anceps				1	1	3	2	1	2	2
— var. *linearis*							1			
S. phoenicenteron						1	1		1	
Surirella biseriata var. *constricta*							1			
S. elegans					1					
S. ovalis					1					
S. tenera				1					1	
Synedra nana						1				
S. ulna						1				1
Tabellaria fenestrata	2	1				1				1
T. flocculosa					1	11	24	15	11	15
Tetracyclus lacustris		1								

Diatomeenflora

Die Diatomeensukzession im unteren Abschnitt der Schichtenfolge vom Suksilampi ist aus Tabelle II ersichtlich. In dem in der Jüngeren Dryaszeit abgelagerten Schluff-Feinsand sind am zahlreichsten Diatomeenarten süsser Kleingewässer repräsentiert: *Fragilaria construens*, *F. pinnata*, *Navicula radiosa* und *Tabellaria flocculosa*. Eine merkwürdige Entwicklungsphase macht sich in 270 cm Tiefe im Sediment der Zone IV geltend, wo in dem oben beschriebenen Floratypus die Grosssee-Diatomeen 11 % ausmachen, und zwar sind es folgende Arten: *Campylodiscus noricus* var. *hibernica* (2), *Cymatopleura elliptica*, *Cymbella ehrenbergii* (4), *Epithemia hyndmanni* und *Gyrosigma attenuatum* (3). Es muss sich aber dennoch um einen Kleinsee gehandelt haben, denn aufgrund der Topographie des Geländes kann in dem Gebiet kein vom Baltikum getrennter Grosssee bestanden haben. Eine mögliche Erklärung für die Erscheinung könnte sein, dass die Diatomeenformen der Grossseen im allgemeinen auch Formen klaren Wassers sind, und anfänglich ist das Wasser der Seen klarer gewesen als gegenwärtig.

Schichtenfolge eines Moors E von der Anhöhe Hernevaara

Die Schichtenfolge stammt aus einem Zwergstrauch-Reisermoor am Rand eines kleinen Weihers, der im Kirchspiel Värtsilä, unmittelbar östlich von der Anhöhe Hernevaara gelegen ist (Abb. 2, Punkt 4). Der erbohrte Teil der Lagerfolge enthält die Ablagerungen auf dem Grund des Moores in 5.5—4.35 m Tiefe (Abb. 7). Die Probeserie ist zuvörderst deswegen interessant, weil es nur hier gelungen ist, auf dem Grund des Moors glazialen Bänderton zu bekommen. Das Moor hat eine Höhe von ca. 105 m und liegt distalwärts vom 1. Salpausselkä.

Pollenflora

Die Pollenflora zeigt die Verhältnisse von Zone III (Jüngere Dryaszeit) bis Zone V (Boreal). Der Bänderton und der Feinsandschluff sind den Pollen gemäss in der Jüngeren Dryaszeit abgelagert worden. Die Sedimentation von organischem Material hat um die Wende von der Jüngeren Dryaszeit zum Präboreal eingesetzt. Ungefähr aus der gleichen Zeit stammen die zwei aufgefundenen *Ephedra*-Pollenkörner. Im Material des Untersuchungsgebiets sind sonst keine *Ephedra*-Pollen gefunden worden, woraus zu schliessen sie hier selten und wahrscheinlich vom Wind aus weiterer Entfernung herbeigetragen sind. Bortenschlager (1965) hat festgestellt, dass im Firngebiet der Ötztaler Alpen u.a. Pollen afrikanischer *Ephedra*-Arten *(E. alata* und *E. altissima)* angeweht werden, so dass die *Ephedra*-Pollen also eine grosse Verbreitungsfähigkeit besitzen. Die zahlreichen *Ephedra*-Pollenkörner, die in Südostfinnland in den spätglazialen, vorwiegend schluffigen Sedimenten von Onttola gefunden worden sind (Repo 1963), sprechen jedoch ihrerseits dafür, dass *Ephedra* vielleicht in der Spätglazialzeit in Finnland gewachsen sein könnte.

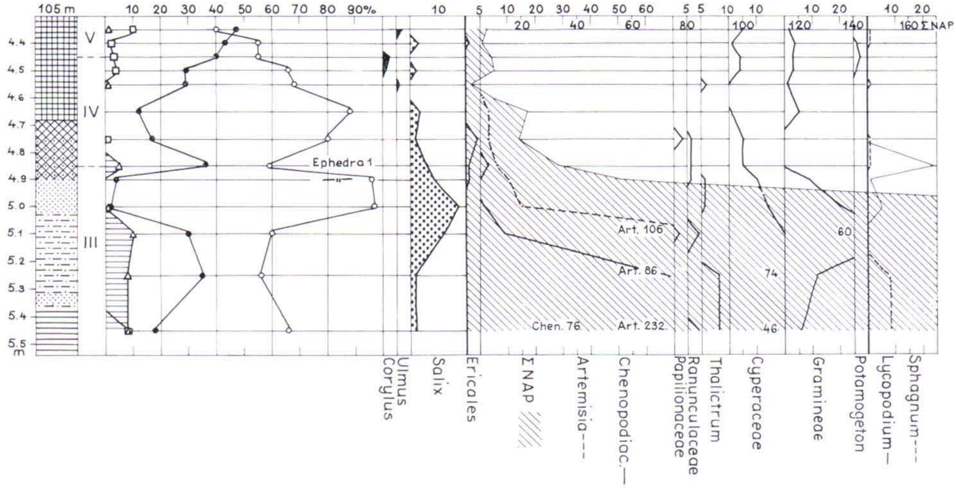

Abb. 7. Pollendiagramm der Schichtenfolge Hernevaara E.

Die irreguläre Pollensukzession in der im Präboreal und Boreal entstandenen Gyttja und Diatomeengyttja legt Zeugnis davon ab, dass in dem Seebecken in der fraglichen Zeit der Schlamm umgelagert worden ist, weshalb die Sedimente der Zonen IV und V miteinander vermengt sind. Auch heute noch geht durch den Weiher eine beträchtliche Strömung, die das lockere Bodensediment umlagern kann.

Diatomeenflora

Der obere Abschnitt des untersuchten Teils (4.7—4.3 m) der Schichtenfolge aus dem Moor östlich von Hernevaara enthält viele Kieselalgen, denn in Frage steht eine um die Wende von Präboreal und Boreal entstandene Diatomeengyttja. Der Artenbestand setzt sich aus Kleinseeformen zusammen; an den untersuchten Stellen sind die vorherrschenden Arten *Melosira italica*, *M. distans*, *Fragilaria construens*, *F. pinnata* und *Navicula anglica*. In der Gyttja der Zonenwende III/IV ist die maximale Art *Cocconeis diminuta*, aber in 5.25 m Tiefe kommt in dem in der Jüngeren Dryaszeit abgelagerten Schluff-Feinsand als vorherrschende Planktonart *Melosira islandica* ssp. *helvetica* (14 %) zusammen mit *Stauroneis phoenicenteron* (14 %) vor. Damals bestand wahrscheinlich eine Verbindung zum Baltischen Eissee, denn wegen der topographischen Verhältnisse kann in dem Gebiet kein getrennter lokaler Grosssee gewesen sein.

Im untersten Abschnitt der Lagerfolge im Schluff-Feinsand enthält der gebänderte Schluffton nur sehr spärlich Diatomeen. Das in 5.35 m Tiefe angetroffene *Stephanopyxis turris* var. *polaris*-Fragment dürfte sekundär dorthin gelangt sein. Die fragliche, in Finnland seltene Salzwasserform kommt nach Mölder in den Yoldiameersedimenten

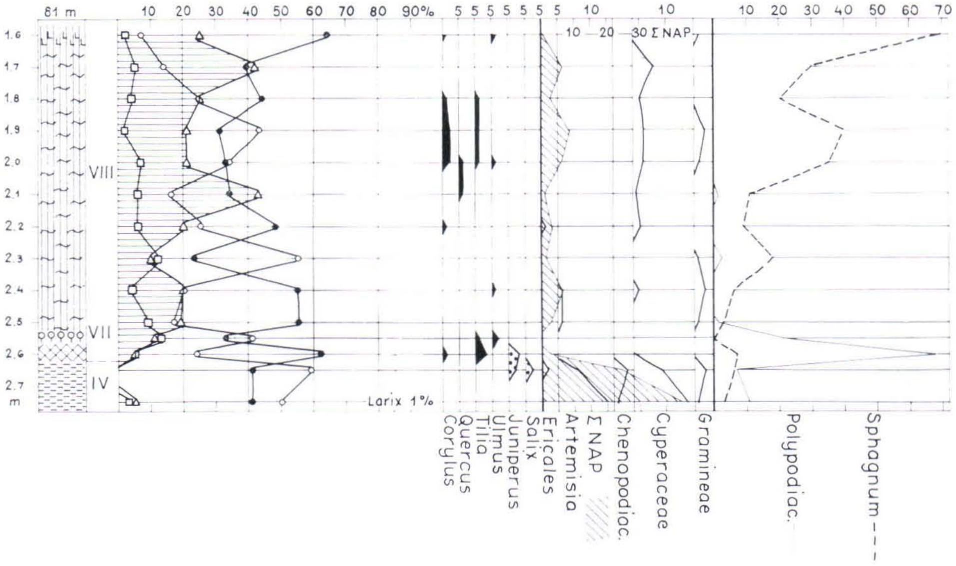

ABB. 8. Pollendiagramm der Schichtenfolge vom Moor Suursuo.

vor. In der hier besprochenen Schichtenfolge kämen als eventuelle Lebensstätte der Art eine interglaziale Meer- oder spätglaziale Yoldiameerphase in Betracht. Eine interglaziale Herkunft ist nicht ausgeschlossen, insbesondere da ziemlich nahe, nämlich in der Gegend des Ladogasees, eine interglaziale Ablagerung angetroffen worden ist, die aus einem zwischen Moränenschichten eingelagerten Tonsediment besteht. Nach Tscheremisinowa (1957) führt es reichlich Salzwasserdiatomeen, die für die Interglazialzeit charakteristisch sind.

Schichtenfolge vom Moor Suursuo

Das Moor Suursuo liegt im Kirchspiel Värtsilä in ca. 81 m Höhe (Abb. 2, Punkt 5) unmittelbar proximal vom 1. Salpausselkä. Die Schichtenfolge betrifft nur die kurze Strecke zwischen 2.75 und 1.6 m. Die Lagerfolge vom Suursuo ist ausgesprochen für die Kenntnis der präborealen Sedimentationsverhältnisse bedeutsam. Betreffs der Pollensukzession dagegen ist die Schichtenfolge unvollständig, weil sie eine beträchtliche Lücke hat (Abb 8).

Pollenflora

Die unterste Partie der Schichtenfolge, symmikter Schluffton, ist aufgrund des Pollenbestandes im Präboreal abgesetzt worden. Hiervon zeugen das *Betula*-Maximum und der noch relativ grosse NBP-Anteil, in welchem die gleichen Arten vertreten sind wie auch sonst in dem Gebiet in den anderen Sedimenten vom Präboreal und aus der Jüngeren Dryaszeit.

Die Ablagerung von organischem Material hat an der Bohrstelle im Frühatlantikum eingesetzt, und zwar etwa zu der Zeit, wo die Fichte sich in der Gegend ausgebreitet hat. In Ostfinnland ist die Fichte verhältnismässig früh eingewandert (Auer 1928, Tolonen 1963). Im *Carex-Sphagnum*-Torf ist die Menge des *Picea*-Pollens in dieser Lagerfolge besonders gross, Maximalwert 43 %.

Diatomeenflora

In dem symmikten Schluffton herrscht eine Süsswasser-Diatomeenflora. Im unteren Abschnitt ist die Menge der Kieselalgen gering. Die dominierenden Gattungen, *Pinnularia* und *Eunotia*, sind Benthosformen. Die Diatomeen sind zum grossen Teil Fragmente, insbesondere die *Pinnularia*-Arten. Dies kommt vermutlich daher, dass die Kieselalgen von Bodenströmungen mitgerissen worden sind, wahrscheinlich in einem Fluss. Obschon Salzwasserformen und Planktonarten fehlen, zeigt schon die Beschaffenheit des Sediments, dass kein Kleinsee in Frage stehen kann. Für das Gleiche spricht auch der geringe Anteil der Epiphytenarten. Die betreffende Kieselalgenflora ähnelt der in Bändertonen, z.B. in Jokela (Mölder, 1956) angetroffenen. Möglicherweise hat es sich um das Yoldiameer gehandelt, in dessen Sedimenten z.B. in der Gegend des Sees Pielisjärvi meistens keine Salzwasserformen vorkommen, wie Hyvärinen 1966 beobachtet hat.

Schichtenfolge vom See Sääperijärvi

Der See Sääperijärvi liegt im Kirchspiel Värtsilä (Abb. 2, Punkt 6) distal vom 1. Salpausselkä an der niedrigsten Stelle der Gegend ca. 67 m ü.d.M. Der Sääperijärvi ist durch den Fluss Jänisjoki mit dem etwas tiefer gelegenen See Jänisjärvi (64 m) verbunden, von wo das Wasser schliesslich in den Ladogasee fliesst. Der See ist relativ eutroph, obschon er ziemlich klares Wasser hat, und darin wachsen u.a. *Stratiotes aloides*, *Potamogeton obtusifolius* und *Myriophyllum spicatum*.

Die aus dem westlich vom See gelegenen Moor erbohrte Schichtenfolge (Abb. 9) grenzt unten an ein Feinsandlager, das eine Mächtigkeit von mehr als 3 m hat, wie an einem nahen Graben zu sehen ist.

Pollenflora

Das Pollendiagramm vom Sääperijärvi ist ähnlich beschaffen wie das vom benachbarten Moor Suursuo. In beiden hat die organische Sedimentation erst im Frühatlantikum eingesetzt, und in beiden tritt der *Picea*-Pollenstreifen ziemlich ausgeprägt hervor. Im Kraut- und Graspollen der untersuchten Lagerfolge trat die eutrophe

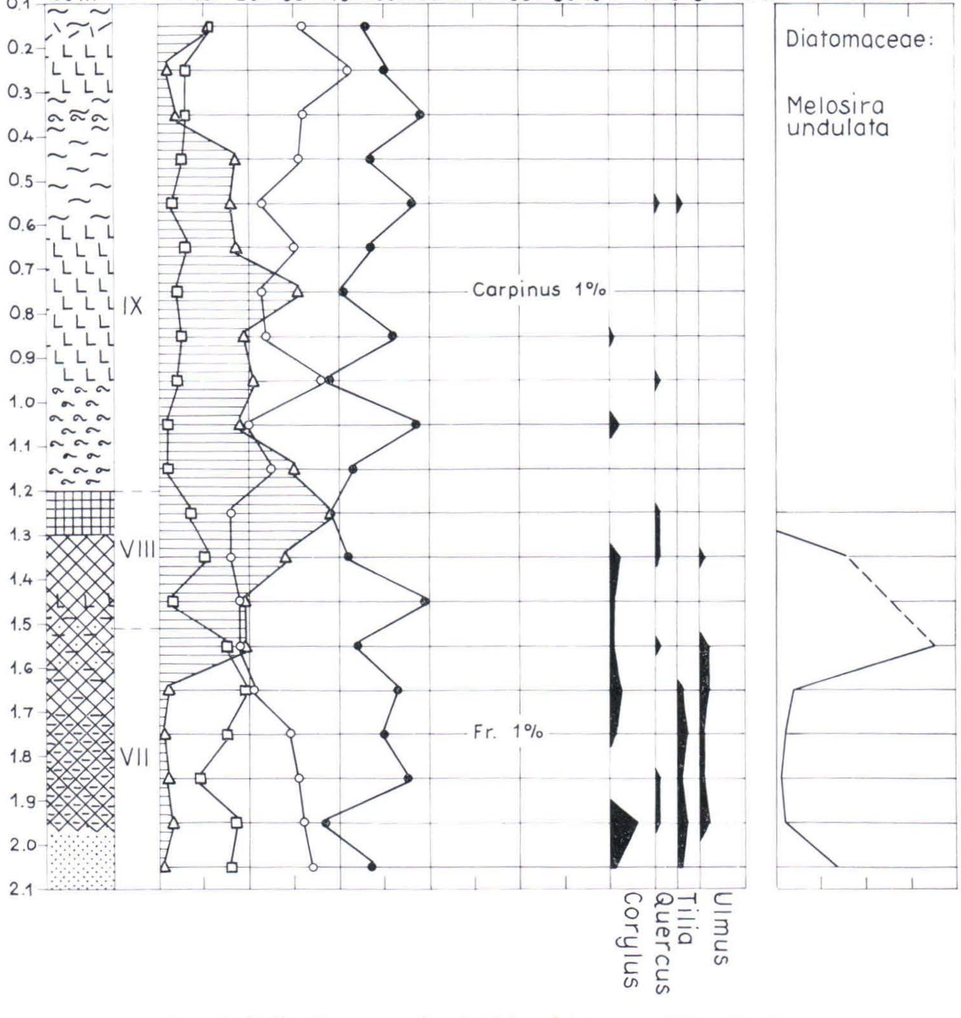

Abb. 9. Pollendiagramm der Schichtenfolge vom Sääperijärvi.

Natur des Sääperijärvi nicht hervor. Zur genaueren Untersuchung des Pollens der Pflanzen in dem See hätten offenbar mehrere hundert Baumpollenkörner pro Probe abgezählt werden müssen. In der fraglichen Arbeit war diese Zahl jedoch auf ca. 200 pro Probe begrenzt, und bei den spätglazialen Ablagerungen sogar auf nur 100 Baumpollenkörner.

Diatomeenflora

Die charakteristische Diatomeenart in der Lagerfolge vom Sääperijärvi war *Melosira undulata* zusammen mit der selteneren var. *normanni*. Der maximale Anteil betrug über 30 % von allen Kieselalgen. Der See muss für das Gedeihen dieser Art also besonders günstig gewesen sein. Obschon die fragliche Art in den Ende Juni genommenen rezenten Proben nicht angetroffen wurde, ist es aufgrund des Gesamtvorkommens nicht ausgeschlossen, dass die Art auch zum gegenwärtigen Diatomeenbestand gehört. Sie ist in Finnland selten und ist nur aus Ilomantsi subfossil gemeldet worden, sowie noch rezent aus drei Seen (Mölder und Tynni 1967).

Zum Diatomeenbestand der gebänderten Schlufftonsedimente

In dem Untersuchungsgebiet liegen bei der Ziegelei von Tohmajärvi in ca. 85 m Höhe (Abb. 2, Punkt 9) sowie in Kiteenlahti in ca. 84 m Höhe (Punkt 8) Tongruben. Die erstere Ablagerung hat eine Mächtigkeit von etwa 6—10 m, an der Bohrstelle ca. 6 m, die letztere wieder ist dünner, an der Bohrstelle ca. 3 m. Insbesondere in Tohmajärvi ist die Bänderung schön ausgeprägt (Abb. 10), die Warven haben eine Stärke von etwa 2 cm. Das Material ist im unteren Abschnitt Tonschluff, aber von ca. 1.5 m Tiefe an aufwärts geht das gebänderte Sediment in gröberen Fein- und Mittelsand über und verliert in ca. 1 m Tiefe die Bänderung. In Kiteenlahti ist kein allmählicher Übergang zwischen dem Oberflächensand und dem darunter liegenden gebänderten Schluffton wahrzunehmen, vielleicht weil der Bodenfrost das superfizielle Sediment vermengt hat.

An manchen Stellen, die wir von der Schichtenfolge analysiert haben, wurden nur in ca. 2 m Tiefe spärlich Kieselalgen und deren Fragmente gefunden, im ganzen 26 Stück. Der Diatomeenbestand weist keinen einheitlichen Florentyp auf, denn mindestens zwei Komponenten lassen sich unverkennbar unterscheiden; Grosssee-Planktonformen repräsentieren die vorherrschende Art *Melosira islandica* ssp. *helvetica* (5) sowie *M. granulata* und *Cyclotella comta*. Von den Benthosformen des Süsswassers waren die *Pinnularia*-Arten *(P. viridis, P. borealis, P. microstauron)* am gewöhnlichsten. Ferner kam *Hantzschia amphioxys* (5) als zweite Hauptart vor. Die Epiphyten machten in der Probe die Minderheit aus: *Epithemia turgida* und *Gomphonema acuminatum*.

In der Schichtenfolge von Kiteenlahti wurden in 1.8 m Tiefe nur 4 Arten gefunden, im ganzen 6 Kieselalgen, und zwar *Asterionella gracillima* (3), *A. formosa*, *Cymbella* sp. fragm. und *Navicula* sp. fragm. Von diesen Arten sind die *Asterionellae* Planktonformen.

Diese wenigen Diatomeenarten stützen die Auffassung, dass der Bänderton an den untersuchten Stellen der Lagerfolge in einem Grosssee abgesetzt worden ist, m.a.W. im Baltischen Eissee. Die Planktonformen repräsentierten demgemäss die Flora des Eissees selbst, und die Benthos- und Epiphytenarten wieder den vom

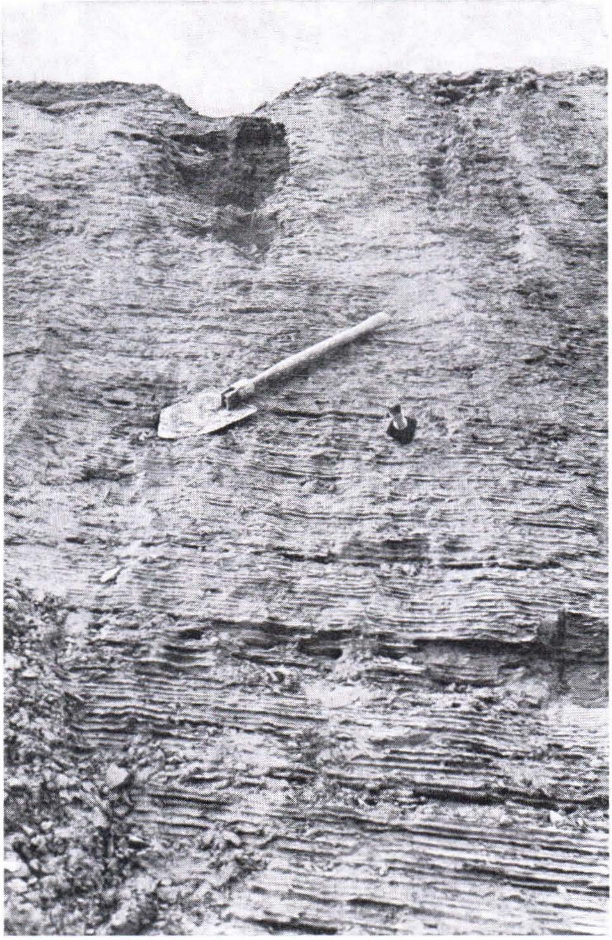

Abb. 10. Bänderstruktur des Schlufftons in der Tongrube der Ziegelei von Tohmajärvi.

Schmelzstrom aus der Eis- und Uferzone mitgebrachten Diatomeenbestand. Zum Vergleich für das Diatomeenplankton eines Grosssees kann der Ladogasee herangezogen werden, wo heutzutage die Arten *Melosira islandica* ssp. *helvetica* und *Asterionella formosa* vorherrschen (Juse 1966).

Den bisherigen Untersuchungen gemäss kommen in den spätglazialen Bändersedimenten unseres Landes stellenweise spärlich Salz- und Brackwasserformen vor, was die Auffassung von einer spätglazialen Meerphase gestützt hat. Die Vorkommen können indessen auch sekundärer Herkunft sein. In den untersuchten Schichtenfolgen des Gebiets konnte freilich keine entsprechende Beobachtung gemacht werden (Ausnahme Salzwasserform im Profil von Hernevaara E, in 5.35 m Tiefe).

DIE GRUNDZÜGE DER UFERVERSCHIEBUNG AUFGRUND DER POLLEN- UND DIATOMEENSTRATIGRAPHIE

Will man die Uferverschiebung in dem Untersuchungsgebiet verfolgen, so geht man von der Lage des Yoldia I-Ufers aus. In Sauramos (1958) Relationsdiagramm ist das Yoldia I-Niveau in der Gegend von Hernevaara in ca. 78 m Höhe eingetragen. In dem Relationsdiagramm von Hyyppä (1966) liegt die Yoldia I-Grenze auf der dem Untersuchungsgebiet entsprechenden Litorina I-Isobase von 30 m ungefähr 60 m ü.d.M. Dem höchsten Uferniveau des Yoldiameers nähert sich von den untersuchten Lagerfolgen am ehesten das in 81 m Höhe gelegene Moor Suursuo, dessen Bodensediment präborealer Ton ist. Ungeachtet seiner Süsswasserdiatomeenflora ist der Ton vielleicht in einer durch einen seichten Sund mit dem Yoldiameer verbundenen Bucht abgelagert worden. Das Moor Rillinkisuo, das etwa 10 km südlich vom Moor Suursuo auf tieferen Landhebungsisobasen in den gleichen Höhen liegt, (Abb, 2, Punkt 7) ist einer orientierenden Pollenuntersuchung gemäss in der Präborealzeit ein See gewesen, in welchem sich Gyttja abgelagert hat.

Der Höhengürtel von 80—90 m entspricht in dem Gebiet einer kurz vor der Yoldiameerphase verlandeten Zone. In diesem Bereich liegen die grössten Ebenen sowie die Moore. Im Bereich der Ziegelei von Tohmajärvi besteht der Boden der Ebene an der Oberfläche aus Sand, aber tiefer unten geht das Sediment ohne Spuren von Erosion in gebänderten Schluffton über. Seiner Lage und Struktur gemäss ist der Bänderton im Spätglazial entstanden. Auch in Kiteenlahti war die Sedimentation des Tons schon in der Spätglazialzeit abgeschlossen.

Das dem Abfliessen des Baltischen Eissees (B III) vorausgegangene Uferstadium lag somit in dem Gebiet in etwa 107 m Höhe ü.d.M. (Yoldia-I 80 m + 27 m), m.a.W. etwas höher als die Schichtenfolge Hernevaara E. Zwischen dem 107 m-Niveau und dem Yoldiameer-Niveau in ca. 98 m Höhe liegt ein gut ausgebildetes Ufer u.a. südlich von der Bucht Kiteenlahti. Dem gleichen Stadium entspricht am Distalhang des 1. Salpausselkä das nördlich vom Sääperijärvi gelegene Ufer.

Die Höhe des Baltischen Eissees, B I, in Hernevaara beträgt nach Sauramo (1958) etwa 112 m ü.d.M. Der Wasserspiegel des Baltischen Eissees I hätte demgemäss um die Wende vom Alleröd zur Jüngeren Dryaszeit etwa 12 m über dem tiefsten Teil der gebohrten Schichtenfolge Hernevaara E gelegen. Der Pollendatierung gemäss ist das Bodensediment des Moors, der gebänderte Schluffton, jedoch in der Jüngeren Dryaszeit entstanden. Sofern in der früheren Phase des Baltischen Eissees (oder in einem spätglazialen Meerstadium) an dieser Stelle Sedimentation stattgefunden hat, sind es so grobe Fraktionen gewesen, dass sie mit den verwendeten Bohrinstrumenten nicht erfasst werden konnten.

Der in ca. 151 m Höhe abgelagerte Feinsand und Schluff vom Moor Mustalampi weist eine ziemlich reiche Kleinsee-Diatomeenflora auf, woraus zu schliessen die Sedimentation in einem abgeschnürten Becken stattgefunden haben muss. Sederholms ursprünglich am Weiher Kukkolampi in Värtsilä beschriebene höchste marine Grenze bei ca. 155 m ü.d.M. entspricht nach Sauramo (1958) dem spätglazialen Uferniveau

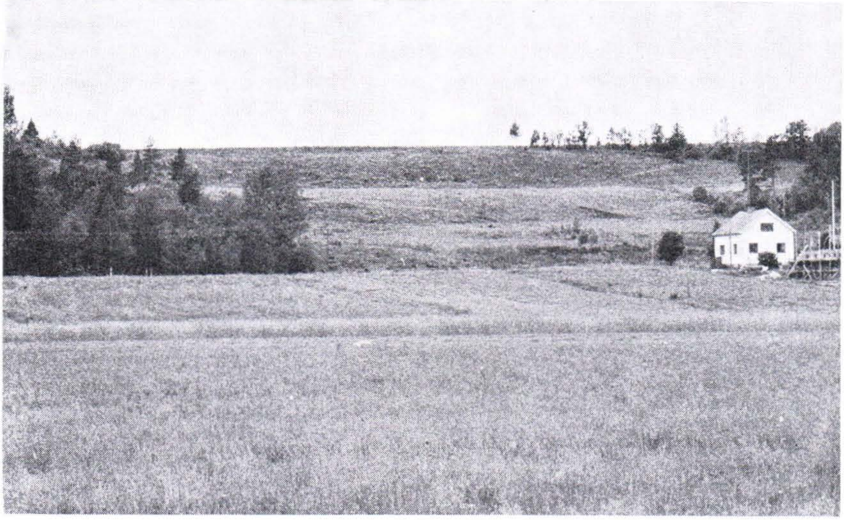

Abb. 11. Gut ausgebildetes Ufer am Distalhang des 1. Salpausselkä in ca. 98 m Höhe nördlich vom Beobachtungspunkt 9.

aus der Älteren Dryaszeit, das seinerseits wieder in Tanners (1930) System dem ältesten und höchsten Eismeer *l*-Niveau entspricht (op.cit.). Die in unserem Gebiet erbohrten Schichtenfolgen enthalten jedoch keine so alten Sedimente. Die fraglichen Sedimente sind in dem Gebiet nicht mit Hilfe der Bändertonchronologie untersucht worden, und die ältere Uferverschiebung ist dort, insbesondere was die Datierung betrifft, deswegen noch nicht sicher geklärt.

DIE WENDE DER SPÄT- UND POSTGLAZIALZEIT AUFGRUND DER C^{14}-DATIERUNG DER SCHICHTENFOLGE VOM MOOR MUSTALAMPI

Die Radiokarbondatierung vom Mustalampi zeigt, dass die beträchtliche BP/NBP-Zunahme des Pollenspektrums in Südostfinnland in den Ausgang der Jüngeren Dryaszeit fällt. Das vorausgegangene NBP-Maximum besteht im Mustalampi zu einem erheblichen Teil aus *Artemisia*- und *Chenopodiaceae*-Pollen. Das fragliche Maximum lässt sich mit dem in gewissen Bändertonhorizonten Südfinnlands vorkommenden Pollenbestand vergleichen (Tynni 1966). Wahrscheinlich liegen die fraglichen verschiedenartigen Sedimente, die Feinsand-Gyttja im Mustalampi und das Bändertonsediment in Südfinnland, die beide die gleiche Pollenflora haben, zeitlich nicht weit auseinander.

Die voneinander wesentlich abweichenden sukzessiven Pollentypen in der Jüngeren Dryaszeit und im Präboreal haben die Anwendung des Pollenverfahrens in den sonst für die Datierung schlecht geeigneten Sedimenten dieser Zeit gerechtfertigt.

Die geringeren BP/NBP-Schwankungen in den anorganischen Sedimenten können durch lokale Faktoren bedingt sein, weshalb sie nicht als Grundlage für die Datierung taugen. Godwin (1956) hat mitgeteilt, dass viele in der Jüngeren Dryaszeit gewöhnliche NBP-Arten in England (grossenteils die gleichen wie in Finnland) noch in der Pollenflora der Präborealzeit auftreten. Andererseits hat u.a. Firbas (1949) zahlreiche Schichtenfolgen aus Mitteleuropa publiziert, in denen die Wende von der Jüngeren Dryaszeit zum Präboreal als ein ausgeprägter BP/NBP-Anstieg zur Geltung kommt.

Der im Vergleich zu den Diagrammen aus Mitteleuropa grössere BP/NBP-Anstieg in Süd- und Südostfinnland entspricht folgerichtig den Erwartungen, denn diese Wandlung betrifft in Finnland in dem fraglichen Gebiet zuerst in der Jüngeren Dryaszeit die Verhältnisse nahe am Eisrand, aber in der Präborealzeit wiederum eine Situation, wo der Eisrand schon erheblich weiter entfernt lag.

Für diese Untersuchung haben wir von der Outokumpu Oy-Stiftung einen Zuschuss erhalten. Die Radiokarbon-Datierung hat im Dezember 1966 die Isotopes, Inc. in USA ausgeführt. Für die Übersetzung des Textes in die deutsche Sprache danken wir Frau Marianne Kahanpää.

Manuskript eingegangen am 6. April, 1967

LITERATURVERZEICHNIS

Auer, V. (1928) Über die Einwanderung der Fichte in Finnland. Comm. Inst. Quaest. Forest. Finl. 13.

Aurola, E. (1955) Die postglaziale Entwicklung des südwestlichen Finnlands. C. R. Soc. Géol. Finlande 11. Bull. Comm. géol. Finlande 121.

Berghell, H. (1903) D 2 Savonlinna, Nyslott; 1 : 400.000. (Bodenkarte). Geologinen Toimisto. Helsinki.

—»— (1904) Geologisk öfversiktskarta öfver Finland. Sektionen D 2. Nyslott. Beskrifning till jordatskartan. Geologiska Kommissionen. Helsingfors.

Bortenschlager, S. (1965) Funde afrikanischer Pollen in den Alpen. Naturwissenschaften, H. 24. S. 663/64.

Donner, J. (1951) Pollen-Analytical Studies of Late-Glacial Deposite in Finland. C. R. Soc. Géol. Finlande 24, S. 1—92. Bull. Comm. geol. Finlande 154.

—»— (1958) The late-glacial period and its correlation with the retreat stages of the ice in Finland. C. R. Soc. Géol. Finlande 30. S. 79—86. Bull. Comm. géol. Finlande 180.

—»— (1967) The Late-glacial and early Post-glacial pollen stratigraphy of southern and eastern Finland. Soc. Sci. Fennica, Commentationes Biol., 29, 9.

Erdtman, G. (1949) Palynological aspects of the pioneer phase in the immigration of the Swedish flora. II. Identification of pollen grains in late-glacial samples from Mt. Omberg. Ostrogothia. Sv. Bot. Tidskr. 43.

Firbas, F. (1949) Spät- und nacheiszeitliche Waldgeschichte Mitteleuropas nördlich der Alpen. I. Allgemeine Waldgeschichte. Jena.

Fromm, E. (1963) Absolute chronology of the Late-Quaternary Baltic. A Rewiew of swedish investigations. Baltica 1, S. 46—59.

Frosterus, Benj. und W. W. Wilkman (1910) D 3 Joensuu; 1 : 400.000. (Bodenkarte). Geologinen Toimisto. Helsinki.

—»— (1917) Suomen Geologinen Yleiskartta. Lehti D 3. Joensuu. Maalajikartan selitys. Geologinen Toimisto. Helsinki.

Godwin, H. (1956) The history of the British flora. Cambridge.

Hyvärinen, H. (1966) Studies on the late-Quaternary history of Pielis-Karelia, eastern Finland. Soc. Scient. Fennica, Comm. Biol. 29, Nr. 4.

—»— (1967) A shore-line diagram for the easternmost section of the Salpausselkäs. Soc. Sci. Fennica, Comm. Phys.-Math., 33, 4.

Hyyppä, E. (1966) The late-Quarternary land uplift in the Baltic sphere and the relation diagram of the raised and tilted shore levels. Ann. Acad. Sci. Fennicae. A. III. 90.

Juse, A. (1966) Diatomeen in Seesedimenten. Arch. Hydrobiol. Beih. Ergebnisse der Limnologie 3/4.

Mölder, K. (1956) Die Diatomeenflora der Bändertone bei Jokela in Südfinnland. Arch. Soc. »Vanamo» 10 : 1.

—»— und R. Tynni, (1967) Über Finnlands rezente und subfossile Diatomeen. I. C. R. Soc. géol. Finlande. 39.

Nilsson, Erik (1964) Geochronological investigations in southern Sweden. Geol. Fören. Förh. Bd. 86.

RAMSAY, W. (1891) Über den Salpausselkä im östlichen Finnland. Fennia 4.

—»— (1931) Material zur Kenntnis der Spätglazialen Niveauverschiebungen in Finnland. Fennia 54.

REPO, R. (1957) Untersuchungen über die Bewegungen des Inlandeises in Nordkarelien. Bull. Comm. géol. Finlande 179.

—»— (1963) On the late-Glacial vegetation of Jaamankangas, Finland. Arch. Soc. »Vanamo» 18 : 2.

SAURAMO, M. (1921) Onkamon keltamulta ja Kannusjärven kehityshistoria. Geol. Kom. geotekn. julk. 31.

—»— (1958) Die Geschicte der Ostsee. Ann. Acad. Scient. Fennicae Ser. A, III, 51.

—»— and V. AUER (1928) On the development of lake Höytiäinen in Carelia and its ancient Flora. Bull. Comm. géol. Finlande 81.

TANNER, V. (1930) Studier över kvartärsystemet in Fennoskandias nordliga delar. Bull. Comm. geol. Finlande 88.

TOLONEN, K. (1963) Über die Entwicklung eines nordkarelischen Moores im Lichte der C^{14}-Datierung. Das Moor Puohtiinsuo in Ilomantsi (Ost-Finnland). Arch. Soc. »Vanamo» 18 : 1.

TSCHEREMISINOWA, E. A. (1957)

Черемисинова, Е.А. (1957) Морская диатомовая флора четвертичных отложений котловины Дадожского озера. Бюлл. КЧ, Ио. 21.

TYNNI, R. (1966) Über spät- und postglaziale Uferverschiebung in der Gegend von Askola, Südfinnland. Bull. Comm. géol. Finlande 223.

WILKMAN, (1917) siehe Frosterus, Benj. und W. W. Wilkman (1917).

Comptes Rendus de la Société géologique de Finlande
N:o XXXIX (1967), pp. 161—172

AN ELECTRON MICROPROBE STUDY OF THE DISTRIBUTION OF IRON, MANGANESE, AND PHOSPHORUS IN CONCRETIONS FROM THE GULF OF BOTHNIA, NORTHERN BALTIC SEA

BY

BORIS WINTERHALTER and JAAKKO SIIVOLA

Geological Survey of Finland, Otaniemi

ABSTRACT

Fe-Mn-concretions of a spheroidal type were found according to electron probe determinations to consist of alternating iron- and manganese-rich layers. This pattern was ascribed to seasonal variations in the physicochemical conditions governing the precipitation of the hydrous oxides of iron and manganese. Calculations based on the rhythmic growth of the concretions investigated gave a mean accumulation rate of 0.15—0.20 mm/yr.

The rather high phosphorus content (average 3.5 % P_2O_5) of the concretions was found to be concentrated in the iron-rich layers, probably as a result of the scavenging effect of ferric hydroxide.

INTRODUCTION

The recent expansion in marine geological research is also reflected in the increasing number of reports dealing with the occurrences of sea-floor precipitates of hydrous iron and manganese compounds. Even though the chemical and mineralogical composition of deep-sea iron-manganese concretions and their shallow-water counterparts in shelf areas, and also in many fresh water lakes, has already been studied in quite some detail (*e.g.*, Aarnio 1917, Buser 1959, Manheim 1965, Mero 1965, Strakhov 1966), considerable differences of opinion still prevail as to the origin and the causes of the formation of such precipitates. This is probably to a large extent due to the scarcity of accurate data on their internal structure and inter-element relationships. Especially bulk chemical analyses of whole concretions or even parts of them have in some cases been a source of misleading information. The recent progress in electron probe microanalysis techniques has, however, opened up new possibilities for studying the distribution of elements in different parts of a single nodule with a dimensional accuracy of the order of one micron.

The present paper describes the results of an electron microprobe investigation of iron-manganese concretions occurring abundantly in the Gulf of Bothnia, in the northern Baltic Sea. Special emphasis is placed on the relative concentrations of manganese, iron, and phosphorus across a nodule, which is of great importance in any attempt to solve the actual processes leading to the formation of concretions of hydrous iron and manganese oxides.

IRON-MANGANESE CONCRETIONS

Considerable areas of the sea-floor in the Gulf of Bothnia is more or less covered under a blanket of iron-manganese concretions. The occurrence and chemical composition of these precipitates as well as similar concretions from other parts of the Baltic Sea have been described by several authors (Gripenberg 1934, Gorshkova 1961, Manheim 1961 and 1965, Winterhalter 1966). Even though the Baltic concretions closely resemble deep-sea manganese nodules, many significant differences, especially in chemical composition and inter-element relationships, can be noticed.

A striking phenomenon, not described in the literature dealing with deep-sea manganese nodules, is a clear correlation between the manganese/iron ratio and the type of Baltic Sea concretion. Winterhalter (1966) has found that the concretions, which are divided into three separate groups according to their physical form, are characterized by definite manganese/iron ratios: I spheroidal — $MnO/Fe_2O_3 > 0.5$; II discoidal — $MnO/Fe_2O_3 = 0.2$—0.5; and III others varying from thin sheets to thick slabs of concretionary material — $MnO/Fe_2O_3 < 0.2$.

A second major difference was the high phosphorus content of Baltic concretions, averaging 3.5 % P_2O_5, as compared to concentrations of well under 1 % P_2O_5 in manganese nodules from the Atlantic and Pacific Oceans (Mero 1965). Lacustrine ores from Finnish and East Karelian lakes are also generally very poor in phosphorus (Aarnio 1917, Strakhov 1966). Only concretions from the Barents Sea (Strakhov, *op.cit.*), White Sea (Gorshkova 1931) and the Kara Sea (Gorshkova 1957) have phosphorus in concentrations comparable with those from the Gulf of Bothnia. According to Winterhalter *(op.cit.)* a correlation between the iron and phosphorus concentrations in Baltic concretions seemed to exist, although the exact relationship between these elements could not be satisfactorily ascertained by available chemical means. This was one of the reasons why several samples of iron-manganese concretions from the Gulf of Bothnia were subjected to the present electron microprobe study.

EXPERIMENTAL PROCEDURES

Owing to the relative softness of the concretionary material, each specimen had to be impregnated in epoxy resin prior to preparation and polishing for microprobe determinations. The procedure was as follows: A cross-section of the nodule was first cut and trimmed with a knife, after which it was immersed in a crucible containing araldite mixed with hardener. Water and air trapped in the porous material were evacuated in a vacuum desiccator until no more bubbles could be seen to arise from the sample. When the desiccator was opened, ambient air pressure forced the resin into the cracks and voids of the concretionary material. The surface of the impregnated concretion was trimmed and polished after the araldite had hardened. To produce as perfect a surface as possible, the sample was re-impregnated several times with successive re-polishing.

Prior to analysis the surface of the polished section was metalized with copper in a vacuum vapour chamber.

The electron probe determinations were made with a Cambridge Geoscan two-channel EP-microanalyzer at the Geological Survey of Finland. The main purpose of the analyses was to determine the relationships between Fe, Mn, P and Ca in the concentric structures of the iron-manganese concretions. The following working constants were used: excitation potential 25 kV; specimen current 60 mμA; analyzed lines Fe K_{α_1}, Mn K_{α_1}, P K_{α} and Ca K_{α}.

Because of the experimental nature of the present work, qualitative determinations were made at first to get a general idea of the composition of the concretions. At a later stage emphasis was placed on the recording of relative variations in the concentrations of the main conctituents. Minor elements were not analyzed owing to their low concentrations in Baltic concretions (*cf.*, Winterhalter 1966, Table 8) and to the poor quality of the polish attainable on this type of material. In fact, the unevenness of the final polished surface was considerably greater than required by the accuracy of the electron probe. Thus irregularities would be registered as variations in the X-ray intensity. Also grit formed during polishing may be trapped in minute cracks and hollows in the specimen and cause distortions in the picture of element concentrations.

It must be pointed out that the sensitivity of the microanalyzer is not uniform across the entire electron beam scan when a low magnification is used in conjunction with a mica crystal. Thus the black areas on both sides of the central vertical zone in Fig. 1 D are caused by properties of the mica crystal and do not indicate a deficiency in phosphorus. The LiF-crystal used in analyzing manganese and iron, however, gives a more uniform distribution photograph (*cf.*, Figs. 1 B and 1 C).

RESULTS

As previously anticipated according to bulk chemical analyses and optical observations (Winterhalter 1966), the concretions were found to consist of alternating iron- and manganese-rich layers. The electron beam scanning photographs in Fig. 1, covering an area of 700 × 700 microns from a cross-section of a spheroidal concretion, clearly show this concentric pattern. The cracks in the polished section, evident especially in the lower part of the Fe distribution photograph (Fig. 1 C), are due to disintegration (dehydration) of hydrous iron oxides in vacuum and under the heat

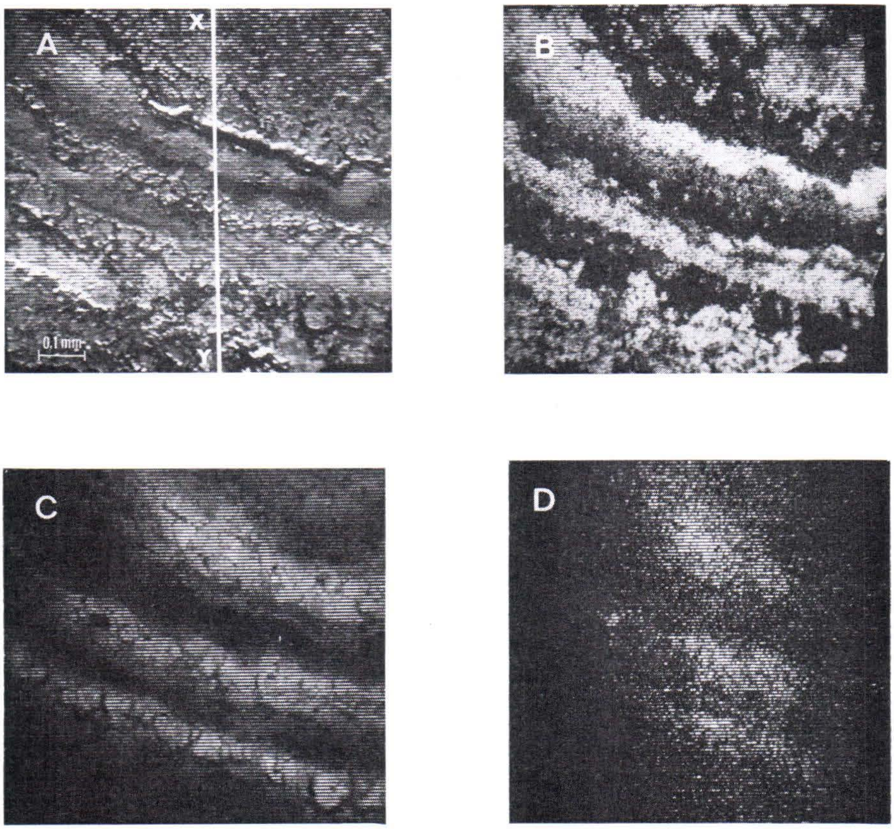

FIG. 1. Electron beam scanning photographs which show part of the concentric layering comprising a spheroidal concretion. A. Electron image. The line XY indicates the traverse of the Fe-Mn-intensity profile in Fig. 2. B. Distribution of manganese, X-ray image, Mn $K_{\alpha 1}$. C. The distribution of iron is clearly complementary to that of manganese. X-ray image, Fe $K_{\alpha 1}$. D. X-ray image, P K_{α}. Note the similar distribution of phosphorus and iron.

effect of the electron beam during scanning. The lack of such cracks in the manganese-rich layers possibly is an indication that the water is chiefly bound to iron.

Burns and Fuerstenau (1966) found in an electron probe investigation of some Pacific manganese nodules that the iron concentration fluctuates whereas the manganese concentration is relatively uniform throughout a nodule, being only slightly higher where the iron is low. This does not, however, seem to be the case with Baltic concretions, as can be inferred from the iron and manganese distribution photographs in Figs. 1 B and 1 C. The distribution profile in Fig. 2 shows the relative concentrations of iron and manganese along the vertical traverse marked XY in Fig. 1 A. The inverse relationship between iron and manganese is obvious.

Evidently it is possible to distinguish three different types of layers in Baltic spheroidal concretions according to their iron and manganese concentrations:

1. an iron-rich phase practically void of manganese;
2. a manganese phase containing at most only minor quantities of iron; and
3. an intermediate layer consisting of both iron and manganese phases, possibly in the form of a layer lattice structure with alternating sheets of ordered manganese dioxide and disordered iron-manganese hydroxides reported by Buser (1959) to be found in manganese nodules.

Even though ionic diffusion in concretionary aggregates may sometimes cause segregation of constituents into separate layers, the alternating iron and manganese phases in the present spheroidal concretions must be considered as primary features, *i.e.* depositionary. There are at least two factors clearly speaking against a post-depositionary segregation. Firstly, the occurrence of alternating iron- and manganese-rich layers is consistent throughout a sample, *i. e.*, there is no detectable difference in the distribution pattern of the elements between the central and the peripheral parts of a nodule. Secondly, the accumulation rate of the concretionary material is too great (up to 0.1 mm/yr. according to Manheim, 1965) to allow for ionic diffusion of a magnitude capable of explaining the formation of separate Fe and Mn phases.

The iron and manganese in sea water occur mostly as colloidal hydrous oxides (Fe^{3+} and Mn^{4+}) (cf., Krotov 1951, Hartmann 1964). The coagulation of the colloids is governed by the pH of the sea water. According to Krotov *(op.cit.)* colloidal ferric hydroxide coagulates at pH-values as low as 6.6 while manganous hydrosols are precipitated first at pH-values exceeding 8. The pH of Baltic waters is generally around 7, which during intense biological activity in the summer season can, however, reach values considerably over 8.

Other factors reflecting seasonal and climatic variations, such as fluctuations in oxygen content, temperature and biological activity, typical of a shallow sea like the Baltic, are also capable of influencing the precipitation of iron and manganese. Consequently, it seems feasible to consider the seasonal changes in the physicochemical conditions of Baltic waters sufficient to cause the rhythmic precipitation of separate iron and manganese layers. Thus, an iron and a manganese phase may together constitute an annual growth layer. It should be pointed out that climatic fluctuations may occasionally distort this sequence. Variations in bottom currents, which directly affect sedimentation conditions on the sea-floor, are capable of influencing the formation of concretions.

In Fig. 2, the part of the concretion between 0 and 160 microns has been precipitated during conditions of environmental instability. After this the seasonal influence on the precipitation of both iron and manganese has become more distinct causing the formation of three clearly discernible, consecutive, annual, growth layers (first: 160—320 microns; second: 320—520 microns; and third: 520—720 microns). This gives an accumulation rate of nearly 200 microns/year. From another electron probe

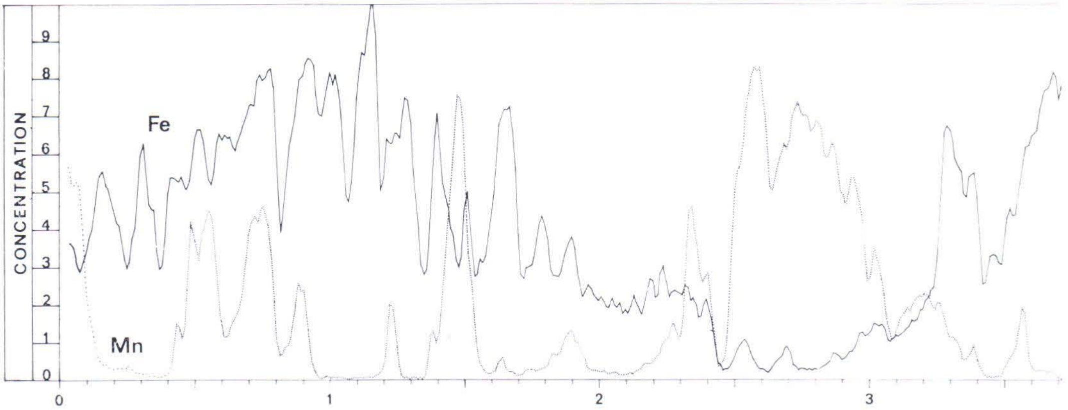

FIG. 2. The relative concentrations of iron and manganese along line XY in Fig. 1 A. Specimen traversing
caused either by an irregularity in the polished section

profile (length 1.1 mm), radially across a sample of a spheroidal concretion from a different location in the Bothnian Bay, seven distinct pairs of iron and manganese rich layers were observed. This corresponds to a mean accumulation rate of 160 microns per year.

Discoidal concretions, characterized by a girdle of concretionary material around some nucleus, *e.g.*, a pebble, exhibit a concentric growth structure. The annual growth pattern of altenating iron and manganese rich layers typical of the spheroidal nodules (Figs. 1 and 2) is not, however, evident in the discoidal type (Figs. 3 and 4). This is

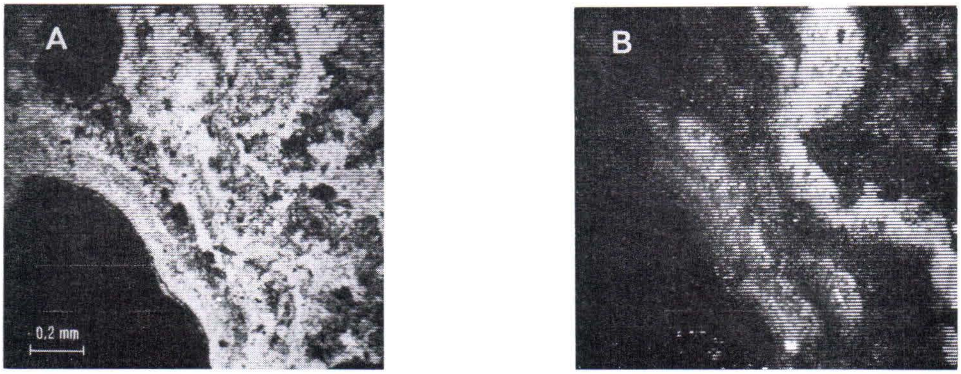

FIG. 3. Electron beam scanning photographs of part of a discoidal concretion. Part of the nucleus (a granitic pebble) is visible as a black area in the lower left-hand corner of the pictures. A. The distribution of manganese, X-ray image, Mn $K_{\alpha 1}$. B. The distribution of iron, X-ray image, Fe $K_{\alpha 1}$. Owing to differences in the X-ray intensities and in photographic exposure times, the specimen seems to contain more manganese than iron, although in reality the opposite is the case.

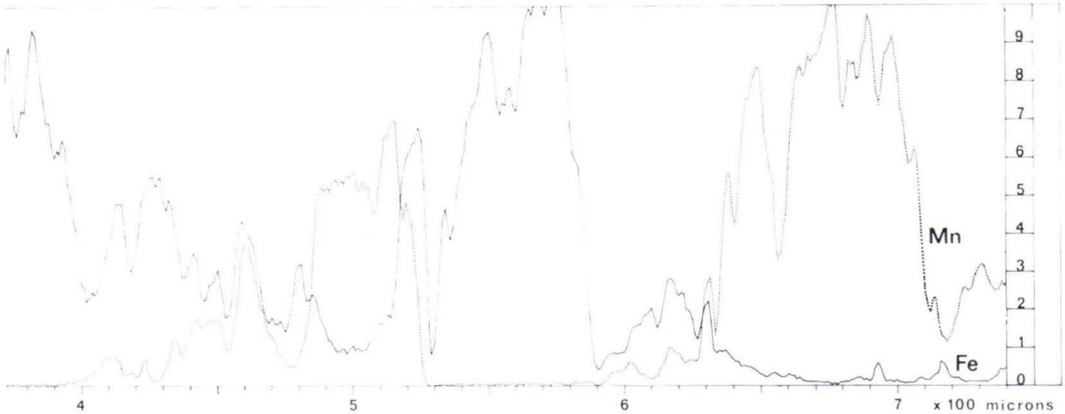

at 10 microns per minute. A drop in the Fe and Mn intensities (*e.g.* at 243 and 258 microns in the figure) is
or by the presence of a quartz or similar grain.

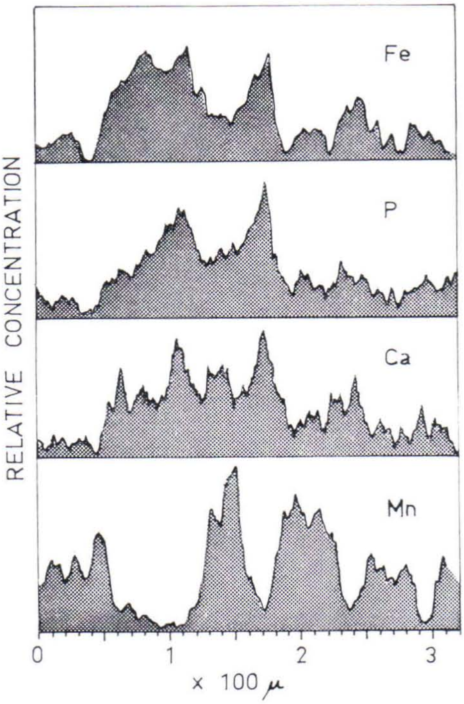

FIG. 4. Electron beam scan profiles showing the relative X-ray intensities of Fe $K_{\alpha 1}$, P K_{α}, Ca K_{α} and Mn $K_{\alpha 1}$ radially across the lower part of a discoidal concretion. The intensities have not been calibrated against standards and thus the concentrations of the different elements are not comparable

TABLE 1.

Iron, manganese, and phosphorus concentrations in Fe-Mn-concretions from the Gulf of Bothnia

Sample No	Station No	Location of sampling station		Depth meters	Percentages on dry weight basis			$\frac{P_2O_5}{Fe_2O_3}$	Remarks
		Longitude	Latitude		MnO	Fe_2O_3	P_2O_5		
1	CIII	64° 42′N	23° 05′E	74	3.5	38.2	6.4	0.168	Flat concretion 4—5 mm thick
2	US4a	62° 39′N	19° 30′E	140	5.67 1)	34.33 1)	4.88 1)	0.143	Spheroidal conretions < 0.8 cm Ø
3	Ä3	64° 51′N	22° 18′E	59	17.0	41.2	4.33 2)	0.105	Discoidal concretion around a pebble nucleus
4	S3	63° 57′N	21° 45′E	70	15.5	30.0	4.0	0.133	Discoidal concretion around a pebble nucleus
5	BII	61° 29′N	19° 48′E	93	10.04 1)	30.95 1)	3.90 1)	0.126	Spheroidal concretions < 0.5 cm Ø
6	P2O	65° 04′N	23° 21′E	77—92	7.8	39.3	3.63 2)	0.092	Spheroidal concretion ~ 2 cm Ø
7	Ä7 (a)	64° 51′N	22° 47′E	78	17.3	26.9	3.3	0.123	Spheroidal concretion ~ 1.5 cm Ø
8	P9 (b)	64° 38′N	22° 55′E	79	4.5	33.1	3.02 2)	0.092	Corroded flat concretion
9	BIII	61° 37′N	19° 48′E	90	9.92 1)	29.66 1)	2.98 1)	0.101	Spheroidal concretions < 0.4 cm Ø
10	P9 (a)	64° 38′N	22° 55′E	79	21.8	27.5	2.97 2)	0.108	Spheroidal concretion ~ 1.3 cm Ø
11	SM2	64° 04′N	21° 27′E	88	17.07 1)	26.92 1)	2.59 1)	0.096	Spheroidal concretions < 1 cm Ø
12	KÅ4	62° 15′N	19° 16′E	94	17.98 1)	20.79 1)	2.59 1)	0.125	Spheroidal concretions 3—7 mm Ø
13	Ä7 (b)	64° 51′N	22° 47′E	78	23.5	22.5	2.5	0.111	Spheroidal concretion ~ 0.5 cm Ø
14	RR5	64° 50′N	23° 10′E	71	18.32 1)	27.77 1)	2.13 1)	0.077	Spheroidal concretions 5—10 mm Ø

Anal.: T. Koljonen 1), Meeri Taug 2), the rest of the data is from Winterhalter (1966).

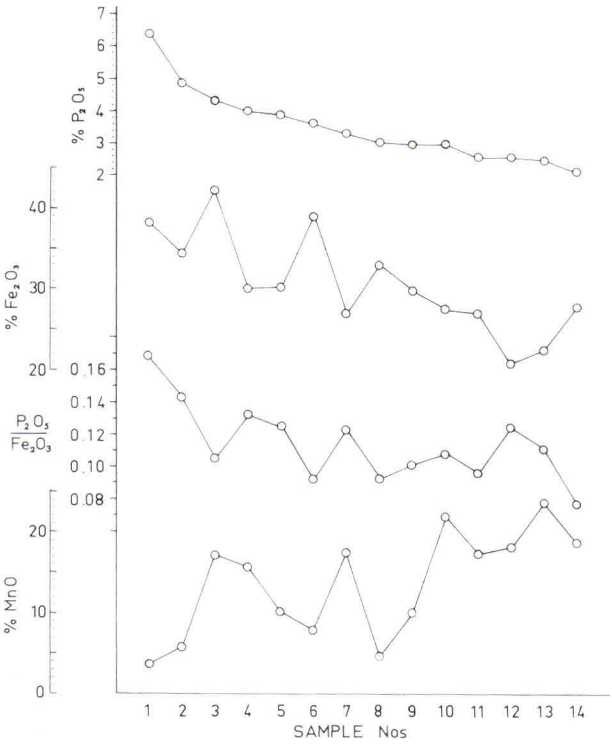

FIG. 5. The assay data from Table 1 have been plotted to show the relationship between phosphorus, iron and manganese.

probably due to the difference in environmental factors governing the formation of the concretions. Spheroidal nodules are generally found in marginal areas of active and in some cases semi-stagnant sedimentary basins, where physicochemical conditions are mostly governed by seasonal changes in the overlying water-masses. Discoidal concretions, on the other hand, are typical of rather hard sandy or gravelly sea-floors swept clear of fine detrital material by bottom currents, which are often induced by surface winds. Any seasonal pattern in the conditions governing the precipitation of iron and manganese, which could be effective in a calm environment (*e.g.* in the formation of spheroidal concretions), would be disguised or obliterated by bottom currents bringing water-masses of varying physicochemical properties over regions where discoidal concretions are forming.

Despite this difference, both spheroidal and discoidal concretions show equally well the striking correlation between iron and phosphorus. A set of bulk chemical analyses are given in Table 1 to show the concentrations of P, Fe and Mn in concretions from various parts of the Gulf of Bothnia. The assay data have been plotted in Fig. 5 in the order of decreasing phosphorus concentration from left to right. The

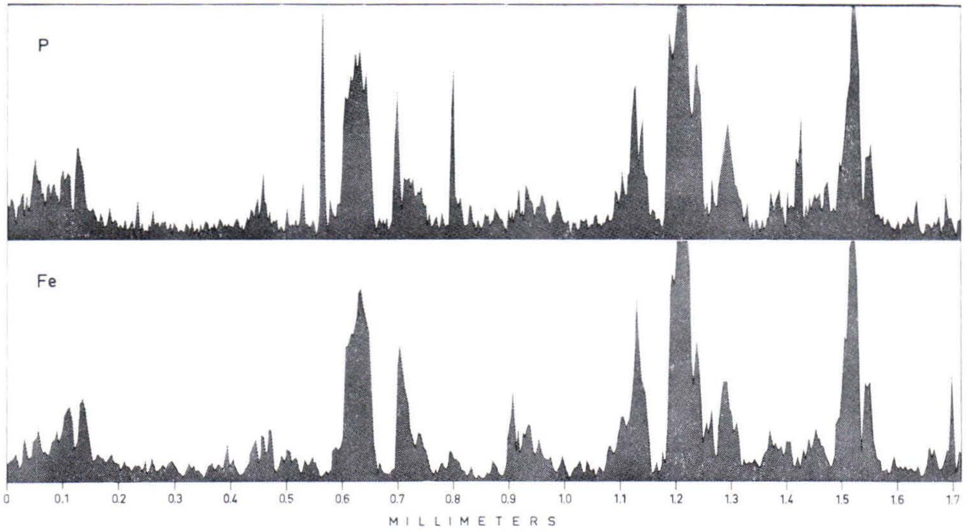

FIG. 6. Specimen traversing profiles (30 microns per minute) showing the relative X-ray intensities of phosphorus and iron. It should be stressed that the concentrations of the elements are not comparable.

phosphorus/iron ratio seems to decrease slightly with an increase in the manganese content of the sample.

According to studies in the lacustrine environment made by Hutchinson (1957), iron and phosphorus tend to from a highly insoluble precipitate. If however, tetravalent manganese is present, he found, that the iron will be preferentially precipitated as a hydroxide instead of phosphate. This would mean that the more manganese is present the less phosphorus can be fixed by iron. Whether the inverse relationship between the phosphorus/iron ratio and the manganese in Fig. 5 is only apparent or actually is a result of the afore mentioned effect cannot, however, be concluded on the basis of the available data.

It is evident from the assay data in Table 1 that the concretions contain considerably more iron than can be bound in ferric phosphate stoichiometrically. The excess iron would be fixed as a hydrous oxide. Microprobe determinations show the fluctuations in the distribution of both iron and phosphorus across a sample to be strikingly identical. This is especially discernible in concentration profiles (*cf.*, Figs. 4 and 6). The few odd deviations in the phosphorus profile in relation to the iron profile can be explained if a comparison is made between the phosphorus and calcium concentrations. Thus the phosphorus highs with no equivalent maxima in the iron profile (*e.g.* Fig. 6 at 0.53, 0.57, 0.80, 1.42 mm, etc.) were found to correspond to definite calcium concentrations indicating the occurrence of eitner detrital apatite or authigenic calcium phosphate.

The exceedingly close relationship between phosphorus and iron would imply a simultaneous precipitation of ferric phosphate and ferric hydroxide and the maintenence of a fairly constant ratio between both elements. This seems to be fairly improbable, and the presence of phosphorus in Baltic concretions seems rather to be due to the scavenging effect of ferric hydroxide on the PO_4^{-3}-anion (*cf.* Borchert, 1965 p. 179).

Acknowledgements — The authors are grateful to Professor Vladi Marmo, Director of the Geological Survey of Finland, for having read the manuscript and recommended its present publication. Mr. Boris Saltikoff, M. Sc., has been very helpful in preparing the samples and in doing electron probe investigations. Miss Meeri Taug and Mr. Tapio Koljonen, M. Sc., have made the chemical determinations. To these and other persons who have aided us in our work we owe our sincere thanks.

Manuscript received, April 11, 1967

REFERENCES

Aarnio, B. (1917) Järvimalmit eräissä Pusulan, Pyhäjärven, Lopen, Somerniemen ja Tammelan järvissä. Geotekn. Tied. No 20.

Borchert, H. (1965) Formation of Marine Sedimentary Iron Ores. *In* Chemical Oceanography II (ed. by J. P. Riley & G. Skirrow), Academic Press, London. pp. 159—204.

Burns, R. G. and D. W. Fuerstenau (1966) Electron-probe Determination of Inter-element Relationships in Manganese Nodules. Am. Mineral. No. 5—6, vol. 51, pp. 895—902.

Buser, W. (1959) The Nature of the Iron and Manganese Compounds in Manganese Nodules. Oceanographic Cong. Pre-prints, pp. 962—964.

Gorshkova, T. I.

Горшкова, Т. И. (1931) Химико-минералогическое исследование осадков Баренцова и Белого морей. Труд. Гос. океанограф. ин—та т. I, вып. 2—3. с. 83—127.

—»—(1957) Осадки Карского Моря. Тр. Всесоюзн. гидробиол. об—ва, т. VIII. с. 68—99.

—»—(1961) Осадки Рижкого залива. Тр. НИИРХ СНХ Латв. ССР, III.

Gripenberg, Stina (1934) A Study of the Sediments of the North Baltic and Adjoining Seas. Merentutk.lait.julk. No. 96 pp. 1—231.

Hartman, M. (1964) Zur Geochemie von Eisen und Mangan in der Ostsee. Meyniana, Bd. 14, pp. 3—20.

Hutchinson, G. E. (1957) A Treatise on Limnology — I. Geography, Physics and Chemistry. John Wiley & Sons, New York.

Krotov, B. P. (1951)

Кротов, Б. Р. (1951) О разделении алюминия, железа н марганца при выпадении из раствора в водных бассеинах. Акад. Наук СССР Докл, т. 78, Но. 3, с. 531—534.

Manheim, F. T. (1961) A Geochemical Profile in the Baltic Sea. Geochim. Cosmochim. Acta, Vol. 25, pp. 52—70.

—»— (1965) Manganese-iron Accumulations in the Shallow Marine Environment. Symp. Marine Geochemistry, Occ. Publ. No. 3—1965; Narragansett Marine Lab., Univ. Rhode Island. pp. 217—276.

Mero, J. L. (1965) The Mineral Resources of the Sea. Elsevier, London, 312 pp.

Strakhov, N. M. (1966) Types of Manganese Accumulation in Present-day Basins: Their Significance in Understanding of Manganese Mineralization. Internat. Geology Rev., vol. 8, No. 10, pp. 1172—1198. Transl. from Litologiya i poleznyye iskopayemyye, 1965, No. 4, pp. 18—49.

Winterhalter, B. (1966) Pohjanlahden ja Suomenlahden rautamangaani-saostumista. (With English summary and figure captions) Geotekn.julk. No. 69, pp. 1—77.

Comptes Rendus de la Société géologique de Finlande
N:o XXXIX (1967), pp. 173—187

SUKULAITE* — $Ta_2Sn_2O_7$ — AND WODGINITE AS INCLUSIONS IN CASSITERITE IN THE GRANITE PEGMATITE IN SUKULA, TAMMELA IN SW FINLAND

BY

ATSO VORMA and JAAKKO SIIVOLA

Geological Survey of Finland, Otaniemi, Finland

ABSTRACT

Sukulaite, a new mineral with the formula $(Ta, Nb)_2Sn_2O_7$, was found as narrow rims surrounding wodginite inclusions in tantalian cassiterite in a specimen from the granite pegmatite in Sukula, Tammela, SW Finland. Under a binocular microscope the color of sukulaite is yellowish brown, translucent; in reflected light, light gray with a reddish or lilac tint. Reflectivity in oil is 3.4 % in Xe light. Polishing hardness is greater than that of cassiterite and wodginite. X-ray powder photograph shows the mineral to be isotypic with microlite. The space group is *Fd3m* with $a_0 = 10.57$ Å.

Chemical analyses of the wodginite suggest a variety with iron prevailing over manganese. Precession photographs show the systematic extinctions to be consistent with the space groups *C2/c* and *Cc*. Cell parameters are given for two wodginite crystals, microprobe analyses for three. The mineral is twinned on (100). The nature of oriented intergrowth with cassiterite is discussed.

INTRODUCTION

In a recent paper by one of the authors (Vorma, 1965) three columbite specimens associated with ainalite, the tantalian cassiterite of A. E. Nordenskiöld (1863) from the Penikoja granite pegmatite in Somero, SW Finland and two columbite specimens from the adjacent Torro pegmatite area were described. The columbite in all the five investigated specimens was in a disordered state. During the same study tapiolite from two specimens from the same pegmatite province was investigated and the disordered state was noted. The present work is a continuation of the study of ainalite specimens from the same pegmatite province (Tammela-Somero pegmatite province). This time the inclusions in the ainalite specimens from the pegmatite at Sukula in

---

*) The name sukulaite is from the locality. The name is approved by the Commission on New Minerals and Mineral Names, IMA, May 1967.

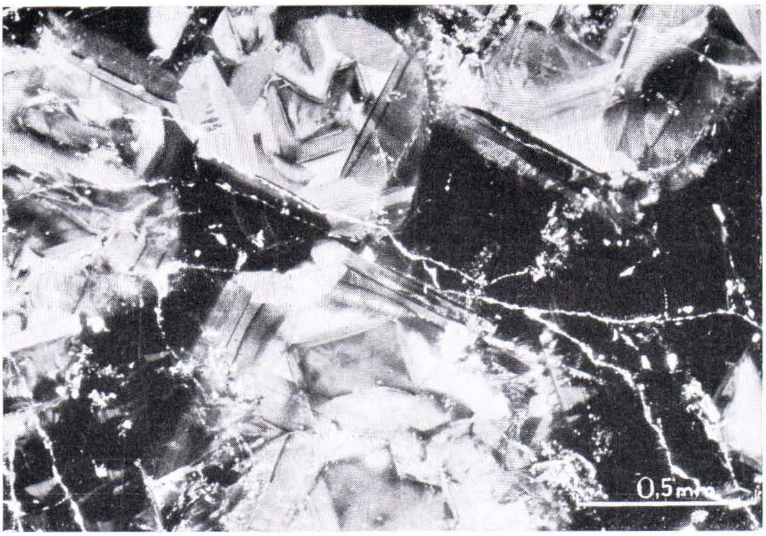

FIG. 1. Zoned cassiterite. Polished section, oblique illumination. Specimen no. 439. Sukula, Tammela, SW Finland.

Tammela will be described. The study shows sukulaite — a new Ta-Sn oxide —, iron rich wodginite, tapiolite and native bismuth occurring as inclusions in cassiterite. This paper is mainly concerned with sukulaite and wodginite.

The pegmatite province of Tammela-Somero was described by Mäkinen in 1913 and recently by Aurola, 1963. The specimens investigated during the present study are from the collection of Dept. of Geology and Mineralogy, University of Helsinki, *viz.* nos. 439, 440, 443, 444, 445 and 446. All of these specimens were collected about one hundred years ago.

OCCURRENCE

Numerous pegmatite exposures with small abandoned quartz quarries are met with in the Sukula village and its surroundings. A small pegmatite quarry near the Kulmala farm house in Sukula is known, due to the type material for tapiolite (Nordenskiöld, 1863, p. 445). From the same quarry the occurrence of triphylite has been reported (*ref.* in Mäkinen, 1913, p. 96). An adjacent small quarry is mentioned by Nordenskiöld (*op.cit.*, p. 449) as a locality from which he described columbite. In one pegmatite dike at Sukula, triplite has been described (*ref.* in Mäkinen, 1913, p. 100). The Sukula pegmatite is characterized by quartz, microcline, albite, muscovite, biotite, tourmaline and beryl.

The specimens investigated during this study are listed in Table 1. No closer locality for these specimens is given than Sukula, Tammela. It is, however, highly

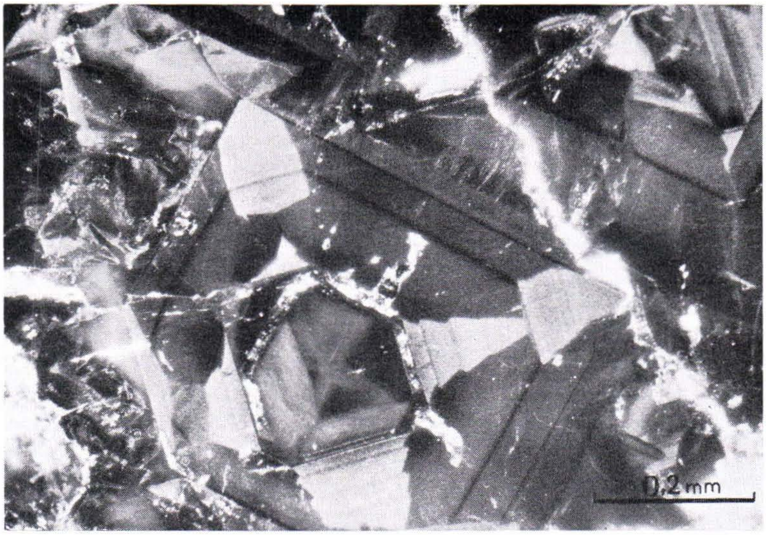

FIG. 2. Zoned cassiterite with overgrowth pyramids well developed. Polished section, oblique illumination. Specimen no. 439. Sukula, Tammela, SW Finland.

probable that the specimens originate from the quarry near the Mäkitulokas farm house in Sukula. This quarry is distinct from both the above mentioned quarries where tapiolite and columbite have been described. The quarry at Mäkitulokas was mentioned by Nordenskiöld in 1863 (*op.cit.*, p. 452) as the locality where ainalite was found in Sukula.

The specimens consist of cassiterite in coarse granular masses, grain size being mostly about 1 mm, occasionally up to a few centimeters. When a polished section is studied under a binocular microscope (oblique illumination), very marked zoned structure is often observed in cassiterite. The cores of cassiterite grains are usually light yellow, transparent (diameter 0.2 mm). The transparent cores are then surrounded by numerous opaque, in obliquely illuminated light steel gray, zones of tantalian cassiterite. In places the growth bands are parallel to the bounding faces, in places the growth is sectoral (Figs. 1 and 2). Microprobe analyses of cassiterite indicate Ta_2O_5 amounts varying from point to point and from specimen to specimen between 0.*x* and 6 wt.- %. The highest Nb_2O_5 content is about 1 wt.- % (in specimen no. 445; 6 % for Ta_2O_5 was recorded at the same point). FeO contents amount in places up to 1 wt.- %, MnO and TiO_2 up to 0.*x* %. In addition to the Ta and Nb concentrations above, in the cassiterite structure (solid solution of tapiolite in cassiterite), numerous inclusions of opaque minerals were found in cassiterite, occurring partly as oriented intergrowths. So far iron rich wodginite, tapiolite, native bismuth and sukulaite have been identified (Table 1).

TABLE 1.
Identification of Sukula specimens

Specimen no.	Label	Phases observed and method of identification
439	Ainlite, Sukula, Tammela, 1861.	Zoned tantalian cassiterite (1, 3, 4) with inclusions of wodginite (1, 4), tapiolite (3, 4) and native bismuth (3, 4).
440	Ainalite, Sukula, Tammela, 1861. A present from A. E. Nordenskiöld.	Zoned tantalian cassiterite (1, 3, 4) with inclusions of wodginite (1, 2, 3, 4), sukulaite (1, 3, 4) and native bismuth (4).
443	Ainalite, Sukula, Tammela.	Tantalian cassiterite (1, 2, 3, 4) with inclusions of wodginite (1, 3, 4) and native bismuth (4).
444	Ainalite, Sukula, Tammela, 1870, F. J. W. (the initials of prof. F. J. Wiik).	Tantalian cassiterite (1, 3, 4) with inclusions of wodginite (1, 2, 3, 4), tapiolite (3, 4) and native bismuth (3, 4).
445	Ainalite, Sukula, Tammela, 1861.	Tantalian cassiterite (1, 3, 4) with inclusions of tapiolite (1, 3, 4) and native bismuth (3, 4).
446	Ainalite, Tammela.	Zoned tantalian cassiterite (1, 3, 4) with inclusions of wodginite (1, 4), tapiolite (3, 4) and native bismuth (4).

(1) = X-ray powder determination
(2) = X-ray single crystal study
(3) = electron probe microanalysis
(4) = detected on polished section

The sizes of the wodginite and tapiolite inclusions in cassiterite are mostly between 0.01 and 0.2 mm. The inclusions are sometimes quite irregular in shape, sometimes, however, lathlike. Due to the difficulty in distinguishing wodginite from tapiolite under reflected light no estimation is given of their relative abundance. Sukulaite has been identified so far in one specimen (no. 440). In this specimen the small wodginite inclusions are often surrounded by narrow ($< 20\ \mu$) rims of sukulaite (Figs. 3 and 4); in places sukulaite replaces wodginite almost completely. It should be mentioned that specimen no. 440 is rather strongly disintegrated pointing to the possible role of supergene processes in the origin of sukulaite.

Native bismuth occurs in each investigated specimen as very small inclusions in cassiterite. The grain size varies from 0.01 to 0.03 mm. Only some few grains were found in each polished section.

Point count analyses were made of the polished sections. The opaque inclusions in cassiterite amounted from 0.6 % to 3.6 % (wodginite + tapiolite + native bismuth + sukulaite). The silicate inclusions were present about 2—4 %, in specimen no. 443 this figure amounted to 19 %.

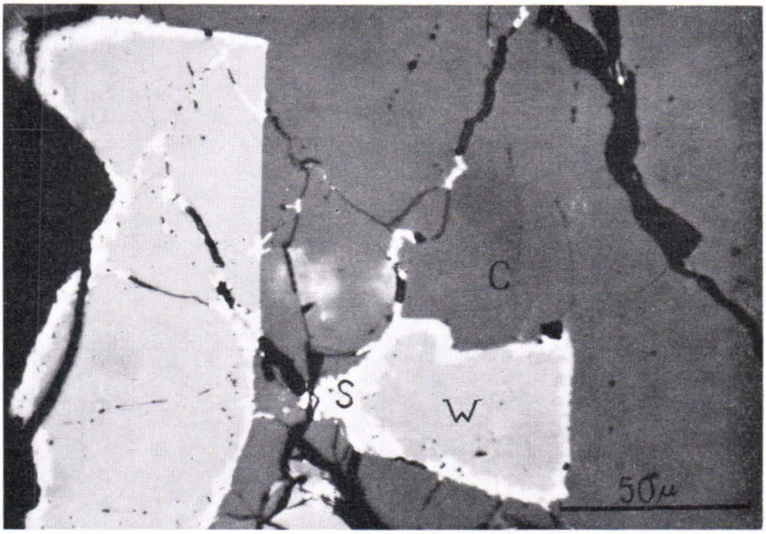

FIG. 3. Sukulaite (s), wodginite (w) and cassiterite (c). Polished section. Specimen no. 440. Sukula, Tammela, SW Finland.

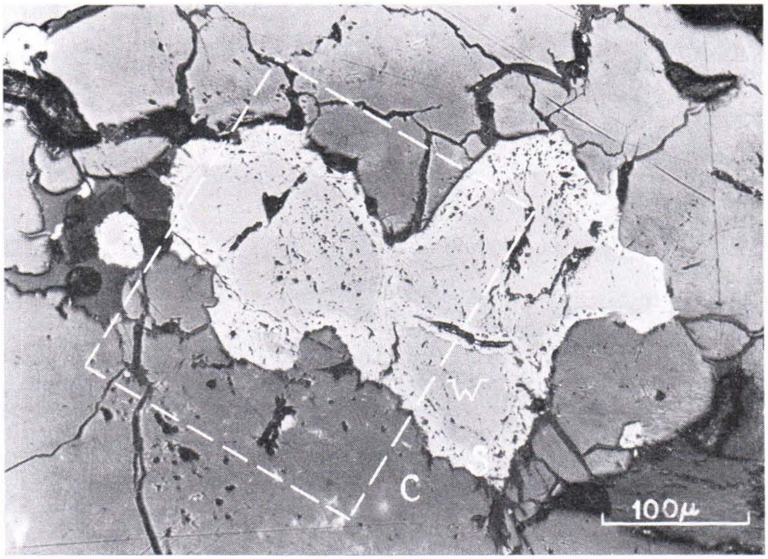

FIG. 4. Sukulaite (s) occurring as a rim between wodginite (w) and cassiterite (c). The area bounded by the broken line refers to the Fig. 5. Polished section. Specimen no. 440. Sukula, Tammela, SW Finland.

TABLE 2.

Chemical composition of sukulaite. Electron microprobe analysis by J. Siivola

	Wt.-%		Atomic prop.	
Ta_2O_5	47	Ta	313	286
Nb_2O_5	8	Nb	60	
TiO_2	1	Ti	13	
MnO	2	Mn	28	336
FeO	1.7	Fe	24	
SnO_2	40	Sn	284	
	(99.7)	O	1 328	

SUKULAITE

Physical properties

Under a binocular microscope the color of sukulaite is yellowish brown, translucent, under reflected light gray with a reddish or lilac tint. The color is lighter than that of cassiterite and wodginite. Between crossed nicols the mineral has strong internal reflections, certainly partly due to the small grain size, in reddish brown, making it impossible to judge whether the mineral is optically isotropic or not.

The reflectivity of sukulaite was measured in xenon light in oil immersion with a photomicrographic exposure meter. *R* turned out to be 13 % higher than that of cassiterite, relatively. If taking $R = 3\ \%$ for cassiterite in oil, then $R = 3.4\ \%$ for sukulaite in oil. This also concerns the pigmentation on the grain boundaries of sukulaite.

The polishing hardness of sukulaite is greater than that of cassiterite and wodginite. Due to the scantity of material, density could not be determined. For synthetic $Ta_2Sn_2O_7$, Gasperin (1955) gives the density as 8.34.

Chemical composition

There was insufficient sukulaite material for wet chemical analysis. The composition could be tested only with an electron probe microanalyser (model Geoscan). All the elements between Na and U were scanned, but only Ta, Nb, Sn, Mn, Fe and Ti were found (see Fig. 5). The result of the analysis is given in Table 2. The analysis nearly corresponds to $(Ta, Nb)_2Sn_2O_9$ with Ta : Nb = 78 : 22.

The role of iron and manganese in sukulaite is questionable. The mineral occurs as aggregates, the grain size being approximately 5 μ. The grains are often thinly coated with an unidentified mineral (Fig. 6). Because the diameter of the electron beam used was of the same magnitude ($< 2\mu$) as the grain size of sukulaite, and the effective penetration of the beam is of the same order, it is quite possible that the analysis given also includes the coating on the sukulaite grains.

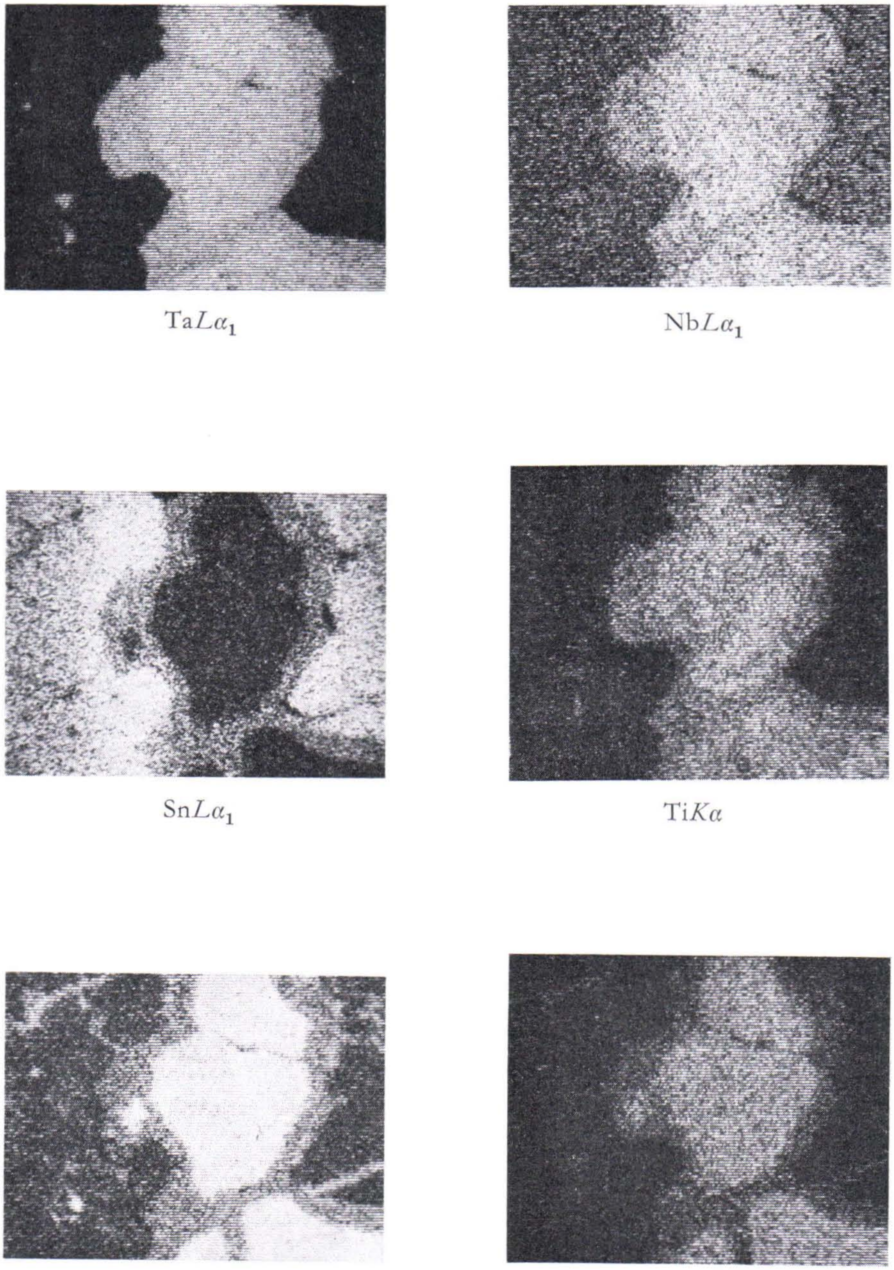

$\mathrm{Ta}L\alpha_1$ $\mathrm{Nb}L\alpha_1$

$\mathrm{Sn}L\alpha_1$ $\mathrm{Ti}K\alpha$

$\mathrm{Fe}K\alpha_1$ $\mathrm{Mn}K\alpha_1$

FIG. 5. Electron probe scanning pictures showing the distribution of Ta, Nb, Sn, Ti, Fe and Mn in sukulaite, wodginite, and cassiterite. *Cf.* Fig. 4. Specimen no. 440. Sukula, Tammela, SW Finland.

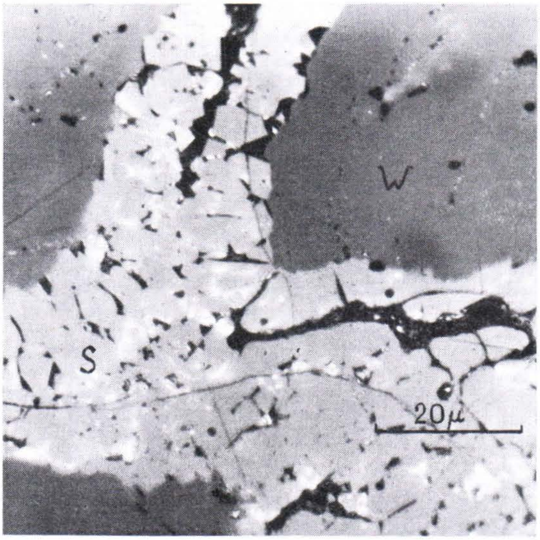

FIG. 6. Idiomorphic sukulaite (s) and wodginite (w). Polished section. Oil immersion. Specimen no. 440. Sukula, Tammela, SW. Finland.

X-ray crystallography

Debye-Scherrer photographs from an aggregate of sukulaite showed the mineral to be cubic with $a_0 = 10.57$ Å. The powder data are given in Table 3. These also contain some diffraction lines of the adjacent cassiterite which could not be completely separated from sukulaite. Due to the aggregate nature of the preparate (grain size in it $\sim 5\ \mu$) the intensities of reflections may be affected by preferred orientation if present.

The powder data show sukulaite to be isotypic with microlite and thus to have the space group *Fd3m*. No work could be done on single crystals due to their very small grain size.

Gasperin, 1955, synthesized the compound $Ta_2Sn_2O_7$ by heating equal weights of powdered SnO_2 and Ta_2O_5 with a globule of tin. According to Gasperin the compound is isotypic with the minerals of the microlite-pyrochlore group. The material synthesized by Gasperin is yellow, transparent. Measured density is 8.34 and calculated density 8.21 (Structure Reports for 1955, vol. 19, p. 392). Cubic system, $a_0 = 10.48$ Å. The work of Gasperin indicates the tin to be in the Sn^{2+} state. As shown, sukulaite is isotypic with microlite as is also the compound synthesized by Gasperin. Thus we can conclude that sukulaite is rather $Ta_2Sn_2O_7$ than $Ta_2Sn_2O_9$ (*cf.* p. 178), in consistency with the structure formula of the atopite structure type.

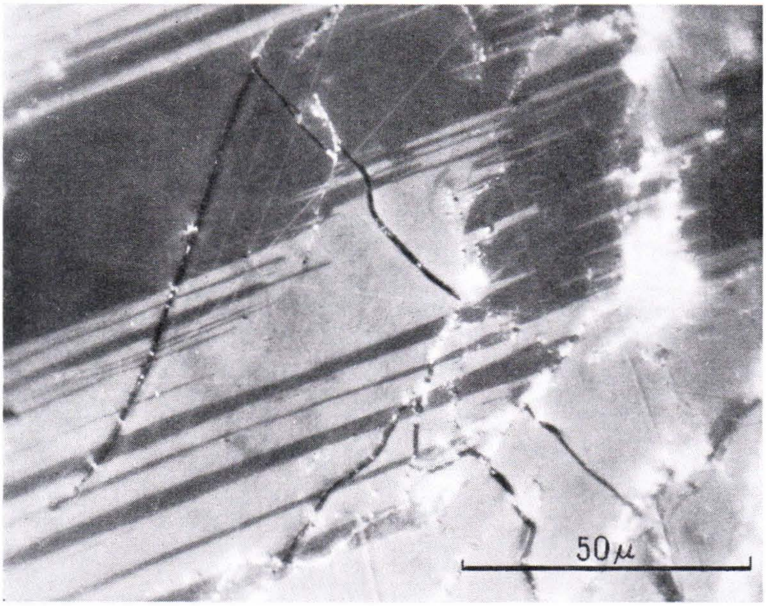

FIG. 7. Lamellar twinning in wodginite. Polished section. Nicols + —8°. Specimen no. 440. Sukula, Tammela, SW Finland.

Gasperin *(op.cit.)* claims Ta to be in the position 16(c) and Sn in 16*(d)* in the synthetic $Ta_2Sn_2O_7$ while in microlite the position 16*(d)* is occupied by Ta. The structure determination by Gasperin is based on the 28 strongest reflections of the powder data. It must be emphasized that in a structure of microlite type all the reflections with h, k and $l =$ even have the same contribution from Sn and Ta regardless of their distribution between the positions 16*(c)* and 16*(d)*. All the reflections with h, k and $l =$ odd, however, have contributions from atoms in these positions with opposite signs; thus these reflections are weak compared with most of those with h, k and $l =$ even. To judge whether sukulaite does belong to the microlite-pyrochlore group or not (Ta in the position 16*(d)* or in 16*(c)*) one ought to record accurate intensity data from the reflections with h, k and $l =$ odd. Due to the very small size of the preparate and its aggregate nature with possibly some preferred orientation, it has been impossible for us to get such data *.

WODGINITE

In five out of the six investigated ainalite specimens a mineral, at first regarded as columbite, was found as inclusions. The identification was carried out by means

---

*) The X-ray scattering curve for ($Ta_{0\cdot78}Nb_{0\cdot22}$) is practically the same as that of dysprosium (at least up to $sin\Theta/\lambda = 0.8$ Å^{-1}). The intensities of the reflections in the powder data of $Dy_2Sn_2O_7$ (ASTM 13—187) are very similar to those of sukulaite.

TABLE 3.

X-ray powder data for sukulaite from Sukula granite pegmatite in Tammela, SW Finland. Camera dia. 57.3 mm, Cu$K\alpha$

hkl	I_o	d_o(Å)	d_c(Å)
111	vw	~6.04*	6.10
(cassit.)	w	3.351	
311	w	3.175	3.187
222	vs	3.046	3.051
400, (+ cassit.)	ms	2.640	2.642
511, 333	vvw	2.034	2.034
?	vvw	1.953	
440	s	1.866	1.869
(cassit.)	vw	1.767	
620, (+ cassit.)	vw	1.670	1.671
622	s	1.589	1.593
444	m	1.524	1.526
711, 551	w	1.479	1.480
(cassit.)	vw	1.440	
642, (+ cassit.)	vw	1.415	1.412
731, 553	vw	1.374	1.376
?	vvw	1.340	
800	mw	1.3189	1.3213
662	m	1.2105	1.2125
840	m	1.1796	1.1818
911, 753	vw	1.1587	1.1602
844	mw	1.0780	1.0788
933, 771, 755	vw	1.0635	1.0623
10.2.2; 666	m	1.0171	1.0171
880	vw	.9346	.9343
11.3.1; 971; 955	w	.9228	.9235
10.6.2	m	.8938	.8933
12.0.0; 884	mw	.8811	.8808
11.5.1; 777	vw	.8716	.8718
11.5.3; 975	w	.8485	.8490
12.4.0	mw	.8360	.8356
13.1.1; 11.7.1; 11.5.5; 993	w	.8085	.8083
10.6.6	mw	.8065	.8060
12.4.4	w	.7973	.7967
13.3.1; 11.7.3; 997	w	.7905	.7900

*) Due to the very small preparate and long exposure time the background at small Θ angles is very strong and hence the data are not very accurate at small Θ angles.

of Debye-Scherrer photographs (camera dia. 57.3 mm). Subsequent electron microprobe analyses (Table 4) and X-ray single crystal study showed that the mineral, thought to be columbite, was iron rich wodginite. No phase corresponding in composition to columbite was detected. Tapiolite was encountered as inclusions in cassiterite in four specimens. Presumable wodginite and tapiolite were present as inclusions in every specimen concerned (see Table 1).

In polished section under reflected light wodginite is grayish white and weakly pleochroic. Anisotropism is distinct. Twinning is often observed; occasionally the twinning is lamellar (Fig. 7).

TABLE 4.

Chemical data and the unit cells of wodginites

	1	2	3	4	5	6
Ta_2O_5 . . .	70.49	70.05	74.1	65	60	61
Nb_2O_5 . .	7.63	1.35	14.5	9	16	13
SnO_2	8.92	13.20	—	10	10	10
MnO	10.87	9.04	5.5	5	2	2
FeO	1.34	1.87	5.9	8	6	7
TiO_2	—	2.39	—	2	3	4
CaO	0.42	—	—	—	—	—
MgO	0.37	—	—	—	—	—
SiO_2	—	0.60	—	—	—	—
Loss of ignition	0.18	—	—	—	—	—
	100.22	98.50	100.0	99	97	97
			Unit cell contents			
Ta	8.29	8.40	8.45	7.4	6.7	6.8
Nb	1.49	0.27	2.74	1.7	3.0	2.4
Sn	1.54	2.32	—	1.7	1.6	1.6
Mn	3.98	3.38	1.95	1.8	0.7	0.7
Fe	0.48	0.69	2.07	2.8	2.1	2.4
Ti	—	0.79	—	0.6	0.9	1.2
O	32.00	32.00	32.00	32.0	32.0	32.0
			Cell parameters			
a_o	9.52Å	9.47Å	9.46Å	9.48Å	—	9.48Å
b_o	11.47	11.42	11.50	11.44	—	11.45
c_o	5.10	5.09	5.14	5.11	—	5.11
β	91° 18′	91° 02′	90° 53′	90° 37′	—	90° 42′

1. Wodgina, Australia (Nickel *et al.*, 1963).
2. Bernic Lake, Manitoba (Nickel *et al.*, 1963).
3. Ruanda (Bourguignon and Mélon, 1965). Corrected for impurities.
4. Sukula, Tammela, SW Finland. Specimen no. 440. Electron microprobe analysis by J. Siivola.
5. » » » » » » 443. » » » » » »
6. » » » » » » 444. » » » » » »

Chemical composition

The analyses in Table 4 reveal that the wodginite from Sukula is characterized by high Ta_2O_5, Nb_2O_5 and SnO_2 contents (see also Fig. 5). The Fe/Mn ratio exceeds one. The other published wodginite analyses are given in the same Table 4. The unit cell contents are calculated assuming 32 oxygen atoms per cell (Nickel *et al*, 1963). It is seen that the Tammela wodginite is the iron richest so far recorded. The mineral originally named wodginite is a manganese tin tantalate. In the case of the Tammela mineral we are dealing with an iron tin tantalate. As the crystal chemistry of wodginite is only slightly known we think it unwise to give any special name to the iron rich wodginite. Mention should be made that also the Ruanda wodginite (Table 4, column 3) is richer in iron than in manganese.

The tapiolite inclusions in the ainalite specimens concerned are richer in tantalum than the wodginite. The composition in each of the six quantitatively analyzed crystals is practically the same, viz. Ta_2O_5 74 %, Nb_2O_5 8 %, FeO 10 %, MnO 1 %, TiO_2 3 % and SnO_2 2 %. These electron microprobe analyses indicate that the Ta/Nb ratio is much higher than that in wodginite. The same also applies to the Fe/Mn ratio. The low figure for SnO_2 in tapiolite compared with that in wodginite is also noteworthy.

X-ray crystallography

Two crystals of Tammela wodginite were investigated by single crystal methods. The Buerger precession photographs showed the mineral to have systematic extinctions consistent with the space groups $C2/c$ and Cc. The cell parameters of the investigated specimens are given in Table 4, columns 4 and 6. The space groups are the same and the cell parameters very similar to those given for wodginite by Nickel *et al.* (1963). The β angle, however, is smaller than that of any previously published wodginite. Bourguignon and Mélon (1965, p. 299) recognize that some of the Ruanda wodginite specimens do not exhibit the doubling of some characteristic reflections in their powder data, even though these have all the other characteristics of wodginite. The authors mentioned attribute this to the variation of the β angle. Comparing the Fe/Mn ratio in the wodginites in Table 4 with the β angle it is presumable that the increasing Fe content decreases β. The synthetic compound *G* of Moreau and Tramasure (1965, p. 354) corresponding to iron free Mn rich wodginite with cell parameters $a_o = 9.45$ Å, $b_o = 11.40$, $c_o = 5.09$ and $\beta = 91°14'$ also supports this. If this assumption is correct the identification of iron rich wodginites using X-ray powder methods must be carried out with care. Mention should also be made that the Tammela wodginites do not show the 110 reflection (at 7.2 Å) in their single crystal photographs even though this reflection is allowed in the space groups $C2/c$ and Cc. All the other low angle reflections characteristic of wodginite (see Nickel *et al.*, 1963), however, are present in the single crystal data of Tammela wodginites.

Both single crystals of the Tammela wodginites investigated by the Buerger precession method were twinned on (100). The β angle deviates in both cases so much from 90° (90°42' and 90°37') that there was no difficulty in detecting the twinning law.

The orientation law of wodginite inclusions in respect to their host, cassiterite, was revealed by precession photographs. These show in addition to the wodginite phase weak extra diffractions which could easily be attributed to cassiterite. The oriented intergrowth was observed to obey the rule *:

---

*) The same orientation law was also verified by X-ray single crystal photographs for a disordered columbite intergrown with cassiterite (specimen from the Penikoja pegmatite quarry, Somero, SW Finland).

$x_c \| x_w$, *i.e.*,	the 4.73 Å axis of cassiterite is parallel to the 2 × 4.73 Å axis of wodginite and hence the *yz*-plane of cassiterite is almost parallel to the *yz*-plane of wodginite, on which plane
$z_w \perp (011)_c$, *i.e.*, $z_w \| [10\bar{1}]_c$	and hence $y_c \wedge y_w \approx 34°$, where the subscripts *c* and *w* refer to cassiterite and wodginite, respectively.

Ramdohr showed 1961 (p. 478) that in exsolved columbite in cassiterite the columbite *a* axis (3 × 4.75 Å axis) is parallel to the cassiterite *a* axis (4.73 Å axis). Thus it seems that the exsolved wodginite phase and columbite phase in cassiterite are oriented according to the same rule (*cf.* Haapala *et al.*, 1967).

DISCUSSION

Comparing the chemical analyses of the Sukula wodginites (Table 4) with those of the coexisting tapiolite (p.184) it is seen that the Ta/Nb ratio is considerably lower in wodginite than in tapiolite. The fractionating of Ta and Nb is more advanced in tapiolite than in wodginite. This is evidently partly due to the fact that the exsolution of wodginite in cassiterite takes place earlier than that of tapiolite. Cassiterite is isotypic with tapiolite and heterotypic with columbite-tantalite. This explains why more tapiolite than columbite-tantalite is dissolved in cassiterite (Schröcke, 1966, p. 9) and why the columbite-tantalite phace exsolves before the tapiolite phase (Ramdohr, 1961, p. 478). This same explanation can certainly be extended to the assemblage wodginite-tapiolite in cassiterite.

The stability range and crystal chemistry of wodginite is not fully known. The experimental works of Turnock (1965, 1966) and Schröcke (1966) indicate that the occurrence of wodginite, either without other tantalates or with tantalite, indicates relatively high oxygen pressure of the genetic conditions while tantalite is stable over a relatively large range of oxygen pressure. The occurrence of tapiolite is indicated by relatively low oxygen pressure. According to Turnock the partial pressure of oxygen will control which of the above mentioned minerals will form.

Turnock prepared synthetic wodginite in the system $MnTa_2O_6$-$FeTa_2O_6$-O as well as in the system $FeTa_2O_6$-$MnTa_2O_6$-$FeTaO_4$ in the join $MnTa_2O_6$-$FeTaO_4$. The wodginite phase produced was $Mn^{2+}_{2-2w}Fe^{3+}_{3w}Ta_{4-w}O_{12}$ with $0.08 < w < 0.29$ (Turnock, 1966). According to Turnock wodginite may contain ferric but not ferrous iron. Tin is not an essential element. Wodginite is a solid solution between AB_2O_6 and ABO_4 types.

Moreau and Tramasure 1965 (p. 354) prepared the *G* phase, analogous in cell dimensions to the wodginite phase, by heating Mn_2O_3 and Ta_2O_5 (1 : 1) in air at 1 050° for 95 hrs. The authors mentioned also produced the wodginite phase in the binary system $FeTa_2O_6$-$MnTa_2O_6$ (*op.cit.* pp. 376—378). For a composition

$(Fe_{0.1}Mn_{0.9})Ta_2O_6$ the wodginite phase was produced at 1 050°C in nitrogen in 50 hrs simultaneously with tantalite, while for the compositions $(Fe_{0.2}Mn_{0.9})Ta_2O_6$ and $(Fe_{0.3}Mn_{0.7})Ta_2O_6$ the wodginite phase was produced simultaneously with tapiolite.

Schröcke (1966, pp. 33—34, 46) has described a monoclinic phase analogous to wodginite in the quaternary system $FeNbO_4$-(Fe, Mn) $(Nb, Ta)_2O_6$. According to him: »Im Bereich von 900—1 100°C gibt es 3 quaternäre, homogene Mischkristallräume: einen alseitig um $FeNbO_4$ mit α-PbO_2- bzw. Wolframitstruktur, einen um $FeTa_2O_6$ mit Rutil- bzw. Trirutilstruktur und einen randlich um das Columbitsystem, ausgehend von dessen Zweistoffsystemen $FeNb_2O_6$-$MnNb_2O_6$-$MnTa_2O_6$ mit α-PbO_2- bzw. Columbitstruktur. Dieser wird sich bei 1 100° kaum mehr als 10—15 Mol.-% in den quaternären Raum erstrecken und sich mit sinkender Temperatur wesentlich verkleinern. Auch der $FeNbO_4$-Raum verkleinert sich bis auf 900° beträchtlich ausser der Ecke gegen $MnTa_2O_6$. An diesen Bereich des $FeNbO_4$-Raumes ist die monocline Aufspaltung analog dem Wodginit gebunden». On pp. 46—47 Schröcke discusses the role of Fe^{3+} in the columbite-, α-PbO_2- and wolframite structures with Fe : (Ta, Nb) > 1 : 2 as a cause of monoclinic distortion. Schröcke's statement, after discussing the chemical analyses of Bernic Lake and Wodgina wodginites, »Wenn an der Richtigkeit der Analysen nicht gezweifelt wird, muss es offenbar mehrere Gebiete der komplexen Mischkristalle vom ABO_4 und AB_2O_6 geben mit monoklin deformierter α-PbO_2-, Wolframit- oder Columbitstruktur. Das Wodginitproblem bedart offenbar noch weiterer Mineralanalysen und experimentaller Arbeit», receives additional support from a comparison of the compositions of Ruanda and Tammela wodginites with those of synthetic wodginites. So far synthetic wodginite, corresponding in composition (Fe/Mn ratio) either to Ruanda or Tammela wodginites, has not been produced. Certainly the extensive replacement of manganese by tin should have some influence on the stability field of wodginite.

In one of the investigated specimens from Sukula the new mineral sukulaite — $Ta_2Sn_2O_7$—replaces wodginite. The given formula is derived on crystallochemical bases. In tapiolite Ta occurs as pentavalent, in cassiterite Sn as tetravalent. In sukulaite at least one of these cations has to occur in a lower oxidation state. The sequence wodginite-tapiolite-sukulaite possibly reflects the gradual decrease of the partial pressure of oxygen.

Acknowledgments — The authors are indebted to Prof. Ahti Simonen and Dr. Kai Hytönen for the critical reading of the manuscript. Our thanks are also due to Mr. Erkki Halme for taking the photographs and for the reflectivity measurement of sukulaite.

Manuscript received, May 20, 1967

REFERENCES

Aurola, Erkki (1963) On the pegmatites in the Torro area, Southwestern Finland. Bull. Comm. Géol. Finlande, 206, 1—32.

Bourguignon, P. and Mélon, J. (1965) Wodginite du Rwanda. Ann. Soc. Géol. de Belg., t. 88, 291—300.

Gasperin, Madeleine (1955) Synthèse et identification de deux oxydes doubles de tantale et d'étain. Comptes Rendus Acad. Sci. Paris, Tome 240, no. 24, 2340—2342.

Haapala, Ilmari, Siivola, Jaakko and Löfgren, Arvo (1967) On the Haapaluoma Sc-bearing columbite and its inclusions. Bull. Comm. Géol. Finlande 229, 95—100.

Mäkinen, Eero (1913) Die Granitpegmatite von Tammela in Finland und ihre Minerale. Bull. Comm. Géol. Finlande, 35, 1—101.

Moreau, J. and Tramasure, G. (1965) Contribution a l'étude des séries columbite-tantalite et tapiolite-mossite. Ann. Soc. Géol. de Belg, 8. t. 88, 301—390.

Nickel, E. H., Rowland, J. F. and McAdam, R. C. (1963) Wodginite—a new tin-manganese tantalate from Wodgina, Australia and Bernic Lake, Manitoba. Can. Mineral., 7, 3, 390—402.

Nordenskiöld, A. E. (1863) Om tantalitartade mineralier från nejden af Torro. Öfv. af kongl. vet. akad. förh. 20, 443—453 (republished in 1864 in German: Ueber tantalitartige Mineralien aus Gegend von Torro. Pogg. Ann., 122, 604—615).

Ramdohr, Paul (1961) Magnetische Cassiterite. Bull. Comm. Géol. Finlande, 196, 473—481.

Schröcke, Helmut (1966) Über Festkörpergleichgewichte innerhalb der Columbit-Tapiolitgruppe, sowie der Columbit-Tapiolitgruppe mit $YTi(Nb, Ta)O_6$, Euxenit, und mit $FeNbO_4$. N. Jb. Miner. Abh., B. 106, H. 1, 1—54.

Turnock, A. C. (1965) Synthetic wodginite, tapiolite and tantalite. Can. Mineral., 8, 3, 402.

—»— (1966) Synthetic wodginite, tapiolite and tantalite. Can. Mineral., 8, 4, 461—470.

Vorma, Atso (1965) Notes on columbite and tapiolite from the pegmatite area of Tammela and Somero in SW Finland. Bull. Comm. Géol. Finlande, 218, 169—176.

Comptes Rendus de la Société géologique de Finlande
N:o XXXIX (1967), pp. 189—197

WORM-SHAPED CASTS IN PRECAMBRIAN QUARTZITE FROM KUUSAMO, NORTHEASTERN FINLAND

BY

RAIMO LAUERMA

Geological Survey of Finland, Otaniemi

and

RISTO PIISPANEN

Department of Geology, University of Oulu

ABSTRACT

Sinuous, worm-shaped bodies occurring on the ripple-marked surfaces of Precambrian quartzite are described, and their possible origin is discussed. One new age determination is reported, giving an U-Pb age of 1,800 million years for uraninite from a veinlet in the Karelian schist belt of Kuusamo.

INTRODUCTION

The authors took part in geological field work in the commune of Kuusamo, northeastern Finland, during the month of July, 1966. One of them (R.P.) found two slabs of quartzite the ripple-marked surfaces of which contained odd worm-shaped bodies. The find was made in connection with the geological remapping of the Kuusamo schist belt begun by the Geological Survey of Finland in the summer of 1965. The two slabs were discovered lying by the side of a tractor trail made for timber haulage on a steep hillside. The slabs had evidently been thrust to the surface when the trail was made, and the finder's attention was first drawn to them on account of their conspicuous ripple-marked surfaces.

At the site and in the vicinity of the find, the overburden is thin, apparently less than a meter thick. A few dozen meters northeast of the place where the find was made, there is a steep wall of rock in the rugged exposures of which the same kind of quartzite is to be seen as the two slabs. And also the boulders lying around in the immediate surroundings of the spot where they were found consist of the identical rock. The quartzite has obviously been broken up by the frost action typical of conditions in northern Finland. The boulders have sharp edges (see Figs. 2 and 3) and no signs are to be detected of the rounding produced by glacial transportation. Considering these facts, it seems rather obvious that the boulders are quite local in origin.

A careful search failed to bring to light any additional slabs containing worm-shaped bodies. The search was considerably hampered by the circumstance that the local boulders have a fairly strong cleavage subparallel or parallel to the bedding, in consequence of which the rock does not split off under hammer blows along the ripple-marked surfaces, where similar worm-like bodies might be seen.

LOCATION

The site of the find is in northeastern Finland some fifteen kilometers northwest from the church at Kuusamo (see Fig. 1). More exactly stated according to the available map (Topographical Map of Finland, 1 : 20 000, Sheet 4522 11, 1966), it is situated about 800 meters to the southwest from the northwestern end of Hietalampi (lake) at an altitude of 320 meters. According to the general geodetic coordination of Finland, its coordinates are: y = 450 350, x = 7 328 950.

GEOLOGICAL SETTING AND AGE OF THE QUARTZITE

The Precambrian geology of the Kuusamo schist belt, with its surroundings, is outlined in Fig. 1 according to the geological maps by V. Hackman (1910) and V. Hackman and W. W. Wilkman (1925). In the light of these maps and other geological investigations (e.g., Simonen 1960, pp. 6—10), the Karelian supracrustal rocks rest unconformably on the pre-Karelidic basement. Age data reported e.g. by Kouvo and Tilton (1966, p. 421) indicate that the rocks in the basement complex crystallized between 2,600 and 2,800 million years ago, and that the sedimentary column overlying the basement rocks was intruded by syntectonic plutonic rocks 1,800—1,900 million years ago.

Recently, Dr. O. Kouvo made an age determination of a small sample containing uraninite, which was forwarded to him by Mr. Y. Vuorelainen from the Outokumpu Company. The sample (No. A 185 of the Outokumpu Co.) was taken from a veinlet associated with albite diabase, which forms a sill in the schist formation. The source of the sample is about 200 m north of the Jyrävä waterfall in the central part of the Kuusamo schist belt (Y. Vuorelainen, personal communication). This uraninite yielded following radiometric ages: Pb^{207}-Pb^{206} 1,800 m.y., Pb^{207}-U^{235} 1,790 m.y. and Pb^{206}-U^{238} 1,780 m.y. The result is nearly concordant and the parent-daughter ratios fit a 1,800 m.y. diffusion curve when plotted on a concordia diagram (O. Kouvo, personal communication) On geological grounds it is obvious that this uraninite is younger than the sediments in the Kuusamo schist belt, and this age

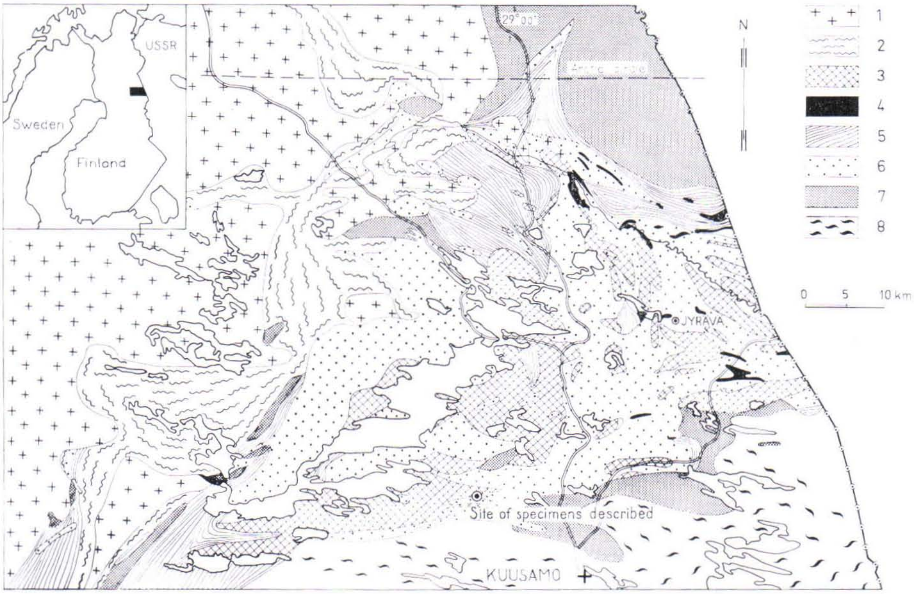

FIG. 1. Source of the specimens described, and the main geological features of the Kuusamo schist belt according to Hackman (1910) and Hackman and Wilkman (1925). 1. Late Karelian granite. 2. Migmatitic mica gneiss. 3. Metabasite (metadiabase) 4. Dolomite. 5. Mica schist and hornblende schist. 6. Quartzite. 7. Metabasite and tuffite. 8. Pre-Karelidic basement gneiss.

determination thus gives a reliable minimum age also for the quartzite in which the worm-shaped bodies are embedded. This quartzite is thus with a high degree of certitude older than 1,800 million years and, on the other hand, considerably younger than 2,600—2,800 million years. Accurately determining the age of sedimentation of the quartzite on the basis of the data at present available is difficult and the result is bound to be uncertain, but it probably is roughly 2,000 million years. The place where the quartzite slabs were discovered is situated, according to the map drawn by Hackman and Wilkman, approximately three kilometers from the contact of the pre-Karelidic basement and the Karelian schists, as measured over the ground. The geological remapping operations are still in progress in the area, and they may bring more light on the relations between the quartzite under our scrutiny and the other local rocks.

DESCRIPTION OF THE QUARTZITE SLABS AND THE WORM-SHAPED BODIES

The larger of the two slabs is 30 cm long, 25 cm wide and 3 cm thick. The smaller slab is 21 cm long, 18 cm wide and 5 cm thick. Both slabs are platy parallel to the

FIG. 2. Overlapping of the quartzite slabs, shown in normal position. Counterpart at left. The vertical surface of the larger slab at right has been sawed.

bedding and interference ripple marks can be seen on both of them. Both are parts of the same original boulder because the ripple-marked surfaces fit together exactly in the way shown in Fig. 2. The smaller slab is the counterpart. The wave length of the main set of ripple marks ranges from 5 cm to 7 cm, and the crests are 5 to 8 mm higher than the troughs. The ripple index is about 10. The other set of ripple marks are approximately at right angles to the main set and their wave length and amplitude are slightly smaller than those of the main set. The ripple-marked surfaces of both slabs are shown in Fig. 3.

On the freshly broken surfaces the quartzite is pale gray in color, whereas on the weathered surfaces the color is brownish gray. The ripple-marked surface of the smaller slab (counterpart) has a brownish color which is evidently due to a very thin mica film. The ripple-marked surfaces of both slabs contain also splotches of mica here and there. The X-ray data of this mica are consistent with those of muscovite. In places the ripple-marked surfaces have a sheared appearance, but the shearing has been quite weak and with respect to the genesis of the worm-shaped bodies altogether a secondary phenomen. The maximum thickness of the mica splotches is approximately 0.5 mm and the average thickness of the mica-bearing layer only a fraction of this figure.

According to the microscopic evidence, the rock contains approximately 70 per cent of quartz, 20 per cent sericite, and 10 per cent potassium feldspar, plagioclase and accessory minerals. The grain size of the rock is 0.05—0.1 mm. The texture is shown in Fig. 7.

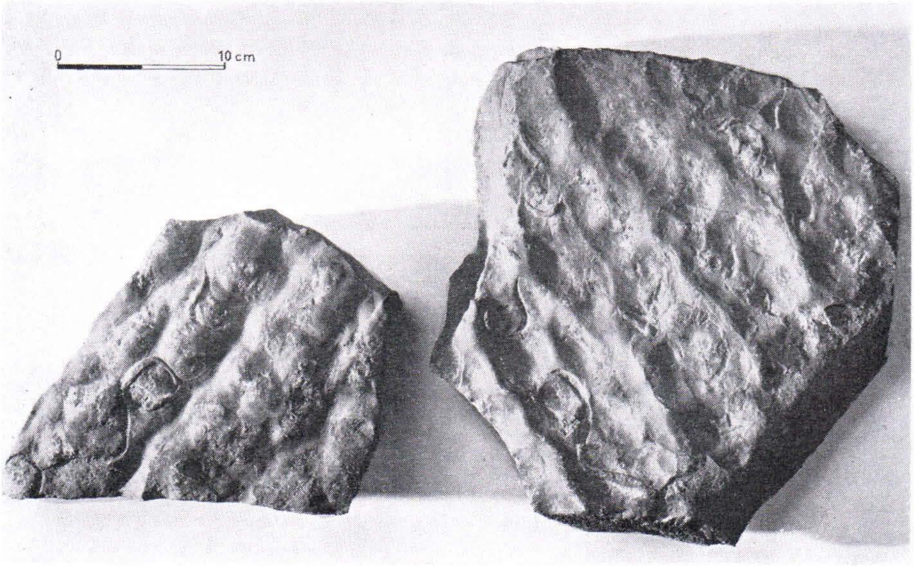

FIG. 3. Ripple-marked bedding surfaces of the quartzite slabs with worm-shaped bodies. Counterpart at left.

The ripple-marked surface of the larger slab contains several worm-shaped bodies (see Figs. 3—5). Two of them are to be seen also on the surface of the counterpart. The two slabs have separated exactly along the rippled-marked surface so that two worm-shaped bodies are shared by each slab, a portion of each of these bodies being on the ripple-marked surface of the larger slab and a portion on the surface of the obverse slab.

The longest of the worm-shaped bodies is 17 cm long and the shortest one 2.5 cm long. In thickness they vary between two and seven millimeters. The longest of the bodies is 2 mm thick in the middle, and on both sides of this portion it expands to 7 mm and 5 mm in thickness. The thickest portions are situated in throughs of the interference ripple marks and narrowest at the crests. All the bodies have tapering ends. The shape of the bodies can be seen in Figs. 3—5. In cross section it approximates an ellipse, the longer axis of which is parallel to the bedding surface. (Fig. 6).

The worm-shaped bodies follow precisely the ripple-marked bedding surface. No sign of penetration can be observed either upwards or downwards. On the walls of the mold of one body there can be detected under suitable illumination minor corrugations, which are about one millimeter apart (Fig. 5).

One transverse thin section was made of one of the bodies. Under the microscope it was observed to consist of material almost identical with the quartzite, that is to say, of lithified sand (Fig. 6). Megascopically, the worm-shaped bodies are on freshly broken surfaces slightly lighter in color than the matrix.

FIG. 4. Detailed photograph of one worm-shaped body occurring partly as a cast and partly as a mold.

FIG. 5. Detailed photograph of a worm-shaped body occurring as a cast at left and as a mold at right. Faint corrugations to be seen within the walls of the mold are shown with arrow.

FIG. 6. Photomicrograph of cross-section of worm-shaped body.

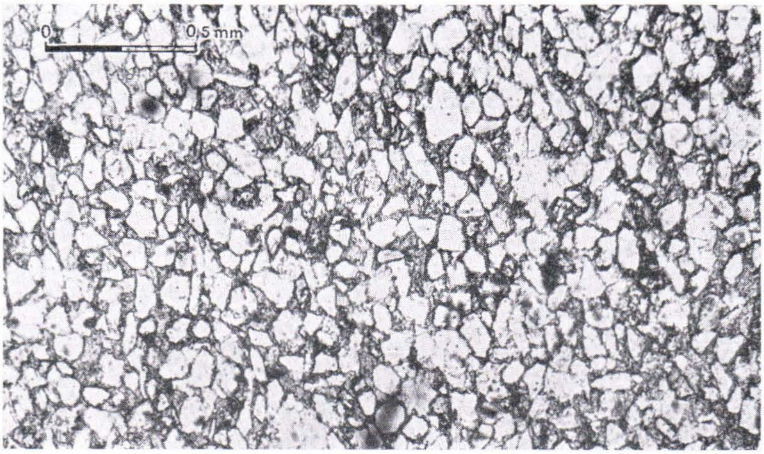

FIG. 7. Photomicrograph of texture of the quartzite.

DISCUSSION

Similar sinuous, worm-shaped or ropelike structures occurring on the ripple-marked bedding planes of arenaceous rocks have been described from different parts of the world during the past three decades, and the question of their origin has provoked considerable controversial discussion. Endo (1933) reported the observation of »branching tubular bodies with numerous microscopic filaments still preseved within their wall» in a quartzite from South Manchuria. He considered them to be algal remains and proposed the name of a new genus, Manchuriophycus, for them. The organic origin of Manchuriophycus was later disputed by Häntzschel (1949), who regarded the tubular bodies as infilled mud-cracks. From Montana, U.S.A., Fenton and Fenton (1937) described filled, non-annulate burrows from a Precambrian quartzite in the Belt series. This discovery seems to be accepted by Glaessner (1966) as trace fossil.

Faul (1950) described sinuous markings on the bedding surfaces of Precambrian Ajibik quartzite occurring in Michigan U.S.A. He interpreted the markings as burrows made by some small unknown organism. Subsequently, Frarey and McLaren (1963) reported similar features from Huronian quartzites and interpreted them to be metazoan relics. Wheeler and Quinlan (1951) and Barnes and Smith (1964) have interpreted similar structures as mud-crack infilling on ripple-marked surfaces.

Recently, Hofmann (1967) has described complex structures in Upper Huronian quartzite in Ontario, Canada, and interpreted them as probable metazoan fossils. They are preserved as sand casts in the form of curved spindles having inclined lateral corrugations, axial marking, and apparent bilateral symmetry. According to this source it seems likely that similar structures described from many geologic systems are polygenetic, and that one single explanation cannot apply to all the similar-looking forms.

The specimens with the worm-shaped bodies described in the present paper closely resemble those described by Hofmann, including the corrugated structures, which he considers to be among the most significant evidence of the biological origin of the bodies. The geological age of the two finds is also approximately the same. Our own material is slightly smaller, consisting of only two slabs, and the bodies contained in them are apparently somewhat less well preserved; yet, their origin seems to be identical. It is nevertheless clear that many more similar specimens — or ones whose origin is more unambiguous — must be found and studied in detail, with careful comparisons made, before the problem of the origin of the structures of this description can be deemed solved.

Acknowledgments: The authors are indebted to Dr. H. Faul from the University of Pennsylvania, U.S.A., Dr. M. F. Glaessner from the University of Adelaide, South Australia, Drs. G. Kautsky and F. Brotzen from the Geological Survey of Sweden, and Professor O. Sotavalta from the Institute of Zoology, University of Oulu, Finland, for valuable advice and information concerning similar structures and problems. We are also grateful to Mr. Y. Vuorelainen from the Outokumpu Company for field data concerning the uraninite-bearing sample used for age determination, to Dr. O. Kouvo for permission to use the unpublished results of his age determination, and to Professor P. Haapala for permission to publish data concerning the material of the Outokumpu Company. We also wish to thank Professor A. Simonen of the Geological Survey of Finland for kindly reading our manuscript and giving valuable criticism and advice, Mr. E. Halme for taking the photographs, Mrs. L. Pipinen for drawing the appended map and Mr. P. Sjöblom, M. A., for correcting the English manuscript.

Manuscript received, May 25, 1967

REFERENCES

BARNES, W. C. and SMITH, A. G. (1964) Some markings associated with ripple-marks from the Proterozoic of North America. Nature, Vol. 201, No. 4923, pp. 1018—1019.

ENDO, R. (1933) Manchuriophycus, nov. gen., from Sinian Formation of South Manchuria. Japanese Journ. Geol. and Geogr. Vol. XI. Nos 1—2, pp. 43—48.

FAUL, H. (1950) Fossil burrows from the Precambrian Ajibik quartzite of Michigan. Journ. of Paleontology. Vol. 24, No. 1, pp. 102—106.

FENTON, C. L. and FENTON, M. A. (1937) Belt Series of the North: Stratigraphy, Sedimentation, Paleontology. Bull. Geol. Soc. Am. Vol. 48, pp. 1873—1970.

FRAREY, M. J. and MCLAREN, D. J. (1963) Possible Metazoans from the early Proterozoic of the Canadian Shield. Nature, Vol. 200, No. 4905, pp. 461—462.

GLAESSNER, M. F. (1966) Precambrian Paleontology. Earth-Science Reviews. Vol. 1, No. 1, pp. 29—50.

HACKMAN, V. (1910) Suomen geologinen yleiskartta. The general geological map of Finland. Lehti — Sheet C 6. Rovaniemi.

HACKMAN, V. and WILKMAN, W. W. (1925) Suomen geologinen yleiskartta. The general geological map of Finland. Lehti — Sheet D 6. Kuolajärvi.

HOFMANN, H. J. (1967) Precambrian fossils (?) near Elliot Lake, Ontario. Science, Vol. 156, No. 3774, pp. 500—504.

HÄNTZSCHEL, W. (1949) Zur Deutung von Manchuriophycus Endo und ähnlichen Problematika. Mitt. Geol. Staatsinstitut Hamburg. Heft 19, pp. 77—84.

KOUVO, O. and TILTON, G. R. (1966) Mineral ages from the Finnish Precambrian. Journal of Geology. Vol. 74, No. 4, pp. 421—442.

SIMONEN, A. (1960) Pre-Quaternary rocks in Finland. Bull. Comm. géol. Finlande. 191, pp. 1—49.

WHEELER, H. E. and Quinlan, J. J. (1951) Pre-Cambrian sinuous mud cracks from Idaho and Montana. Journ. Sediment. Petrology, Vol. 21, No 3, pp. 141—146.

Comptes Rendus de la Société géologique de Finlande
N:o XXXIX (1967), pp. 199—217

ÜBER FINNLANDS REZENTE UND SUBFOSSILE DIATOMEEN I

VON

KARL MÖLDER [1]) und RISTO TYNNI

Geologische Forschungsanstalt in Finnland, Otaniemi

ZUSAMMENFASSUNG

Die Arbeit behandelt 16 *Melosira*-Arten sowie *Hyalodiscus*, *Pyxidicula*, *Stephanopyxis*, *Sceletonema* und *Thalassisira*. Bei jeder Art finden sich Angaben über die Verbreitung und Ökologie.

INHALT

EINLEITUNG

Vorliegende Untersuchung befasst sich mit der Diatomeenflora Finnlands in systematischer, ökologischer, quartärgeologischer und geographischer Hinsicht. Auch die Beziehungen der Arten und Varietäten zu der Trophie und zum pH des Wassers werden behandelt. Bei der Beschreibung der Arten und Varietäten werden aus Finnland bisher vorliegende Diatomeenarbeiten berücksichtigt. Weil die Verfasser bei der Umgrenzung ihrer Taxa die Hustedtschen Grundlagen befolgt haben, mussten viele

---

[1]) Anschrift: Dr. Karl Mölder, Kelohongantie 2 C, Tapiola, Finnland.

Formen wieder eingezogen werden und als Synonyme stehen bleiben. Es ist schon seit langem üblich, dass man kleine Abweichungen vom Typus nicht mehr als neue Formen beschreibt. Neue Kombinationen werden nur dann vorgenommen, wenn zwingende Gründe dazu vorliegen.

Die Diatomeen oder Kieselalgen sind mikroskopisch kleine einzellige Algen, deren Zelle aus zwei schachtelartig übereinandergreifenden Teilen besteht und Kieselsäure enthält. Die Zellwand ist mehr oder minder stark verkieselt und von Poren, Poroiden und Kanälen durchbrochen. Ebenso kommen an ihr verschiedene Verdickungen als Rippen, Warzen, Punkte usw. in mannigfaltigster Weise vor. Die Zellen haben einen Zellkern und einen bis mehrere Plattenchromatophoren. Als Assimilationsprodukt findet man meistens gelbbraunes fettes Öl.

Die Diatomeen leben im Wasser, auf feuchtem Gestein, auf feuchter Erde, auf den Bäumen oder überall, wo Wachstumsbedingungen für sie vorhanden sind. Viele Arten leben einzeln und frei, andere Arten wieder haften mit Hilfe von Gallertstielen oder Gallertpolstern an der Unterlage. Einige Arten, wie z. B. *Asterionella formosa Bacillaria paradoxa* und *Tabellaria fenestrata* var. *asterionelloides* bilden Kolonien, Sterne und Ketten oder leben in Gallertschläuchen oder in formlosen Gallertlagern.

Trotzdem Nitzsch schon im Jahre 1817 seine Untersuchung über die Diatomeen veröffentlichte, dauerte es 65 Jahre, bevor die erste Arbeit (Juhlin-Danfelt 1882) erschien, die mit der Diatomeenflora Finnlands im Zusammenhang steht.

Im Jahre 1891 veröffentlichte sodann P. T. Cleve seine Untersuchung über die Diatomeenflora Finnlands, in welcher neben den rezenten auch subfossile Formen behandelt sind. Neben den systematischen Angaben findet man hier auch ökologische Bemerkungen über Kaltwasserdiatomeen.

Hiernach vergingen 25 Jahre, ehe Astrid Cleve-Euler, die Tochter P. T. Cleves, im Jahre 1915 wieder eine Untersuchung über die Diatomeen Finnlands herausgab. Im gleichen Jahre veröffentlichte K. M. Levander seine Untersuchung »Zur Kenntnis der Bodenfauna und des Planktons der Pojovik» und auch einige andere Arbeiten, in denen er im Plankton vorkommende Melosiren behandelt.

Im Jahre 1920 erschien von Caroline Leegaard die Untersuchung: »Microplancton from the Finnish waters during the month of May 1912», in welcher die Verfasserin auch einige neue Diatomeen beschreibt. Fünf Jahre später veröffentlichte H. Järnefelt (1925) seine Dissertation »Zur Limnologie einiger Gewässer Finnlands». Das Diatomeenmaterial ist von Fr. Hustedt bestimmt worden und enthält viele neue Arten aus Finnland.

Im Jahre 1926 erschien von C. W. Fontell eine kleine Untersuchung »Om brack- och saltvattendiatomaceers förekomst i sött vatten i närheten av kusten». Der Verfasser hat aus kleinen Binnengewässern in der Nähe des Finnischen und des Bottnischen Meerbusens Salz- und Brackwasserformen gefunden, die jetzt als Relikte im Süsswasser wachsen.

Im gleichen Jahre 1926 verteidigte I. Välikangas an der Universität Helsinki seine Dissertation »Planktologische Untersuchungen im Hafengebiet von Helsinki», in welcher er neben dem Zooplankton auch planktische Diatomeen und andere Algen behandelt. Der Verfasser wendet sich in dieser Untersuchung besonders den ökologischen Fragen zu.

In den Jahren 1927—34 folgen sodann mehrere Untersuchungen in der Reihe »Zur Limnologie einiger Gewässer Finnlands» von H. Järnefelt. Da aber die in diesen Arbeiten erwähnten Diatomeen nicht aus Dauerpräparaten bestimmt sind, müssen diese Bestimmungen mit Vorsicht genommen werden.

Astrid Cleve-Euler besuchte im Jahre 1932 Finnisch-Lappland, und als Ergebnis dieser Reise erschien die Arbeit »The Diatoms of Finnish Lapland», in welcher neben der Diatomeensystematik auch geologische Fragen im Untersuchungsgebiet Behandlung finden. Auch hat die Verfasserin viele neue Varietäten und Formen aufgestellt.

In der Arbeit von 1937 (Mölder) »Die rezente Eunotienflora Finnlands» werden aus Finnland 39 *Eunotia*-Arten und 24 Varietäten angeführt. Dazu werden unterschieden die Ubiquisten, die Arten mit ausgeprägt nördlicher Verbreitung und die Kaltwasserformen. Im gleichen Jahre erschien von Mölder auch die Arbeit »Einige neue Diatomeen aus Finnland und Estland».

Im Jahre 1938 erschien von H. Luther die Untersuchung über die Algen im westlichen Inari (Enare) in Lappland. Die Bestimmungen der in der Arbeit enthaltenen Diatomeen sind von Mölder. Zwei Jahre später (1939) veröffentlichte Mölder 7 neue Diatomeen aus finnischen Gewässern.

Im Sommer 1933 bereiste Astrid Cleve-Euler wieder die nördlichsten Teile Finnlands und sammelte Material für eine neue Diatomeen-Untersuchung, die dann im Jahre 1939 erschien. In dieser Arbeit versucht sie mit Hilfe der Diatomeen auch geologische Fragen ihres Untersuchungsgebietes zu lösen und unterscheidet die Arenariaflora, die Rhoicospheniaflora, die Saimaflora und die lappländisch-arktische Kälteflora. Auch zahlreiche neue Taxa werden beschrieben. Weil aber mehrere Abbildungen unzulänglich gezeichnet sind, lässt sehr schwer kontrollieren, welche Formen sie tatsächlich darstellen.

Im Jahre 1942 erschien von derselben Autorin die Untersuchung »Coscinodisci et Thalassiosirae Fennosueciae», wo sie kritisch diese Diatomeen behandelt. Diese Arbeit bringt viel Neues und befasst sich auch mit systematischen Fragen.

Im folgenden Jahre 1943 erschienen von Mölder zwei Arbeiten: »Rezente Diatomeen in Finnland als Grundlage quartärgeologischer Untersuchungen» und »Studien über die Ökologie und Geologie der Bodendiatomeen in der Pojo-Bucht». Erstere behandelt rezente Diatomeen der Meeresufer bei Kemi und Helsinki nebst einigen Diatomeen aus dem Süsswasser, die zweite die rezenten Diatomeen des Litorals und des tieferen Wassers, mit Angaben über die ökologischen Verhältnisse im Untersuchungsgebiet.

Gleichzeitig mit diesen veröffentlichte G. Krasske (1943) seine Untersuchung »Zur Diatomeenflora Lapplands» und im Jahre 1949 noch eine ergänzende Arbeit. In diesen Arbeiten hebt der Verfasser nordische Arten, nordisch-alpine Arten und Kaltwasserformen hervor.

Astrid Cleve-Euler hat während der Jahre 1951—55 fünf grosse Arbeiten unter dem Titel »Die Diatomeen von Schweden und Finnland» herausgegeben. Aus ihnen erhält man eine gute Vorstellung von der Diatomeenflora dieser Gebiete. Die Verfasserin beschreibt auch viele neue Arten, Varietäten und Formen und bildet sie ab, leider aber in manchen Fällen so, dass es Schwierigkeiten bereitet, diese Diatomeen in den Präparaten zu identifizieren.

Im Jahre 1958 erschien von E. Halme und K. Mölder eine umfassende Untersuchung über das Phytoplankton der Pojo-Bucht an der finnischen Südküste. Darin werden genaue Angaben über die Temperatur und den Salzgehalt des Wassers gemacht, in denen die im Plankton vorkommenden Algen wachsen. Hier wurden insgesamt 502 Diatomeen-Arten festgestellt.

Im Jahre 1959 veröffentlichte F. E. Round aus Finnland zwei Arbeiten, in denen er neben anderen Algen aus den Flüssen Tornionjoki, Muonionjoki und Könkämäeno sowie aus Tvärminne auch Diatomeen angibt.

In den Jahren 1959 und 1960 erschienen von R. Simonsen zwei Arbeiten, »Neue Diatomeen aus der Ostsee» I und II, in denen er für die Wissenschaft neue Formen beschreibt.

In einer grösseren Untersuchung über die Diatomeenflora des Bottnischen Meerbusens und der Ostsee behandelt Mölder 1962 ausführlich die Wirkung der im Wasser gelösten Salze und der Temperatur auf die Diatomeen. Planktische Formen wurden im Untersuchungsgebiet nur wenig gefunden, der Schwerpunkt liegt deutlich bei den Formen des Meeresbodens.

Im Jahre 1966 erschien von K. Mölder und R. Tynni die Untersuchung »Diatomeen im Plankton bei der Stadt Helsinki und in der Stromschnelle Putaankoski im Kirchspiel Askola, Südfinnland, im Jahre 1964». In dieser Arbeit konnten die Verfasser z. B. feststellen, dass *Achnanthes taeniata* im April bei 3.6°C am besten wächst. *Sceletonema costatum* dagegen hat ihr maximales Vorkommen im Juli bei 23°C warmem Wasser.

Ausser den vorhin schon genannten Untersuchungen hat H. Järnefelt noch einige Arbeiten veröffentlicht, in denen die Diatomeen von K. Mölder an Dauerpräparaten bestimmt wurden. Dazu gibt es eine Menge quartärgeologischer Arbeiten, in denen die subfossile Diatomeenflora aus Vertikalprofilen bestimmt worden ist. (Siehe Literaturverzeichnis.)

DIE DIATOMEEN, IHRE ÖKOLOGIE, VERBREITUNG UND SUBFOSSILES VORKOMMEN

Die Diatomeen zerfallen in zwei Gruppen, die sich sowohl morphologisch als auch biologisch voneinander unterscheiden lassen. Die erste Gruppe, *Centricae* oder *Centrales*, bilden Diatomeen mit zentrisch gebauten Zellen und radiärer bis unregelmässiger Struktur, ohne Rhaphe oder Pseudorhaphe. Chromatophoren zahlreich, meist klein und rundlich. Die zweite Gruppe, *Pennatae* oder *Pennales* bilden Diato-

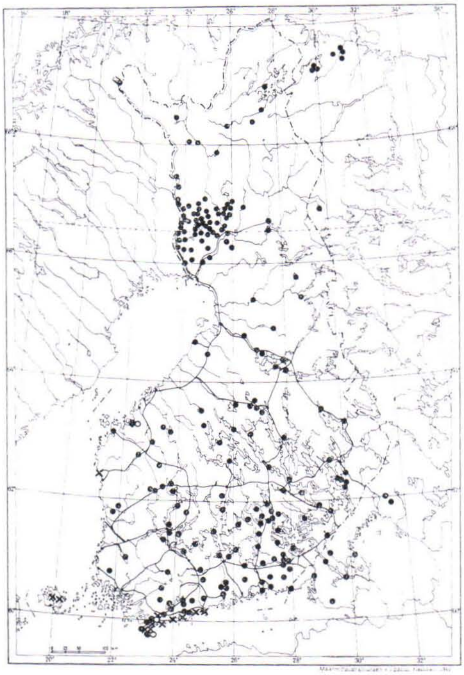

Abb. 1.

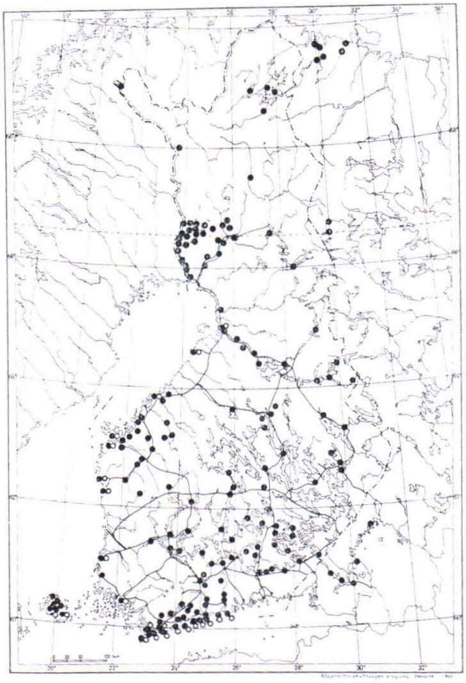

Abb. 2.

Abb. 1. Rezente Verbreitung von *Melosira ambigua* (Punkte), *Melosira sulcata* (Ringe) und *Melosira moniliformis* (Kreuze).

Abb. 2. Rezente Verbreitung von *Melosira islandica* ssp. *helvetica* (Punkte) und *Melosira arctica* (Ringe).

meen mit zygomorph gebauten Schalen, mit Rhaphe oder Pseudorhaphe und fast stets mit fiedriger und regelmässiger Struktur. Chromatophoren klein und zahlreich, oft gelappt.

Melosiren

Melosiren gehören zu der ersten Gruppe und die Zellen sind stets zylindrisch, trommelförmig oder beinahe kugelförmig. Frusteln bilden lange perlschnurartige Ketten oder walzenförmige lange Fäden. Die Valvarfläche ist immer kreisförmig und die Endfläche der Valva flach oder konvex. Die Schalen sind regellos oder radial punktiert, am Rande häufig gezähnt. Chromatophoren sind als kleine rundliche oder gelappte Plättchen vorhanden.

Melosira ambigua (Gun.) Müller

Synonyme: *Melosira crenulata* var. *ambigua* Grun., *M. crotonensis* Wolle, *M. crenulata* var. *Pantocseki* De Toni, *M. ambigua* ssp. *variata* Müller, *M. ambigua* ssp. *puncticulosa* Müller, *M. polymorpha* ssp. *italica* var. *ambigua* Bethge, *M. italica* var. *ambigua* A. Cleve.

Sehr verbreitet in den Seen und Flüssen. Reichlicher im Plankton der eutrophen Seen und im Wasser mit pH 5—7. Individuenzahlen sehr klein in den alkalischen Seen. Abb. 1. Subfossil selten in den Eisseesedimenten und individuenreich in Binnensee- und den Ancylusseesedimenten.

Melosira arctica (Ehr.) Dickie

Synonyme: *Gaillonella arctica* Ehr., *Melosira nummuloides* var. *hyperborea* Grun., *Gaillonella nummuloides* var. *hyperborea* De Toni, *Melosira hyperborea* (Grun.) Schütt, *M. nummuloides* Vanhöffen, *M. juergensi* Vanhöffen, *M. nummuloides* var. *arctica* P. T. Cleve, *M. arctica* var. *bornholmiensis* Cleve-Euler.

In arktischen Meeren im Wasser mit 2 bis 3 % Salz gemein. In Finnland an den Meeresküsten von Oulu bis Helsinki im Wasser mit 0.5 bis 0.8 % Salz individuenarm, im Frühling und im Herbst häufiger vorhanden. Abb. 2. Subfossil in den Yoldia- und Litorinameersedimenten recht selten vorhanden.

Melosira arenaria Moore

Synonyme: *Gaillonella varians* Ehr., *G. biseriata* Ehr., *G. vermicularis* Bréb., *Orthosira arenaria* Smith, *Melosira arenaria* var. *hungarica* Pantocsek, *M. hisbida* Peragallo, *M. arenaria* var. *granulata* Gutwinski, *M. Csákyana*, *M. neogena* et *M. arenaria* var. *tertiaria* Pantocsek, *M. arenaria* var. *vestita* Pantocsek.

Kommt rezent in Finnland in der Litoralregion der grösseren Seen selten vor. Cleve-Euler (1951) hat sie jedoch auch zu den Planktonformen gerechnet. Im vorliegenden Material ist *Melosira arenaria* nicht im Plankton angetroffen worden. Subfossil kommt sie als typische Ancylusseediatomee in den Ancylusseesedimenten vor.

Melosira distans (Ehr.) Kützing

Synonyme: *Gaillonella distans* Ehr., *Coscinodiscus minor* Smith, *Orthosira nivalis* Kitton, *Gaillonella gallica* Ehr., *Melosira distans* var. *nivalis* Grun., *M. solida* var. *Sarsii* Gran, *M. polymorpha* ssp. *distans* Bethge, *M. polymorpha* ssp. *distans* var. *nivalis* Bethge, *M. distans* var. *genuina* Grun., *M. distans* var. *humilis* A. Cleve, *M. distans* var. *humilis* f. *validior* A. Cleve, *M. distans* var. *humilis* f. *clinostriata* A. Cleve, *M. distans* var. *decipiens* Grove, *M. decipiens* Grove, *M. Pfaffiana* Reinsch, *M. distans* var. *Pfaffiana* (Reinsch) Grun., *M. distans* var. *africana* Müller, *M. laevissima* Grun., *M. lirata* var. *exigua* A. Cleve, *M. distans* var. *exigua* A. Cleve, *M. scalaris* Grun., *M. distans* var. *scalaris* Grunow.

Sehr verbreitet im Litoral in süssen Gewässern Finnlands besonders in oligotrophen Seen. Selten im Plankton und dann in Ufernähe. Abb. 3. Subfossil in allen Wassersedimenten in Finnland.

Var. *lirata* (Ehr.) Bethge

Synonyme: *Gaillonella lirata* Ehr., *Melosira lirata* Kütz., *M. distans* var. *lirata* f. *lacustris* (Grun.) Bethge.

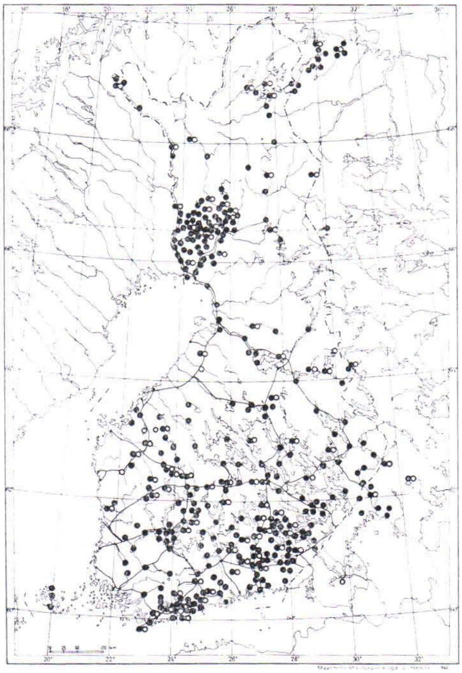
Abb. 3.

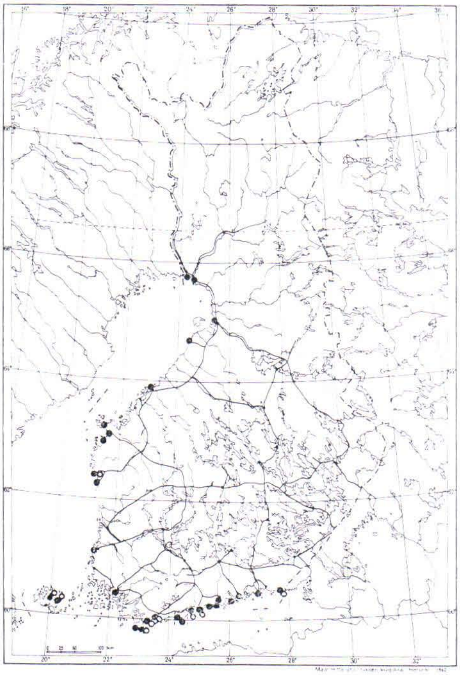
Abb. 4.

ABB. 3. Rezente Verbreitung von *Melosira distans* (Punkte) und *M. d.* var. *lirata* (Ringe).
ABB. 4. Rezente Verbreitung von *Melosira juergensi* (Punkte) und *Melosira dubia* (Ringe).

Kommt häufig zusammen mit der Hauptart besonders in den Seen vor. Abb. 3. Subfossil seltener in den Sedimenten als Hauptart.

Forma *seriata* Müller

Unterscheidet sich von voriger durch unvollständige Porenreihen, von denen 1—2 Querreihen am Diskusrand vorhanden sind. Der übrige Teil des Mantels ist strukturlos. Kommt selten in den Seen vor.

Als Variationen von *M. distans* hat Cleve-Euler (1951) *M. distans* var. *humilis* aus Kuusamo beschrieben, *M. distans* var. *africana* aus dem Fluss Poukanijoki, *M. distans* var. *nivalis* insbesondere aus Nordfinnland sowie *M. distans* var. *exigua* aus dem Fluss Kemijoki und dem See Höytiäinen.

Melosira dubia Kützing

Synonym: *Podosira dubia* Grun.

Gedeiht im Wasser mit 1.5 bis 2.5 % Salz in der Litoralregion der europäischen Meeresküsten. Kommt in Finnland selten und individuenarm an den Meeresküsten vor. Abb. 4. Subfossil sehr selten in den Litorinameersedimenten.

Melosira granulata (Ehr.) Ralfs

Synonyme: *Gaillonella granulata* Ehr., *G. decussata* Ehr., *Orthosira punctata* Smith, *Melosira decussata* Kütz., *M. decussata* var. *ordinata* Kütz., *M. granulata* var. *maxima* Ehr., *M. granulata* var. *decussata* Grun., *M. granulata* var. *jeremiae* Grun., *M. granulata* var. *jonensis* Grun., *M. lineolata* Grun., *M. punctata* Juhlin-Dannfelt, *M. granulata* var. *boryana* Pantocsek, *M. granulata* var. *attenuatum* Pantocsek, *M. granulata* var. *spinosa* Balachoncew, *M. granulata* var. *maeotica* Pantocsek, *M. granulata* ssp. *mutabilis* Müller, *M. granulata* ssp. *punctata* Müller, *M. granulata* f. *reticulata* Müller, *M. polymorpha* ssp. *granulata* Bethge, *M. granulata* var. *typica* A. Cleve, *M. granulata* var. *curvata* Grun., *M. granulata* f. *curvata* Grunow.

Findet sich besonders im Plankton der grösseren Seen und Flüsse Finnlands. Gedeiht in eutrophen bis oligotrophen Gewässern mit 4.5—6.5 pH. Gelegentlich trifft man sie in kleineren Wasseransammlungen. Wächst auch in den ziemlich ausgesüssten Flussmündungen des Finnischen Meerbusens. An der Station I in der Pojo-Bucht ist beobachtet worden, dass die optimalen Wachstumsbedingungen im Hochsommer bei einer Wassertemperatur von 22°C und einem Salzgehalt von 0.08 % gegeben sind (Halme und Mölder, 1958). Nach Cleve-Euler (1951) liegen keine rezenten Funde aus Lappland vor. Neueren Untersuchungen gemäss ist die Art aber doch vielerorts in Lappland angetroffen worden (Abb. 5).

Subfossil kommt sie häufig in den Ancylusseesedimenten und auch in den Sedimenten der grösseren Binnenseen vor, nicht selten auch in den Eisseesedimenten.

Var. *angustissima* Müller

Synonyme: *Gaillonella tenerrima* Ehr., *Melosira arundinacea* Castracane, *M. granulata* var. *procera* f. *tenerrima* Müller.

Kommt häufig zusammen mit der Hauptart vor. Abb. 5. Bevorzugt saures Wasser. Subfossil in den Ancylusseesedimenten und auch in den Binnenseesedimenten häufig.

Var. *muzzanensis* (Meister) Bethge

Die Art wurde nur 3 Mal aus Lappland in den Flüssen festgestellt. Abb. 5.

Melosira islandica Müller

Synonyme: *Melosira transsilvanica* Pantocsek, *M. granulata* var. *hungarica* Pantocsek, *M. Temperi* Pantocsek, *M. polymorpha* ssp. *granulata* var. *islandica* Bethge, *M. venerensis* A. Cleve.

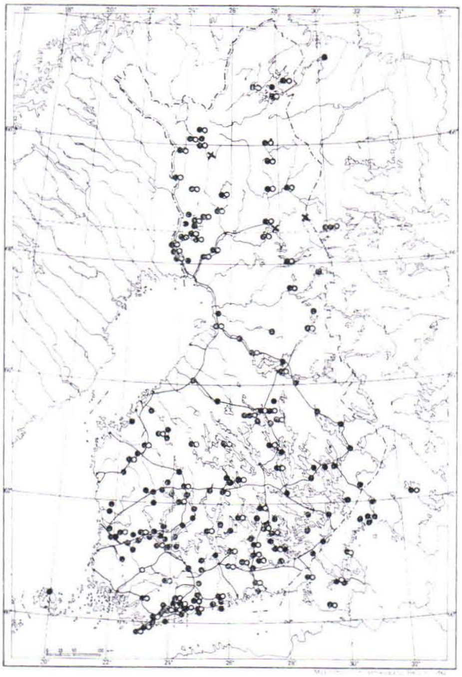
Abb. 5.

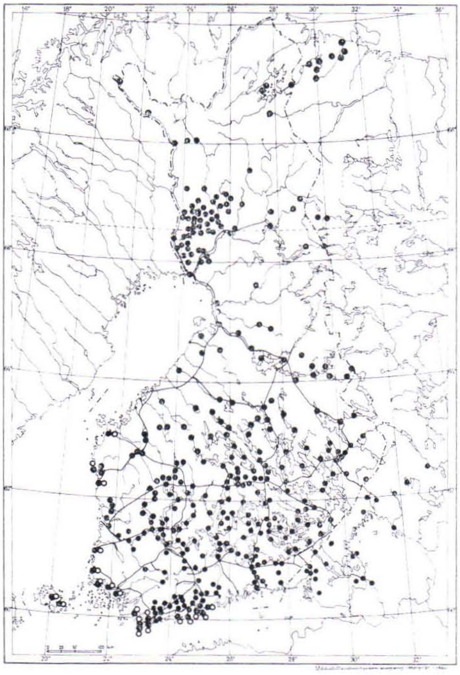
Abb. 6.

Abb. 5. Rezente Verbreitung von *Melosira granulata* (Punkte), *M. g.* var. *angustissima* (Ringe) und *M. g.* var. *muzzanensis* (Kreuze).

Abb. 6. Rezente Verbreitung von *Melosira italica* (Punkte) und *Melosira nummuloides* (Ringe).

Kommt in Lappland in den grösseren Seen selten vor. Subfossil selten in den Ancylusseesedimenten.

Ssp. *helvetica* Müller

Synonyme: *Melosira lineolata* Grun., *M. granulata* ssp. *helvetica* A. Cleve, *M. polymorpha* ssp. *granulata* var. *helvetica* Bethge.

Sehr verbreitet im Plankton der Seen und Flüsse und in den Bächen. Wächst auch in den kälteren Zeiten des Jahres in eutrophen bis oligotrophen Gewässern mit 4—8 pH. Gedeiht auch in schwachem Brackwasser. Abb. 2. In der Pojo-Bucht entsprachen den optimalen Wachstumsverhältnissen eine Temperatur von 9.4°C und Salzgehalt von 0.17 ‰. Oligohaline eurytherme Kaltwasserform (Halme & Mölder, 1958).

Subfossil individiuenreich in den Ancylusseesedimenten und auch in den Binnenseeablagerungen vorhanden. Selten in den Eissee- und anderen spätglazialen Süsswassersedimenten.

Melosira italica (Ehr.) Kützing

Synonyme: *Gaillonella italica* Ehr., *G. crenulata* Ehr., *G. crenata* Ehr., *G. laevis* Ehr., *G. crotonensis* Bailey, *Aulacosira crenulata* Thwaites, *Orthosira tenuis* Rabenh., *Melosira tenuis* Kütz., *M. crenulata* Kütz., *M. laevis* Ralfs, *M. crenulata* var. *italica* Grun., *M. crenulata* var. *laevis* Grun., *M. crenulata* var. *semilaevis* Grun., *M. crenulata* var. *tenuis* Grun., *M. crenulata* var. *fossilis* Pantocsek, *M. crenulata* var. *debilis* Pantocsek, *M. crenulata* var. *hungarica* Pantocsek, *M. Zeileri* Mauler, *M. italica* var. *tenuis* Müller, *M. laevis* var. *elongata* Lauby, *M. laevis* var. *fuegiana* Frenguelli, *M. polymorpha* ssp. *italica* Bethge, *M. crenulata* var. *tenuissima* Grun., *M. crenulata* var. *ambigua* Grun.

Wächst besonders häufig im Litoral der oligotrophen und dystrophen Seen, in Teichen, Flüssen, Bächen und Gräben. Kommt auch in schwachem Brackwasser an den Flussmündungen im Plankton vor. Abb. 6. Subfossil in den Eissee-, Ancylussee- und Kleinseesedimenten sehr verbreitet.

Var. *valida* Grun.

Synonyme: *Melosira valida* Meister, *M. polymorpha* ssp. *distans* var. *valida* Bethge, *M. crenulata* var. *valida* Grun.

Wächst in der Litoralregion der Seen und Teiche, seltener in den Flüssen und Bächen zusammen mit der Hauptart. Abb. 7. Subfossil in den Ancylusseesedimenten und in anderen Süsswasserseenablagerungen.

Ssp. *subarctica* Müller

Synonyme: *Melosira polymorpha* ssp. *italica* var. *subarctica* Bethge.

Sie ist eine Kaltwasserdiatomee und kommt in den Gewässern Lapplands sehr individuenreich vor. Sie wächst hauptsächlich in den oligotrophen Gewässern. Abb. 7. Subfossil in den Sedimenten der Binnenseen.

Nach Cleve-Euler (1951) entspricht die von Hustedt (1930) beschriebene Form *M. italica* var. *subarctica* der Form *M. italica* var. *valida*. Cleve-Euler hat aus Inari auch *M. italica* var. *alpigena* gemeldet (Järnefelt: vorherrschende Planktonform im See Kaskenjärvi). Die in Frage stehende Varietät ähnelt der von Hustedt beschriebenen kleinen Form *M. distans* var. *alpigena*. Cleve-Euler hat ausserdem eine auf der Insel Kärnäsaari gefundene, fossile *M. ludica*-Art beschrieben.

Melosira juergensi Agardh

Synonyme: *Melosira subflexilis* Kütz., *M. subangularis* Grun., *M. Borreri* var. *bothnica* Grunow.

Sehr verbreitet an den Meeresküsten in ganz Europa und seltener im Brackwasser des Binnenlandes. Beste Wachstumsbedingungen hat sie im Wasser mit 1.5 bis 2.5 % Salz. In Finnland kommt sie häufig an den Meeresküsten als Benthosform

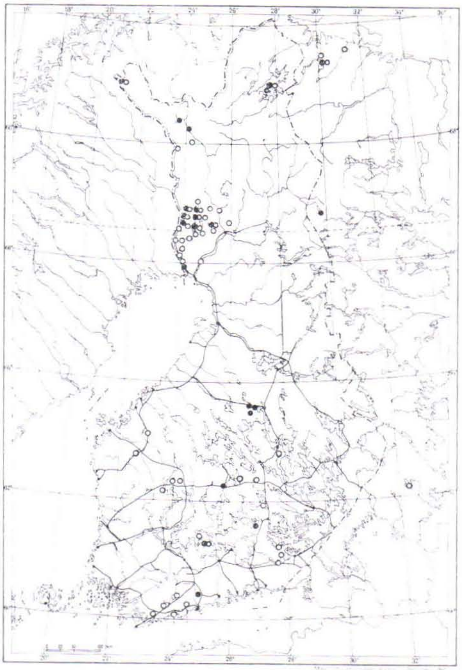

Abb. 7.

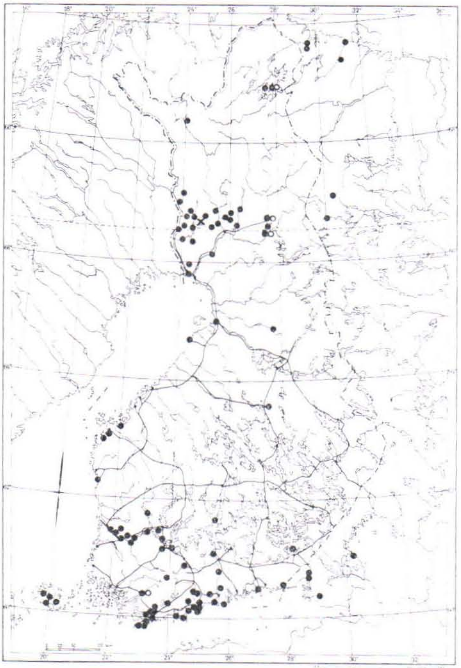

Abb. 8.

Abb. 7. Rezente Verbreitung von *Melosira italica* var. *subarctica* (Punkte) und *M. i.* var. *valida* (Ringe).
Abb. 8. Rezente Verbreitung von *Melosira varians* (Punkte), *Melosira undulata* (Ringe) und *M. u.* var. *normanni* (Kreuze).

vor, wo im Wasser 0.5 bis 1 % Salz vorhanden ist. Sie ist eine Brackwasserdiatomee. Abb. 4. Subfossil in den Yoldia- und Litorinameersedimenten vorhanden, wo sie in den letzteren in einigen Proben recht grosse Individuenzahlen hat.

Melosira moniliformis (Müller) Agardh

Synonyme: *Conferva moniliformis* Müller, *C. lineata* Dillwyn, *C. nummuloides*, *Fragilaria lineata* Lyngbye, *Lysigonium lineatum* Link, *L. moniliforme* Link, *Gaillonella moniliformis* Bory, *G. lineata* Ehr., *G. Borreri* Pelletan, *Melosira lineata* Ag., *M. Borreri* Greville, *M. lentigera* Harvey, *M. Borreri* var. *moniliformis* Grunow. Der Name hat sich nicht eingebürgert, denn u.a. Cleve-Euler (1951) und M.-B. Florin (1957) gebrauchen begründet die Bezeichnung *M. lineata*.

Im Litoral des gesamten europäischen Küstengebietes, besonders in Nordeuropa. Planktondiatomee im Wasser mit 0.5 bis 3 % Salz. In der Ostsee, wo weniger Salz im Wasser gelöst vorhanden ist, sind die Punkte auf den Schalen nicht so deutlich entwickelt. Kommt hauptsächlich am Südwestende des Landes vor. Abb. 1. Subfossil häufig in Litorina- sehr selten in den Yoldiaseesedimenten.

M. moniliformis (Agardh) A. Cleve ähnelt *M. arctica*, aber die Art ist aus Finnland nicht gemeldet.

Melosira nummuloides (Dillw.) Agardh

Synonyme: *Conferva nummuloides* Dillw., *Fragilaria nummuloides* Lyngbye, *Gaillonella nummuloides* Bory, *Sphaerophora globulifera* Hassall, *Melosira discigera* Ag., *M. salina* Kütz., *M. salina* var. *concatenata* Kütz., *M. nummuloides* var. *elestdana* Pantocsek.

Als Aufwuchsdiatomee wächst sie im Wasser mit 1—3 % Salz in allen Küstengebieten. Abb. 6. Von den Wellen wird sie u.a. von Wasserpflanzen losgerissen, und man findet sie auch im Plankton an den Küsten. An den finnischen Meeresküsten kommt sie von Vaasa bis Helsinki rezent vor. Subfossil in den Litorinameersedimenten.

Melosira roeseana Rabenhorst

Synonyme: *Orthosira spinosa* Smith, *O. Roeseana* O'Meara, *Melosira spinosa* Brun.

In Finnland aus folgenden Stellen festgestellt: Fluss Muonionjoki, Fluss Vaskojoki, See Inarinjärvi, See Kemijärvi und See Konttajärvi. Alle Fundorte in Finnland sind aus Lappland, und sie ist demgemäss eine Kaltwasserdiatomee. Subfossil nur aus Lappland bekannt.

Melosira sulcata (Ehr.) Kützing

Synonyme: *Gaillonella sulcata* Ehr., *G. coronata* Ehr., *G. plana* Ehr., *Orthosira marina* Smith, *O. sulcata* O'Meara, *Paralia marina* Heiberg, *P. sulcata* P. T. Cleve, *P. sulcata* f. *radiata* Van Heurk, *Melosira marina* Janisch.

Häufig im Litoral an den Meeresküsten ganz Europas. Selten an den Meeresküsten Finnlands (Mölder 1962). Vereinzelt auch im Plankton. Optimale Wachstumsbedingungen im Wasser mit 2.5—3 % Salz. Abb. 1. Subfossil in Yoldia- und Litorinameersedimenten.

Melosira undulata (Ehr.) Kützing

Synonyme: *Gaillonella undulata* Ehr., *G. punctata* Ehr., *G. punctigera* Ehr., *Melosira punctigera* Ralfs.

Nur aus 4 oligotrophen Seen in Finnland rezent festgestellt. Abb. 8. Subfossil in Wärtsilä und Ilomantsi gefunden.

Var. *normanni* Arnott

Synonyme: *Melosira gownii* A. Schmidt.

Nur im See Raanujärvi aus Lappland festgestellt. Abb. 8. Subfossil selten in den Binnensee- und Ancylusseesedimenten gefunden.

Melosira varians Agardh

Synonyme: *Conferva hiemalis* Roth, *C. fasciata* Dillwyn, *Nematoplata çuadrata* Bory, *Gaillonella varians* Ehr., *Vesiculifera composita* Hassall, *Lysigonium varians* De Toni, *Melosira aeçualis* Ag., *M. coarctata* Ehr., *M. varians* var *aeçualis* Kützing.

Sehr verbreitet in den Gewässern Finnlands. Häufig auch an den Meeresküsten, wo das Wasser 0.5 bis 1 % Salz enthält. Abb. 8. Benthosform. Subfossil in den Yoldia-, Ancylus- und Litorinaseesedimenten sowie in Binnenseesedimenten, fehlt aber in den Baltischen Eisseesedimenten.

Melosira westii Smith

Synonyme: *Discoplea umbilicata* Ehr., *Cyclotella umbilicata* Ralfs, *Lysigonium Westii* O'Meara, *Gaillonella Westii* De Toni.

Litoral im Salz- und Brackwasser. Optimale Wachstumsbedingungen im Wasser mit 3 % Salz. Subfossil in Litorinameersedimenten relativ gemein (kleine Form, forma *parva* Brander), selten in den Yoldiameersedimenten.

Hyalodiscus

Linsenförmige, kurze Ketten bildende Zellen. Die Randzone der Schale zart areoliert, Scheitel sehr zart punktiert.

Hyalodiscus scoticus (Kützing) Grun.

Synonyme: *Cyclotella scotica* Kütz., *C. ligustica* Kütz., *Podosira hormoides* Smith, *P. Smithiana* Grun., *P. Franklini* Grun., *Hyalodiscus subtilis* var. *scotica* Peragallo.

An den Küsten des Salz- und Brackwassers verbreitet. Optimale Wachstumsbedingungen im Wasser mit 1.5—3 % Salz. In Finnland kommt sie selten an den Meeresufern vor. Subfossil in den Yoldia- und Litorinameersedimenten recht häufig.

Pyxidicula

Zellen kugelig bis ellipsoid mit hochgewölbten Schalen, einzeln oder kurze Ketten bildend.

Pyxidicula mediterranea Grun.

Rezent aus Finnland nicht bekannt. Im Mittelmeergebiet verbreitet. Subfossil sehr selten in Yoldiameersedimenten.

Stephanopyxis

Zellen zylindrisch, kugelig oder ellipsoid.

Stephanopyxis turris var. *polaris* Grun.

Pelagisch an den europäischen Meeresküsten verbreitet. Rezent aus Finnland nicht bekannt. Subfossil selten in den Yoldiameersedimenten.

Sceletonema

Dünnwandige, zylinder-ellipsoidförmige Zellen, die mit Kieselstäbchen zu fadenförmigen Kolonien vereinigt sind.

Sceletonema costatum (Grev.) Cleve

Synonyme: *Melosira costata* Greville.

Sehr gewöhnliche Planktondiatomee an den Meeresküsten. Eurytherme und euryhaline Form (Hustedt 1930), deren optimale Wachstumsbedingungen bei Helsinki i. J. 1964 im Juli herrschten (Temperatur 23°, Salzgehalt $5^0/_{00}$) (Mölder & Tynni 1966). Nach Cleve-Euler (1951) hat die Art ein beträchtliches Wintermaximum. Den oben genannten Beobachtungen gemäss ist die Art jedoch eurytherm und gedeiht am besten in warmem Wasser. Wegen ihrer schwachen Schale hält sich die Art nicht in Sedimenten und ist subfossil nicht beobachtet worden.

Thalassiosira

Zellen trommelförmig, seltener zylindrisch, durch zentralen Gallertstrang zu Ketten verbunden.

Thalassiosira baltica (Grun.) Ostenfelt

Synonyme: *Coscinodiscus polyacanthus* var. *baltica* Grun., *C. balticus* P. T. Cleve.

Eine typische Brackwasserdiatomee und sehr verbreitet im Bottnischen- und Finnischen Meerbusen sowie in der Ostsee (Mölder 1962). Häufige Planktondiatomee. Subfossil häufig in den Yoldia- und Litorinameersedimenten.

Thalassiosira decipiens (Grun.) Joergensen

Im Küstenplankton ganz Europas verbreitet. An den Küsten Finnlands von Vaasa bis Helsinki und im Plankton der Ostsee häufig (Mölder 1962). Subfossil in den Yoldia- und Litorinameersedimenten nicht häufig.

Manuskript eingegangen am 3, April 1967

TAFEL I

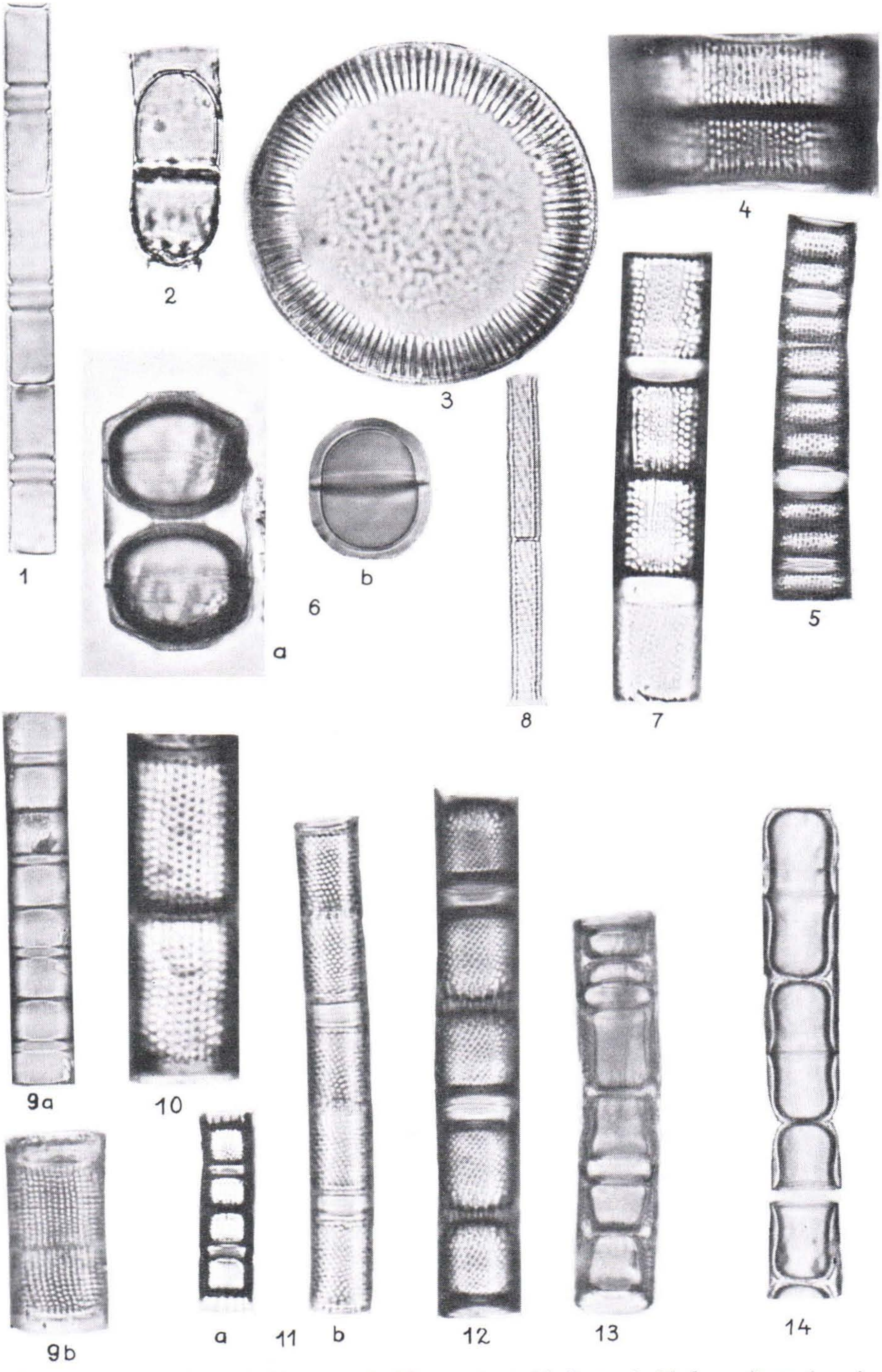

Fig. 1. *Melosira ambigua*, 2. *M. arctica*, 3. *M. arenaria*, 4. *M. distans*, 5. *M. d.* var. *lirata*, 6. a—b. *M. dubia*, 7. *M. granulata*, 8. *M. g.* var. *angustissima*, 9. a—b. *M. islandica* ssp. *helvetica*, 10. *M. islandica*, 11 . a—b. *M. italica*, 12. *M. i.* var. *subarctica*, 13. *M. i.* var. *valida*, 14. *M. juergensi*.

TAFEL II

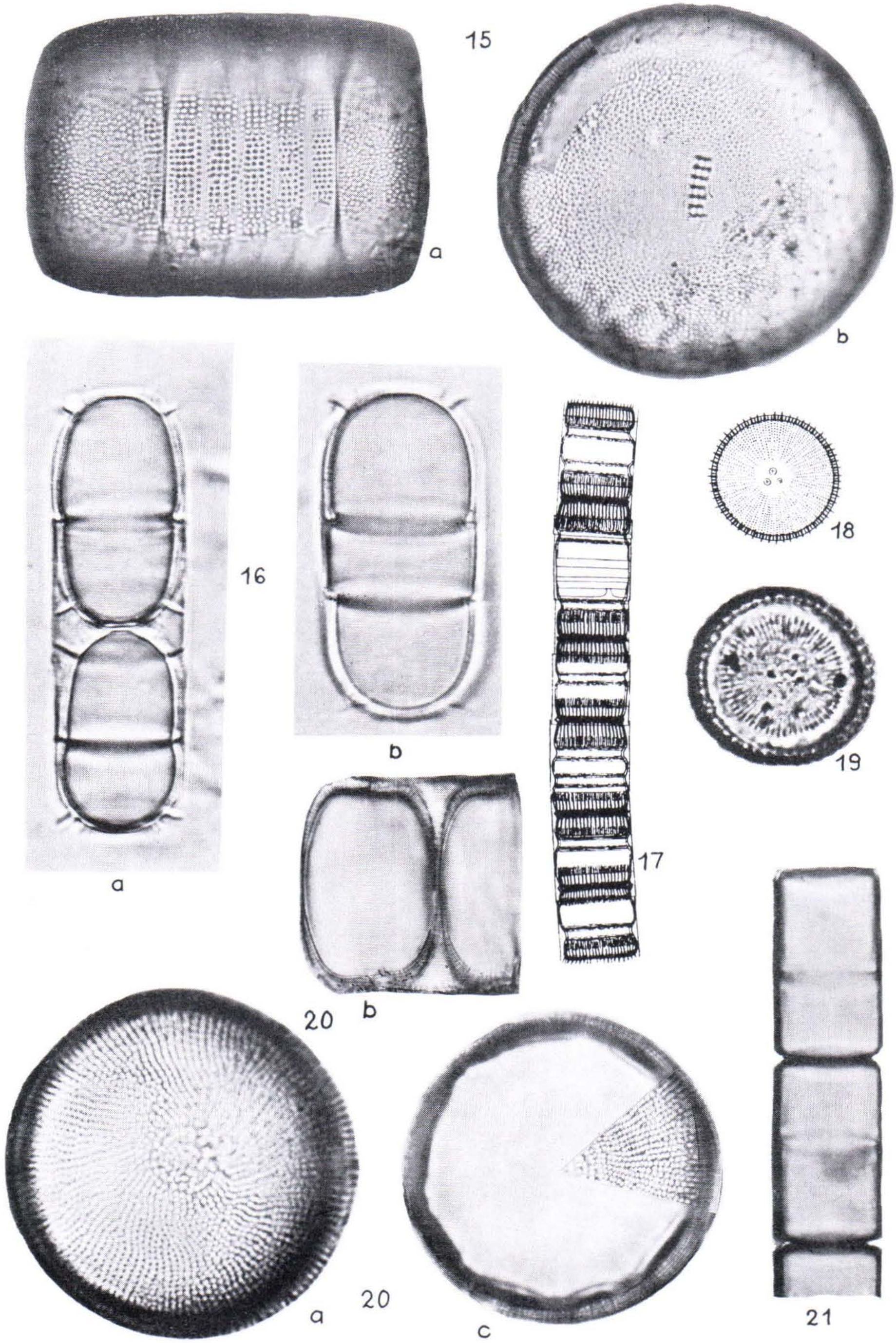

Fig. 15. a—b. *Melosira moniliformis*, 16. a—b. *M. nummuloides*, 17. *M. roeseana* nach (Hustedt), 18. *M. r.* var. *epidendron* (nach Hustedt), 19. *M. sulcata*, 20. a—b. *M. undulata*, c. *M. u.* var. *normanni*, 21. *M. varians*.

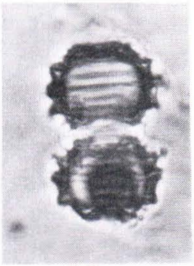

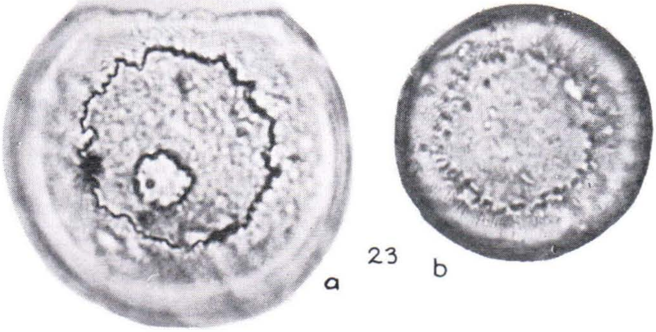

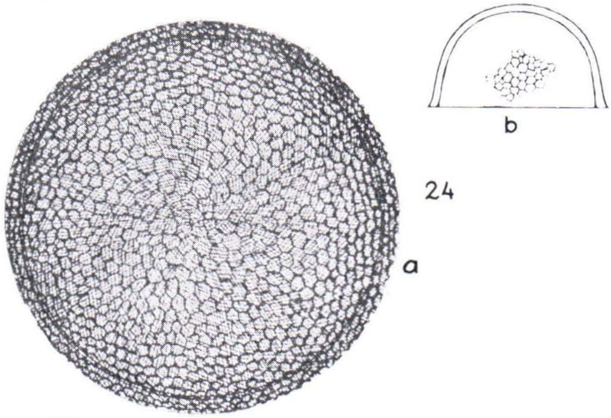

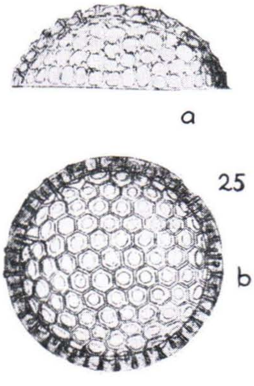

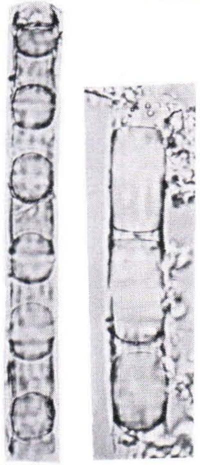

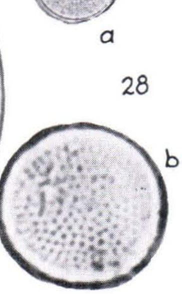

Fig. 22. *Melosira westii*, 23. a—b. *Hyalodiscus scoticus*, 24. a—b. *Pyxidicula mediterranea* (Original), 25. a—b. *Stephanopyxis turris* var. *polaris* (nach Grunow), 26. a—b. *Sceletonema costatum*, 27. *Thalassiosira baltica*, 28. a—b. *T. decipiens*. Photo E. Halme.

(etwa 1500-fache Vergr. in Fig. 4, 23a; 1000-fach 1, 3, 5—8, 9b, 10, 11b—16b, 19—22, 23b, 24, 26—28; 800-fach 2; 500-fach 9a, 11a, 17, 18; 400-fach 25.)

LITERATURVERZEICHNIS

Aario, R. (1965) Development of ancient Lake Päijänne and the history of the surrounding forests. Ann. Acad. Scient. Fennicae, Ser. A, III, 81.

—»— (1966) Kieselgur in fluvioglazialen Ablagerungen in Haapajärvi in Ostrobottnien. C. R. Soc. Géol. Finlande 38.

Alhonen, P. (1965) C_{14}-Datierung der vorgeschichtlichten Schlittenkufe aus Kullaa in Satakunta (Westfinnland). Suomen Museo 72.

Aurola, E. (1938) Die postglaziale Entwicklung des südwestlichen Finnlands. C. R. Soc. Géol. Finlande 11. Bull. Comm. géol. Finlande 121.

Backman, A. L. et Cleve-Euler, Astrid, (1922) Die fossile Diatomeenflora in Österbotten. Acta Forest. Fenn., 22, no 4.

Brander, G. (1935) Die baltische Diatomeen-Succession des Bålen-Beckens. Geol. Fören. Förhandl., 57.

—»— (1937) Ein Interglazialfund bei Rouhiala in Südfinnland. Bull. Comm. géol. Finlande 118.

—»— (1937) Zur Deutung der intramoränen Tonablagerung an der Mga, unweit von Leningrad. Ibid. 119.

Cleve, P. T. (1891) The Diatoms of Finland. Acta Soc. F. Fl. Fenn. 8, no 2.

Cleve-Euler, Astrid, (1915) New Contributions to the Diatomaceous Flora of Finland. Arkiv för Bot., 14, no 9.

—»— (1934) The Diatoms of Finnish Lapland. Soc. Scient. Fennica, Comm. Biol., 4, Nr. 14.

—»— (1939) Bacillariaceen-Assoziationen im nördlichsten Finnland. Acta Soc. Scient. Fenn., N. S., B 2, Nr. 3.

—»— Coscinocisci et Thalassiosirae Fennosueciae. Eine kritische Übersicht. Bot. Not. 1942.

—»— (1951—1955) Die Diatomeen von Schweden und Finnland. I—V. Kungl. Svenska Vetenskapsakademiens Handlingar 4. Ser., 2 : 1 (1951), 4 : 1, 5 (1953), 5 : 4 (1955), 3 : 3 (1952).

Donner, J. (1952) On the early Post-Glacial shore-line displacement in southeast Finland. Ann. Acad. Scient. Fennicae Ser. A. III, 29.

Florin, Maj-Britt (1957) Plankton of fresh and brackish waters in the Södertälje area. Acta Phytogeographica Suecica 37.

Fontell, C. W. (1926) Om brack- och saltvattendiatomacéers förekomst i sött vatten i närheten av kusten. Acta Soc. F. Fl. Fenn., 55, no 7.

Halme, E. et Mölder, K. (1958) Planktologische Untersuchungen in der Pojo-Bucht und angrenzenden Gewässern. III. Phytoplankton. Ann. Bot. Soc. Vanamo, Tom. 30, no 3.

Hustedt, Fr. (1927—1930 a) Die Kieselalgen Deutschlands, Österreichs und der Schweiz. I. Teil. Rabenhorst: Kryptogamenflora, 7. Leipzig.

—»— (1930 b) Bacillariophyta (Diatomeae). Bascher: Süsswasserflora, 10. Jena.

Hyvärinen, H. (1966) Studies on the late-Quaternary history of Pielis-Karelia, eastern Finland. Soc. Scient Fennica, Comm. Biol. Vol 29 Nr 4.

Hyyppä, E. (1937) Postglacial changes of shore-line in Sout Finland. Bull. Comm. géol. Finlande 120.

Juhlin-Dannfelt, H. (1882) On the Diatoms of the Baltic Sea. Bih. K. Sv. Vet.-Ak. Handl., 6, no 21.

Järnefelt, H. (1925) Zur Limnologie einiger Gewässer Finnlands. I. Ann. Soc. Vanamo. 2.

Krasske, G. (1943) Zur Diatomeenflora Lapplands. Ber. Deutsch. Bot. Gesell. Bd. 61, H. 3.

—»— (1949) Zur Diatomeenflora Lapplands II. Ann. Soc. Vanamo. Tom. 23, no 5.

Lappalainen, V. (1962) The shore-line displacement on southern Lake Saimaa. Acta Bot. Fennica 64.

Leegaard, Caroline, (1920) Microplankton from the Finnish waters during the month of May 1912. Acta Soc. Scient. Fenn. 48, no 5.

Levander, K. M. (1915) Zur Kenntnis der Bodenfauna und des Planktons der Pojoviek. Fennia, 35, Nr. 2.

Luther, H. (1938) Algen aus dem westlichen Enare in Lappland. Memor. Soc. F. Fl. Fenn., 14.

MÖLDER, K. (1937 a) Die rezente Eunotienflora Finnlands. Ann. Bot. Soc. Vanamo. Tom. 8, no 7.

—»— (1937 b) Einige neue Diatomeen aus Finnland und Estland. Ibid., Tom. 8, no 7.

—»— (1938) Die rezente Diatomeenflora Estlands. Ibid. Tom. 12, no 2.

—»— (1939) Einige neue Diatomeen aus Finnland. Ibid., Tom. 11, no 3.

—»— (1943 a) Studien über die Ökologie und Geologie der Bodendiatomeen in der Pojo-Bucht. Ibid. Tom. 18, no 2.

—»— (1943 b) Rezente Diatomeen in Finnland als Grundlage quartärgeologischer Untersuchungen. Geol. der Meere und Binnengew. 6.

—»— (1944 a) Die Postglaziale Klimaentwicklung im Lichte der fossilen Diatomeenfunde in Südfinnland. C. R. Soc. Géol. Finlande. 16.

—»— (1944 b) Das Karelische Eismeer im Lichte der Fossilen Diatomeenfunde. Ibid. 16.

—»— (1944 c) Die Entwicklungsgeschichte des Sees Vieljärvi in Ostkarelien und die Klimaschwankung im Lichte der Fossilen Diatomeenfunde aus den Seesedimenten. Ibid. 16.

—»— (1946 a) Zwei Tonprofile aus Süd-Pohjanmaa. Ibid. 19.

—»— (1946 b) Beiträge zur Kenntnis der rezenten Diatomeenflora von Åland (Ahvenanmaa). Ann. Soc. Vanamo. Tom. 21, no 5.

—»— (1951) Beiträge zur Kenntnis der rezenten Diatomeenflora Ostkareliens. Ibid. Tom. 25, no 1.

—»— (1955) Die Entwicklungsgeschichte des Sees Siikajärvi im mittleren Uusimaa. Acta Geographica. Bd. 14.

—»— (1956) Die Diatomeenflora der Bändertone bei Jokela in Südfinnland. Arch. Soc. Vanamo. 10 : 1.

—»— (1961) Diatomeen aus Kenia, Ostafrika. Ibid., 15 : 1—2.

—»— (1962 a) Über die Diatomeenflora des Bottnischen Meerbusens und der Ostsee. Merentutk. julkaisu. Nr. 203.

—»— (1962 b) Diatomeen aus den Gebirgen Sula und Kangari in Sierra Leone Westafrika. Bull. Comm. géol. Finlande. Nr. 198.

—»— (1964) Abhängigkeit der Diatomeen vom Felsgrund in Mittelfinnland. Ann. Bot. Fenn. 1.

—»— und TYNNI, R. (1966) Diatomeen im Plankton bei der Stadt Helsinki und in der Stromschnelle Putaankoski im Kirchspiel Askola, Südfinnland, im Jahre 1964. Ibid., 3.

—»— VALOVIRTA, V. und VIRKKALA, K. (1957) Über Spätglazialzeit und frühe Postglazialzeit in Südfinnland. Bull. Comm. géol. Finlande. Nr. 178.

REPO, R. (1963) On the Late-Glacial vegetation of Jaamankangas. Arch. Soc. »Vanamo» 18 : 2.

ROUND, F. E. (1957) The Late-Glacial and Post-Glacial Diatom succession in the Kentmere Valley Deposit. Part 1. Introduction, methods and flora. New Phytologist. 56.

—»— (1959) The composition of some algal communities living in rock pools on skerries near the Zoological Station at Tvärminne, S. Finland. Soc. Sci. Fennica, Comm. Biol. 21, Nr. 1.

—»— (1959) The algal flora of the Tornionjoki, Muonionjoki and Könkämäeno in North Finland. Ibid. 21, Nr. 2.

SALMI, M. (1949) Die Litorinagrenze in der Umgebung von Alajärvi in Süd-Ostbottnien. C. R. Soc. géol. Finlande 22.

SAURAMO, M. (1958) Die Geschichte der Ostsee. Ann. Acad. Scient. Fennicae, Ser. A, III, 51.

SIMONSEN, R. (1959) Neue Diatomeen aus der Ostsee I. Kieler Meeresforschung. 15 : 1.

—»— (1960) Neue Diatomeen aus der Ostsee II. Ibid. 16 : 1.

TYNNI, R. (1966) Über spät- und postglaziale Uferverschiebung in der Gegend von Askola, Südfinnland. Bull. Comm. géol. Finlande. Nr. 223.

VALOVIRTA, V. (1965) Zur spätquartären Entwicklung Südost-Finnlands. Ibid., Nr. 220.

VIRKKALA, K. (1948) Late-Glacial Development of Schore-Lines in Southern Kainuu and Northern Karelia. Bull. Comm. géol. Finlande Nr. 142.

—»— (1959) Über die spätquartäre Entwicklung in Satakunta, W-Finnland. Ibid., Nr. 183.

VÄLIKANGAS, I. (1926) Planktologische Untersuchungen im Hafengebiet von Helsingfors. Acta Zool. Fenn., 1.

THE GEOLOGICAL SOCIETY OF FINLAND

Founded in 1886

Officers for 1967

Heikki Tuominen, President

Nils Edelman, Vice-President

Valto Veltheim, Past President

Veikko Lappalainen, Councillor

Pentti Rouhunkoski, Councillor

Heikki Niini, Secretary
Natronal Board of Public Roads and
Waterways, Water Division, Mikonkatu 2 D,
Helsinki 10, Finland

Kauko Meriläinen, Treasurer
Geological Survey of Finland,
Otaniemi, Finland

MEMBERSHIP

Membership is open to any Finnish national interested in geoscience. Foreign membership is open to any foreign geologist on the recommendation of two Finnish members.

Members receive the following publications: Suomen Geologisen Seuran Julkaisuja» (Comptes Rendus de la Société géologique de Finlande), founded in 1929, one issue per year, containing scientific articles; »Geologi», founded in 1949, 10 issues per year, containing short articles in Finnish or Swedish on geoscientific subjects, book reviews, membership news, etc.

The annual membership fee is 20 Finnish marks. Lifetime membership fee 400 Finnish marks.